Synthesis and Characterization of Poly(arylene ether sulfone)s for Reverse Osmosis Water Purification and Gas Separation Membranes

Benjamin James Sundell

Dissertation submitted to the faculty of the Virginia Polytechnic Institute and State University in partial fulfillment of the requirements for the degree of

Doctor of Philosophy

in

Macromolecular Science and Engineering

James E. McGrath, Chair
Judy S. Riffle, Chair
S. Richard Turner
Alan R. Esker
Richey M. Davis
Sue J. Mecham

(08/25/14)
(Blacksburg, VA)

Keywords: Reverse osmosis water purification, gas separation, polymer synthesis, poly(arylene ether sulfone), crosslinking, membrane fabrication

ABSTRACT

Synthesis and Characterization of Poly(arylene ether sulfone)s for Reverse Osmosis Water Purification and Gas Separation Membranes

Benjamin James Sundell

Crosslinking is an effective technique for increasing the salt rejection of water purification membranes and the selectivity of gas separation membranes. An abundance of monomers, telechelic oligomers, and novel polymers were synthesized for use as separation membranes. These materials were often imbued with crosslinking functionalities to increase their performance during testing at the University of Texas-Austin.

Crosslinking of sulfonated poly(arylene ether sulfone) oligomers was studied systematically with regard to end-group functionality, polymer composition, and polymer hydrophilicity. Sulfonated bisphenol A based poly(arylene ether sulfone) random copolymers were synthesized with reactive amine endgroups and further functionalized with a tetra-epoxy resin, acryloyl chloride, phenylethynyl phthalic anhydride, and maleic anhydride. The reaction between amine terminated oligomers and a tetra-epoxy produced large, ductile membranes with gel fractions approaching 99%, the highest reported for crosslinked sulfonated polysulfone oligomers. This crosslinking reaction was studied by synthesizing two series of oligomers, one based on a bisphenol A monomer and the other based on a 4,4'-biphenol monomer. Both series were synthesized with 40, 50 and 60% degrees of sulfonation, so that hydrophilicity and composition could be studied with regard to water purification properties. All six oligomers

were produced with a gel fraction exceeding 90%, and the membranes were evaluated at the University of Texas-Austin. The crosslinked oligomers demonstrated relatively constant salt rejection across a range of hydrophilicity values, which proved that crosslinking restricted the large amount of swelling that non-crosslinked sulfonated polysulfones undergo. The crosslinked oligomers had the best water purification properties reported for sulfonated polysulfone, with similar water permeabilities and an order of magnitude higher selectivity (P_w/P_s = 1.69 ± 0.13 x 10^3) than analogous linear copolymers (P_w/P_s = 3.67 ± 0.53 x 10^2). An additional series of linear sulfonated copolymers were also synthesized based upon a hydroquinone bisphenol, which also had superior water purification properties (1.06 ± 0.06 L μm m^{-2} h^{-1} bar^{-1}, P_w/P_s = 2.44 ± 0.15 x 10^3) compared to previously synthesized linear copolymers.

Poly(arylene ether)s were also investigated for use as gas separation membranes. A poly(arylene ether ketone) and poly(arylene ether sulfone) were both synthesized with moieties capable of oxidation and/or photocrosslinking through benzylic hydrogen abstraction by an excited ketone. The polymers produced tough, ductile films. Gas transport properties of the linear polymers and crosslinked polymer were compared. The O_2 permeability of one exemplary non-crosslinked poly(arylene ether) was 2.8 Barrer, with an O_2/N_2 selectivity of 5.4. Following UV crosslinking, the O_2 permeability decreased to 1.8 Barrer, and the O_2/N_2 selectivity increased to 6.2.

In memory of Professor James E. McGrath, beloved educator, advisor and friend

ACKNOWLEDGEMENTS

The work embodied in a Ph.D. dissertation is not solely a mark of personal effort and I am tremendously grateful to the aid, support and love of numerable individuals.

First, I am extremely fortunate to have had Dr. James E. McGrath as a research advisor, a great man and scientist. He taught me an immeasurable amount about polymer chemistry and encouraged my growth from student to scientist. It was a privilege to work for such an iconic figure in polymer science, and I'll always remember his kindness and generosity for his students. The research performed in this dissertation can all be traced back towards his brilliant mind, and I hope he would be proud to see it brought to fruition.

I'm thankful for the rest of my doctoral committee; Dr. McGrath couldn't have identified better scholars to oversee my graduate school journey. Dr. Riffle and Dr. Mecham contributed tremendously towards much of my scientific writing, and selflessly led our research group throughout this last year. Dr. Turner's industrial class was very helpful in my job search and will continue to serve me well in my industrial career. I appreciate the scientific discussion and help from Dr. Davis and Dr. Esker, ranging from the polyelectrolyte effect to chemical potential gradients, their passion for others research was always evident. Though not a member of my committee, I'm extremely grateful to Dr. Benny D. Freeman of the University of Texas-Austin for his collaboration with our research group and contribution of transport results.

I'd like to thank Ms. Laurie Good for all of her help in keeping our research group running, organizing our travel to conferences, support and friendship. I'm also grateful to the rest of the McGrath research group, especially Jarrett Rowlett, Hailun Borjigin, Joshua Moore and Ali Nebipasagil for their scientific discussions, collaboration and friendship.

I'm fortunate to have a very loving family including parents Tim and Mary who instilled intellectual integrity and personal responsibility in me from a young age, my sister Kate who has always been excited and cheered for my progress, and grandparents Ron and Mary for their warmth, kindness and love. My mother-in-law Becky, father-in-law Bob and all my brothers and sisters-in-law also mean the world to me, and have made me a part of their family and consistently motivated my scientific career. Finally, thanks to my little brother Dezmen for inspiring me to be a better man and thanks to my furry footed companions Kai and Arya.

Most of all, I'd like to thank my wife Courtney. Graduate school has been a roller-coaster of highs and lows that I could not have weathered without her steadfast encouragement and unconditional love. We've both grown so much these last four years and can be proud of all we've accomplished as we complete this first chapter of our married life. I couldn't have asked for a better partner in life and can't wait to start our next journey in Boston. This is truly your accomplishment as well, and I'll never forget the personal and professional sacrifices you took to get me here. I love you Courtney, always and forever.

ATTRIBUTION

Chapter 3: Crosslinking Disulfonated Poly(arylene ether sulfone) Telechelic Oligomers Part 1: Synthesis, Characterization and Membrane Preparation

Chapter 3 was published in Industrial and Engineering Chemistry Research

Kwan-soo Lee, Ph.D. (Department of Macromolecular Science and Engineering) is currently a post-doctoral researcher at Los Alamos National Lab. Dr. Lee was a co-author on this paper and assisted with the preparation of the amine terminated telechelic oligomer.

Ali Nebipasagil, M.S. (Department of Macromolecular Science and Engineering) is currently a Ph.D. candidate at Virginia Tech. Mr. Nebipasagil was a co-author on this paper and performed the initial photochemical crosslinking of the acrylamide terminated oligomer.

Andrew Shaver, B.S. (Department of Macromolecular Science and Engineering) is currently a graduate student at Virginia Tech. Mr. Shaver was a co-author on this paper and assisted in the thermal analysis of the oligomers.

Joseph R. Cook, Ph.D. (Department of Chemical Engineering) is currently a post-doctoral researcher at the University of Texas at Austin. Dr. Cook was a co-author on this paper and contributed to the water purification property testing of the crosslinked films.

Eui-Soung Jang, B.S. (Department of Chemical Engineering) is currently a graduate student at the University of Texas at Austin. Mr. Jang was a co-author on this paper and contributed to the water purification property testing of the crosslinked films.

Benny D. Freeman, Ph.D. (Department of Chemical Engineering) is currently a professor at the University of Texas at Austin. Dr. Freeman was a co-author on this paper, co-principal investigator for one of the grants supporting this research and contributed revisions to the final document.

James E. McGrath, Ph.D. (Department of Macromolecular Science and Engineering) was a professor at Virginia Tech. Dr. McGrath was a co-author on this paper, co-principal investigator for the grant supporting this research and contributed revisions to the final document.

Chapter 4: Crosslinking Disulfonated Poly(arylene ether sulfone) Telechelic Oligomers Part 2: Effect of Backbone Structure, Degree of Sulfonation and Crosslinking on Transport Properties
To be submitted

Eui-Soung Jang, B.S. (Department of Chemical Engineering) is currently a graduate student at the University of Texas at Austin. Mr. Jang was a co-author on this paper and contributed to the water purification property testing of the crosslinked films.

Chang Hyun Lee, Ph.D. (Department of Macromolecular Science and Engineering) was a post-doctoral research at Virginia Tech. Dr. Lee was a co-author on this paper and performed the initial thin film fabrication of the amine terminated oligomer.

Joseph R. Cook, Ph.D. (Department of Chemical Engineering) is currently a post-doctoral researcher at the University of Texas at Austin. Dr. Cook was a co-author on this paper and contributed to the water purification property testing of the crosslinked films.

Ozma Lane, M.S. (Department of Macromolecular Science and Engineering) is a Ph.D. candidate at Virginia Tech. Ms. Lane was a co-author on this paper and performed the AFM microscopy on the crosslinked copolymers.

Benny D. Freeman, Ph.D. (Department of Chemical Engineering) is currently a professor at the University of Texas at Austin. Dr. Freeman was a co-author on this paper and contributed revisions to the final document.

Judy S. Riffle, Ph.D. (Department of Macromolecular Science and Engineering) is a professor at Virginia Tech. Dr. Riffle was a co-author on this paper and contributed revisions to the final document.

James E. McGrath, Ph.D. (Department of Macromolecular Science and Engineering) was a professor at Virginia Tech. Dr. McGrath was a co-author on this paper and principal investigator for the grant supporting this research.

Chapter 5: Synthesis and Characterization of Sulfonated Hydroquinone Based Poly(arylene ether sulfone) Random Copolymers for use as Water Purification Membranes

To be submitted

Eui-Soung Jang, B.S. (Department of Chemical Engineering) is currently a graduate student at the University of Texas at Austin. Mr. Jang was a co-author on this paper and contributed to the water purification property testing of the copolymer films.

Andrew Shaver, B.S. (Department of Macromolecular Science and Engineering) is currently a graduate student at Virginia Tech. Mr. Shaver was a co-author on this paper and assisted in the thermal analysis of the copolymers.

Priya Pisipati, B.S. (Department of Macromolecular Science and Engineering) is currently a Ph.D. candidate at Virginia Tech. Ms. Pisipati was a co-author on this paper, and contributed to the IR spectroscopy performed on the sulfonated copolymers.

Benny D. Freeman, Ph.D. (Department of Chemical Engineering) is currently a professor at the University of Texas at Austin. Dr. Freeman was a co-author on this paper and co-principal investigator for one of the grants supporting this research.

Judy S. Riffle, Ph.D. (Department of Macromolecular Science and Engineering) is a professor at Virginia Tech. Dr. Riffle was a co-author on this paper and contributed revisions to the final document.

James E. McGrath, Ph.D. (Department of Macromolecular Science and Engineering) was a professor at Virginia Tech. Dr. McGrath was a co-author on this paper and co-principal investigator for the grant supporting this research.

Chapter 6: Synthesis, Oxidation and Crosslinking of Tetramethyl Bisphenol F (TMBPF)-Based Polymers for Oxygen/Nitrogen Gas Separations

Article in press in Polymer

Andrew Shaver, B.S. (Department of Macromolecular Science and Engineering) is currently a graduate student at Virginia Tech. Mr. Shaver was a co-author on this paper and assisted in the thermal analysis of the polymers.

Qiang Liu, B.S. (Department of Chemical Engineering) is currently a Ph.D candidate at the University of Texas at Austin. Mr. Liu was a co-author on this paper and contributed to the gas transport testing of the polymer films.

Ali Nebipasagil, M.S. (Department of Macromolecular Science and Engineering) is currently a Ph.D. candidate at Virginia Tech. Mr. Nebipasagil was a co-author on this paper and performed the NMR analysis on one of the polymer samples.

Priya Pisipati, B.S. (Department of Macromolecular Science and Engineering) is currently a Ph.D. candidate at Virginia Tech. Ms. Pisipati was a co-author on this paper and contributed to the IR spectroscopy performed on the polymers.

Sue J. Mecham, Ph.D. (Department of Macromolecular Science and Engineering) is currently a research scientist at the University of North Carolina at Chapel Hill. Dr. Mecham was a co-author on this paper and contributed to the SEC analysis of the polymers.

Benny D. Freeman, Ph.D. (Department of Chemical Engineering) is currently a professor at the University of Texas at Austin. Dr. Freeman was a co-author on this paper, co-principal investigator for one of the grants supporting this research and assisted in revisions of the final document.

Judy S. Riffle, Ph.D. (Department of Macromolecular Science and Engineering) is a professor at Virginia Tech. Dr. Riffle was a co-author on this paper and contributed revisions to the final document.

James E. McGrath, Ph.D. (Department of Macromolecular Science and Engineering) was a professor at Virginia Tech. Dr. McGrath was a co-author on this paper and co-principal investigator for one of the grants supporting this research.

TABLE OF CONTENTS

LIST OF FIGURES

LIST OF TABLES

CHAPTER 1: LITERATURE REVIEW

1.1. Introduction

1.1.1. Reverse Osmosis

The lack of accessibility of fresh drinking water creates physical and economic water scarcity and is a global issue impacting billions of people.[1] The vast majority of water on Earth, near 97%, is seawater. Thus, the production of fresh potable drinking water from seawater is of tremendous global importance. Water purification is not a new challenge and historical methods such as flash distillation are still relevant today. However, multi-stage flash distillation (MSF) and multiple-effect distillation (MED) have a relatively high cost because of their thermal energy requirements. Rising fuel prices and environmental concerns are driving society and industry to seek alternative technologies that reduce our reliance on natural resources. One remarkable technology that already has widespread implementation is reverse osmosis (RO). Desalination of water by MSF and MED have energy demands in the range of 15-58 [(kW h m^{-3}] while RO is as low as 2-4 [(kW h m^{-3}].[2] The minimum energy required for RO will vary based upon system design and operating conditions. For example, higher saline concentrations of the feed or raising the percent recovery (the amount of seawater converted to desalinated water) will increase the minimum energy needed.[3] The theoretical minimum for typical conditions, a 35,000 parts per million salt feed and 50% percent recovery is 1.06 [(kW h m^{-3}]. Figure 1.1 shows that the change in power consumption for seawater RO (SWRO) plants has decreased drastically over the last 40 years and now approaches the theoretical minimum.[3]

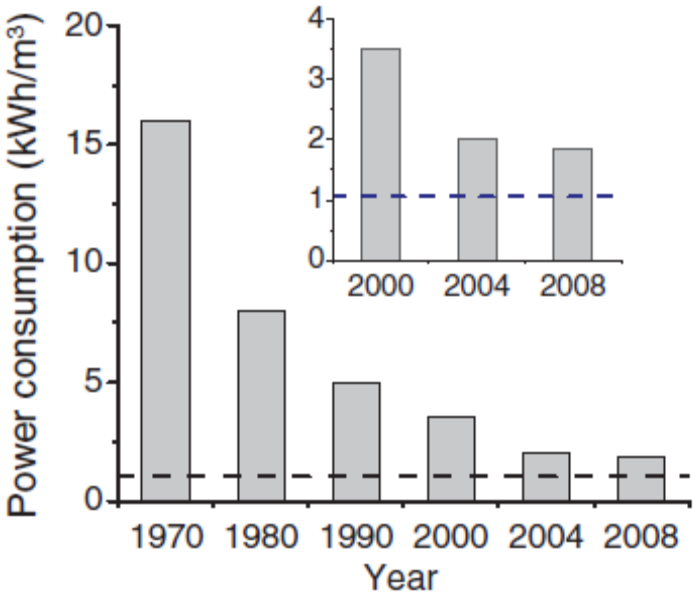

Figure 1.1 Power consumption for SWRO plants, dashed line represents theoretical minimum. From Science 2011, 333, 712. Elimelech M.; Phillip W. A. The future of sweater desalination: energy, technology, and the environment. Used with permission of American Association for the Advancement of Science, 2011[3]

In regular osmosis, diffusion of water across a semipermeable membrane occurs as a result of a concentration gradient. This spontaneous flow of water from a lower salt concentration solution to a higher salt concentration solution can be quantified by the osmotic pressure ($\prod$). The osmotic pressure is thermodynamically determined by the activity of the solvent (a_w), the partial molar volume of the solvent (V_w) and the temperature and gas constant.

Equation 1.1 $\prod = - \ln (a_w) \frac{RT}{V_w}$

For dilute solutions the osmotic pressure can be reduced to the van't Hoff equation and is proportional to the molar concentration of solute (C_s).

Equation 1.2 $\prod \approx C_s RT$

Figure 1.2[4] shows that RO achieves the exact opposite transport phenomenon with the aid of an applied pressure on the higher concentration side that exceeds the osmotic pressure.

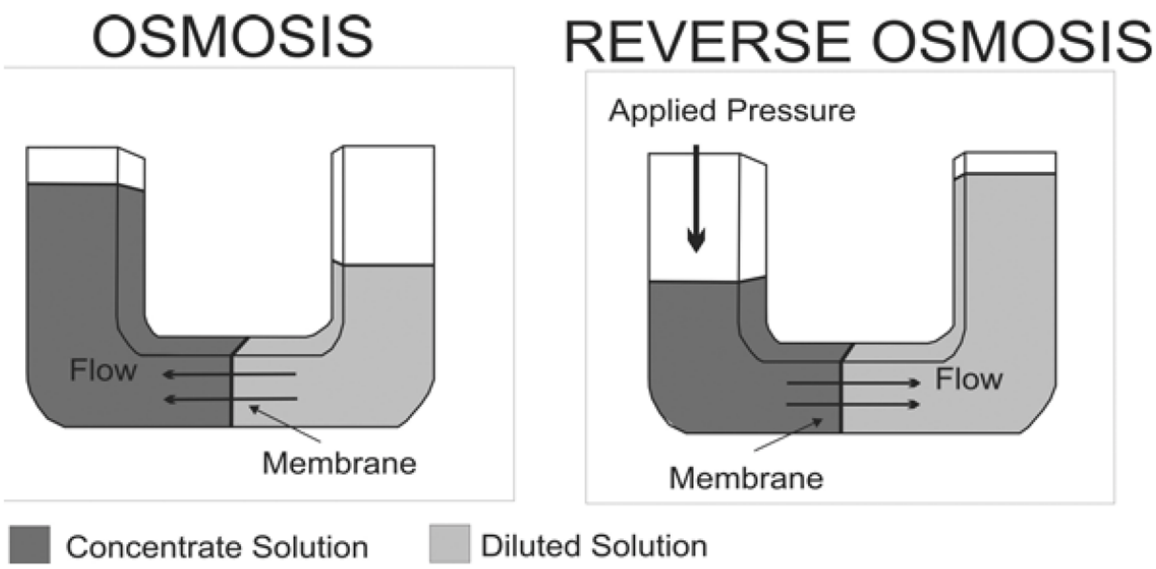

Figure 1.2 Overall principle of osmosis compared to reverse osmosis. From Desalination 2007, 216, 1. Fritzmann, C.; Löwenberg, J.; Wintgens, T.; Melin, T. State-of-the-art of reverse osmosis desalination. Used with permission of Elsevier, 2007[4]

RO can be applied to purify brackish, waste and sea water. RO can also be used to produce high purity rinse water for electronics manufacturing, food and beverage production and several other industrial processes.[5] Purification occurs by applying a high pressure (usually greater than 145 psi) to the feed side (e.g. salt water) which forces the water through the semipermeable membrane, but only if the membrane has significant rejection properties by allowing water to pass through while also blocking salt transfer.

1.1.1.1. History of RO

Normal osmosis was first coined by Abbé Nollet in 1748 to describe the movement of water through a pig bladder.[6] Much work was done in the 1800s in developing theories regarding osmotic pressure, ultimately leading to discoveries such as the van't Hoff equation and fundamental solution properties. Membranes during this period were still largely based upon animal products and could not achieve any consistent separation properties which could be used

on a commercial level. Membranes based upon nitrocellulose were developed in 1865 and because of their reproducibility were used in the pioneering solution work done by van't Hoff and others.[7] In 1907, Bechhold devised controlled evaporation techniques to regulate the pore size of the nitrocellulose membrane, and over the next several decades these techniques were refined and applied to other polymers.[6] The importance of membrane technology was demonstrated in war-torn Europe in the 1940s where water filters were desperately needed. During this time, research sponsored by the United States government began driving technical innovation which led to the first industrial membrane producers. Significant growth in the microfiltration area sparked interest in the ability to separate salt from water, especially after Yuster predicted this was possible in the early 1950s. Membranes during this time weren't selective enough to separate salt from water and suffered from other problems such as low water flux and poor mechanical properties. A monumental discovery occurred in the 1960s when Loeb and Sourirajan first produced an asymmetric cellulose membrane that had a thin selective layer cast on a permeable support layer, allowing an order of magnitude flux increase while still maintaining the mechanical strength and transport performance of the selective layer.[8] Developments in membrane modules quickly followed. General Atomic produced the first practical spiral-wound system and DuPont soon after commercialized a hollow fiber module.[7] Synthetic developments in membranes led to interfacially polymerized skins supported by a foam, called a thin film composite, eventually resulting in fully aromatic polyamide membranes capable of producing potable water in one pass. During the 1980s thin film composite membranes continued to improve and non-cellulosic materials became prominent in industry. Since the 1980s there have been numerous improvements in the areas of salt rejection and water flux on industrially used membranes synthesized from aromatic polyamides, cellulose acetate

and cellulose triacetate. By the year 2000, RO was used to treat over 1 billion gallons of water a day and by 2010 that number had increased to over 10 billion gallons per day.[4] The importance of fresh drinking water combined with rising population levels ensure that desalination will play an even more vital role in this century, and the improved economic efficiency of RO compared to multi-stage flash distillations will ensure the growth of RO for the foreseeable future.

1.1.1.2. Principles of RO

1.1.1.2.1. Solution-Diffusion

The exact mechanism by which a RO membrane discriminates between water and solutes was very controversial in the 1960s and early 1970s.[9] Because of ultrafiltration and other less selective membranes, there was an initial bias towards the more developed and perhaps more intuitive pore-flow model. In the pore-flow model a net movement occurs across a porous membrane from an area of higher pressure to an area of lower pressure. When the higher pressure stream meets the membrane some species may permeate through because they are smaller than the pores in the membrane while other species may be too large and thus excluded. Essentially, membranes that separate based on the pore-flow model operate by size-sieving mechanisms. Transport is described by the Hagen-Poiseuille equation and is dependent on mass flux, porosity, solution density and viscosity.[10] By the 1980s this model for RO was largely dismissed in favor of the solution-diffusion model.

The solution-diffusion model is distinct in that some solutes become soluble in the membrane and diffuse through the membrane to the permeate side, finally desorbing at the permeate side of the membrane. Figure 1.3 shows how several theoretical terms vary throughout the membrane in a pressure driven separation process such as RO.[9,11]

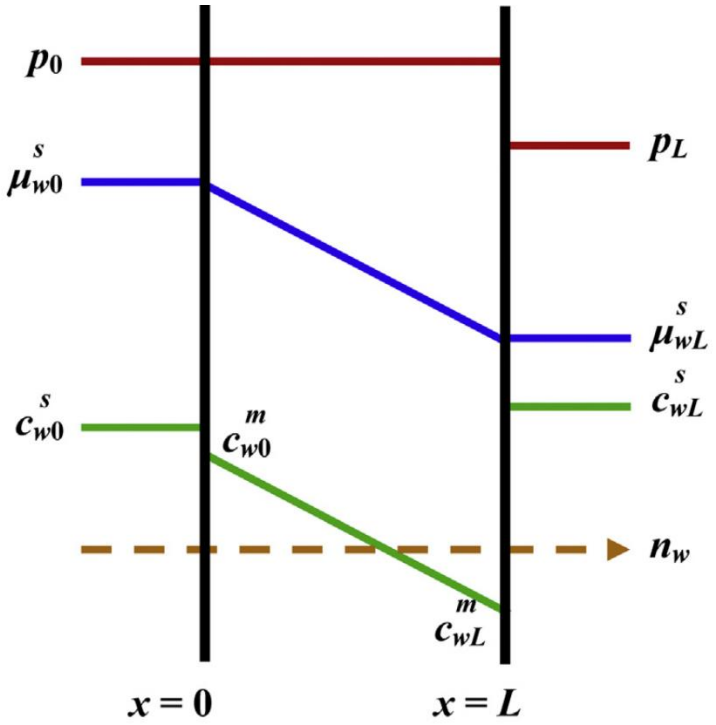

Figure 1.3 Water permeation through a membrane by solution-diffusion. From Prog. Polym. Sci. 2014, 39, 1. Geise, G. M.; Paul, D. R.; Freeman, B. D. Fundamental water and salt transport properties of polymeric materials. Used with permission of Elsevier, 2014[11]

The chemical potential will always dictate the direction of flow across the membrane from the higher side to the lower chemical potential side. In regular osmosis the high concentration of the solute in the saline solution results in a lower water chemical potential than the less concentrated solution, which drives water flow in an undesirable direction. However, chemical potential is affected by pressure, temperature and other forces in addition to concentration.[11] The application of a pressure higher than the osmotic pressure allows the flow across the membrane to be reversed and thus the chemical potential and concentration gradient instead decrease continuously from the saline/concentrated feed to the pure water solution.

Transport equations predicting water permeability and salt permeability were developed for both the pore-flow and solution-diffusion models, some of which are detailed in later sections. The adoption of the solution-diffusion model occurred as a result of experimental

evidence[12] fitting much more closely to theoretical values than those hypothesized by the pore-flow model. The agreement between experimental data over the last 30 years shows that the model is self-consistent.[9]

1.1.1.2.2. Membrane Flux

The two most essential parameters in any RO membrane are the membrane flux and the salt rejection. The following transport equations are applicable to uncharged polymer materials. Polymers with immobile ions attached throughout the matrix will have additional frictional forces and Donnan exclusion effects with diffusing ions that must be taken into account.[10] Flux refers to the transfer rate of water through a membrane of a certain thickness. The solution-diffusion model describes flux (J_A) as a Fickian diffusion process which has the general form

Equation 1.3 $J_A = -D_{AB}(\frac{d_{CA}}{d_x})$

Where D is the diffusion coefficient and $(\frac{d_{CA}}{d_x})$ describes the driving force, a gradient in chemical potential across a distance x. An RO specific equation can be derived from this when combined with expressions for chemical potential and treated with respect to membrane variables. In RO the driving force for water flux is the applied pressure difference across the membrane, leading to the membranes water concentration gradient.[10] Equation 4[9] describes the water flux (J_w) with respect to molar volume (v_w), water diffusion and sorption coefficients (D_w and K_w), water concentration at the feed/membrane interface (c_{w_0}), hydrostatic pressure across the membrane (Δp), osmotic pressure ($\Delta\pi$), and membrane thickness (l)

Equation 1.4 $J_w = \frac{D_w K_w v_w \, c_{w_0} \, (\Delta p - \Delta\pi)}{lRT}$

Water sorption is defined as the ratio of water concentration in the membrane to water concentration in the feed $\left(\frac{C_{W,F}^{m}}{C_{W,F}}\right)$. The water permeability is a product of the water sorption and the average water diffusion coefficients

Equation 1.5 $P_w = K_w D_w$

This expression is usually simplified by replacing $D_w K_w c_{w_0} v_w / lRT$ with the water permeability constant (A).

Equation 1.6 $J_w = A\,(\Delta p - \Delta \pi)$

Figure 1.4 and 1.5 shows the theoretical expectation of a linear increase in water flux with increasing applied pressure.[6]

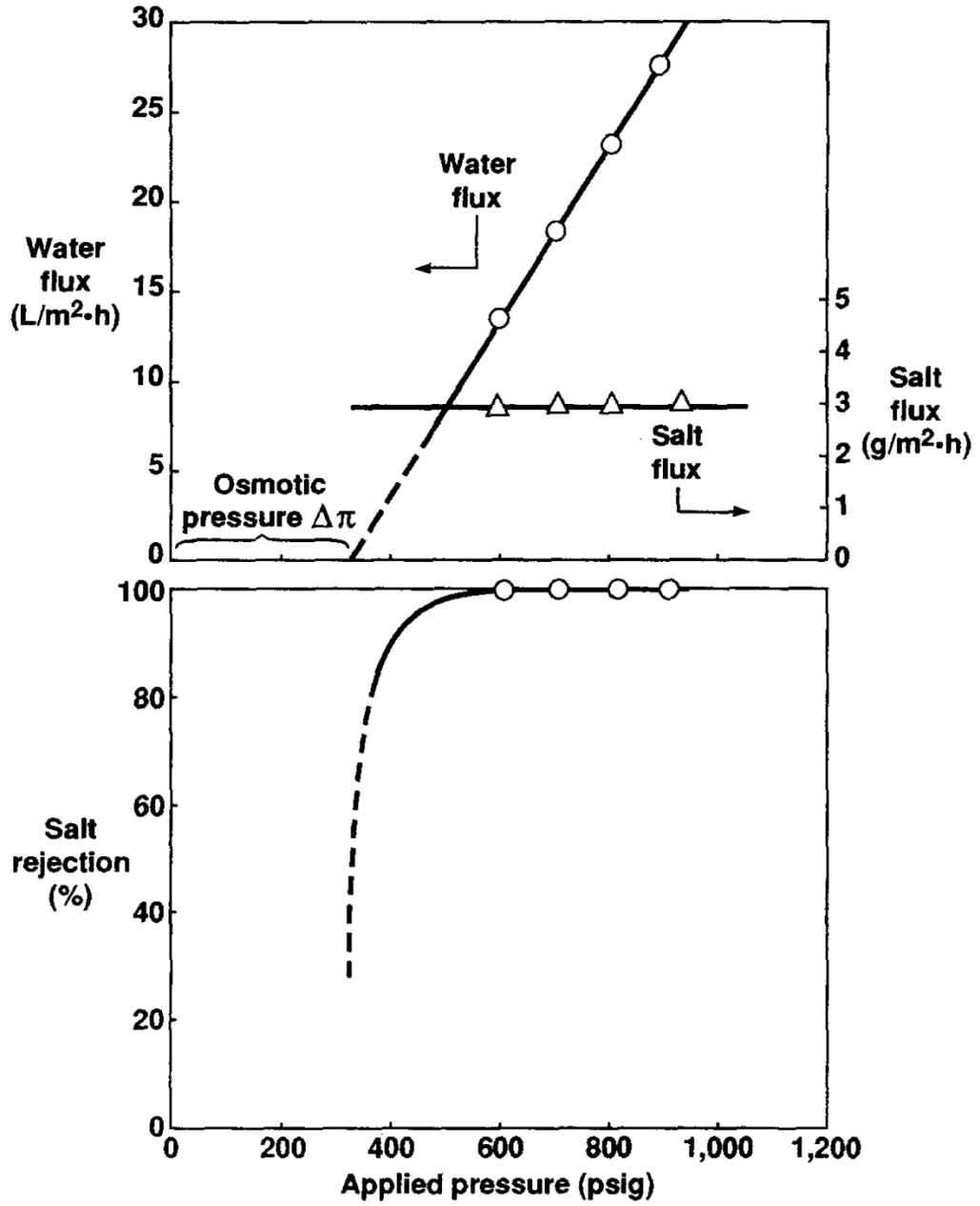

Figure 1.4-5 Flux and rejection data for FilmTec Corp., FT30 membrane. From J. of Membr. Sci. 1995, 107, 1. Wijmans, J. G.; Baker, R. W. The solution-diffusion model: a review. Used with permission of Elsevier, 1995[6]

Notably there is no water flux when the applied pressure is equal to the osmotic pressure. The flux will become negative if the osmotic pressure is greater than the applied pressure; in this situation water will flow in the direction of higher solute concentration. This figure also demonstrates that the salt flux is independent of pressure, which on a practical level means that

higher applied pressures can generally increase the economic efficiency of RO systems. Typical operating pressures for seawater purification range from 800-1,000 psi. At these pressures commercial polyamide membranes have water permeability constants around 0.61-5.46 L/m^2 h bar.[13,14]

1.1.1.2.3. Membrane Selectivity

Selectivity refers to the ability of a membrane to discriminate between different components in the feed so that only certain species permeate through the membrane. In the purification of seawater the most abundant species that needs to be separated from water are the salt ions Na^+ and Cl^-. The salt flux (J_s) can be calculated similarly to the water flux, with the exception that salt flux is concentration dependent, but not pressure and temperature dependent.[9]

Equation 1.7 $J_s = \frac{D_s K_s (c_{s0} - c_{sl})}{l}$

The salt permeability is also analogous in form to the water permeability

Equation 1.8 $P_s = K_s D_s$

These expressions are usually simplified to the following form

Equation 1.9 $J_s = B\,(c_{s0} - c_{sl})$

where B is simply called the salt permeability constant. The measurement of salt flux is important, however many researchers prefer to describe the separation efficiency by a rejection coefficient (R)

Equation 1.10 $\%\, R = \left(1 - \frac{c_{sl}}{c_{s0}}\right) * 100\%$

In these equations (c_{sl}) describes the salt concentration at the membrane/permeate interface and (c_{s0}) is the salt concentration at the membrane/feed interface. The target for total dissolved

solids left in the desalination permeate are usually under 500 mg L^{-1} and typical commercial rejection coefficients are greater than 99 percent.[5,10]

An important qualitative relationship between permeability and selectivity was recognized in the 1980s. Researchers noted that improving membrane permeability for the desired permeate resulted in a loss of selectivity, thereby increasing the permeability of undesirable species. An upper bound relationship for dense film water purification membranes was investigated by Geise et al. in order to further elucidate the transport relationships governing RO.[15] The data available in the literature is complicated because many industrial figures report membrane properties by water flux and salt rejection, properties that do not reflect the fundamental transport behavior and depend on membrane thickness and other often unreported parameters. The fundamental membrane properties of interest are water and salt solubility coefficients and water and salt diffusion coefficients. These intrinsic parameters can be used to calculate water and salt permeability and give rise to the following expression for selectivity

Equation 1.11 $$\alpha_{w/s} = \frac{P_W}{P_S} = \frac{K_W}{K_S} * \frac{D_W}{D_S}$$

These coefficients were found for several series of polymers including: polyamides, polyimides, sulfonated poly(arylene ether sulfones) and crosslinked poly(ethylene glycol). The water permeability and theoretical selectivity were calculated and are summarized in Figure 1.6.[15]

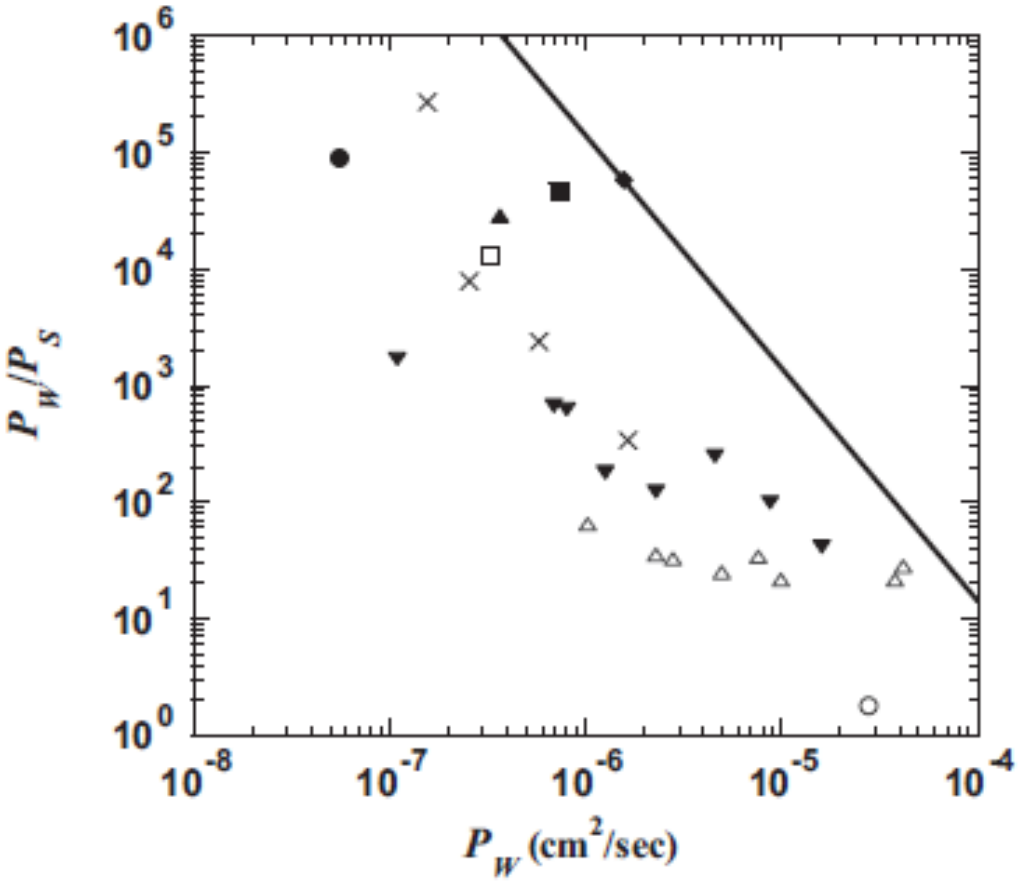

Figure 1.6 Relationship between selectivity and water permeability for RO. From J. of Membr. Sci. 2011, 369, 130. Geise, G. M.; Park, H. B.; Sagle, A. C.; Freeman, B. D.; McGrath, J. E. Water permeability and water/salt selectivity tradeoff in polymers for desalination. Used with permission of Elsevier, 2011[15]

This figure shows that an upper bound does exist for RO dense film membranes. The tradeoff between selectivity and permeability for gas separation is backed by theory and relates to molecular diameter and solubility into the polymer matrix.[16] This tradeoff relationship is less known for RO, although it is also likely based upon physical characteristics and other factors such as the ionic strength of polymer and salt.[15]

1.1.1.2.4. Fouling

Previous sections have dealt with elucidating the fundamental transport equations of the solution-diffusion mechanism. While fouling is not a quantitatively derived property of membranes, it has important real world consequences in both membrane and module design. Fouling refers to any undesirable formation on the membrane and may include microbial adhesion and growth, inorganic or colloidal deposits, and organic molecule adsorption.[5] The problem of fouling was noticed very quickly after the industrial implementation of RO membranes. Biofouling is an especially notorious problem that lowers membrane flux, reduces membrane selectivity/performance and lowers membrane lifetime. Figure 1.7 shows a SEM micrograph of a fouling layer (fl) deposited on a reverse osmosis membrane (rom) and support layer (tex).[17]

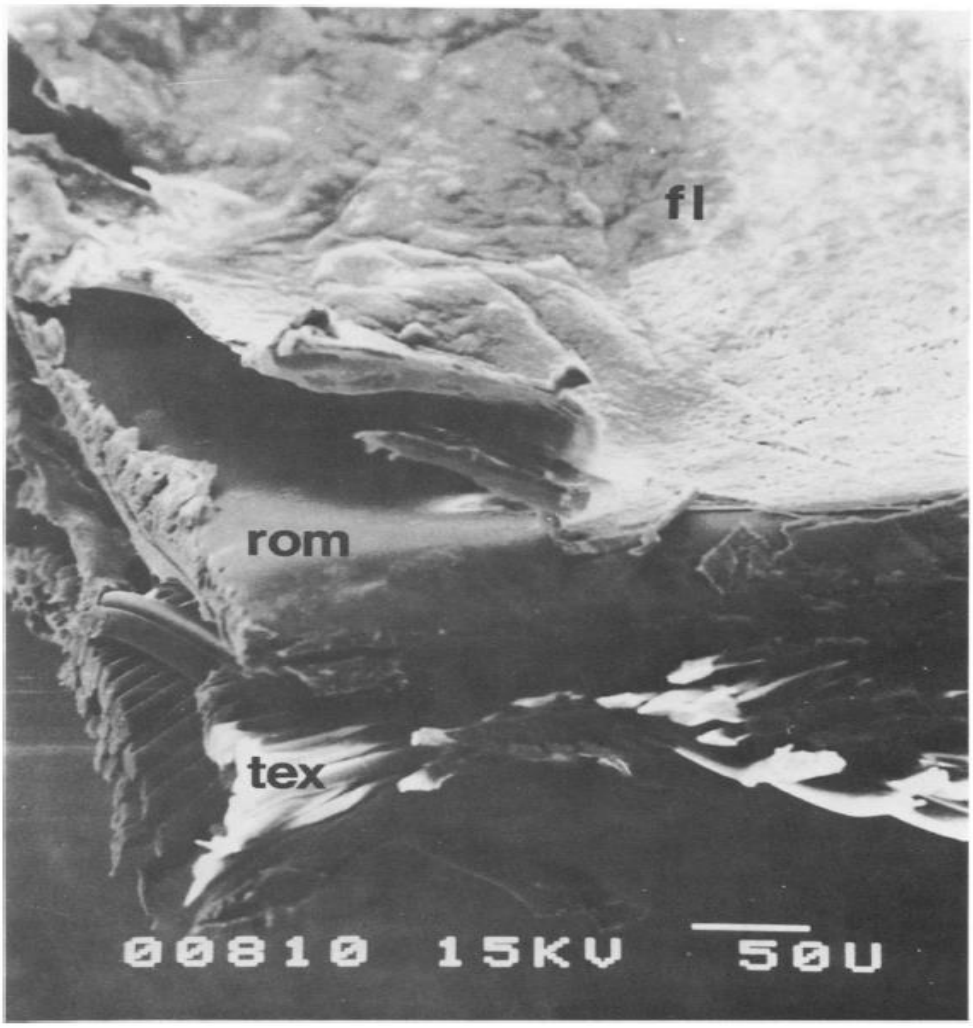

Figure 1.7 RO membrane fouling. From Applied and Enviromental Microbiology 1983, 45, 1066. Ridgway, H. F.; Kelly, A.; Justice, C.; Olson, B. H. Microbial Fouling of Reverse-Osmosis Membranes Used in Advanced Wastewater Treatment Technology: Chemical, Bacteriological, and Ultrastructural Analyses. Used with permission of American Society for Microbiology, 1983[17]

Early work by Kissinger et al. looked at the effect of bacteria deposition on a cellulose acetate membrane used for concentrating maple sap for maple syrup production.[18] The experimental conditions promoted slime build up on the membrane, which may not have damaged the material, but did reduce water flux. This initial work also showed that the application of an acidic chlorine solution or the use of ultraviolet lamps on the supply line greatly reduced bacterial populations on the membrane. Chlorine is so effective against biofouling that almost all seawater is treated with it, although this gives rise to additional problems because the

most commonly used RO membranes will degrade when exposed to chlorine.[19] Fouling is ubiquitous in RO processes, and different methods of treatment need to be developed for each system to minimize the negative influence on water flux and overall unit performance.

1.1.1.2.5. Concentration Polarization

An additional phenomenon that reduces water permeability and may lead to membrane fouling is concentration polarization. Different species permeate through the membrane at different rates and cause concentration gradients, notably a large buildup of salt at the membrane/feed solution interface. This "cake layer" will lower water flux by physical resistance to flow and increased osmotic counter-pressure.[20] Concentration polarization's effect on RO performance was noted in the literature as early as 1965 when Brian mathematically solved for optimal flux values at a given salt concentration to minimize concentration polarization.[21] Operating below a critical flux can reduce the thickness of the cake layer and increase the time between a cleaning of a membrane. Concentration polarization becomes more important at higher fluxes and higher percentages of salt rejection, necessitating continued consideration as membrane technology improves.

1.1.2. Pressure Retarded Osmosis

Reverse osmosis is an established technology that can reliably produce potable water from seawater with the aid of an applied pressure that exceeds the osmotic pressure. The paradigm of using energy to produce drinking water is reversed in a process known as pressure retarded osmosis (PRO), where energy is produced at the expense of fresh water. The principle behind PRO is that some of the free energy of mixing may be captured in aqueous salt

solutions.[10] Pressure retarded osmosis is very similar to forward osmosis (FO) in that the net flow of water goes from the less concentrated solute side to the more concentrated solute side of the membrane. Figure 1.8 depicts the fundamental differences between the three processes.[22]

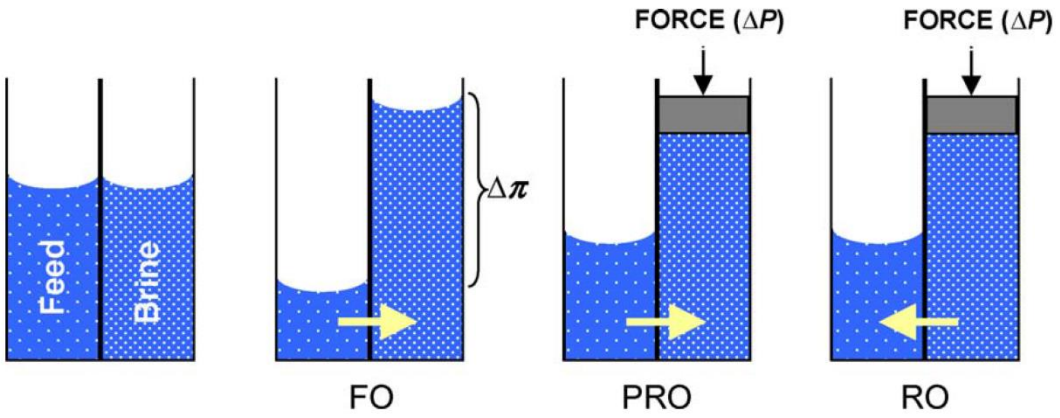

Figure 1.8 Flow of water and pressures present in FO, PRO and RO. From J. of Membr. Sci. 2006, 281, 70. Cath, T.; Childress, A.; Elimelech, M. Forward osmosis: Principles, applications, and recent developments. Used with permission of Elsevier, 2006[22]

In FO the applied pressure (ΔP) on the brine side is 0, so the minimum requirement for RO is $\Delta P > \Delta\pi$, and PRO operates at $\Delta\pi > \Delta P > 0$. In PRO, with regard to Figure 1.8, 80-90% of the water with a low salt concentration will flow across the semipermeable membrane and create a large pressure gradient, towards a theoretical maximum of 26 bars.[23] The pressure created from this system can then be used for mechanical work, such as spinning a turbine, in order to produce electricity. Pressure retarded osmosis is a practical source of renewable energy wherever fresh water meets salt water, such as a river flowing into an ocean. The estimated worldwide potential for PRO is 1655 TWh/year, making it an attractive addition to other renewable forms of energy such as wind and solar power.[23]

1.1.1.1. History of PRO

The first appearance of PRO in the literature occurred in 1954, where it was mentioned that the entropy of mixing water with different salt concentrations could result in free energy equivalent to that of a 680 ft waterfall.[24] This early work used alternating acidic and basic membranes to achieve a maximum external power of 15 mW, demonstrating proof of concept but lack of economic feasibility. Loeb first coined the term PRO in 1976, following recent improvements in membrane technology and RO's early industrial implementation.[25] Loeb demonstrated working small scale PRO systems using hollow-fiber seawater RO membranes, though the energy cost remained too high. In the early 1980s, researchers developed improved models that could predict PRO performance based upon RO and FO measurements.[26] These models showed that PRO could not achieve economic feasibility with current state-of-the-art membranes, largely because of internal and external concentration polarization drastically lowering membrane flux. Continued improvements in membrane technology and growing emphasis on renewable energy generated increased industrial interest in PRO in the late 1990s. Statkraft, a northern European power producer, investigated large scale implementation of this technology which led to the first prototype in 2009. Figure 1.9 shows a simplified schematic of the entire PRO process.[27]

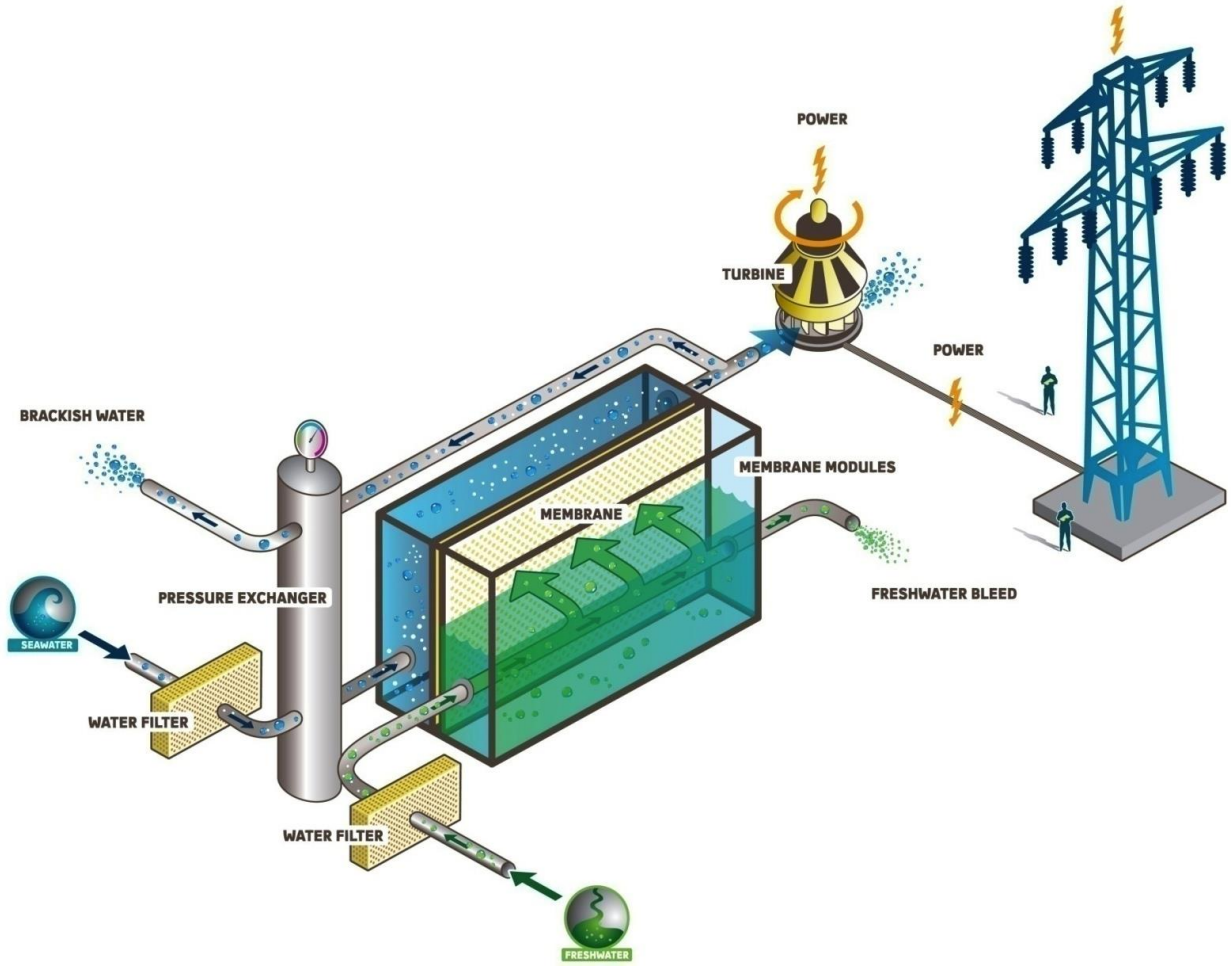

Figure 1.9 Graphic of PRO process. From Polymers 2013, 5, 303. Alsvik, I. L.; Hagg, M. B. Pressure Retarded Osmosis and Froward Osmosis Membranes: Materials and Methods. Used with permission of Polymers, 2013[27]

Statkraft initially used cellulose acetate membranes and later installed thin-film composite aromatic polyamide systems. Currently the focus of research continues on membrane development to produce a material with a power efficiency greater than 4 W/m^2, the minimum needed for large scale economic viability.[23]

1.1.1.2. Principles of PRO

PRO and RO both use similar semipermeable membranes and are both governed by the solution-diffusion mechanism. Most of the fundamental transport equations remain the same for

PRO. The expression for water flux looks almost identical, except that the applied pressure and osmotic pressure terms are switched by convention to give a positive flux value.[26]

Equation 1.12 $J_w = A\,(\Delta\pi - \Delta p)$

The PRO equation for salt rejection remains unchanged. Usually salt flux is not a serious effect, but selectivity remains crucial because any salt that contaminates the pure water feed will reduce the overall net osmotic pressure, which in turn reduces the power density of the membrane.[28]

The PRO process should maximize the power density to achieve the most energy efficiency. The power per membrane area (W) is equal to the product of water flux and applied pressure. Differentiation of this expression finds minimum power generation at $\Delta p = 0$ or $\Delta p = \Delta\pi$, and a maximum power density occurs when the applied pressure equals half of the osmotic pressure $\left(\Delta p = \frac{\Delta\pi}{2}\right)$.[25]

Equation 1.13 $W = J_w \Delta p = A(\Delta\pi - \Delta p)\Delta p$

Equation 1.14 $W_{max} = \frac{A\Delta\pi^2}{4}$

The problem of concentration polarization worsens in PRO, because of the pressures applied on both sides of the semipermeable membrane. A dilutive external concentration polarization arises on the saline side that lowers the effective salt concentration at the membrane interface, causing a reduced osmotic pressure. A concentrative internal concentration polarization acts in the porous support layer, as a buildup of salt at the support layer/dense layer interface reduces effective water flux. The concentrative internal concentration polarization is not a problem in RO, as the water flow will clear any salt from the membrane by convection. Figure 1.10 models both types of concentration polarization[28].

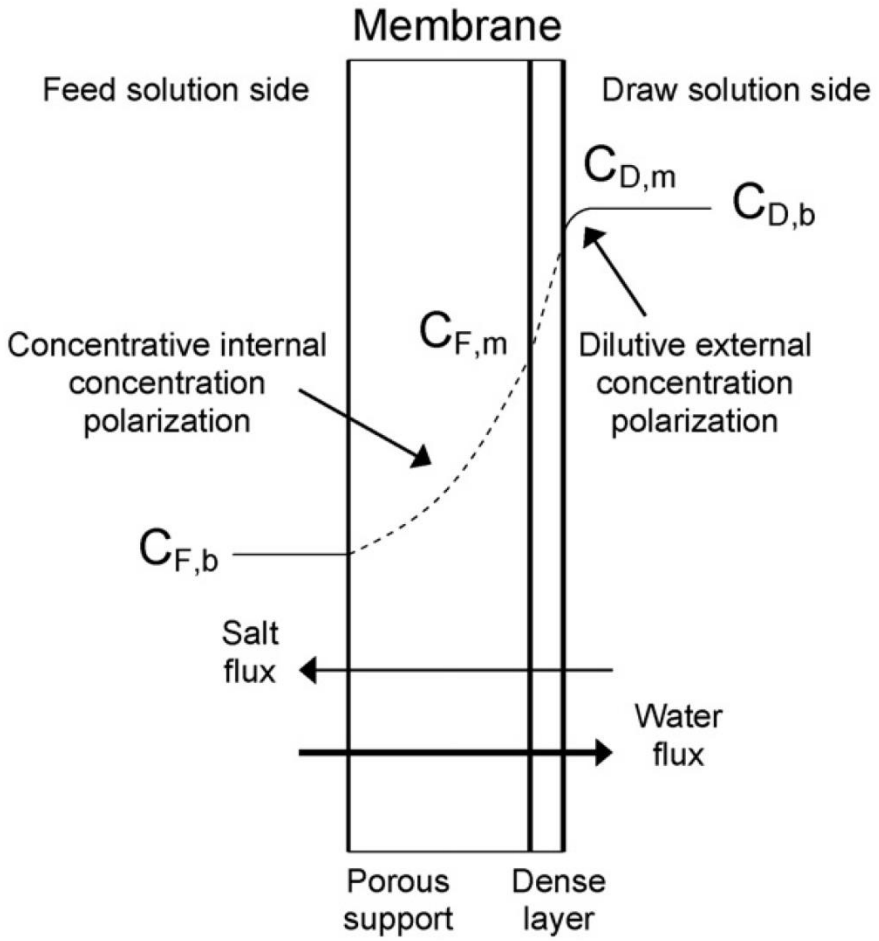

Figure 1.10 Concentration polarization in PRO membranes. From J. of Membr. Sci. 2009, 343, 42. Achilli, A.; Cath, T. Y.; Childress, A. E. Power generation with pressure retarded osmosis: An experimental and theoretical investigation. Used with permission of Elsevier, 2009[28]

Much literature exists that derives dilutive external concentration polarization[29,30] and concentrative internal concentration polarization.[26] The increased complexity of concentration polarization leads to a more rigorous definition of water flux[31] and power density[28] that has been appropriately modeled elsewhere. One consequence of this increased complexity is that the thickness (t), porosity ($D\varepsilon$) and tortuosity (τ) of the membrane and the support layer become much more important in their effect on water flux. Tortuosity qualitatively relates to the length and difficulty of the path the solute takes during transport in the membrane. Most literature

combine these terms as an expression for resistivity of salt diffusion within the porous support layer (K)[26,28], Statkraft denotes this value as the structure parameter (S).[27]

Equation 1.15 $K = S = \frac{\tau t}{D\varepsilon}$

Minimizing the structural parameter increases water flux and power density which makes it an important parameter to optimize for PRO membranes.

1.1.3. Gas Purification Membranes

Gas purification membranes are an industrially important technology that can separate mixed gas streams into relatively pure gases. The first gas purification membranes were used to purify hydrogen from purge gas streams in ammonia plants.[32] Today, gas purification is a versatile platform to separate nitrogen from air, carbon dioxide from methane, and hydrogen from numerable gases. Natural gas processing is a tremendous application, as the world uses about 100 trillion standard cubic feet of natural gas each year which must be treated before entering the pipeline.[33] Gas purification membranes compete against pressure swing absorption and cryogenic distillation, and their benefits include lack of a phase change, small membrane modules and absence of moving parts.[34,35]

1.1.3.1. History of Gas Purification Membranes

Gas separations have been of academic interest for a very long time, 1848 if Graham's law of effusion is considered its birth. One hundred years later, Doolittle described the dependence of viscosity and diffusion on free volume elements in the chemical environment.[36] These theories were used to describe molecular transport in liquids and glasses, which may be extended to polymeric materials.[37] During this time, the potential of polymeric membranes for

gas purification was widely known, but industrial development was frustrated by the inability to develop highly permeable membranes and consistent membrane modules.

The first large scale gas purification membrane was the hydrogen separating Prism membrane, pioneered by Permea in 1980.[32] The first gas separation membranes were inspired by work done in the RO area, which was adapted to produce the asymmetric hollow-fiber polysulfone Prism membrane. A depiction of a hollow fiber membrane module compared to the previously mentioned spiral wound module is shown in Figure 1.11.

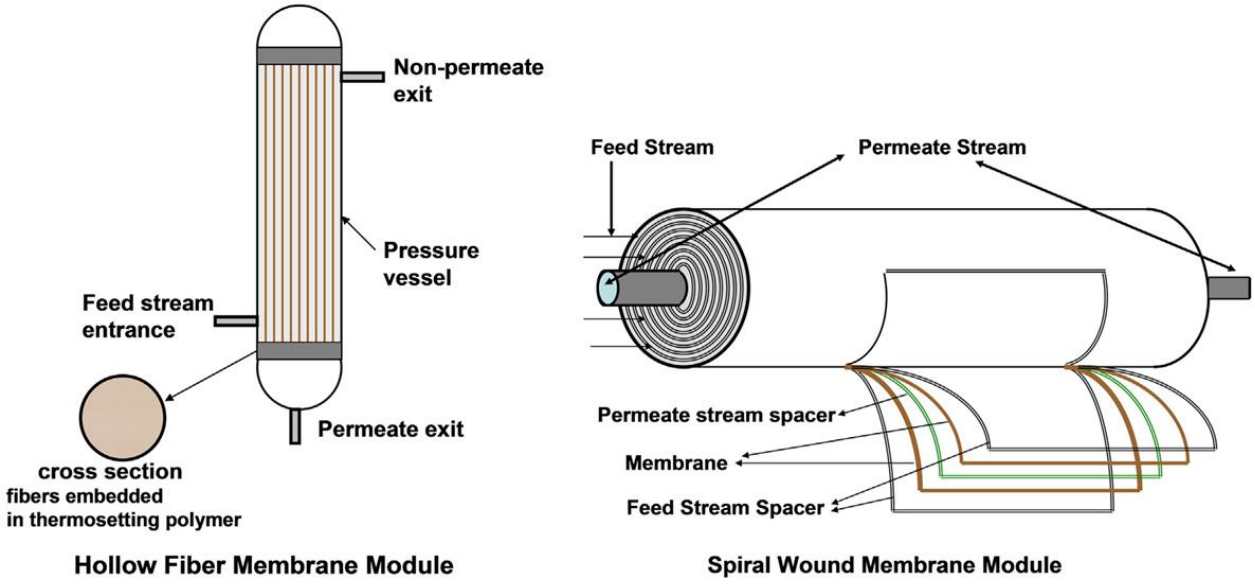

Figure 1.11 Membrane modules for separation applications. From Polymer 2013, 54, 4729. Sanders, D. F.; Smith, Z. P.; Guo, R.; Robeson, L. M.; McGrath, J. E.; Paul, D. R.; Freeman, B. D. Energy-efficient polymeric gas separation membranes for a sustainable future: A review. Used with permission of Elsevier, 2013[35]

Since the introduction of the Prism membrane, polyimides,[38-42] polyaramides, polycarbonates, cellulose acetate, polyphenylene oxide and silicone rubbers have all found use as gas separation materials for a wide variety of applications.[32] A timeline of gas separation membranes is shown in Figure 1.12.

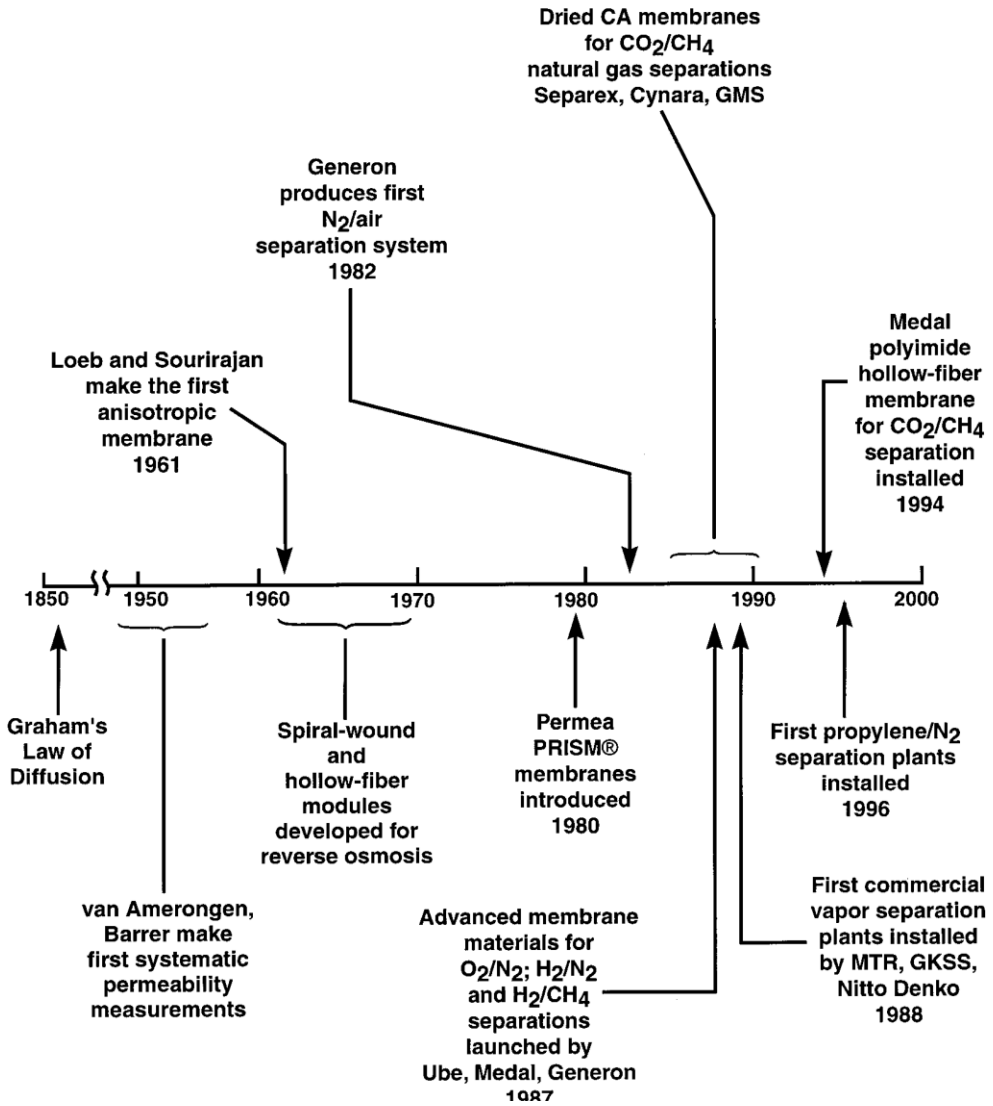

Figure 1.12 Timeline of industrial development for gas separation membranes. From Ind. Eng. Chem. Res. 2002, 41, 1393. Baker, R. W. Future Directions of Membrane Gas Separation Technology. Used with permission of American Chemical Society, 2002[32]

Polymer membranes for gas purification face several challenges. These include: an inability to withstand high temperatures and chemically harsh environments, plasticization in the presence of hydrocarbons or CO_2, and difficulty in achieving breakthrough performances in selectivity and permeability which is limited by the "upper-bound", described in the following section.[34]

1.1.3.2. Principles of Gas Purification Membranes

Similar to RO, the transport of gases in a dense polymer membrane occurs by the solution-diffusion model. Therefore, the three previously discussed sections on solution-diffusion, membrane flux and membrane selectivity all hold true for gas separation membranes. The permeability of gas across the membrane can be described by Equation 5, and the membrane efficiency, i.e. selectivity may be described by Equation 11. Of course, it is desirable in these separations to increase both permeability and selectivity, and the challenge of this is encapsulated by the upper-bound phenomenon.

An inherent trade-off relationship between selectivity and permeability has been identified; membranes with high gas permeability tend to have lower selectivity, and vice-versa. This observation was meticulously assembled into an upper-bound plot by Robeson by plotting much of the available permeability and selectivity values from the literature for various polymeric membranes.[16] The upper-bound plot has been revised in recent years, and is shown in Figure 1.13.[43] The upper-bound has a mathematical and theoretical basis derived by Freeman and others,[44] and describes the efficiency of polymeric membranes for gas separations as limited by the size of the diffusing gases and availability of free volume in the membrane.

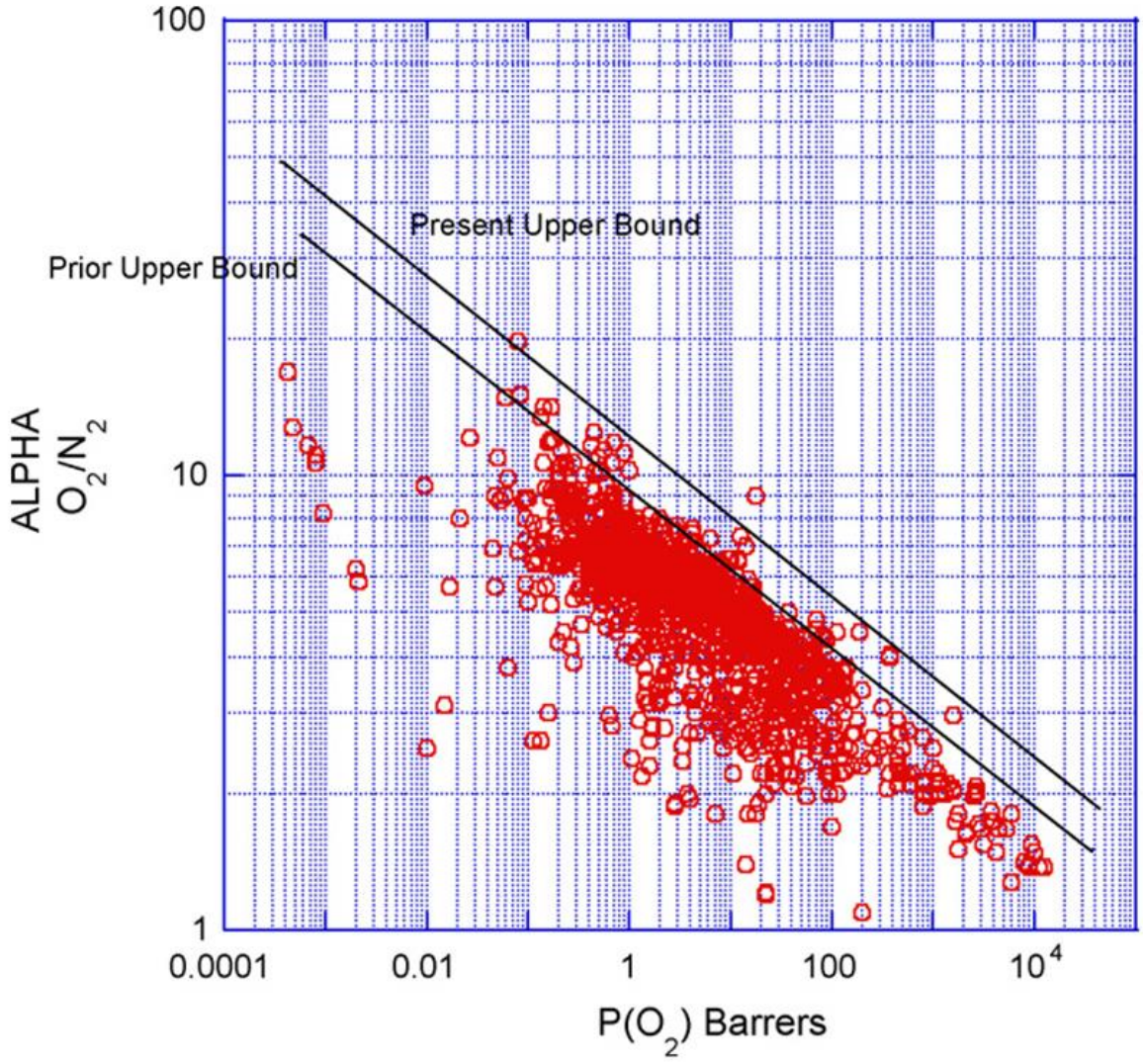

Figure 1.13 Upper-bound plot for oxygen/nitrogen separations. From J. of Membr. Sci. 2008, 320, 390. Robeson, L. M. The upper bound revisited. Used with permission of Elsevier, 2008[43]

1.2 Reverse Osmosis Membranes

The semipermeable membrane is the heart of the RO process, shown in Figure 1.14.

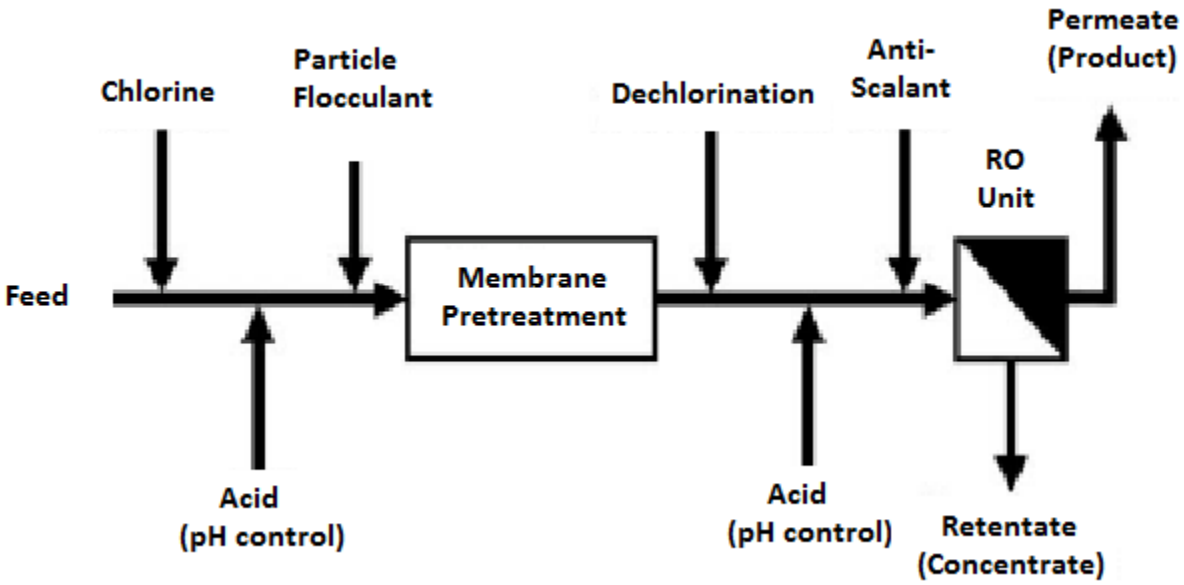

Figure 1.14 Simplified flow diagram of an RO Process. From J. Polym. Sci. 2010, Part B: Polym. Phys., 48, 1685. Geise, G. M.; Lee, H.-S.; Miller, D. J.; Freeman, B. D.; McGrath, J. E.; Paul, D. R. Water purification by membranes: the role of polymer science. Used with permission of John Wiley and Sons, 2010[10]

The importance of reverse osmosis has driven researchers to continuously investigate and synthesize new membrane materials for over 50 years. The field is largely dominated by cellulose acetate and aromatic polyamide based materials, though many classes of polymers have shown promise that they could compete against the industrially used membranes. The following is a short list of properties that potential membranes must demonstrate to be applicable in RO:[10,45,46]

- High salt rejection
- High water flux

- Ability to form thin films with high strength and about 100 nm in thickness, or fabrication into high surface-to-volume ratio constructs (e.g. hollow fibers). This is necessitated by the high water flux requirement.
- Ability to be incorporated into one of the four standard membrane modules: tubular, plate and frame, hollow fibers or spiral wound
- Wide operating range for ion content, pressure and temperature
- Resistance to chemical attack and fouling
- Resistance to compaction under high pressure
- Long service life
- Low cost

1.2.1. Cellulose Acetate membranes

Cellulosic derivatives have a storied history in reverse osmosis, largely because they were the first asymmetric materials produced by Loeb and Sourirajan that demonstrated the viability of reverse osmosis technology. This was achieved by hand casting a solution of polymer in water and acetone with aqueous magnesium perchlorate. The solution was dried for a short period of time on glass before being immersed in cold water to produce the asymmetric membrane.[8] A final wet annealing step was also used to ensure that pores were eliminated in the membrane skin and this resulted in a dense membrane.

Cellulose acetate is made from reacting acetic anhydride and acetic acid with cellulose,[8] the naturally occurring polysaccharide that is the most common organic compound found on Earth. The number of hydroxyl groups that are replaced by acetate is quantified by a degree of substitution, often referred to as D.S. Cellulose acetate materials generally have a D.S. in the

range of 2.4-2.5, while materials with a D.S. above 2.75 (to the maximum value of 3) are referred to as cellulose triacetate. Figure 1.15 shows cellulose triacetate with a D.S. of 3. The degree of acetylation has a profound influence on the membrane transport properties, and high levels of acetylation increase salt rejection and lower water flux.[47]

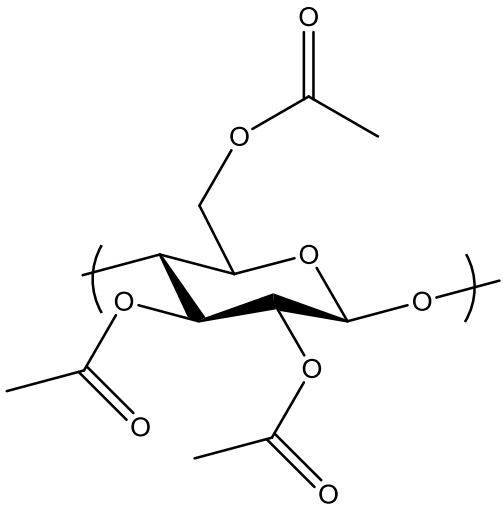

Figure 1.15 Cellulose triacetate

The choice of cellulose acetate by Loeb and Sourirajan was well founded, Reid and Breton showed it was the most permiselective material available at the time.[8,47] The early research performed by Reid et al. showed that a salt rejection of up to 97.4% was obtainable, though permeability was still low, despite film thicknesses less than 10 microns. These early films had a D.S. of 2.6. The apparent semipermiability of cellulose acetate was suggested to be the amorphous portions of the membrane binding to water through hydrogen bonding.[48] The transport of salt and other molecules that cannot participate in hydrogen bonding travel by a hole-type diffusion, but as water binds to the membrane these holes shrink and less solute can pass through the material.[47] As the applied pressure increases, more water binds to the membrane and hole-type diffusion decreases. Water retains a high permeability as an equilibrium develops, causing hydrogen bonded water to make discrete jumps among hydrogen

bonded sites down the length of the membrane and eventually permeating on the other side.[48] The equilibrium water sorption of cellulosic materials generally falls in the range of 15-30 weight %.[10] The following empirical results helped develop and prove this theory: salt rejection was poor at low pressures and increased quickly in the 150 to 250 psi range before approaching an asymptote at 100%;[48] electrical measurements showed that semi-permeability was correlated with ions not able to hydrogen bond, but no such relationship was found when the ions could participate in hydrogen bonding[48] and finally that larger multivalent salts had enhanced rejection compared to NaCl.[49]

Cellulosic membranes have a lower acceptable pH range, lower hydrolytic stability, less versatility and a shorter service life than polyamide materials, but their high flux and salt rejection, relatively high resistance to chlorine and low cost have enabled their continued importance.[10,45] The membranes are used at a pH of 4.7, and values higher or lower than this tend to accelerate hydrolytic and membrane degradation.[50] Typical membranes are made from a cellulose acetate/cellulose triacetate blend; cellulose triacetate has better chemical and hydrolytic stability, but if not blended compacts easily leading to flux decline.[5] Although cellulosic materials do not have as high rejection as the aromatic polyamide thin film composites, their enhanced chlorine tolerance makes them ideal for applications such as waste water treatment.

1.2.2. Polyamide Membranes

Polyamides are the preferred chemical structure for state-of-the-art membranes in reverse osmosis water purification. The initial research into polyamides investigated the commercially important linear aliphatic systems such as Nylon 6,6, but these were rejected because of poor mechanical stability and relatively low separation potential. Industrial scientists and engineers

worked throughout the 1970s developing these materials and found that the aromatic systems could achieve much higher separations, but in their infancy they still lagged behind the high flux high rejection properties of cellulosic materials.[8] Aromatic polyamides finally achieved commercial importance after patents and literature described the formation of a thin-film composite system in the late 1970s.[46] The state-of-the-art FT-30 polyamide membrane was reported in 1980 with initial investigations describing optimal conditions.[51] Over the last 30 years, the processing, synthesis and transport properties of these materials have been widely investigated.

Several choices of monomers are available to produce the aromatic polyamides and polyureas used for reverse osmosis, but usually they are phenylene diamines reacted with various acyl chlorides or isocyanates.[52,53] Different isomers of phenylenediamines may be combined to afford high chain stiffness while giving a kinked microstructure that helps avoid crystallization. The interfacial polymerization proceeds through two stages. The first fast stage forms the initial polyamide separation skin layer, then diamine diffusion through this layer into the phase rich with chloride monomer results in further reaction and increased film thickness.[54] The acid chlorides are insoluble in the aqueous solution, ensuring that polymerization occurs at the interface and not in solution.[55] A key feature of the state-of-the art materials is a high degree of crosslinking. The films with the highest flux and salt rejection are ones where crosslinking occurs simultaneously with polymer film formation at the interface.[56] Additional post-polymerization curing and/or heat treatment may sometimes be utilized to further increase the salt rejection while maintaining high water fluxes.[54] Figure 1.16 shows a reaction scheme between m-phenylene diamine and trimesoyl chloride to produce the crosslinked polyamide selective layer.[56]

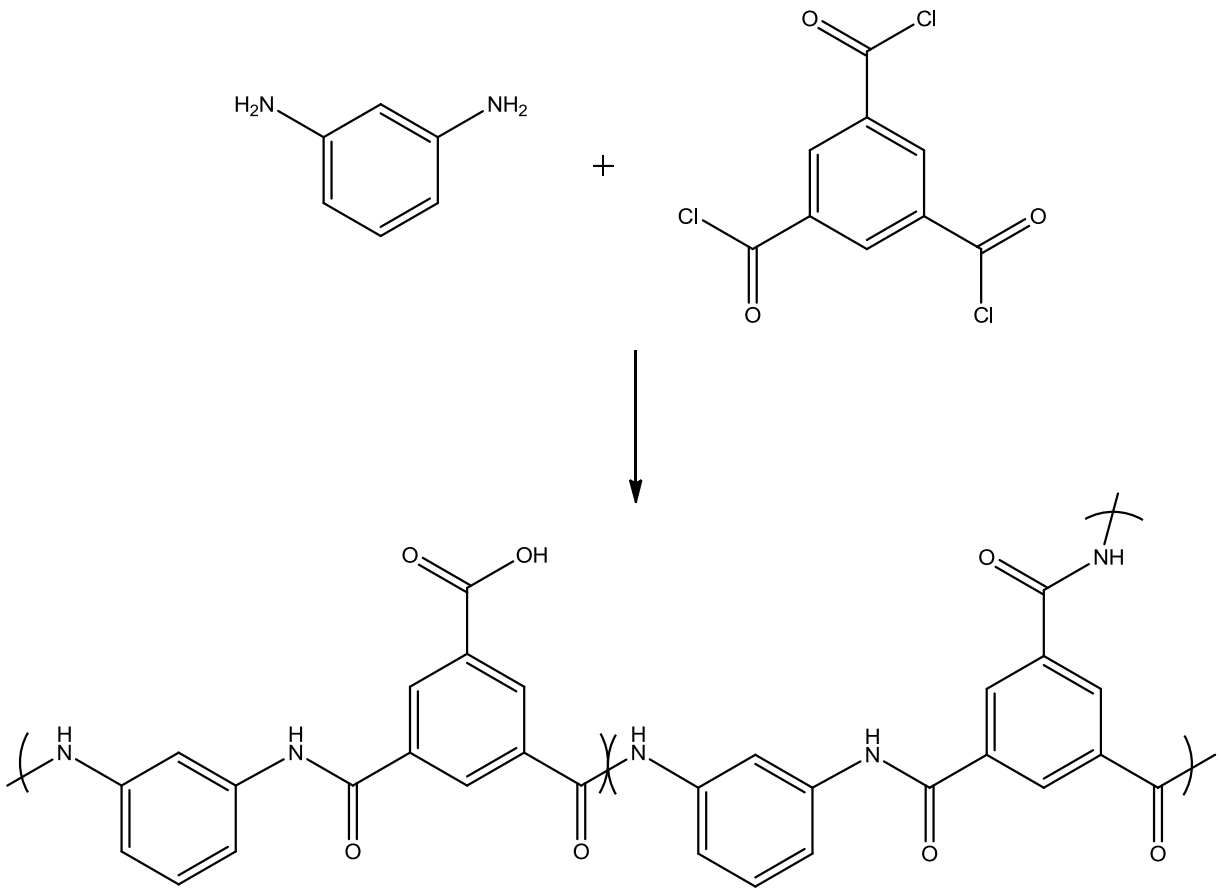

Figure 1.16 FilmTec FT-30 schematic with linear and crosslinked repeat units shown

Variations of the above membrane have been developed for tapwater, brackish, and seawater purification. Aromatic polyamides are advantageous relative to cellulosic materials in several areas beyond their enhanced salt rejection. They are relatively resistant to acid or base induced hydrolysis and can be used over a wider pH range.[51] The high extent of crosslinking reduces swelling and helps resist compaction under high pressures, a problem that the asymmetric cellulose membranes consistently suffer.

The importance of the thin-film composite on reverse osmosis technology is tremendous and warrants closer examination. The culmination of this research and initial use of this technology occurred in the early 1980s. However investigation of applying selective membranes in-situ on polysulfone supports started in 1967.[51] Early researchers dissolved a commercially

available polysulfone in dimethylformamide at 15% solids, cast the solution on a glass plate and subsequently precipitated it in a water bath by one quick immersion. A microporous sheet around 40 microns thick[56] lifted off of the glass plate spontaneously and was washed with deionized water before further use.[46] The microporous membrane was then soaked in an aqueous solution with a very low concentration of diamine. Excess aqueous solution was removed by a rubber roller before exposing it to an organic solution of isophthaloyl chloride in hexanes. This interfacial polymerization produces a selective "skin" membrane that generally ranges from 0.1-3 microns thick.[52] In commercial applications the polysulfone support layer is additionally supported by a woven or nonwoven polyester web with a thickness on the order of 100 microns.[46,56]

One advantage of the thin-film composite is that very thin layers of the selective membrane are possible, and because of the polysulfone support, mechanical failure is less likely to occur even if the highly crosslinked polymer is extremely brittle and weak.[51] The ability to produce an extremely thin selective layer results in a much enhanced water flux, predicted by Equation 4. Both linear and crosslinked polymers may be used as the skin layer, whereas only linear soluble materials may be used in asymmetric systems.[56] One advantage of the thin-film composite approach is that producing the selective skin and porous support layer separately allows additional optimization. Polyamide membranes may also be modified post polymerization to further improve their transport properties. One example is to apply poly(ethylene oxide) to the polyamide and crosslink it photochemically to produce a smoother membrane that enhances resistance to biofouling.[57]

The enhanced structural stability from the thin-film composite alleviated the problem of mechanical stability, but the lack of chemical and biological resistance remained an issue. The

largest problem is the lack of resistance to the chlorine biocide in the feed solution.[55] Membrane performance deteriorates in long term tests with even low levels of chlorine concentration.[53,58] Treatment of drinking water with parts-per-million levels of chlorine greatly improves the water quality by killing pathogens and other bacteria carried in water.[55] The lack of chlorine resistance by polyamides leads to higher costs. The feed must be chlorinated to reduce biofouling, de-chlorinated to protect the membrane during permeation, and finally chlorinated again after permeation to protect against microbial contaminants. Studies showed that a low pH accelerates membrane degradation under these conditions, and that the membrane may degrade by two mechanisms, one that leads to an increased molecular weight of the polymer film and one that lowers the molecular weight. An increase in molecular weight could occur by chloramination of the amide bond and subsequent attack by an amine terminated chain, producing a crosslinked site.[58] A decrease in molecular weight arises from chain scission after the chloramination reaction.[56] Figure 1.17 shows the incorporation of chlorine into the polymer system, the reactive species are aqueous chlorine derivatives such as the hypochlorite ion.[53]

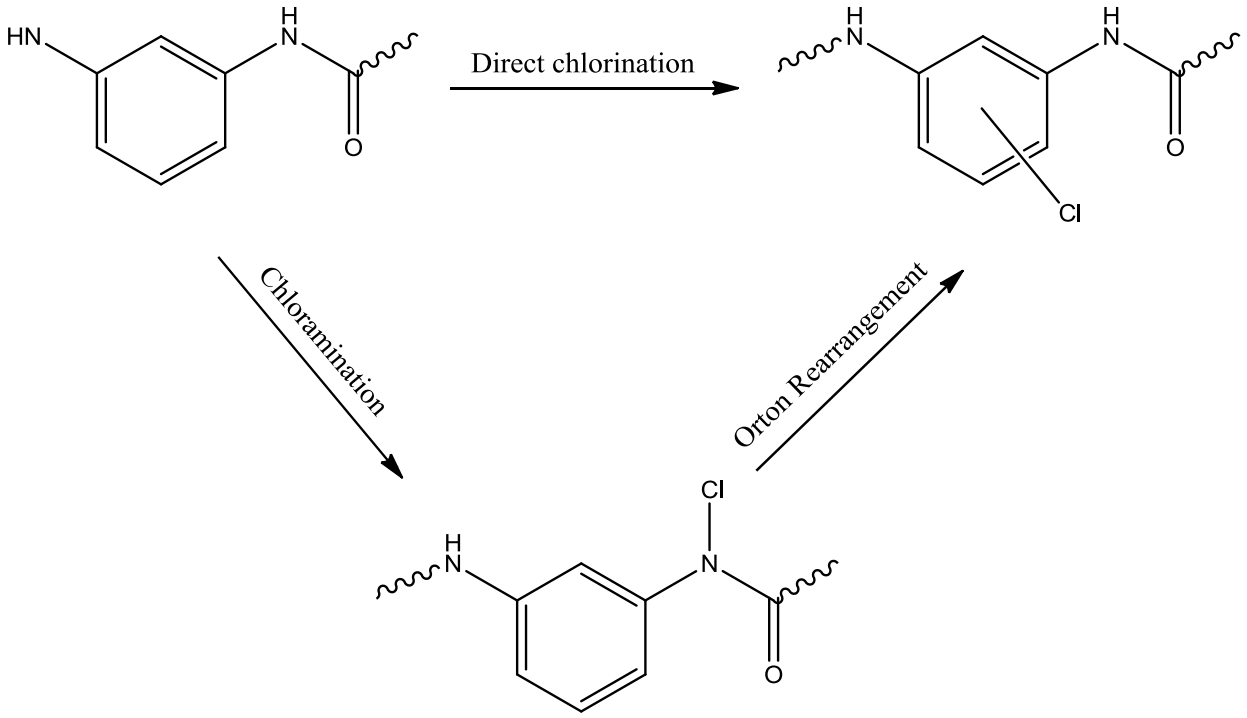

Figure 1.17 Pathways to chlorination in polyamides[53]

The nitrogen in the amide bond is readily attacked by chlorine because of the neighboring electron withdrawing carbonyl group. It has been proposed that this reaction proceeds through an amide oxygen intermediate before rearranging to the chloramide. The chlorine can further become incorporated into the adjacent aromatic ring by the Orton rearrangement.[59] Recent studies have suggested that the extent of Orton rearrangement is largely due to amine end groups instead of the amide bond on the backbone of the polymer.[55] It has also been suggested that direct ring chlorination may occur through electrophilic aromatic substitution. There is a significant effect of pH on the rate of chlorination, with model studies demonstrating no chloramide formation above a pH of 10.[55] The subsequent mechanism of amide bond cleavage is unknown, although hydrolysis and oxidative cleavage have been proposed.[53] Degradation by chlorine can be lessened by alkyl substitution at the amide nitrogen[60] and the use of protecting groups on the adjacent aromatic ring,[61] though the transport properties of the material are always

affected as a consequence. Different isomers of the phenylene diamine also respond differently to chlorination, the 1,3 isomer being the most vulnerable and the 1,2 isomer being the least vulnerable to attack.[55]

1.2.3. Sulfonated PPO Membranes

It has been demonstrated that several classes of polymers can be fabricated into thin-film composites, including sulfonated polyphenylene oxide (PPO), shown in Figure 1.18.

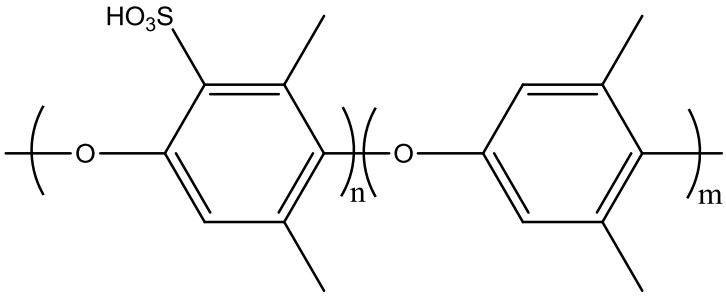

Figure 1.18 Repeat unit of sulfonated PPO with "n" degree of sulfonation

Sulfonated PPO is produced by the facile chlorosulfonation of PPO, and the transport properties of these materials are strongly correlated with the ion exchange capacity (IEC), a measure of the degree of sulfonation of the polymer. Higher amounts of sulfonation lead to a more hydrophilic material with increased water uptake and permeability, at the expense of lower levels of salt rejection.[62] Highly sulfonated materials also swell tremendously in water, leading to large increases in flux and additional loss of salt rejection.[63] Reverse osmosis studies demonstrated that sulfonated PPO has very high chemical stability and excellent resistance to acidic and basic environments, but cannot achieve the high flux and high rejection transport properties of the traditional cellulosic or polyamide systems.[8,64-66]

1.2.4. Sulfonated Poly(arylene ether sulfones)s Membranes

The development of poly(arylene ether sulfone)s, commonly called polysulfones, for reverse osmosis began in the 1970s in both academic labs and industry. At this time the cellulosic asymmetric materials suffered stability issues because of chemical and biological attack. Polysulfones famously demonstrate high chemical inertness and the rigid backbone of these polymers make it mechanically attractive as well. The commercially available hydrophobic polysulfones can also be sulfonated to increase hydrophilicity. Typically 20-50% of the repeat units are sulfonated. Below this range polysulfones have prohibitively low water uptake and above this range they are highly swollen and eventually water soluble.[67] Figure 1.19 shows a repeat unit of a sulfonated UDEL polysulfone, with a random composition of sulfonated moieties.

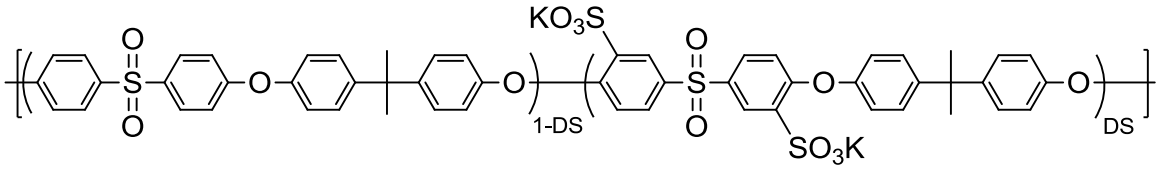

Figure 1.19 Random copolymer of sulfonated UDEL polysulfone

The first sulfonated polysulfones tested for reverse osmosis showed transport properties in line with cellulose acetate.[68] Later these were fabricated into composite hollow fiber systems with 98% salt rejection and reasonable water flux, useful for brackish water purification but not selective enough for seawater desalination.[56] Early studies showed a very strong Donnan exclusion effect that was enhanced by high operating pressures and water flux. This Donnan effect actively pulls cations into the membrane and repels anions into the solution.[10] The membranes additionally demonstrated high resistance to water fouling and thus permitted high pressure operations.

Sulfonated polysulfones were eventually made by direct sulfonation methods that were not only more reproducible, but also increased the regularity of sulfonated units in the microstructure.[67] Recently McGrath and Freeman et al. began studying the fundamental transport characteristics of these polymers and synthesized several novel structures. They found that varying the sulfonation level (often expressed as the ion-exchange capacity with the units of milliequivalents per gram), altering the hydrophobic structure and changing the sulfonate group to sulfonic acid all had a pronounced effect on the membrane's transport properties.[15,54,69-71] Generally these membranes are used in the salt form, as an acidified material would slowly be converted to the salt form because of the high NaCl concentration in RO applications. The thermal processing history of the films also affected the transport properties obtained.

The sulfonate groups strongly repel anions by the aforementioned Donnan exclusion effect, however they also lead to high amounts of membrane swelling that can lower salt rejection and worsen mechanical properties.[14] The salt permeability will also depend upon the salt concentration in the feed solution, because high concentrations will lower the Debye length and screen anionic repulsions between polymer and salt.[10,68] Water permeability depends upon the self-diffusion coefficient of water through the material, which is proportional to the volume fraction of water in the polymer and thus related to the free volume of the system.[70] Positron annihilation lifetime spectroscopy has been used to probe the free volume of these polymers.[71]

Morphological studies using atomic force microscopy revealed that the sulfonated polysulfones contain two distinct regions. The ionic regions of the copolymer aggregated together to form hydrophilic areas amongst a matrix of hydrophobic segments.[70] As sulfonation levels increased, the hydrophilic regions expanded, until a critically high level of sulfonation changed the ionic regions so that they became continuous and formed large channels through the

material. Literature attempting to probe Fickian diffusion with these charged membranes generally assumes that the charged units on the membrane are homogeneously distributed throughout the polymer matrix to simplify the mathematics.[10]

Paul et al. showed that the loss of selectivity could be greatly mitigated by controlling membrane swelling through chemical crosslinking.[14] Table 1.1 shows a crosslinked highly sulfonated material with greatly enhanced rejection compared to the linear control. The state-of-the-art SW30HR-380 polyamide membrane is also shown for comparison.[14]

Table 1.1 Effect of crosslinking on membrane selectivity. From Polymer 2008, 49, 2243. Paul, M.; Park, H. B.; Freeman, B. D.; Roy, A.; McGrath, J. E.; Riffle, J. S. Synthesis and crosslinking of partially disulfonated poly(arylene ether sulfone) random copolymers as candidates for chlorine resistant reverse osmosis membranes. Used with permission of Elsevier, 2008[14]

System	Curing time (min)	Water permeability (L μm/m^2 h bar)	NaCl rejection[a] (%)	NaCl permeability[b] ($\times 10^{-8}$, cm^2 s^{-1})
BPS-5k-2E-15M	15	3.2	87.8	6.5
BPS-5k-2E-45M	45	1.5	96.1	3.8
BPS-5k-2E-90M	90	1.4	97.2	1.1
Uncrosslinked BPS50	0	3.5	73.4	—
SW30HR-380[c]	—	0.61[d]	99.7	—

Crosslinking also reduces the free volume by lowering membrane swelling and restricting the polymer matrix, thus the effective permeability of water through the membrane is lowered[14]. Polysulfones may also be physically crosslinked by various methods, such as blending with cationic polyethylene oxide derivatives.[69]

Sulfonated polysulfones are particularly attractive because of their hydrolytic stability and high chlorine resistance. This resistance comes from the particularly strong bonds between carbon, oxygen and sulfur, and polysulfones also lack the amide linkages for chlorine to attack.

The enhanced chlorine tolerance of sulfonated polysulfones compared to polyamides is shown in Figure 1.20.

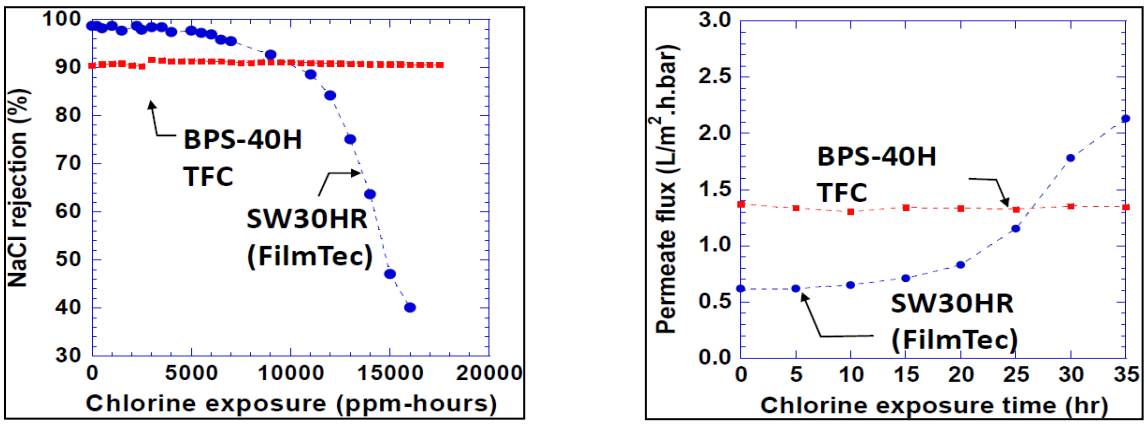

Figure 1.20 Degradation of SW30HR polyamide membrane compared to sulfonated polysulfone. From Angew. Chem., Int. Ed. 2008, 47, 6019. Park, H. B.; Freeman, B. D.; Zhang, Z.-B.; Sankir, M.; McGrath, J. E. Highly chlorine-tolerant polymers for desalination. Used with permission of John Wiley and Sons, 2008[72]

Currently water must be chlorinated to disinfect the water and reduce biofouling, and then the disinfectant must be removed before passage through the membrane. Finally the water must be re-chlorinated before distribution for human consumption.[67] A chlorine resistant reverse osmosis membrane could remove several of these steps, leading to lower operational costs and possibly a longer lifetime of the materials. The major challenge for achieving commercial viability of sulfonated polysulfones is to bring their transport properties in line with the state-of-the-art membranes and to develop comparable methods of fabrication of thin film composites, asymmetric membranes or hollow fibers.

1.3. Poly(arylene ether sulfone)s

Polysulfones belong to a high performance poly(arylene ether) class of polymers that includes polyetheretherketones (PEEK) amongst other aromatic polyethers. The amorphous polysulfones are rigid, tough, possess high glass transition temperatures, and have good

mechanical properties, despite lacking the semi-crystalline morphology of PEEK.[73-75] Polysulfones also demonstrate high resistance to acidic, basic, aqueous and oxidative environments.[76]

1.3.1. Synthesis of Poly(arylene ether sulfone)s

1.3.1.1. Electrophilic Aromatic Substitution

An early route to poly(arylene ether sulfone)s used conditions related to the Friedel-Crafts reaction.[77] Two routes were investigated to obtain high molecular weight polysulfones. One involved disulfonyl chlorides reacted with dinuclear aromatic species (A-A + B-B) and the other involved self-condensation of monosulfonyl chlorides (A-B). The two routes are shown in Figure 1.22.[78] Either case requires only catalytic quantities of $FeCl_3$, $AlCl_3$, $SbCl_5$, $SnCl_4$, $InCl_3$ or $TiCl_3$[79] to assist in the formation of an aryl sulfonium cation. Early work used reaction temperatures as high as 250°C, although temperatures in the 120-140°C range were later deemed successful.[77,80]

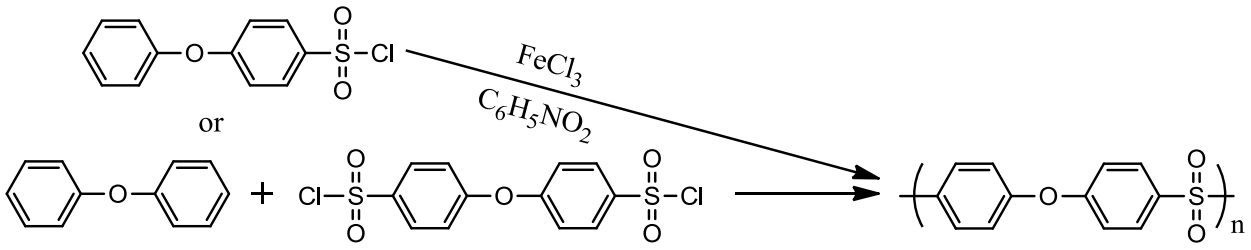

Figure 1.21 Routes to a polysulfone by electrophilic aromatic substitution[78]

The A-B monomer system almost exclusively results in *para* linkages relative to the ether bond, while the A-A + B-B reaction results in more reactivity at the *ortho* position.[78] The sulfone group helps control the regiospecificity and avoid branching because of its electron withdrawing properties, making chain ends much more reactive than rings in the backbone of the

polymer.[77] The electron withdrawing nature of the sulfone group also explains why the monosulfonation route produces less branching and less ortho products than the dinuclear and disulfonyl route.[81] The mechanism for formation of the sulfonium ion followed by substitution is shown below.[82,83]

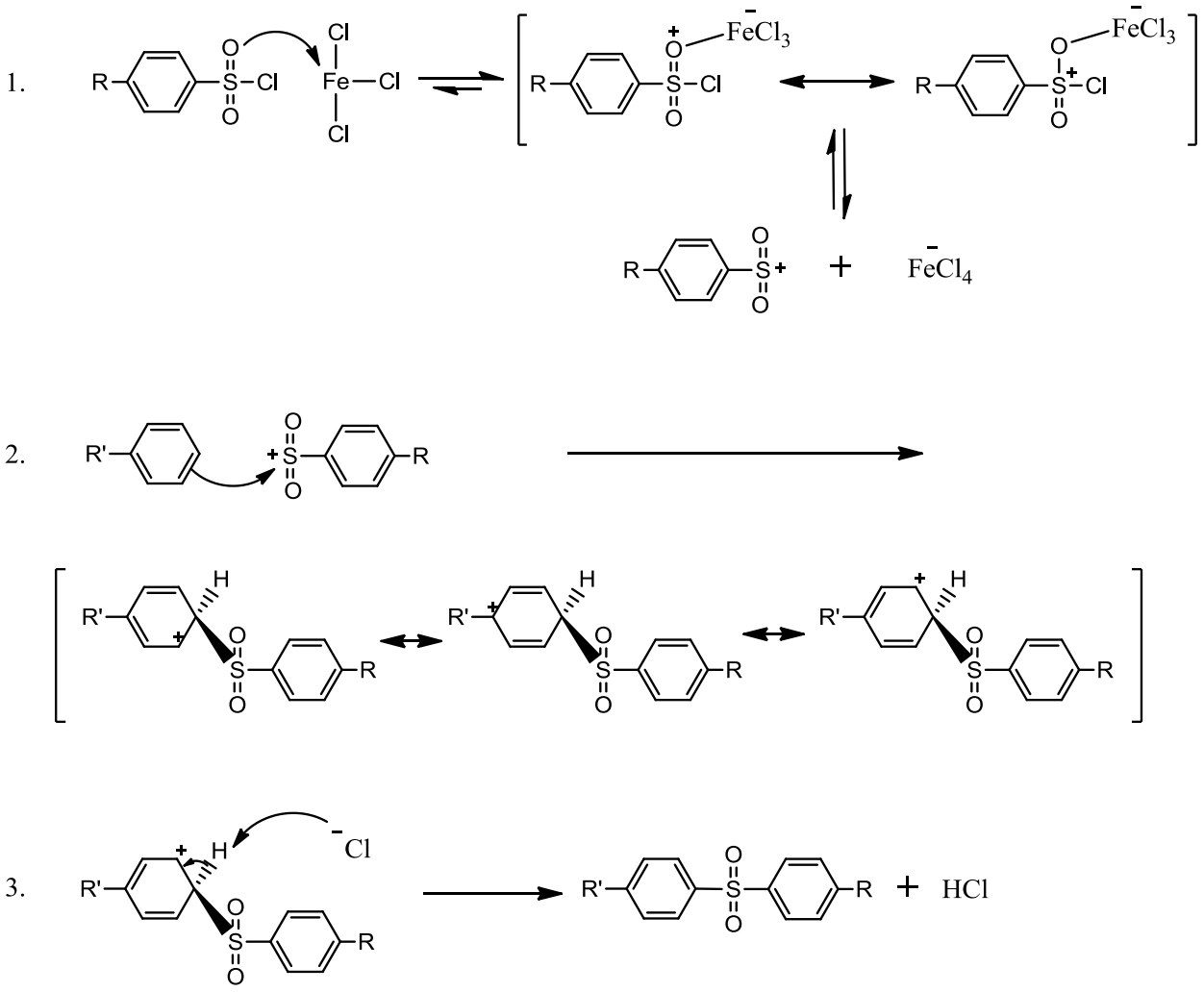

Figure 1.22 Sulfonium ion formation and subsequent electrophilic aromatic substitution[82]

NMR spectroscopy confirmed that the reaction proceeds by an addition-elimination mechanism detailed by Bunnett.[77,84] The monomer bearing the sulfonyl chloride exhibits a strong substitutive effect, in that electron-withdrawing groups increase *ortho* isomer formation while electron-donating groups produce products almost exclusively with *para* substituents.[82]

The mechanism supports this result, as electron-donating groups stabilize the electrophilic cationic intermediate and favor the thermodynamic *para* product formed via a later transition state. Low molecular weights were obtained when the reaction required sulfonium ions to be attacked by a dinuclear species with electron withdrawing groups like benzophenone or diphenylsulfone, as they reduce the reactivity toward electrophilic aromatic substitution.[79,81]

Polysulfones with a significant amount of *ortho* substitution had poorer mechanical properties and sometimes included gel, compared to chains with *para* linkages.[81,85] An excess of sulfonyl chloride sometimes resulted in branching and insoluble material, especially towards the end of the reactions.[77] Additionally, removal of the catalyst was difficult, and in some cases the catalyst caused branching or became incorporated into the polymer backbone by forming an aluminum heterocyclic structure.[86] The nucleophilic aromatic substitution route that is described in the sections below generally eliminates these problems, making it the preferred method for synthesis of polysulfones.

1.3.1.2. Ullmann Reaction

The Ullmann reaction has historically been used to synthesize aromatic ethers by coupling a phenolic derivative with an aromatic halide in the presence of a copper catalyst. Farnham et al. used this reaction to produce wholly aromatic polyethers and noted that weakly acidic dihydric phenols worked best.[88] The Ullmann reaction was also used to successfully synthesize poly(arylene ethers) containing some sulfone bridging units[79,89] and later other structures using halogenated monomers.[90] Figure 1.23 shows a typical route to produce a poly(arylene ether) by the Ullmann reaction. The mechanism of these reactions involve Cu^{+} coordinating to the π system of the aromatic halides and assisting in breaking the carbon-halogen

bond.[80] One consequence of this mechanism is that halide displacement reactivity is I > Br > Cl > F, the opposite order of activated aryl halide nucleophilic aromatic substitution.

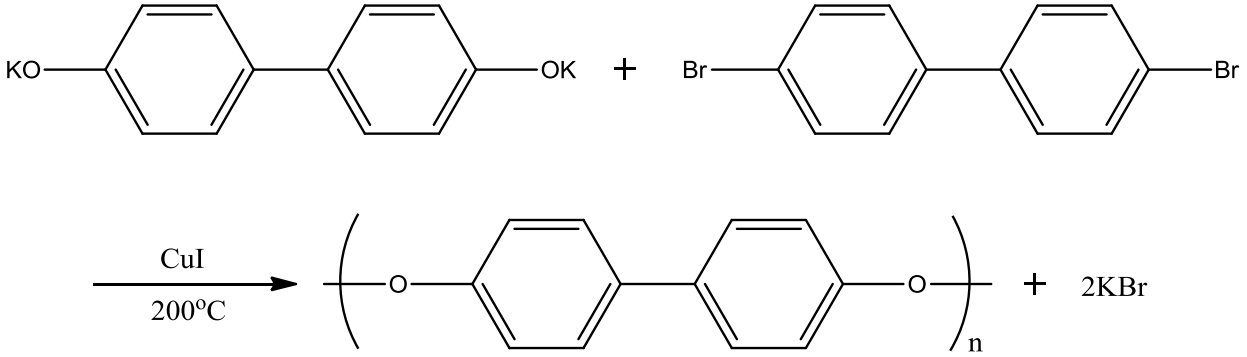

Figure 1.23 Ullmann reaction of bisphenol potassium salt and dibromoarylene[85]

Iodine and bromine functionalized dihalides are much more expensive than chlorine functionalized monomers such as 4,4'-dichlorodiphenyl sulfone, making many of these reactions cost prohibitive. The higher cost of monomers and difficulty of removing copper effectively relegates the synthesis of poly(arylene ethers) by the Ullmann reaction to only non-activated systems that cannot readily undergo nucleophilic aromatic substitution, such as the synthesis of poly(phenylene ethers) and novel aromatic amines and amides.[85,91]

1.3.1.3. Nickel Coupling Reaction

Colon et al. and Ueda et al. developed a more recent approach to synthesize high molecular weight polysulfones in the early 1990s.[50,51] The procedure couples aromatic dichloride monomers using a nickel (0) catalyst in the presence of metallic zinc and a large amount of triphenylphosphine ligand at moderate temperatures. Other routes to polysulfones mentioned in this section involve carbon-heteroatom bond formation to achieve polymer, while this route proceeds by direct carbon-carbon bond formation. The wide availability of dichloride monomers makes this reaction very versatile, although many limitations exist in practice. Any

moieties on the monomers that can react with the nickel catalyst cannot be used, such as nitro groups.[80] A highly inert atmosphere and dehydrated reaction solution is essential. Otherwise water reduces the aryl halides to arenes, deactivates the catalyst, and terminates the polymer chain.[92] The polymer must also remain soluble in the reaction solvent for the polymerization to proceed. In these reactions amorphous polymers proceed to much higher molecular weights than their crystalline analogs and polar aprotic solvents such as DMAc usually lead to higher polymers than THF.[93]

This reaction has not been commercialized because of the difficulty in removing the various catalysts. However, it remains of interest for small scale laboratory purposes because of the versatility of monomer choice compared to other synthetic routes. This reaction has been used to successfully synthesize poly(arylene phosphine oxide)s, poly(arylene fluoro ethylidene) and many other novel materials.[94,95]

1.3.1.4. Nucleophilic Aromatic Substitution

The most commonly used method to synthesize polysulfones is nucleophilic aromatic substitution (S_NAr). Johnson et al. first synthesized a wide variety of high molecular weight polyetherketones and polysulfones by this method in the 1960s,[74] but the basic organic chemistry that drives this reaction was known earlier.

In nucleophilic aromatic substitution the electrons for bond formation are provided by a nucleophilic heteroatom on the aromatic ring, whereas in electrophilic aromatic substitution there is no such group to provide electrons for bonding. This fundamental mechanistic difference results in several important distinctions between the two reactions. In electrophilic aromatic substitution, hydrogen is usually replaced, while in S_NAr, halogens or other groups that are

relatively stable as anions are replaced.[84] In S_NAr directing groups play less of a role, as generally only one group can participate in S_NAr. Usually this group has enhanced reactivity because another substituent on the ring activates it. Figure 1.24 shows a typical S_NAr reaction, which is only possible under these conditions with a strong activating group and good leaving group.[96] Intense academic interest in S_NAr culminated in thorough reviews detailing the mechanism of the reaction, which groups could most easily be replaced, which species were most nucleophilic to S_NAr, and the activating and deactivating influence of other substituents on the ring.[84]

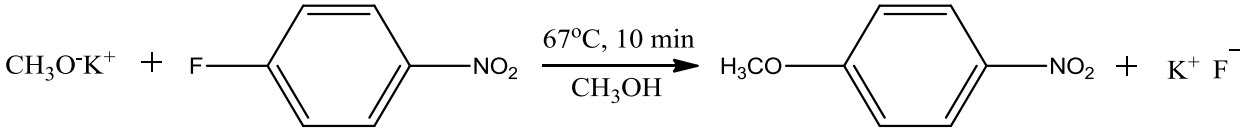

Figure 1.24 Nucleophilic aromatic substitution of *p*-fluoronitrobenzene with methanol[96]

The mechanism for S_NAr shows second-order kinetics, and is first order in both the nucleophile and the aromatic species.[84] The exact mechanism was developed by kinetic data, which demonstrated that reaction rates were much higher with stronger nucleophiles and the reaction was facilitated by electron withdrawing groups on the aromatic species. When the nucleophile attacks the aromatic structure there is no way to maintain aromaticity. Instead the attacked carbon must adopt a sp^3 tetrahedral intermediate. The loss of aromaticity is a huge energetic cost, thus S_NAr is only a reasonable reaction if the resulting anion can be delocalized throughout the aromatic ring and on an electron withdrawing substituent. This relatively stable intermediate, called the Meisenheimer complex, was identified in 1908[97] and has been characterized by both NMR and crystallographic data.[98,99] The initial attack by the nucleophile on the aromatic structure is the rate determining step, as long as the eventual displaced aromatic

group has much greater anionic stability than the nucleophile. Figure 1.25 shows the mechanism for the above reaction, including the formation of a Meisenheimer complex.[96]

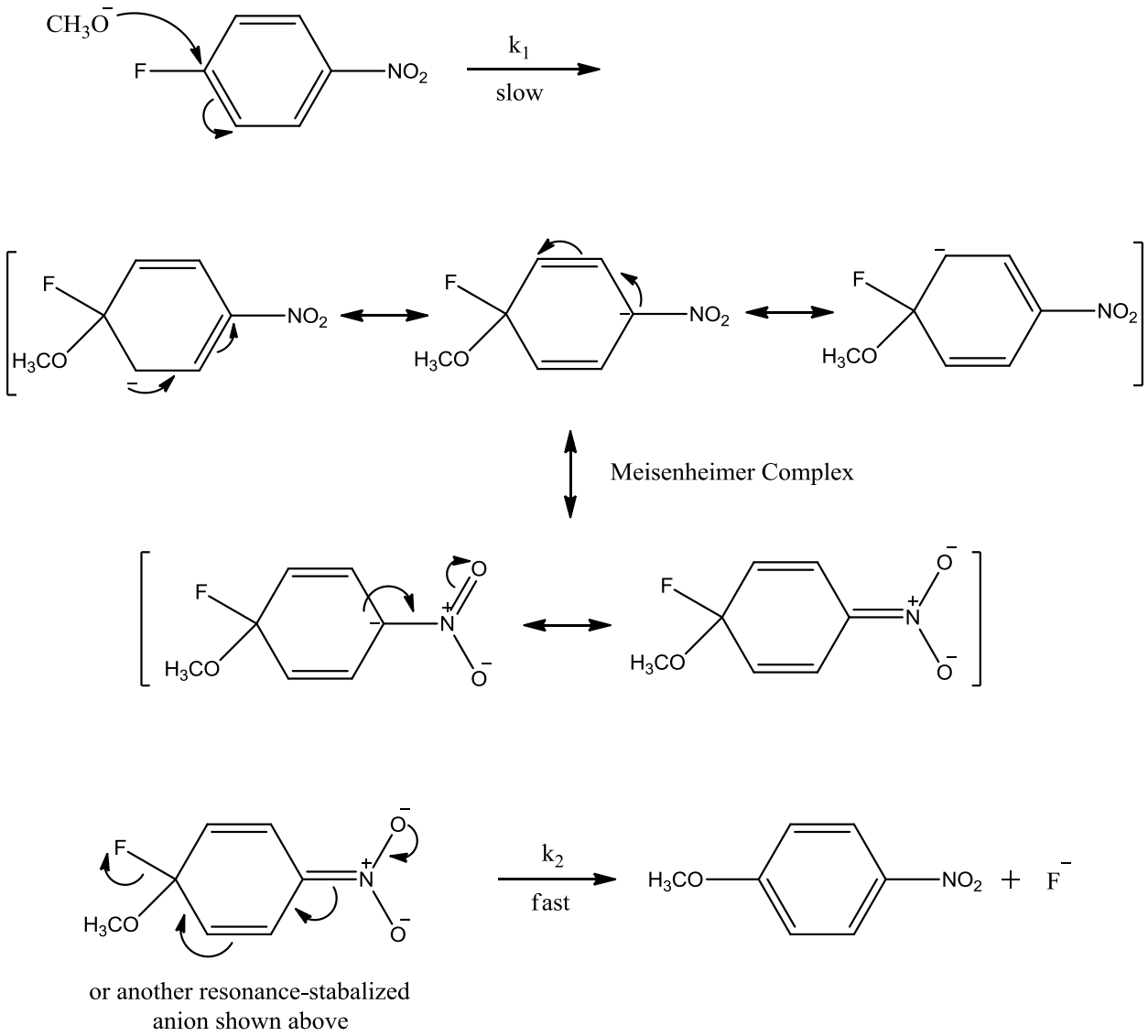

Figure 1.25 Mechanism of nucleophilic aromatic substitution

Leaving group ability in S_NAr differs greatly from other nucleophilic substitution reactions. The largest reason for the order observed is that the rate determining step is the formation of the Meisenheimer complex (k_1 in the above mechanism). The second step of re-aromatizing the ring is fast by comparison. In S_N2 reactions the leaving group ability of

halogens follows the order I > Br > Cl >> F. However, in S_NAr the leaving group ability is F >> Cl > Br > I. The trend normally seen in S_N2 is attributed to the mechanism of bond formation and bond breaking occurring at the same time. The carbon-fluorine bond has a much higher bond strength than other carbon-halogen bonds which inhibits the ability if the fluorine atom to leave. The strength of the carbon-fluorine bond partially results from higher bond polarity relative to other carbon-halogen bonds. When a nucleophile attacks the vacant π^* orbital at the site bearing the aromatic halogen, the enhanced electronegativity of fluorine stabilizes the Meisenheimer complex much more than other halogens.[83] This observation of reactivity proves that bond breaking (k_2 in the above mechanism) is not the rate determining step in most S_NAr reactions.[100] For this same reason, alkoxy groups are readily displaced in S_NAr, though they are poor leaving groups in S_N2 reactions.

Nucleophilic reactivity was investigated by comparing reaction rates and kinetic data. The following series lists species from most nucleophilic to least nucleophilic: $RO^- \approx ArS^-$ > piperidine > ArO^- > $H_2N\text{-}NH_2$ > OH^- > $ArNH_2$.[100] This trend demonstrates that nucleophilicity and basicity may heavily contrast with one another. Nucleophilicity is a kinetic phenomenon while basicity is purely a thermodynamic property, even though OH^- is much more basic than ArO^-, it is much less nucleophilic.

The S_NAr reaction proceeds much more readily in the presence of activating groups for the mechanistic reasons described above. Given the importance of these groups, the relative activating and deactivating power of many substituents has been quantified. Whether the position of the substituent is *ortho, meta* or *para* to the replaced group has a strong effect on substitution rates. However these inductive and resonance effects vary tremendously.[84] The order of activating power of a substituent when *para* to the site of substitution is: NO > NO_2 >

$SO_2R > CF_3 > CN > COH > COR$.[84,101] The order of deactivating power when *para* to the site of substitution is: $NH_2 > OH > NR_2 > OR > R > F > H$.[102]

1.3.1.4.1. Strong Base Approach

S_NAr applied to polysulfone preparation can further be divided into two approaches, synthesis involving strong bases such as NaOH and KOH, or synthesis utilizing weaker bases such as K_2CO_3. The initial research into polysulfone formation used a strong base, and is commonly called the caustic process.

Johnson et al. prepared Udel © polysulfone, then known as Bakelite polysulfone, by reacting the workhorse monomer 4,4'-dichlorodiphenyl sulfone (DCDPS) with the disodium salt of 4,4'-isopropylidene diphenol.[74] Figure 1.26 shows the reaction scheme for formation of this polymer. Their investigations and the work of other researchers determined suitable monomers for the reaction, the role of solvent, the sensitivity to water, and the importance of reaction stoichiometry of not only monomers, but also base. The solubility of the bisphenolate is very important for the aqueous caustic method. The disodium salt of 4,4'-isopropylidene diphenol (Bis-A) met this requirement, however 4,4'-biphenyl does not and thus required development of the potassium carbonate process.[103]

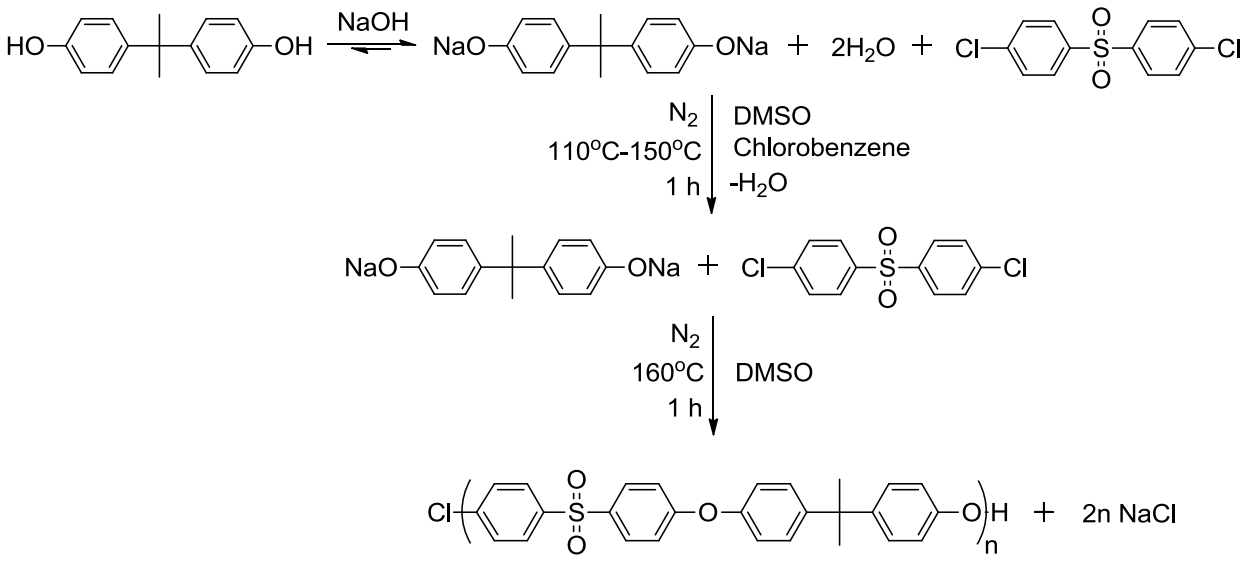

Figure 1.26 Synthesis of polysulfone by the strong base method[74]

The two monomers required to make a polysulfone by an A-A + B-B reaction are a bisphenol and most commonly an activated aryl halide, both with a functionality of two to afford a linear polymerization. Other substituents may replace the role of the halide on the sulfone monomer, such as nitro groups.[104] As stated above, the monomer for an activated dihalide is often DCDPS. Fluorine substituted sulfones react much more quickly, but their much higher price prohibits large scale reactions. For this reason much more variety is seen in the bisphenol monomer structures. While the above reaction uses bisphenol A, an enormous amount of bisphenols react with DCDPS, including biphenol, tetramethylbisphenol A and hydroquinone amongst others.[74] High nucleophilicity in the bisphenol will enhance reactivity, and thus relatively acidic bisphenols like 4,4'-biphenol will react much more slowly than other monomers.[105] A general rule of thumb for this reaction is that electron donating groups *para* to bisphenate anions increase reactivity, while electron withdrawing groups will reduce reactivity.[85]

Dipolar aprotic solvents are the only solvents that have been used successfully to synthesize high molecular weight polysulfones. Initial studies utilized dimethyl sulfoxide

(DMSO) and tetramethylene sulfone ($TMSO_2$). Later *N*,*N*-dimethylacetamide (DMAc), *N*-methyl-2-pyrrolidone (NMP) and dimethylformamide (DMF) also came into use.[106] The solvent must be able to dissolve the alkali bisphenate and also keep the growing polymer chain soluble.[74] It is also desirable to maximize the concentration of monomers and polymer in the reaction flask while maintaining solubility, as second-order kinetics dictate that higher concentrations will require shorter reaction times.[105-107]

Early evidence showed that protic contaminants such as alcohols, or even water in the form of moisture, could inhibit the formation of a high molecular weight polymer.[74] The prevention of high molecular weight comes from side reactions with the activated dihalides and with the polymer. If water attacks the activated halide, it can result in either inactive polymer endgroups or inactive monomer, altering reaction stoichiometry. Moisture is not the only concern involving air. The alkali phenates are readily oxidized in air which also alters reaction stoichiometry, and thus a nitrogen purge is a common requirement in polysulfone synthesis.

The protic contaminant of excess alcohol is of major concern in polysulfone synthesis. The strong base is added in a stoichiometric amount to produce the bisphenate from the bisphenol monomer, and the resulting produced water can be azeotropically removed with solvents such as toluene and chlorobenzene.[74] If too much base is charged to the reaction flask there will be residual base after the azeotropic removal of water. This residual base can lead to hydrolysis of the dihalide, again altering reaction stoichiometry or producing dead chain ends.[85,105] A deficiency of base can result in unreacted bisphenol hydrogen bonding to a phenate anion, reducing nucleophilicity by an order of magnitude.[108] Excess strong base can also lead to ether interchange and lower the degree of polymerization. Even a 1% deviation of base

stoichiometry can decrease the reduced viscosity of polysulfone in chloroform at 25°C from 1.8 dl/g to 0.6 dl/g.[103]

1.3.1.4.2. Weak Base Approach

Patent literature from the late 1970's described polysulfone synthesis using a weaker base such as potassium carbonate, instead of the aforementioned strong bases.[109] This "carbonate" approach was subsequently investigated from a kinetic perspective and compared to the strong base methodology.[103,110,111] The carbonate approach has been successfully applied to other polymeric systems, such as poly(aryl ether) copolymers with poly(phenylquinoxalines).[112] Many of the reaction conditions such as dry atmosphere and polymer workup remain the same.

One motivation behind using a weaker base came from the desire to eliminate the unwanted side reactions of with a strong base. Initial hydrolysis studies proved that even 10-20% of excess weak base did not produce undesirable side reactions with the activated halide.[103] The increased tolerance with excess base does come at an expense. The reaction is slower by approximately an order of magnitude when compared to the strong base route. The slow reaction rates were attributed to hydrogen-bonding between the phenoxide and unreacted phenol groups, the presence of large amounts of azeotropic solvent, or the initial heterogeneity of K_2CO_3. The heterogeneity of K_2CO_3 and the role it plays in converting a phenol to a phenolate is shown in Figure 1.27.

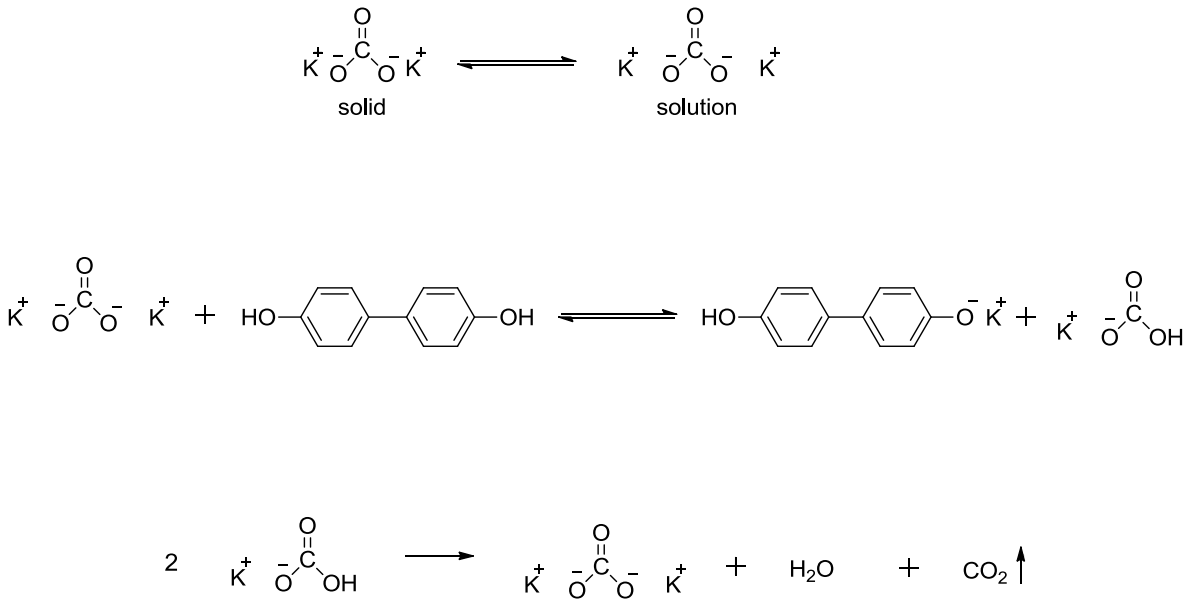

Figure 1.27 Role of potassium carbonate in converting phenols and possible decomposition

The model studies of this reaction used DMAc instead of DMSO, because DMAc has a higher cation solvating power, and increased solubility of the weak base. The poor solubility of the base in the solution also necessitated high temperatures to achieve high molecular weight. An azeotropic solvent must also be used to achieve high molecular weight, often in 50% v/v ratios to the main reaction solvent. Azeotroping the water in the reaction ensures that it cannot act as a nucleophile on the dihalide. The evolution of water will occur throughout this reaction with disproportionation of $KHCO_3$. If water is not azeotropically removed and therefore allowed to react with the activated halide by hydrolysis, the stoichiometry will be upset and high molecular weights may not be obtained.

The reaction temperature of about 165^{o}C for DMAc may not be sufficient for some systems, in which case NMP may be used for reactions up to 190^{o}C.[113,114] A consequence of using higher reaction temperatures is increased ether-ether interchange reactions. While these have no consequence for random composition copolymers, it is a deterrent to synthesizing block copolymers.[112]

The weak base process differs from the strong base approach in a subtle but important mechanistic way. The strong base approach produces bisphenates from bisphenols, and these anionic species proceed to attack the activated aromatic species. Kinetic studies performed by McGrath et al. show that the carbonate process can proceed through a monophenate path.[103,115] Only one phenolic group needs to be converted prior to the initial nucleophilic attack. After this group reacts and forms the dimer species, the other phenol moiety can become converted to a phenate and attack a different sulfone molecule. The monophenate terminated monomers have enhanced solubility compared to the bisphenates, thus allowing more versatility of the bisphenol monomer. Dimer and oligomeric species may form relatively quickly, but the limiting rate constant that influences overall reaction kinetics is the attack of an oligomeric or polymeric phenate on a oligomeric or polymeric halide.[103] Figure 1.28 shows the overall scheme for this reaction below.[101,103,115] The carbonate process to synthesize polysulfones is versatile and a good alternative to the strong base methodology.

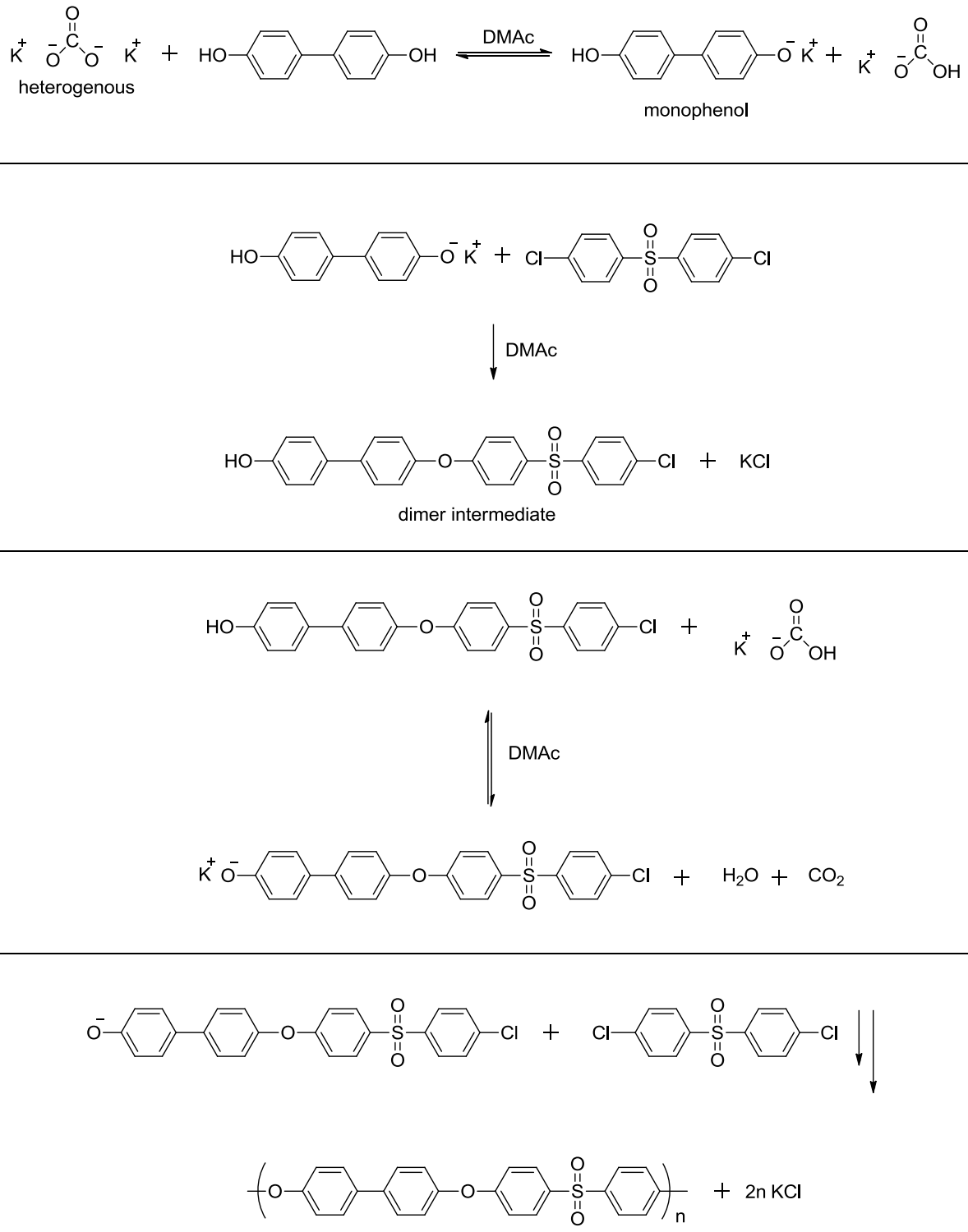

Figure 1.28 Mechanism for synthesis of polysulfone via the weak base "carbonate" process

1.3.2. Post-sulfonation

An important derivative of polysulfones for water purification, fuel cells and other applications involves the addition of ionic groups on the backbone of the polymer.[68,116,117] The most common ionic group included is the sulfonate group, which may be incorporated into the backbone by two different methods. The first method, called post-sulfonation, utilizes an existing polysulfone and harsh electrophilic aromatic substitution conditions to alter the backbone of the polymer chain.

Quentin et al. first investigated sulfonated polysulfones by the post-sulfonation process in the 1970s.[68,118] They dissolved a polysulfone in a polar aprotic solvent and reacted it with chlorosulfonic acid, yielding near quantitative levels of sulfonation on the backbone. Figure 1.29 shows this sulfonation reaction.

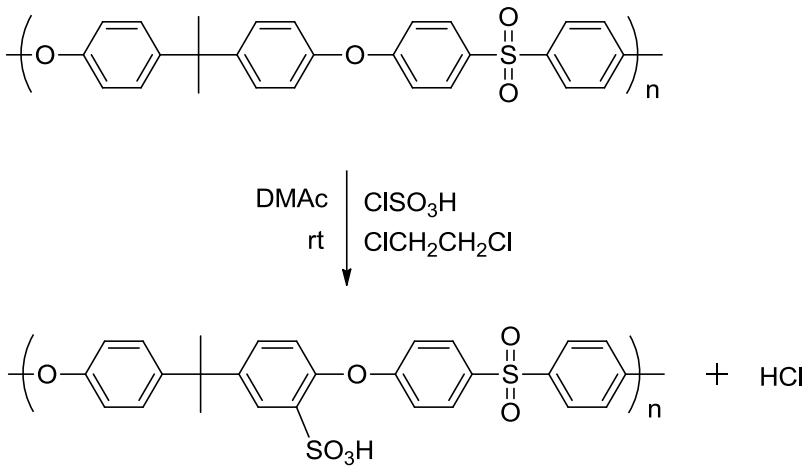

Figure 1.29 Post-sulfonation of a polysulfone with chlorosulfonic acid

At the same time Robeson showed that a 2:1 sulfur trioxide/triethyl phosphate complex (SO_3/TEP) also sulfonated polysulfones quickly at room temperature.[75] Model studies showed that sulfonation preferably occurred on the *ortho* position of the aromatic bisphenol, relative to the ether linkage, owing to the sulfone moiety deactivating electrophilic aromatic substitution.

Robeson later demonstrated that appropriate substitution of the bisphenol regions could result in sulfonation on the phenyl regions adjacent to the sulfone linkage.[116] Post-sulfonation of the position *ortho* to the sulfone linkage without needing substitution on the bisphenol was later accomplished by deprotonating polysulfone with *n*-butyllithium, reacting this group with SO_2, and then oxidizing it to produce sulfonated groups.[119-121] The resulting sulfone moieties are in acidified form, but conversion to a neutral salt yields a more thermally stable polymer.

One concern with the post-sulfonation reaction is that chlorosulfonic acid may react with alkylated portions of the backbone, such as an isopropylidene link and subsequently lead to branching and crosslinking.[68,122] This procedure also results in excess inorganic salts trapped in the polymer matrix that must be removed with extensive Soxhlet extractions.[122,123] The exact regiochemistry of sulfonation also varies, which results in heterogeneous microstructures.[124]

1.3.3. Direct Sulfonation

The second approach toward synthesizing sulfonated polysulfones was pioneered by Ueda et al. in the early 1990s.[125] In this method, known as direct sulfonation, a sulfonated monomer is reacted with other monomers by standard S_NAr, producing a sulfonated polymer without requiring any post-treatment.

Ueda et al. used a monomer first synthesized by Robeson et al., sodium 5,5'-sulfonylbis (2-chlorobenzene sulfonate), also known as SDCDPS, for this direct sulfonation approach.[116] SDCDPS is easily synthesized by the electrophilic aromatic substitution of DCDPS with sulfuric acid and the crude product can then be made monomer grade material by successive recrystallizations. Both the chlorine and the sulfonyl group direct the resulting sulfonate groups to the *meta* position relative to the sulfonyl linkage.[125] McGrath et al. later revised the technique

for synthesizing SDCDPS, demonstrating very high purity by NMR and UV spectroscopy.[126,127] Other sulfonated monomers for sulfonated polysulfone synthesis are present in the literature.[128]

Initial studies demonstrated polymers with up to 30% degree of sulfonation, meaning 30 mol % of SDCDPS was used relative to 70 mol % of DCDPS.[125] All of these polymers were film forming, but it was apparent that higher levels of charged sulfonated monomer resulted in lower molecular weights. Lower molecular weights with increasing degrees of sulfonation can be explained by SDCDPS being less reactive and less soluble than DCDPS. McGrath et al. achieved higher molecular weights with systems up to 100% degree of sulfonation by increasing the reaction temperature to 190°C.[129,130] McGrath et al. also demonstrated that IR, NMR and titrations can determine the degree of sulfonation and that NMR also confirms the polymeric microstructure.[111,129] Figure 1.30 shows a typical reaction scheme for the synthesis of a directly sulfonated polysulfone.

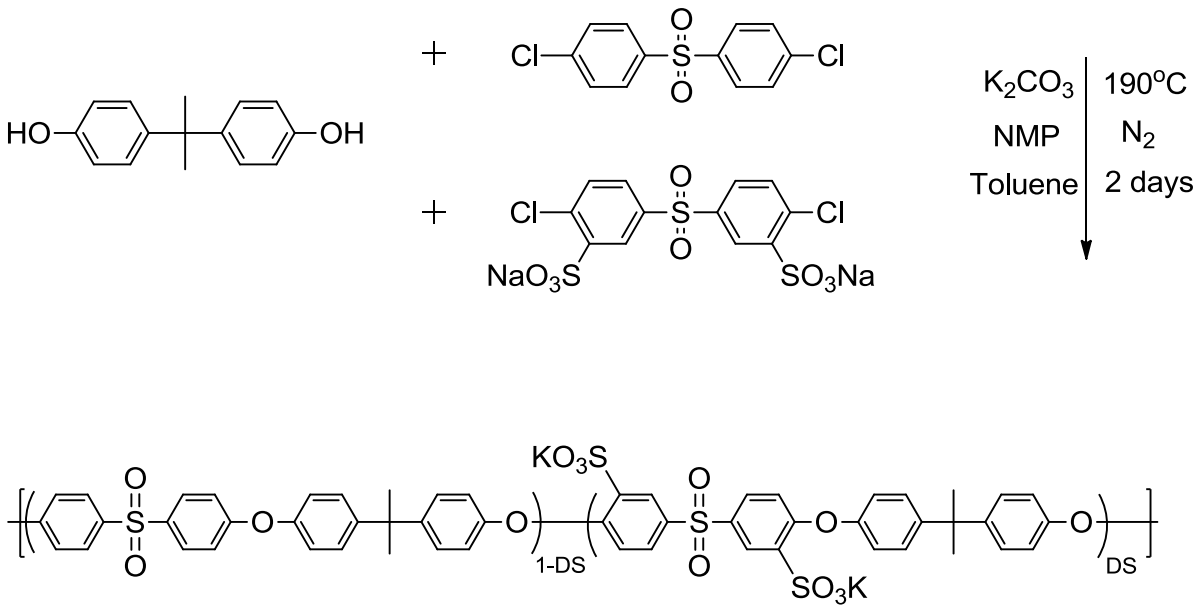

Figure 1.30 Synthesis of a sulfonated polysulfone by direct sulfonation

The direct sulfonation approach has the drawback of additional cost of the SDCDPS monomer and any purification it may need. Thus, very large scale experiments still may prefer to use the post-sulfonation method, especially since the reaction proceeds much more quickly. However, the direct sulfonation method is very successful in controlling the polymer microstructure and generally produces a cleaner, more reproducible product.

1.4. Crosslinking Poly(arylene ether sulfone)s

The crosslinking of polymeric materials is a very important reaction from both a theoretical and industrial perspective. Crosslinks bind polymer chains together through covalent or ionic bonds. The resulting structures are characteristically insoluble and tend to be stronger materials than linear systems, though they are also more brittle.[73] It was mentioned in a previous section that the incredibly high performance of the polyamide water purification membranes is due to the highly crosslinked structure of the polymer, but crosslinking is very important in diverse areas ranging from the vulcanization of rubber for car tires to phenolic resins used in electronics manufacturing.

Crosslinking is especially desirable in polysulfones with large degrees of sulfonation, or any other ionic group that results in a high IEC. Polymers with a high IEC are important for many applications including electrodialysis, water desalination and polymer-electrolyte fuel cells.[119] Unfortunately, these polymers may also swell greatly in solution, leading to a loss in mechanical and transport properties. The following sections give an introduction to the rich chemistry available to crosslink polysulfones.

1.4.1. Covalent

Initial investigations that probed the crosslinking of polysulfones included modifying epoxy resins.[131] Epoxy resins often suffer from high brittleness and lower than desirable impact resistance. The purpose of these studies was not to prove that polysulfones were capable of giving highly crosslinked networks, but rather that small loadings of chemically bound polysulfone could improve the mechanical properties of the epoxy resin. McGrath et al. reacted controlled molecular weight oligomers of Udel polysulfone with an excess of epoxy resin to give an epoxy end-capped polysulfone. The resulting structure was mixed with large amounts of additional epoxy resin and a stoichiometric amount of aromatic diamine at elevated temperatures, resulting in a highly crosslinked network. This synthetic route is shown in Figure 1.31.[131]

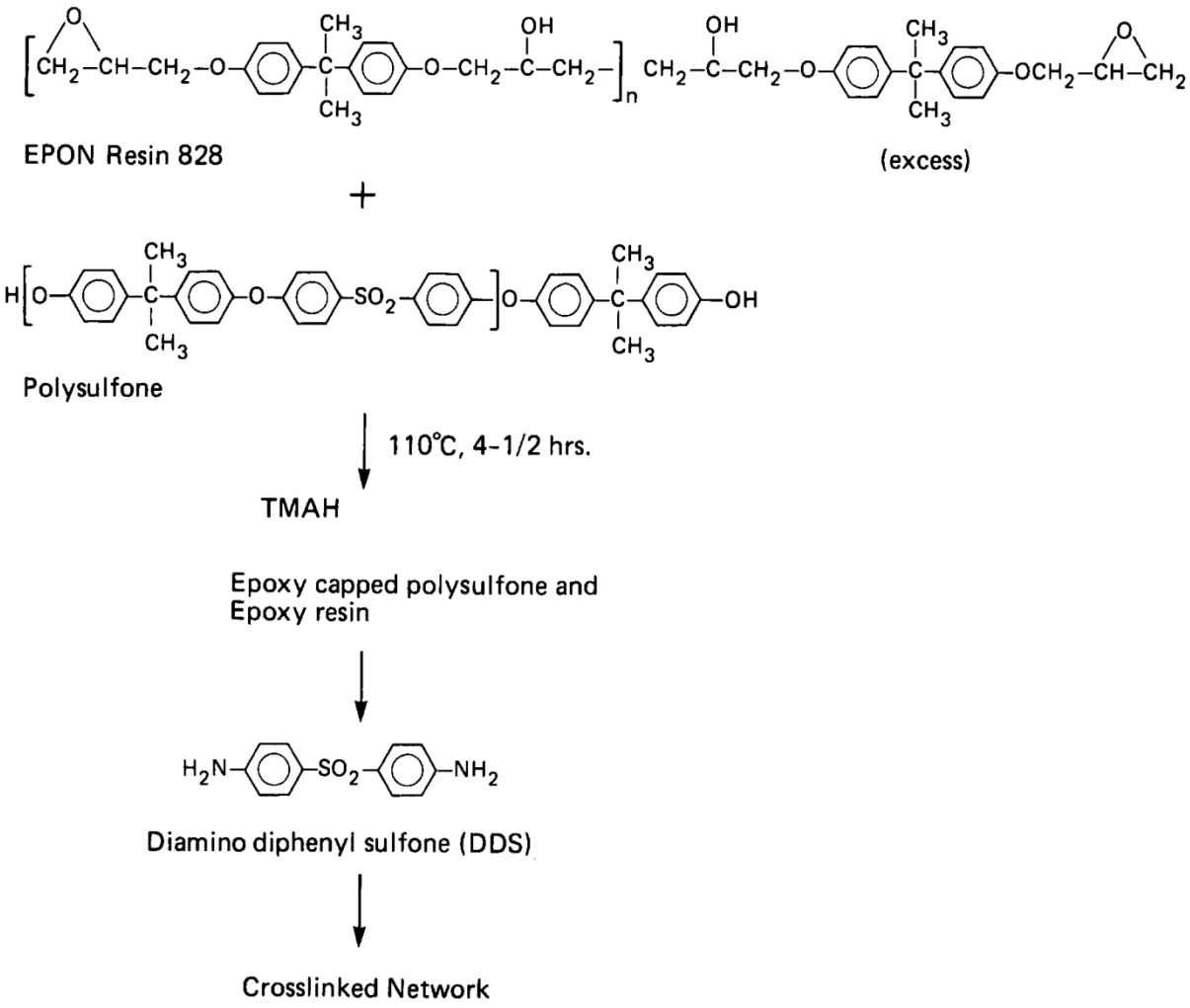

Figure 1.31 Crosslinked epoxy resin modified with 10-15% UDEL polysulfone[131]

The weight percent of polysulfone used in these resins was only 10% to 15%. The resulting fracture toughness was twice as high as the control epoxy resin and only resulted in a small loss of flexural modulus. Scanning electron microscopy showed that both higher weight percentages of polysulfone and higher polysulfone molecular weights contributed to increasingly heterogeneous morphologies and could result in lower chemical resistance.

In 1993 Nolte et al. developed one of the first techniques to crosslink sulfonated polysulfones.[117] Polysulfones were exposed to the conventional post-sulfonation process with chlorosulfonic acid to impart sulfonic acid groups onto the backbone of the polymer. Once the

polymers were cast, they were mixed with small amounts of a diimidazole that activated the sulfonic acid group. This activated group could then react with various diamines, either aliphatic or aromatic, to produce a crosslinked network. Crosslinked structures of this type effectively reduce membrane swelling by 50%, though several issues must be noted. One limit of this technique is that only 50 mol % of the sulfonic groups may be activated, due to imidazole salt formation. An additional problem with this methodology arises from several possible side reactions, including urea and biuret formation.

One particularly versatile approach to covalent crosslinking requires the formation of sulfinate groups along the polymer backbone. An abundant amount of techniques exist to introduce this sulfinate group into aromatic materials including: Friedel-Crafts reactions, sulfonation followed by subsequent reduction to sulfinate, halogen/metal exchange, and the conversion of aromatic diazonium salts.[121] Sulfinate groups may undergo crosslinking by either disproportionation or an S-alkylation reaction with dihaloalkanes. Figure 1.32 depicts both of these routes and the diimidazole crosslinking reactions of polysulfones.[117,121] The sulfinated groups may also be oxidized to sulfonate groups by H_2O_2, $KMnO_4$ or NaOCl prior to the crosslinking reaction. In both of these methods the sulfinated and sulfonated polymers are blended together to form a homogenous solution before crosslinking.[119] These sulfonate groups do not take part in the crosslinking reaction and become entangled in the crosslinked sulfinated network.

Activation with diimidazole

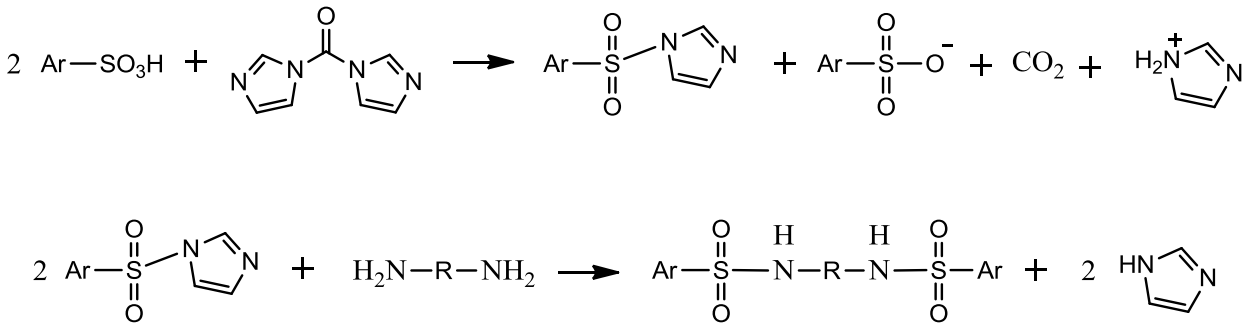

Disproportionation of sulfinic acid

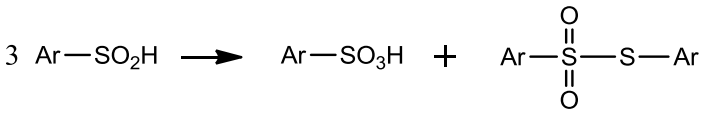

S-alkylation of sulfinate group with dihaloalkane

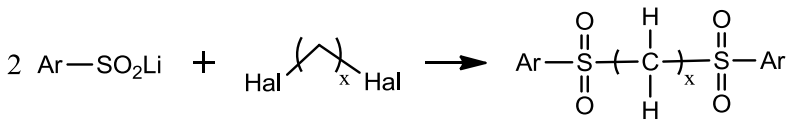

Figure 1.32 Early work in main chain covalent crosslinking[117,121]

The S-alkylation route requires the lithiation of the sulfinated group before crosslinking can occur. The lithiated sulfinate groups can attack a dihaloalkane by a standard nucleophilic substitution reaction, resulting in a crosslinked structure.[120] The preferable nucleophile in this reaction is the sulfur atom, which is predicted by hard/soft-acid/base theory because the sulfur atom is softer than oxygen, and thus its electron shell is more easily perturbed. This crosslinking reaction occurs under very mild conditions and the iodoalkanes in particular are so reactive that membrane fabrication may be impossible because of immediate gelation. A large number of

aromatic crosslinkers have been studied, and the results indicate that changing the crosslinker structure in these reactions does not have a pronounced effect on transport properties, swelling, or gel fraction.[132] Crosslinks generated through this route demonstrate good thermal properties and high stability under basic, acidic and neutral environments.[133]

Crosslinking through disproportionation occurs through an unusual reaction where one sulfinate group acts as the nucleophile and a different sulfinate group acts as an electrophile.[119] Network formation occurs through a stepwise heating regimen up to 120^{o}C under reduced pressure. These membranes also demonstrated good thermal stability and were additionally characterized with regard to IEC, percent swelling, ionic conductivity and ionic permeability. Notably the authors demonstrated that for the crosslinked materials, diffusional permeability remains almost constant in an IEC range of 0.7-1.3, but drastically deviates above or below this region. One disadvantage to both the S-alkylation and disproportionation route is that sulfonic acid moieties are consumed in the crosslinking reaction, lowering the potential IEC of the polymers.[134]

Several other routes have been developed in recent years to crosslink both sulfonated and un-sulfonated polysulfones by reactive moieties along the polymeric backbone. Monomers with pendant hydroxyl groups have been incorporated into the polymer and subsequently reacted with dihaloalkanes in nucleophilic substitution reactions, similar to the chemistry involved in the S-alkylation route.[135,136] Crosslinking reactions of this type use approximately 2-5% by weight of the crosslinking agent. Higher amounts resulted in very fragile materials. Hydroxyl groups may also be used as the crosslinking agent instead of the crosslinking site. Xiao et al. demonstrated that under mild temperatures, sulfonic acid groups will react with poly(vinyl alcohol) to give a crosslinked structure.[137] These materials degrade at temperatures higher than 250^{o}C, though few

applications would require such extreme conditions. Phase transfer catalysts have been utilized to produce polysulfones functionalized with phosphonate and polysulfones functionalized with aldehydes.[138] The functionalized chains react together to form an alkene crosslink site. A novel "hyper-crosslinked" polymer has also been studied by bromomethylation of nearly every aromatic ring on a polysulfone, and then using a Friedel-Crafts catalyst to crosslink the chains.[139] The resulting networks swell less than 3% in any solvent. Figure 1.33 shows several of the aforementioned reactions. Additionally, several groups have synthesized copolymers with pendant allyl,[134] vinyl[140] and propargyl[135] groups that undergo thermal crosslinking. Crosslinking temperatures vary from 180^{o}C when using a free-radical initiator, to 250^{o}C if no initiator is present.

Pendant hydroxyl groups with dihaloalkanes

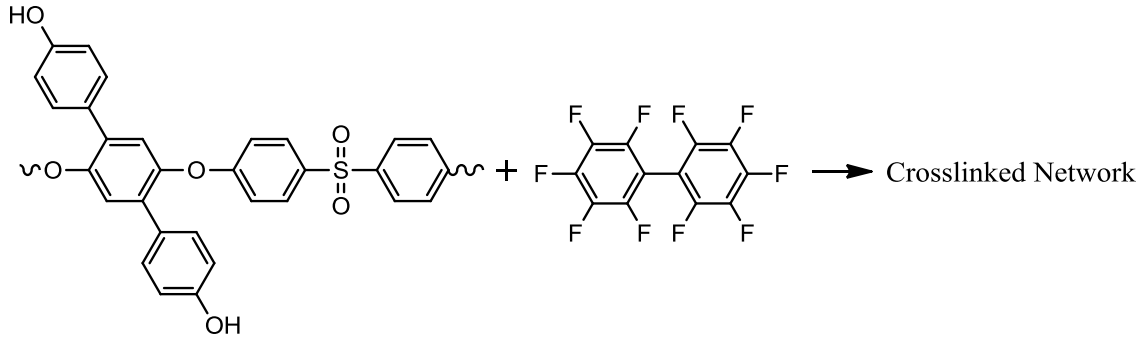

Sulfonic acid with poly vinyl alcohol

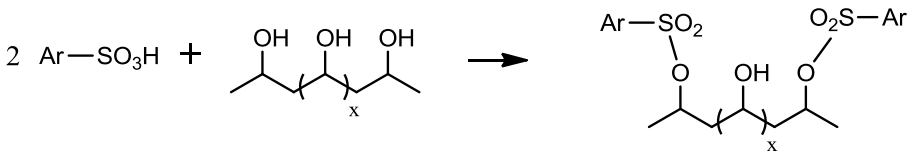

Phosphonates with aldehydes using phase transfer catalyst

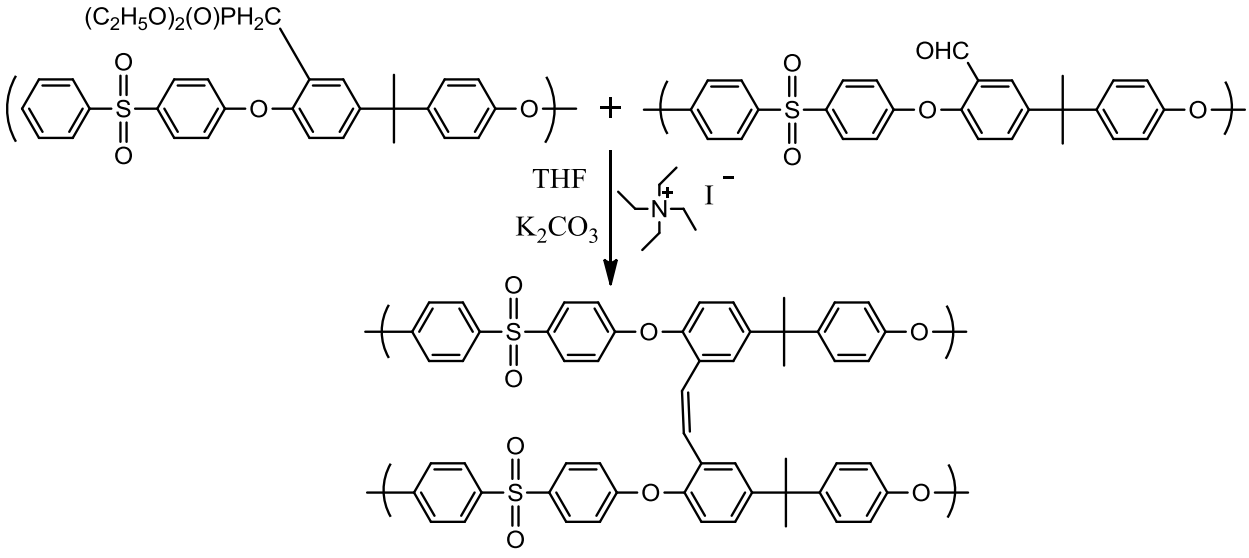

Figure 1.33 Additional synthetic developments in main chain covalent crosslinking[135-138]

Most of the covalent crosslinking chemistry discussed so far utilizes groups along the polymeric backbone as sites for crosslinking. A different approach is to synthesize polysulfones with endgroups capable of chemical crosslinking, structures often referred to as telechilic oligomers. In principle these reactions are similar to the epoxy resins previously discussed, as relatively low molecular weight materials are linked together by chain ends to produce a tough crosslinked film. One advantage of this approach is that lower molecular weight materials are more soluble and easily processed than their high molecular weight equivalents.[141] Much of the chemistry and crosslinkable groups remain the same in this alternate method, especially the use of free radical and thermal crosslinking.

PEEK and PEK type oligomers were crosslinked by McGrath et al. and others prior to polysulfones.[142-144] The crosslinking of polysulfones began in the early 1990's by Delfort and Lucotte et al. Delfort and Lucotte used a monofunctional ethynyl terminated monomer and used the Carothers equation to produce controlled molecular weight oligomers with acetylene endgroups.[141,145] Thermal curing of this system occurred over a wide range, 140 to 300^{o}C, and the resultant networks had T_g's up to 30^{o}C higher than the starting oligomers. Polysulfone oligomers have also been functionalized with allyl and propargyl endgroups that can be crosslinked using high temperature conditions.[146,147] Insoluble fractions as high as 80% were reported and the resulting networks have promising performance in proton exchange membranes.

The telechilic oligomer approach has also been used in condensation reactions as opposed to the free radical processes described above. Paul et al. produced sulfonated polysulfone oligomers that were phenoxide terminated and crosslinked with a multifunctional epoxide at elevated temperatures.[14] The gel fractions obtained from this route are just as high as the free radical cured oligomers and the reduced swelling had a drastic impact on the desalination

properties of the material. One persistent problem with covalently crosslinked materials is that the dry membranes tend to be very brittle and may be prone to mechanical failure.[133]

1.4.2. Ionic/Hydrogen Bonding

The sulfinated polymers described earlier were initially blended with sulfonated polymers, resulting in physical crosslinking by entanglement. This type of physical crosslinking was relatively weak, and any addition of solvent quickly destroyed the network structure. Many types of physical crosslinking suffer from heterogeneous morphologies and unsatisfactorily high swelling. This is especially true of dipole-dipole blends and hydrogen-bonded blends.[133] Physical crosslinking of polysulfones became noteworthy when Kerres et al. pioneered an improved ionically crosslinked approach by blending polysulfones containing basic nitrogen moieties with polysulfones containing sulfonic acid groups.[148,149]

This acid-base approach requires suitably strong basic groups as it was determined that the pK_a of the corresponding acid must be greater than three.[133,150] Examples of the basic polymers used were ortho-sulfone aminated polysulfone, poly(4-vinylpyridine), polyethylenimine and polybenzimidazole.[148] A scheme of the acid-base blend is shown in Figure 1.34.[133]

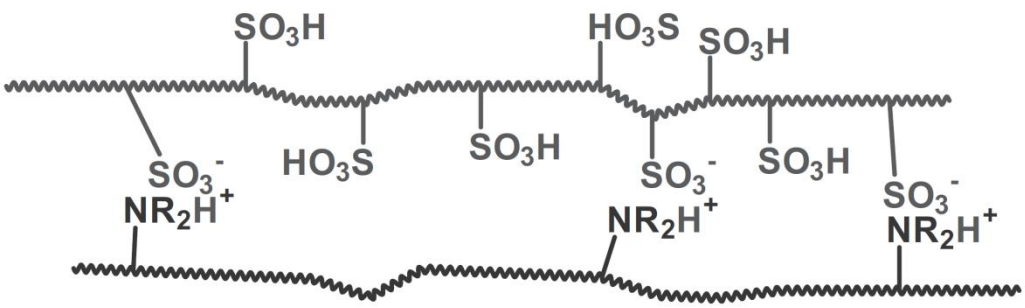

Figure 1.34 Ionically crosslinked polysulfone using acid-base chemistry. From Fuel Cells 2005, 5, 230. Kerres, J. A. Blended and cross-linked ionomer membranes for application in membrane fuel cells. Used with permission of John Wiley and Sons, 2005[133]

Films of these ionic crosslinked systems may be fabricated by mixing both polymers in NMP, casting on a glass plate and evaporating the solvent at 120^{o}C. In some systems it is necessary to convert the sulfonic acid to sulfonate salts prior to mixing, as the interaction between polymers may be significant at low temperatures and prohibit film formation. In these cases the membranes can be post acidified in a hot HCl solution. The acid-base blended membranes may also be doped with phosphoric acid to improve conductivity, at some expense to mechanical strength.[151]

In most cases these acid-base blends result in a homogeneous morphologies.[133] However some results in the literature have shown that miscibility is favored by higher concentrations of the polybenzimidazole and a less sulfonated polysulfone, suggesting that obtaining a homogeneous morphology may not always be guaranteed.[151] Physical crosslinking limits water uptake with increasing crosslink density similar to covalent crosslinking. In some cases the physical crosslinking even has lower swelling at identical IEC's. However, physical crosslinking is unsurprisingly much more temperature dependent. These membranes sorb much more water at elevated temperatures than the corresponding covalently crosslinked materials. The reason for

this phenomenon is that ionic crosslinks and hydrogen bonds undesirably start to separate and break down at higher temperatures.

1.4.3. Covalent/Ionic Mixtures

The acid-base blended ionic membranes had very favorable swelling and conductivity at lower temperatures, and thus researchers sought to extend their temperature use range. One method for doing this is to include covalent crosslinking sites in the backbone of the polymer. One example of this is to use tertiary amine and sulfinate groups that can be crosslinked by alkylation via dihaloalkanes.[132] The resulting ionomer blends had a greatly enhanced homogeneous morphology and lower swelling at higher temperatures. Although this route has had very good initial success on a laboratory scale, the membranes are much more difficult and expensive to prepare and may not be suitable for industrial implementation.[133]

1.5. References

(1) Oki, T.; Kanae, S. *Science* **2006**, *313*, 1068.

(2) Semiat, R. *Enviromental Science & Technology* **2008**, *42*, 8193.

(3) Elimelech, M.; Phillip, W. A. *Science* **2011**, *333*, 712.

(4) Fritzmann, C.; Löwenberg, J.; Wintgens, T.; Melin, T. *Desalination* **2007**, *216*, 1.

(5) Amjad, Z., Ed.; *Reverse Osmosis Membrane Technology, Water Chemistry and Industrial Applications*;Van Nostrand Reinhold, **1993**.

(6) Baker, R. W. *Membrane Technology and Applications*; McGraw-Hill, **2000**.

(7) Systems, A. *Membrane Filtration and related molecular separation technologies*; APV Systems, **2000**.

(8) Sourirajan, S., Ed.; *Reverse Osmosis and Synthetic Membranes*; National Research Council Canada, **1977**.

(9) Wijmans, J. G.; Baker, R. W. *Journal of Membrane Science* **1995**, *107*, 1.

(10) Geise, G. M.; Lee, H.-S.; Miller, D. J.; Freeman, B. D.; McGrath, J. E.; Paul, D. R. *J. Polym. Sci., Part B: Polym. Phys.* **2010**, *48*, 1685.

(11) Geise, G. M.; Paul, D. R.; Freeman, B. D. *Prog. Polym. Sci.* **2014**, *39*, 1.

(12) Lonsdale, H. K.; Merten, U.; Riley, R. L. *Journal of Applied Polymer Science* **1965**, *9*, 1341.

(13) Xie, W.; Geise, G. M.; Freeman, B. D.; Lee, H.-S.; Byun, G.; McGrath, J. E. *Journal of Membrane Science* **2012**, *403-404*, 152.

(14) Paul, M.; Park, H. B.; Freeman, B. D.; Roy, A.; McGrath, J. E.; Riffle, J. S. *Polymer* **2008**, *49*, 2243.

(15) Geise, G. M.; Park, H. B.; Sagle, A. C.; Freeman, B. D.; McGrath, J. E. *Journal of Membrane Science* **2011**, *369*, 130.

(16) Robeson, L. M. *J. Membr. Sci.* **1991**, *62*, 165.

(17) Ridgway, H. F.; Kelly, A.; Justice, C.; Olson, B. H. *Applied and Enviromental Microbiology* **1983**, *45*, 1066.

(18) Kissinger, J. C.; Willits, C. O. *Food Technology* **1970**, *24*, 177.

(19) Mindler, A. B.; Epstein, A. C. *Desalination* **1986**, 343.

(20) Sablani, S. S.; Goosena, M. F. A.; Al-Belushi, R.; Wilf, M. *Desalination* **2001**, *141*, 269.

(21) Brian, P. L. T. *I&EC Fundamentals* **1965**, *4*, 439.

(22) Cath, T.; Childress, A.; Elimelech, M. *Journal of Membrane Science* **2006**, *281*, 70.

(23) Skilhagen, S. E.; Dugstad, J. E.; Aaberg, R. J. *Desalination* **2008**, *220*, 476.

(24) Pattle, R. E. *Nature* **1954**, *174*, 660.

(25) Loeb, S.; Hessen, F. V.; Shahaf, D. *Journal of Membrane Science* **1976**, *1*, 249.

(26) Lee, K. L.; Baker, R. W.; Lonsdale, H. K. *Journal of Membrane Science* **1981**, *8*, 141.

(27) Nielsen, W. K. In *Advances in Materials for Polymeric Membrane Mediated Water Purification* Pacific Grove, California, USA, 2011.

(28) Achilli, A.; Cath, T. Y.; Childress, A. E. *Journal of Membrane Science* **2009**, *343*, 42.

(29) Gekas, V.; Hallstrom, B. *Journal of Membrane Science* **1987**, *30*, 153.

(30) Elimelech, M.; Bhattacharjee, S. *Journal of Membrane Science* **1998**, *145*, 223.

(31) Loeb, S.; Titelman, L.; Korngold, E.; Freiman, J. *Journal of Membrane Science* **1997**, *129*.

(32) Baker, R. W. *Ind. Eng. Chem. Res.* **2002**, *41*, 1393.

(33) Baker, R. W.; Lokhandwala, K. *Ind. Eng. Chem. Res.* **2008**, *47*, 2109.

(34) Bernardo, P.; Drioli, E.; Golemme, G. *Ind. Eng. Chem. Res.* **2009**, *48*, 4638.

(35) Sanders, D. F.; Smith, Z. P.; Guo, R.; Robeson, L. M.; McGrath, J. E.; Paul, D. R.; Freeman, B. D. *Polymer* **2013**, *54*, 4729.

(36) Doolittle, A. K. *J. Appl. Phys.* **1951**, *22*, 1471.

(37) Cohen, M. H.; Turnbull, D. *J. Chem. Phys.* **1959**, *31*, 1164.

(38) Hayes, R. A. Polyimide gas-separation membranes. US4717393A, **1988**

(39) Coleman, M. R.; Koros, W. J. *J. Membr. Sci.* **1990**, *50*, 285.

(40) Bennett, C. L.; Richards, R. E. Copolyimides for use as gas separation membranes. GB2244997A, **1991**

(41) Kita, H.; Inada, T.; Tanaka, K.; Okamoto, K. *J. Membr. Sci.* **1994**, *87*, 139.

(42) Staudt-Bickel, C.; Koros, W. J. *J. Membr. Sci.* **1999**, *155*, 145.

(43) Robeson, L. M. *J. of Membr. Sci.* **2008**, *320*, 390.

(44) Freeman, B. D. *Macromolecules* **1999**, *32*, 375.

(45) Beasley, J. K. *Desalination* **1977**, *22*, 181.

(46) Cadotte, J. E.; King, R. S.; Majerle, R. J.; Petersen, R. J. *J. Macromol. Sci., Chem.* **1981**, *A15*, 727.

(47) Reid, C. E.; Breton, E. J. *J. Applied Polymer Sci.* **1959**, *1*, 133.

(48) Reid, C. E.; Kuppers, J. R. *J. Appl. Polym. Sci.* **1959**, *2*, 264.

(49) Sourirajan, S.; Govindan, T. S. *I&EC Process Design and Development* **1967**; Vol. 1, p 251.

(50) Farooque, A. M.; Al-Amoudi, A.; Numata, K. *Desalination* **1999**, *123*, 165.

(51) Cadotte, J. E.; Petersen, R. J.; Larson, R. E.; Erickson, E. E. *Desalination* **1980**, *32*, 25.

(52) Koros, W. J.; Fleming, G. K.; Jordan, S. M.; Kim, T. H.; Hoehn, H. H. *Prog. Polym. Sci.* **1988**, *13*, 339.

(53) Glater, J.; Hong, S.-k.; Elimelech, M. *Desalination* **1994**, *95*, 325.

(54) Xie, W.; Geise, G. M.; Freeman, B. D.; Lee, H.-S.; Byun, G.; McGrath, J. E. *Journal of Membrane Science* **2012**, *403-404*, 152.

(55) Mickols, W. E. In *Polymer Science: A Comprehensive Reference*; Matyjaszewski, K., Moller, M., Eds.; Elsevier: 2012; Vol. 10, p 1060.

(56) Petersen, R. J. *Journal of Membrane Science* **1993**, *83*, 81.

(57) Sagle, A. C.; Van, W. E. M.; Ju, H.; McCloskey, B. D.; Freeman, B. D.; Sharma, M. M. *J. Membr. Sci.* **2009**, *340*, 92.

(58) Avlonitis, S.; Hanbury, W. T.; Hodgkiess, T. *Desalination* **1992**, *85*, 321.

(59) Orton, K. J. P.; Soper, F. G.; Williams, G. *J. Chem. Soc.* **1928**, 998.

(60) Shintani, T.; Matsuyama, H.; Kurata, N. *Desalination* **2009**, *247*, 370.

(61) Jayarani, M. M.; Rajmohanan, P. R.; Kulkarni, S. S.; Kharul, U. K. *Desalination* **2000**, *130*, 1.

(62) Hickner, M. A.; Fujimoto, C. H.; Cornelius, C. J. *Polymer* **2006**, *47*, 4238.

(63) Fang, J.; Zhai, F.; Guo, X.; Xu, H.; Okamoto, K.I. *J. Mater. Chem.* **2007**, *17*, 1102.

(64) Plummer, C. W.; Kimura, G.; La, C. A. B. *Development of sulfonated polyphenylene oxide membranes for reverse osmosis*, Gen. Elec. Co., 1970.

(65) Chludzinski, P. J.; Fickett, A. P.; LaConti, A. B. *Polym. Prepr., Amer. Chem. Soc., Div. Polym. Chem.* **1971**, *12*, 276.

(66) LaConti, A.B. *In Reverse Osmosis and Synthetic Membranes*, Edited by S. Sourirajan, Ottawa, **1977**. pp.211-229

(67) Park, H. B.; Freeman, B. D.; Zhang, Z.-B.; Fan, G.-Y.; Sankir, M.; McGrath, J. E. *PMSE Prepr.* **2006**, *95*, 889.

(68) Brousse, C.; Chapurlat, R.; Quentin, J. P. *Desalination* **1976**, *18*, 137.

(69) Lee, C. H.; Van, H. D.; Lane, O.; McGrath, J. E.; Hou, J.; Madsen, L. A.; Spano, J.; Wi, S.; Cook, J.; Xie, W.; Oh, H. J.; Geise, G. M.; Freeman, B. D. *Chem. Mater.* **2011**, *23*, 1039.

(70) Xie, W.; Cook, J.; Park, H. B.; Freeman, B. D.; Lee, C. H.; McGrath, J. E. *Polymer* **2011**, *52*, 2032.

(71) Xie, W.; Ju, H.; Geise, G. M.; Freeman, B. D.; Mardel, J. I.; Hill, A. J.; McGrath, J. E. *Macromolecules* **2011**, *44*, 4428.

(72) Park, H. B.; Freeman, B. D.; Zhang, Z.-B.; Sankir, M.; McGrath, J. E. *Angew. Chem., Int. Ed.* **2008**, *47*, 6019.

(73) Odian, G. *Principles of Polymerization* **2004**, *4th Edition*.

(74) Johnson, R. N.; Farnham, A. G.; Clendinning, R. A.; Hale, W. F.; Merriam, C. N. *Journal of Polymer Science: Part A Polymer Chemistry* **1967**, *5*, 2375.

(75) Noshay, A.; Robeson, L. M. *J. Appl. Polym. Sci.* **1976**, *20*, 1885.

(76) Roovers, J.; Ethier, R.; Toporowski, P. M. *High Perform. Polym.* **1990**, *2*, 151.

(77) Cudby, M. E. A.; Feasy, R. G.; Jennings, B. E.; Jones, M. E. B.; Rose, J. B. *Polymer* **1965**, *6*, 589.

(78) Cudby, M. E. A.; Feasey, R. G.; Gaskin, S.; Kendall, M. V.; Rose, J. B. *Polymer* **1968**, *9*, 265.

(79) Jennings, B. E.; Jones, M. E. B.; Rose, J. B. *J. Polym. Sci., Polym. Symp.* **1967**, *16*, 715.

(80) Guo, R.; McGrath, J. E. In *Polymer Science: A Comprehensive Review*; Matyjaszewski, K., Moller, M., Eds.; Elsevier: 2012; Vol. 5, p 769.

(81) Rose, J. B. *Polymer* **1974**, *15*, 456.

(82) Olah, G. A.; Kobayashi, S.; Nishimura, J. *J. Amer. Chem. Soc.* **1973**, *95*, 564.

(83) Carey, F. A.; Sundberg, R. J. *Advanced Organic Chemistry Part A: Structures and Mechanisms*; Springer, 2007.

(84) Bunnett, J. F.; Zahler, R. E. *Chem. Rev.* **1951**, *49*, 273.

(85) Cotter, R. J. *Engineering Plastics, A Handbook of Polyarylethers*; Overseas Publishers Association, 1995.

(86) Cohen, S. N.; Young, R. H. *J. Polym. Sci., Part A-1: Polym. Chem.* **1966**, *4*, 722.

(87) Stamatoff, G. S. Bisphenol polyoxalates. US2989501,**1961**

(88) Farnham, A. G.; Johnson, R. N. Polyarylene polyethers. US3332909,**1967**

(89) Robeson, L. M.; Farnham, A. G.; McGrath, J. E. *Appl. Polym. Symp.* **1975**, *26*, 373.

(90) Jurek, M. J.; McGrath, J. E. *Polym. Prepr. (Am. Chem. Soc., Div. Polym. Chem.)* **1987**, *28*, 180.

(91) Burgoyne, W. F.; Robeson, L. M. Nonhalogenated poly(arylene ether) dielectrics. EP0758664A1, **1997**

(92) Colon, I.; Kwiatokowski, G. T. *J. Polym. Sci., Polym. Chem.* **1990**, *28*.

(93) Bochmann, M.; Kelly, K.; Lu, J. *J. Polym. Sci., Part A: Polym. Chem.* **1992**, *30*, 2511.

(94) Ghassemi, H.; McGrath, J. E. *Polymer* **1997**, *38*.

(95) Havelka-Rivard, P. A.; Nagai, K.; Freeman, B. D.; Sheares, V. V. *Macromolecules* **1999**, *32*, 6418.

(96) Loudon, G. M. *Organic Chemistry*; Fourth ed.; Oxford University Press: New York, New York, 2002.

(97) Meisenheimer, J. *Justus Liebigs Ann. Chem.* **1902**, *323*, 205.

(98) Fyfe, C. A.; Koll, A.; Damji, S. W. H.; Malkiewich, C. D.; Forte, P. A. *Can. J. Chem* **1977**, *55*, 1468.

(99) Messmer, G. G.; Palenik, G. J. *Journal of the Chemical Society D: Chemical Communications* **1969**, 470.

(100) Bunnett, J. F. *Quarterly Reviews, Chemical Society* **1958**, *12*, 1.

(101) Harrison, W. L., Virginia Polytechnic Institute and State University, **2002**.

(102) Berliner, E.; Monack, L. C. **1952**, *74*, 1574.

(103) Viswanathan, R.; Johnson, B. C.; McGrath, J. E., *Polymer* 1984, *25*, 1827.

(104) Beck, J. R. *Tetrahedron* **1978**, *34*, 2057.

(105) Newton, A. B.; Rose, J. B. *Polymer* **1972**, *13*, 465.

(106) Schulze, S. R.; Baron, A. L. *Advan. Chem. Ser.* **1969**, *No. 91*, 692.

(107) Attwood, T. E.; Newton, A. B.; Rose, J. B. *Brit. Polym. J.* **1972**, *4*, 391.

(108) Storozhuk, I. P.; Bakhmutov, V. I.; Mikitaev, A. K.; Valetskii, P. M.; Musaev, Y. I.; Korshak, V. V.; Fedin, E. I. *Vysokomol. Soedin., Ser. A* **1977**, *19*, 1800.

(109) Clendinning, R. A.; Farnham, A. G.; Zutty, N. L.; Priest, D. C.; Patent, C., Ed. 1970; Vol. 847,963.

(110) Mohanty, D. K., Virginia Polytechnic Institute and State University, **1983**.

(111) Johnson, B. C., Virginia Polytechnic Institute and State University, **1984**.

(112) Hedrick, J. L.; Labadie, J. W. *Macromolecules* **1990**, *23*, 1561.

(113) Hedrick, J. L.; Mohanty, D. K.; Johnson, B. C.; Viswanathan, R.; Hinkley, J. A.; McGrath, J. E. *J. Polym. Sci., Part A: Polym. Chem.* **1986**, *24*, 287.

(114) Hedrick, J. L.; Dumais, J. J.; Jelinski, L. W.; Patsiga, R. A.; McGrath, J. E. *J. Polym. Sci., Part A: Polym. Chem.* **1987**, *25*, 2289.

(115) Priddy, D., Virginia Polytechnic Institute and State University, **1994**.

(116) Robeson, L. M.; Matzner, M. Flame retardant polyarylate compositions. EP58403A2,**1982**

(117) Nolte, R.; Ledjeff, K.; Bauer, M.; Muelhaupt, R. *Journal of Membrane Science* **1993**, *83*, 211.

(118) Quentin, J. P. Polysulfones. DE2021383B2,**1970**

(119) Kerres, J.; Cui, W.; Disson, R.; Neubrand, W. *Journal of Membrane Science* **1998**, *139*, 211.

(120) Kerres, J.; Cui, W.; Junginger, M. *Journal of Membrane Science* **1998**, *139*, 227.

(121) Kerres, J.; Zhang, W.; Cui, W. *Journal of Polymer Science, Part A: Polymer Chemistry* **1998**, *36*, 1441.

(122) Johnson, B. C.; Yilgor, I.; Tran, C.; Iqbal, M.; Wightman, J. P.; Lloyd, D. R.; Mcgrath, J. E. *Journal of Polymer Science Part A-Polymer Chemistry* **1984**, *22*, 721.

(123) O'Gara, J. F.; Williams, D. J.; MacKnight, W. J.; Karasz, F. E. *Journal of Polymer Science, Part B: Polymer Physics* **1987**, *25*, 1519.

(124) Bauer, B.; Jones, D. J.; Roziere, J.; Tchicaya, L.; Alberti, G.; Casciola, M.; Massinelli, L.; Peraio, A.; Besse, S.; Ramunni, E. *Journal of New Materials for Electrochemical Systems* **2000**, *3*, 93.

(125) Ueda, M.; Toyota, H.; Ouchi, T.; Suciyama, J.-I.; Yonetake, K.; Masuko, T.; Teramoto, T. *Journal of Polymer Science: Part A Polymer Chemistry* **1993**, *31*, 853.

(126) Sankir, M.; Bhanu, V. A.; Harrison, W. L.; Ghassemi, H.; Wiles, K. B.; Glass, T. E.; Brink, A. E.; Brink, M. H.; McGrath, J. E. *Journal of Applied Polymer Science* **2006**, *100*, 4595.

(127) Li, Y.; VanHouten, R. A.; Brink, A. E.; McGrath, J. E. *Polymer* **2008**, *49*, 3014.

(128) Pang, J.; Zhang, H.; Li, X.; Wang, L.; Liu, B.; Jiang, Z. *J. Membr. Sci.* **2008**, *318*, 271.

(129) Wang, F.; Hickner, M.; Ji, Q.; Harrison, W.; Mecham, J.; Zawodzinski, T. A.; McGrath, J. E. *Macromol. Symp* **2001**, *175*, 387.

(130) Wang, F.; Hickner, M.; Kim, Y. S.; Zawodzinski, T. A.; McGrath, J. E. *Journal of Membrane Science* **2002**, *197*, 231.

(131) Hedrick, J. L.; Yilgor, I.; Jurek, M.; Hedrick, J. C.; Wilkes, G. L.; McGrath, J. E. *Polymer* **1991**, *32*, 2020.

(132) Kerres, J.; Hein, M.; Zhang, W.; Graf, S.; Nicoloso, N. *J. New Mater. Electrochem. Syst.* **2003**, *6*, 223.

(133) Kerres, J. A. *Fuel Cells* **2005**, *5*, 230.

(134) Feng, S.; Shang, Y.; Xie, X.; Wang, Y.; Xu, J. *J. Membr. Sci.* **2009**, *335*, 13.

(135) Voege, A.; Deimede, V. A.; Kallitsis, J. K. *J. Polym. Sci., Part A: Polym. Chem.* **2012**, *50*, 207.

(136) Chikashige, Y.; Chikyu, Y.; Miyatake, K.; Watanabe, M. *Macromol. Chem. Phys.* **2006**, *207*, 1334.

(137) Gu, S.; He, G.; Wu, X.; Guo, Y.; Liu, H.; Peng, L.; Xiao, G. *J. Membr. Sci.* **2008**, *312*, 48.

(138) Popa, A.; Avram, E.; Lisa, G.; Visa, A.; Iliescu, S.; Parvulescu, V.; Ilia, G. *Polym. Eng. Sci.* **2012**, *52*, 352.

(139) Tsyurupa, M. P.; Davankov, V. A. *React. Funct. Polym.* **2002**, *53*, 193.

(140) Kalamaras, I.; Daletou, M. K.; Neophytides, S. G.; Kallitsis, J. K. *J. Membr. Sci.* **2012**, *415-416*, 42.

(141) Delfort, B.; Lucotte, G.; Cormier, L. *J. Polym. Sci., Part A: Polym. Chem.* **1990**, *28*, 2451.

(142) Chan, C. M.; Venkatraman, S. *J. Appl. Polym. Sci.* **1986**, *32*, 5933.

(143) Thompson, S. A.; Farris, R. J. *J. Appl. Polym. Sci.* **1988**, *36*, 1113.

(144) Lyle, G. D.; Senger, J. S.; Chen, D. H.; Kilic, S.; Wu, S. D.; Mohanty, D. K.; McGrath, J. E. *Polymer* **1989**, *30*, 978.

(145) Lucotte, G.; Cormier, L.; Delfort, B. *J. Polym. Sci., Part A: Polym. Chem.* **1991**, *29*, 897.

(146) Chul, G. S.; Chul, K. J.; Ahn, D.; Jang, J.-S.; Kim, H.; Chul, J. J.; Lim, S.; Jung, D.-H.; Lee, W. *J. Membr. Sci.* **2012**, *417-418*, 2.

(147) Oh, Y.-S.; Lee, H.-J.; Yoo, M.; Kim, H.-J.; Han, J.; Kim, T.-H. *J. Membr. Sci.* **2008**, *323*, 309.

(148) Kerres, J.; Ullrich, A.; Meier, F.; Haring, T. *Solid State Ionics* **1999**, *125*, 243.

(149) Kerres, J.; Zhang, W.; Tang, C.-M. Covalently- and ionically-crosslinked polymers for use in membranes. DE10024576A1, **2001**

(150) Kerres, J.; Zhang, W.; Ullrich, A.; Tang, C. M.; Hein, M.; Gogel, V.; Frey, T.; Jorissen, L. *Desalination* **2002**, *147*, 173.

(151) Hasiotis, C.; Li, Q.; Deimede, V.; Kallitsis, J. K.; Kontoyannis, C. G.; Bjerrum, N. J. *J. Electrochem. Soc.* **2001**, *148*, A513.

CHAPTER 2: MONOMER PURIFICATION AND SYNTHESIS

2.1. Introduction

There are several criteria that must be met to obtain high molecular weight in linear step-growth polymerizations. Monomers should exhibit perfect difunctionality, have high reactivity towards one another, and not participate in any side reactions. Additionally, as described by the Carothers equation, the monomers need to be added in a 1:1 molar stoichiometry. Therefore, monomers must be prepared to near 100% purity to ensure that the proper reaction stoichiometry is obtained. The following section discusses the purification of commercially available monomers, as well as monomer synthesis.

Utilizing either novel monomers or specialty organic reagents is an effective route for producing novel polymers. Tetramethyl bisphenol A is reported in the literature, but is relatively expensive and cost prohibitive for large scale polymer synthesis. Thus, a new procedure was utilized to obtain a reagent grade monomer with high yields from inexpensive starting materials. In another case, the synthesis of halide functionalized amine containing premonomer was performed to try to overcome a reactivity issue with the amine containing premonomer. However, most monomer synthesis was performed to produce new monomers, such as tetramethyl bisphenol 3F-phenyl, so that novel polymers could be made. The organic reactions used to produce these novel monomers included electrophilic aromatic substitution, nucleophilic aromatic substitution, and nitration/reduction reactions.

2.2. Monomer and Reagent Purification

2.2.1. *4,4'-Dichlorodiphenyl sulfone (DCDPS)*

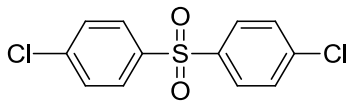

Source: Solvay

Molecular Weight: 287.16 g mol^{-1}

Purification: DCDPS was recrystallized from toluene to produce large white crystals that were pulverized prior to drying. DCDPS was dried under vacuum at 100^{o}C for 12 hours before use in polymerization reactions.

2.2.2. *3,3'-disulfonated-4,4'-dichlorodiphenyl sulfone (SDCDPS)*

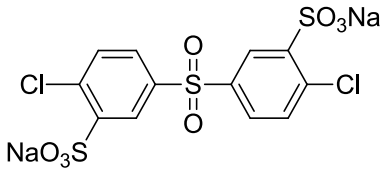

Source: Akron Polymer Systems

Molecular Weight: 491.25 g mol^{-1}

Purification: SDCDPS was used as received, though it may be recrystallized from a 9:1, 2-propanol:DI water (v:v) solution.

SDCDPS contains NaCl impurities from the monomer synthesis, which may be removed by recrystallizing the monomer several times.[1] The amount of NaCl impurity in SDCDPS can be quantified by UV-visible spectroscopy, which was performed by Akron Polymer Systems. The 2-3% NaCl impurity is inert in the nucleophilic step polymerization reactions, and proper

reaction stoichiometry was obtained by adjusting the amount of charged monomer to reflect this impurity. SDCDPS is very hydroscopic, and prior to its use in polymerizations must be dried at 160^{o}C under vacuum for at least 3 days.[1]

During the course of my studies, we interacted with Akron Polymer Systems to further investigate the purity of their SDCDPS. Akron Polymer Systems produced a partially disulfonated polymer based on 4,4'-biphenol, and questioned the purity of their SDCDPS and accuracy of their UV-visible light spectroscopy measurements. Independent analysis of the SDCDPS material was performed in our laboratories to ensure the integrity of their monomer material.

The following experiment was performed on a Shimadzu UV-visible spectrophotometer (UV-1601) using 1 cm cuvettes from Fisher. The SDCDPS monomer provided by Akron Polymer Systems was crushed with a mortar and pestle, and then was dried at 160^{o}C for 72 hours under vacuum. This monomer was cooled to room temperature but kept under vacuum before use to limit ambient water sorption. A previous purchased SDCDPS monomer, initially characterized by Akron Polymer Systems as 98.6% pure, was recrystallized three times by the aforementioned method and used as the "pure" standard for the calibration curve. The pure SDCDPS monomer was also dried at 160^{o}C for 72 hours under vacuum and cooled to room temperature before use.

Three different samples of SDCDPS, purified by recrystallization, were each diluted to three concentrations for a total of 9 data points for the calibration curve. Three samples of the crude SDCDPS monomer were also prepared, and diluted to a similar concentration. The concentrations were in the linear portion of the Beer-Lambert calibration curve (< 3 x 10^{-5} mol L^{-}

[1]). The calibration curve from our results is shown in Figure 2.1, and compared to a previous calibration curve from Li *et al*. shown in Figure 2.2.[1]

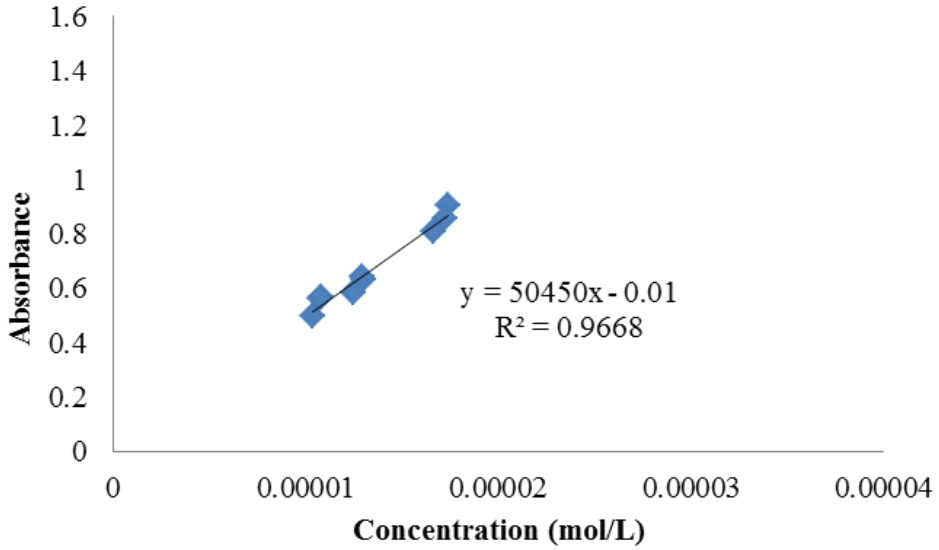

Figure 2.1 Sundell calibration curve for pure SDCDPS

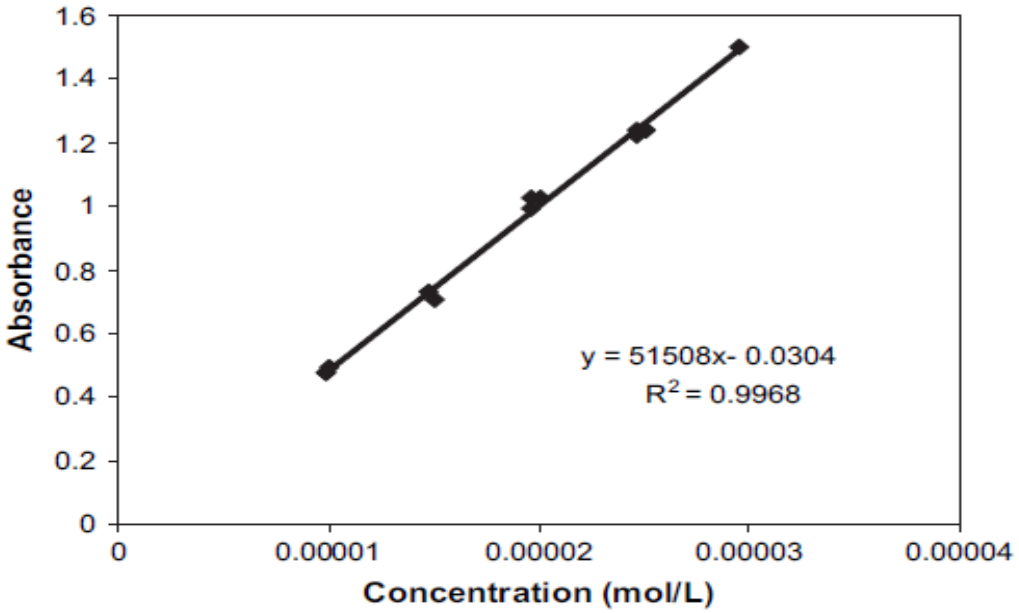

Figure 2.2 Li Calibration curve for pure SDCDPS. From Polymer 2008, 49, 3014. Paul, M.; Park, H. B.; Freeman, B. D.; Roy, A.; McGrath, J. E.; Riffle, J. S. Li, Y.; VanHouten, R. A.; Brink, A. E.; McGrath, J. E. Purity characterization of 3,3′-disulfonated-4,4′-dichlorodiphenyl sulfone (SDCDPS) monomer by UV–vis spectroscopy. Used with permission of Elsevier, 2008[1]

After development of the calibration curves, the relatively new SDCDPS monomer was analyzed for residual NaCl impurities. The crude SDCDPS was found to be 100.4 ± 1.3% pure by the Sundell calibration curve and 101.2 ± 1.5% pure by Li's calibration curve. These two calibration curves indicated that the crude SDCDPS was indeed of monomer grade purity, which is shown in Figure 2.3. The standard deviations on these experiments was slightly higher than those initially performed by Li *et al.*[1] For comparison, the previous crude SDCDPS monomer (purity labeled as 98.6% by Akron Polymer Systems) was calculated to be 98.9 ± 2.8% by the Sundell calibration curve, indicating excellent agreement between the UV-visible spectrometry analysis done between Akron Polymer Systems and the McGrath lab.

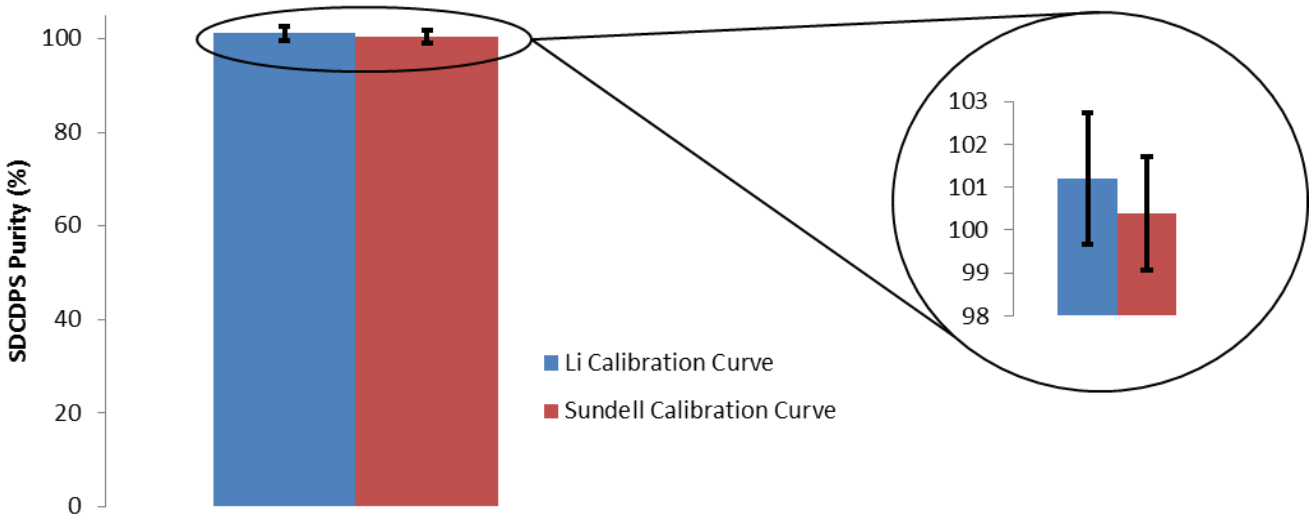

Figure 2.3 Purity of Akron's SDCDPS by different calibration curves

2.2.3. *4,4'-(propane-2,2-diyl)diphenol (Bisphenol A, BisA)*

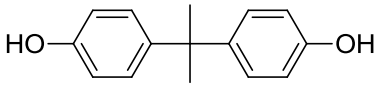

Source: Solvay

Molecular Weight: 228.29 g mol^{-1}

Purification: Bisphenol A was recrystallized from toluene to produce fine, needle-like white crystals. The solubility of Bisphenol A in toluene is somewhat poor, so if large quantities of recrystallized Bisphenol A are desired aqueous methanol may also be used instead. Bisphenol A was dried under vacuum at 100^{o}C for 12 hours before use in polymerization reactions.

2.2.4. *3-Aminophenol (Meta-aminophenol, m-AP)*

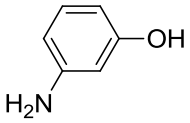

Source: Acros Organics

Molecular Weight: 109.13 g mol^{-1}

Purification: The end-capper *meta*-aminophenol was received as a light tan solid and used without further purification.

2.2.5. *4,4'-Biphenol (Biphenol, BP)*

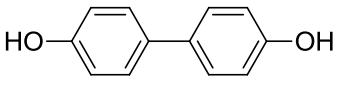

Source: Eastman Chemical Company

Molecular Weight: 186.21 g mol^{-1}

Purification: Monomer grade biphenol was used as received. If necessary, biphenol can be recrystallized from acetone or toluene. Biphenol was dried under vacuum at 100^{o}C for 12 hours before use in polymerization reactions.

2.2.6. *Benzene-1,4-diol (Hydroquinone, HQ)*

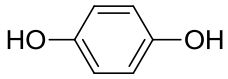

Source: Eastman Chemical Company

Molecular Weight: 110.11 g mol^{-1}

Purification: Hydroquinone as received had a slight pink color which was removed upon recrystallization in methanol. Hydroquinone was dried under vacuum at 80^{o}C for 12 hours before use in polymerization reactions.

2.2.7. *4,4'-Difluorobenzophenone (DFB)*

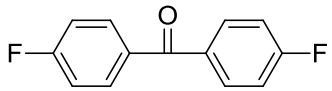

Source: TCI Chemicals

Molecular Weight: 218.20 g mol^{-1}

Purification: Monomer grade difluorobenzophenone was used as received. If necessary, difluorobenzophenone can be recrystallized from petroleum ether. Difluorobenzophenone was dried under vacuum at 60^{o}C for 12 hours before use in polymerization reactions.

2.2.8. *2-Propenoyl chloride (Acryloyl chloride)*

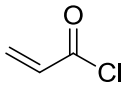

Source: Aldrich

Molecular Weight: 90.51 g mol^{-1}

Purification: Acryloyl chloride was used as received as a transparent and light yellow liquid.

2.2.9. *4-Phenylethynylphthalic anhydride (PEPA)*

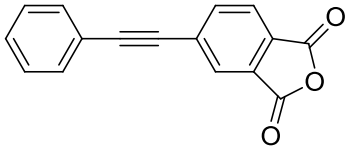

Source: Akron Polymer Systems

Molecular Weight: 248.24 g mol^{-1}

Purification: Phenylethynylphthalic anhydride was obtained as a light yellow solid and used as received.

2.2.10. *Furan-2,5-dione (Maleic anhydride, MA)*

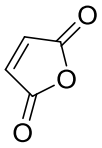

Source: Aldrich

Molecular Weight: 98.06 g mol^{-1}

Purification: Maleic anhydride was obtained as a white solid with an acrid odor and was used without further purification.

2.2.11. *Tetraglycidyl bis(p-aminophenyl)methane (TGBAM)*

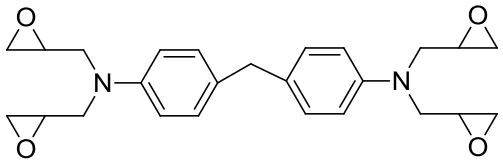

Source: Aldrich

Molecular Weight: 422.52 g mol^{-1}

Purification: TGBAM was obtained as a pale yellow, highly viscous liquid and used without further purification. The average functionality of the epoxy as received was 3.67, as opposed to the theoretical epoxy equivalents of 4. The average functionality was obtained by integrating the epoxy ring protons to those of the methylene protons in the middle of the molecule.[2] This discrepancy was taken into consideration for reaction stoichiometry and additional epoxy was added to account for it.

2.2.12. *Triphenylphosphine (TPP)*

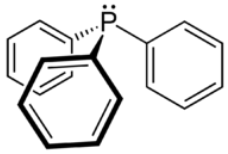

Source: Aldrich

Molecular Weight: 262.29 g mol^{-1}

Purification: Triphenylphosphine was used as received as a white solid. Triphenylphosphine may slowly oxidize to triphenylphosphine oxide, in which case it can be recrystallized from hot ethanol.

2.2.13. *Potassium carbonate (K2CO3)*

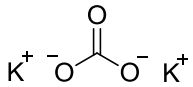

Source: Aldrich

Molecular Weight: 138.21 g mol^{-1}

Purification: Potassium carbonate was received as a white solid and if necessary ground by mortar and pestle. Potassium carbonate was dried under vacuum at 160^{o}C for 12 hours before use as a base in polymerization reactions.

2.2.14. *Additional Reagents/Solvents*

The aforementioned chemicals are not meant to be a comprehensive list of materials used throughout this dissertation. Only commercially available monomers, end-capping reagents and crosslinkers have been described. For a complete list of purchased reagents including solvents, free-radical initiators, desiccants and many others, refer to the experimental sections in Chapters 3-7.

2.3. Monomer Synthesis

2.3.1. *4,4'-(propane-2,2-diyl)bis(2-nitrophenol) (Nitro substituted BisA)*

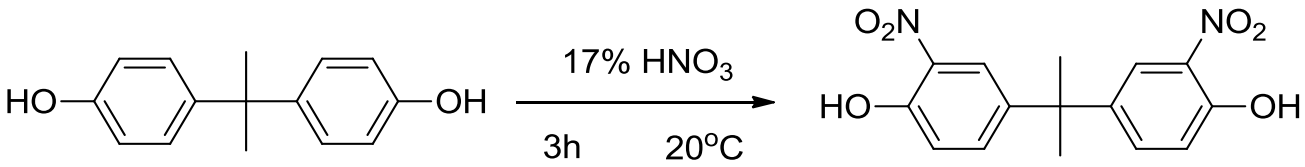

Figure 2.4 Synthesis of nitro substituted BisA

Molecular Weight: 318.28 g mol^{-1}

Experimental: To a 500 mL round bottom flask, 150 mL of 17% w/w aqueous HNO_3 was added, stirred with an egg shaped magnetic stir bar and cooled to 20°C. Bisphenol A (11.4 g, 0.05 mol) was added in 3.8 g increments with five minutes between additions. The reaction was allowed to gradually heat to room temperature and was reacted for 3 h. The reaction turned an opaque yellow during this time. After 3 h, the reaction mixture was poured into 300 mL of stirring DI water. The crude product was filtered and washed with 3 x 100 mL DI water. The crude product was collected and dissolved in toluene to afford a dark green solution. Column chromatography, using silica gel as the stationary phase, was performed on this solution with toluene as the eluent. A black band remained at the top of the column, while a dark yellow band eluted through the column. After the entire product was collected, toluene was evaporated to yield a yellow powder. The yellow powder was recrystallized in hot methanol to produce yellow crystals. The ^{1}H-NMR spectrum is shown below.

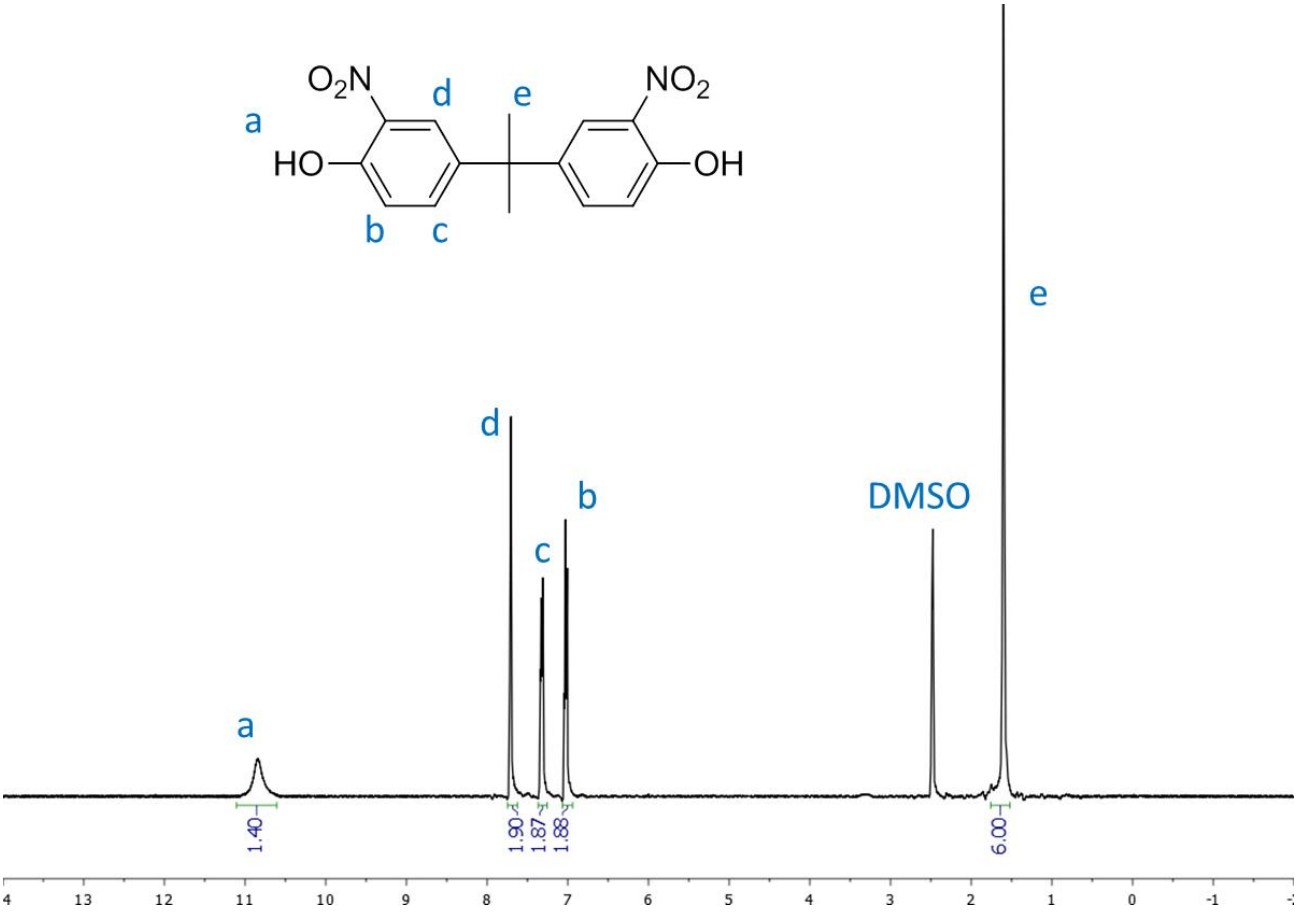

Figure 2.5 [1]H-NMR spectrum of nitro substituted Bisphenol A

2.3.2. *4,4'-(propane-2,2-diyl)bis(2-aminophenol) (Amine substituted BisA, BisAAP)*

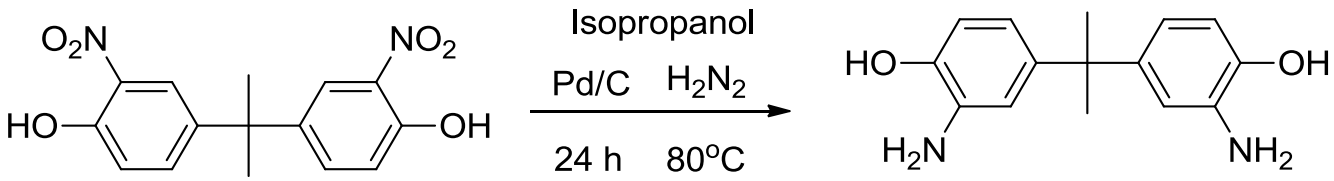

Figure 2.6 Synthesis of amine substituted BisAAP

Molecular Weight: 258.32 g mol^{-1}

Experimental: The reduction of nitrated bisphenol A was performed according to a reduction procedure previously published in our group.[3] A 500 mL three-necked round bottom flask was

equipped with a mechanical stirrer, condenser filled with isopropanol, and nitrogen inlet. Nitro substituted BisA (3.57 g, 0.011 mol) was added with 265 mL of isopropanol to the three-necked flask. The reaction mixture was stirred and brought to reflux. Once dissolved, 0.3 g of palladium on carbon was added, and then hydrazine hydrate (14.5 mL) was added drop wise via an addition funnel. After all of the hydrazine hydrate was added the reaction was refluxed for 2 h, then a second addition of 0.12 g of palladium on carbon was added. The reaction was stirred and refluxed at 80^{o}C overnight. The following morning, 0.24 g of activated charcoal was added to the reaction, and the reaction was then hot filtered over celite to yield a clear solution. The alcohol solvent was evaporated to afford white crystals of pure product. The melting point of the solid was 250^{o}C. Figure 2.7 shows the ^{1}H-NMR spectrum of BisAAP.

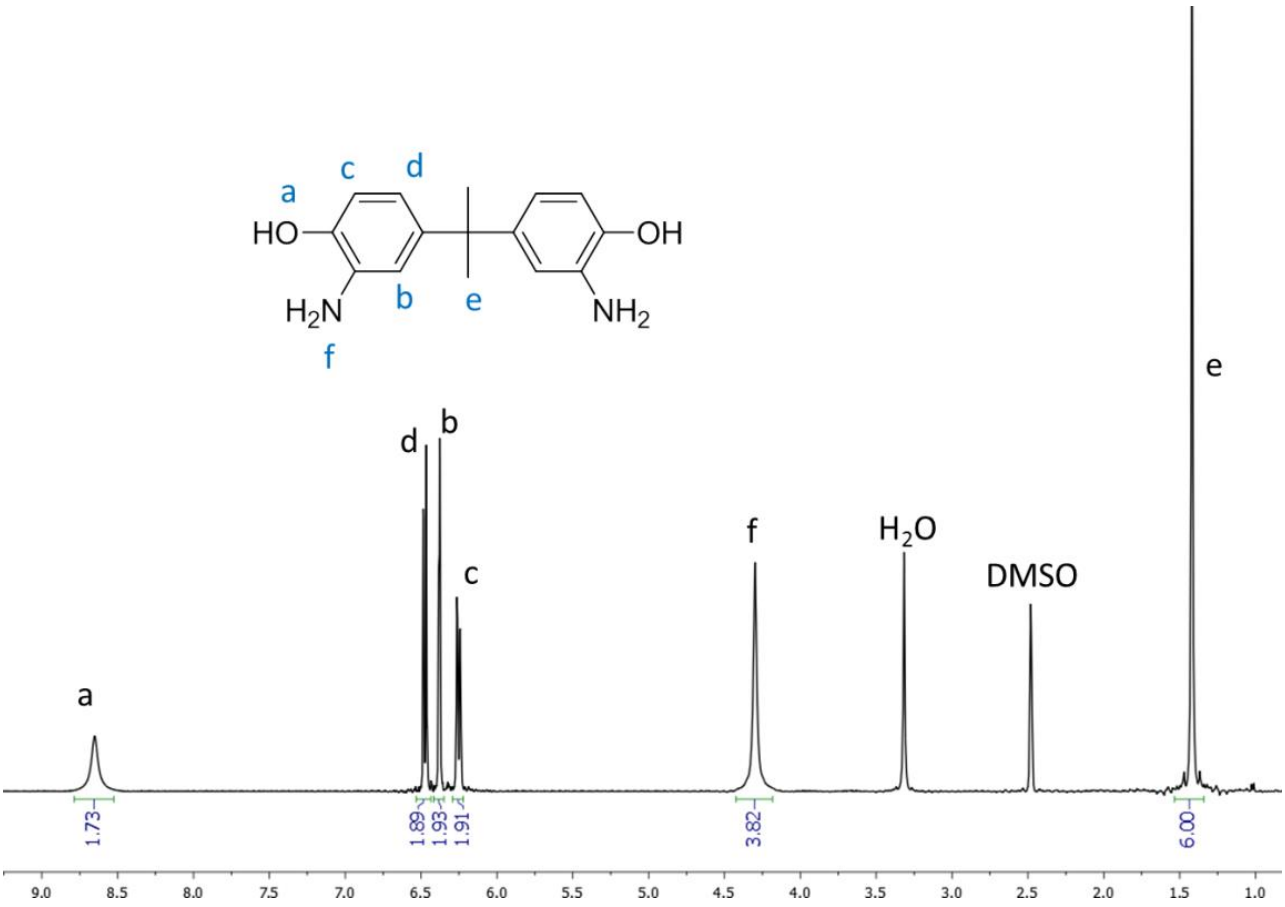

Figure 2.7 ^{1}H-NMR spectrum of BisAAP

2.3.3. *5,5'-(Propane-2,2-diyl)bis(2-(4-((4-chlorophenyl)sulfonyl)phenoxy)aniline) (Halide functionalized BisAAP premonomer, DCDPS-BisAAP-DCDPS)*

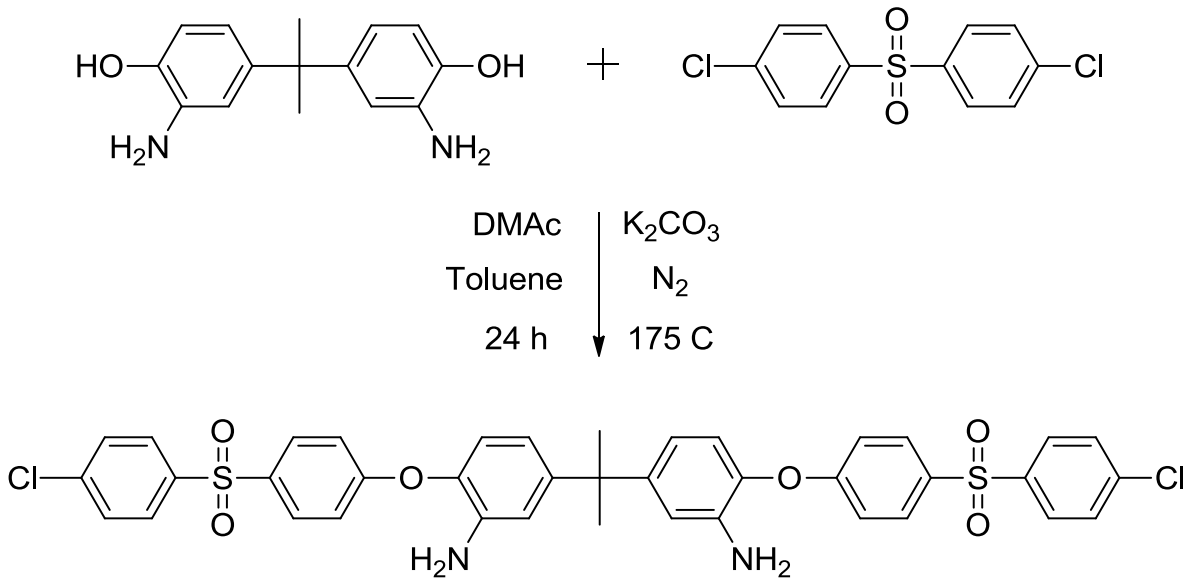

Figure 2.8 Synthesis of DCDPS-BisAAP-DCDPS

Molecular Weight: 759.72 g mol^{-1}

Experimental: To a 50 mL 3-necked flask, BisAAP (0.3000 g, 0.0012 mol), DCDPS (0.7337 g, 0.0026 mol) and K_2CO_3 (0.1927 g, 0.0014 mol) were added with distilled DMAc (4 mL). The reaction flask was equipped with a dean-stark trap filled with toluene, a mechanical stirrer and a nitrogen inlet. A thermocouple was used to regulate the oil bath, which was heated to 155^{o}C to dissolve BisAAP and DCDPS. Toluene (2 mL) was added as an azeotropic solvent to remove water, and the reaction was refluxed for 3 hours. After 3 hours, toluene was drained from the reaction and the oil bath was heated to 175^{o}C. The reaction was stirred at this temperature 12 h. The following day the dark brown solution was cooled to room temperature and filtered through a 1.0 μm syringe filter to remove salts. Additional DMAc (1 mL) was rinsed through the syringe

filter to ensure that the entirety of the product was collected. The product solution was precipitated directly into stirring DI water (100 mL) which afforded a white powder. The white powder was collected on an aspirator and dried in a convection oven at 70^{o}C overnight. The product is highly soluble in acetone, slightly soluble in toluene and insoluble in isopropanol or water. The ^{1}H-NMR of the crude product is shown in Figure 2.9. Both ^{1}H-NMR and thin layer chromatography (ethyl acetate:hexanes, 35:65 (v:v)) showed the presence of small amounts of side products and impurities, but sublimations and recrystallizations from acetone and toluene mixtures were ineffective in further purifying the product.

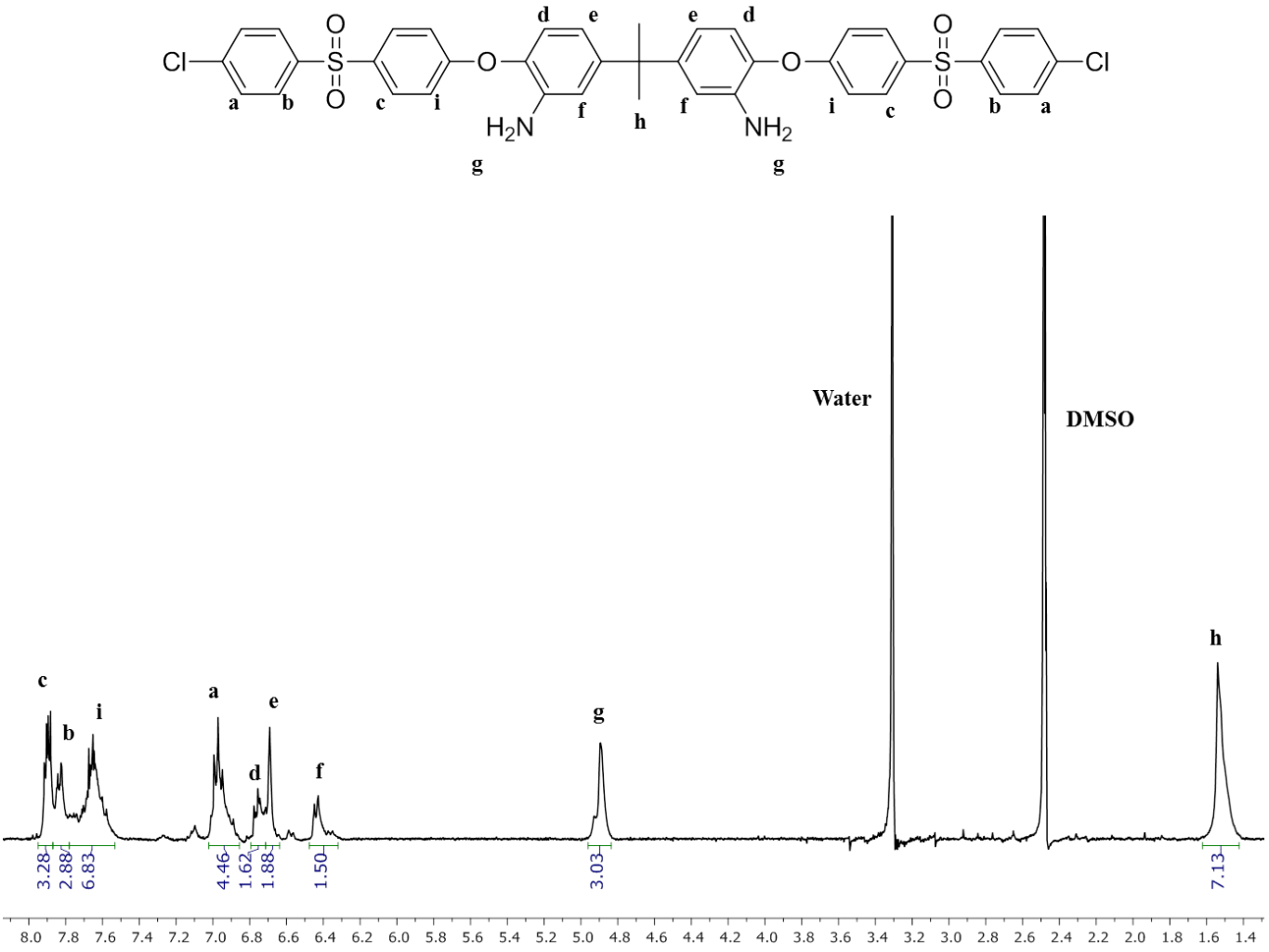

Figure 2.9 ^{1}H-NMR spectrum of DCDPS-BisAAP-DCDPS

2.3.4. *2,2-Bis(4-hydroxy-3,5-dimethylphenyl) propane (Tetramethyl bisphenol A, TMBPA)*

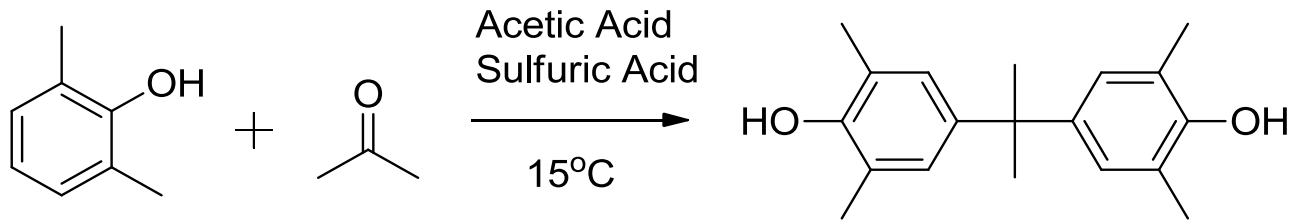

Figure 2.10 Synthesis of tetramethyl bisphenol A

Molecular Weight: 284.40 g mol^{-1}

Experimental: To a 250 mL three-necked flask fitted with a mechanical stirrer, 18.92 g (0.155 mol) of 2,6-xylenol was added with 7.103 g (0.122 mol) of acetone. This was cooled in an ice bath to 15°C and stirred. Using an addition funnel, 16.304 g (0.163 mol) of sulfuric acid mixed with 17.392 g (0.290 mol) acetic acid were added, the acid was cooled in an ice bath before addition. This was reacted overnight at room temperature. The reaction was diluted with 100 mL of water and 150 mL methylene chloride and then transferred to a separatory funnel. The organic layer was washed with water three times before collection. The methylene chloride layer was dried over magnesium sulfate overnight to yield a dry organic layer. Methylene chloride was then evaporated to give crude, slightly yellow product. The product was recrystallized from a 60:40 ethanol:water solution to obtain white crystals. The melting point of the recrystallized solid was 167-168°C, which agreed well with previous literature values. Figure 2.11 shows the ^{1}H-NMR spectrum of tetramethyl bisphenol A.

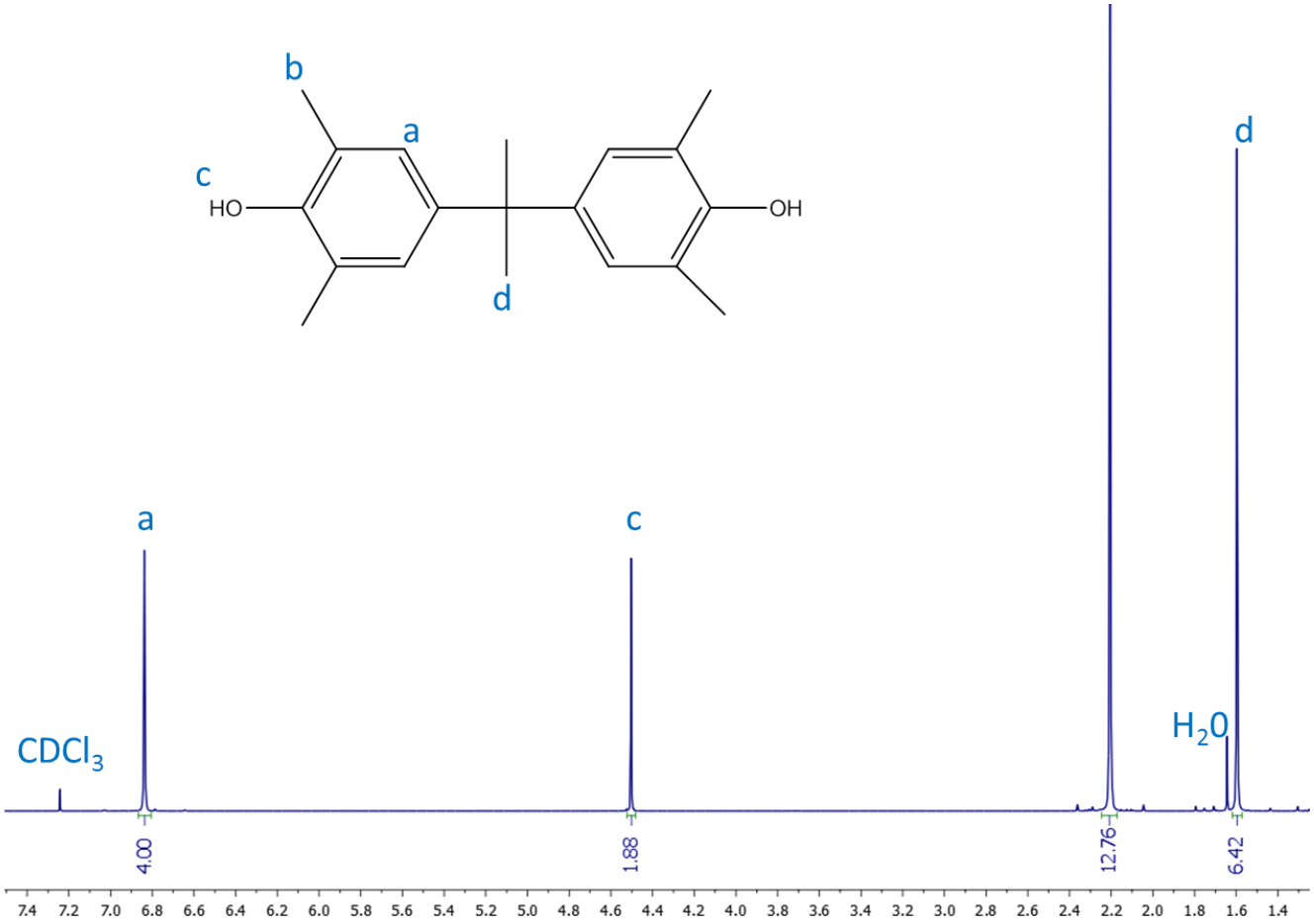

Figure 2.11 ^{1}H-NMR spectrum of tetramethyl bisphenol A

2.3.5. *4,4'-Methylenebis(2,6-dimethylphenol) (Tetramethyl bisphenol F, TMBPF)*

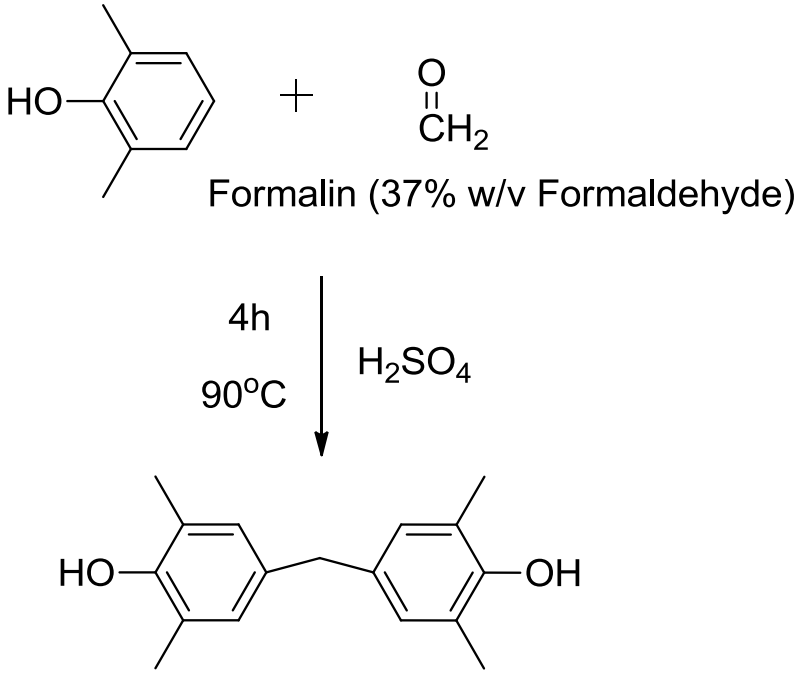

Figure 2.12 Synthesis of tetramethyl bisphenol F

Molecular Weight: 256.34 g mol^{-1}

Experimental: The synthesis of 4,4'-methylenebis(2,6-dimethylphenol), tetramethyl bisphenol F, hereafter referred to as TMBPF, was adapted from a traditional synthesis of a phenol-formaldehyde resin.[4] Excess 2,6-xylenol (415.83 mmol, 50.80 g) was added to a 250-mL three-necked flask equipped with a condenser, mechanical stirrer, and addition funnel. The 2,6-xylenol was heated in a thermocouple regulated oil bath to 90°C and stirred as it began to melt. Sulfuric acid (0.5 g) was added very slowly via the addition funnel, which changed the reaction solution to a dark pink color. The addition funnel was rinsed with DI water to ensure that all of the acid catalyst was transferred into the reaction flask. Formalin (37% by mass formaldehyde in H_2O, 15 mL) was added slowly via the addition funnel over the course of several hours. During this time

the reaction solution turned lighter in color and significantly more opaque. As product continued to form, the reaction mixture transformed from a liquid to a solid. The crude product was removed from the flask and filtered using an aspirator and washed with copious amounts of hot DI water. The crude product was dried at 70^{o}C and was recrystallized from MeOH to obtain white crystals. The melting point of the recrystallized solid was 177^{o}C, which was in the range of reported literature values. Figure 2.13 shows the ^{1}H-NMR spectrum of tetramethyl bisphenol F.

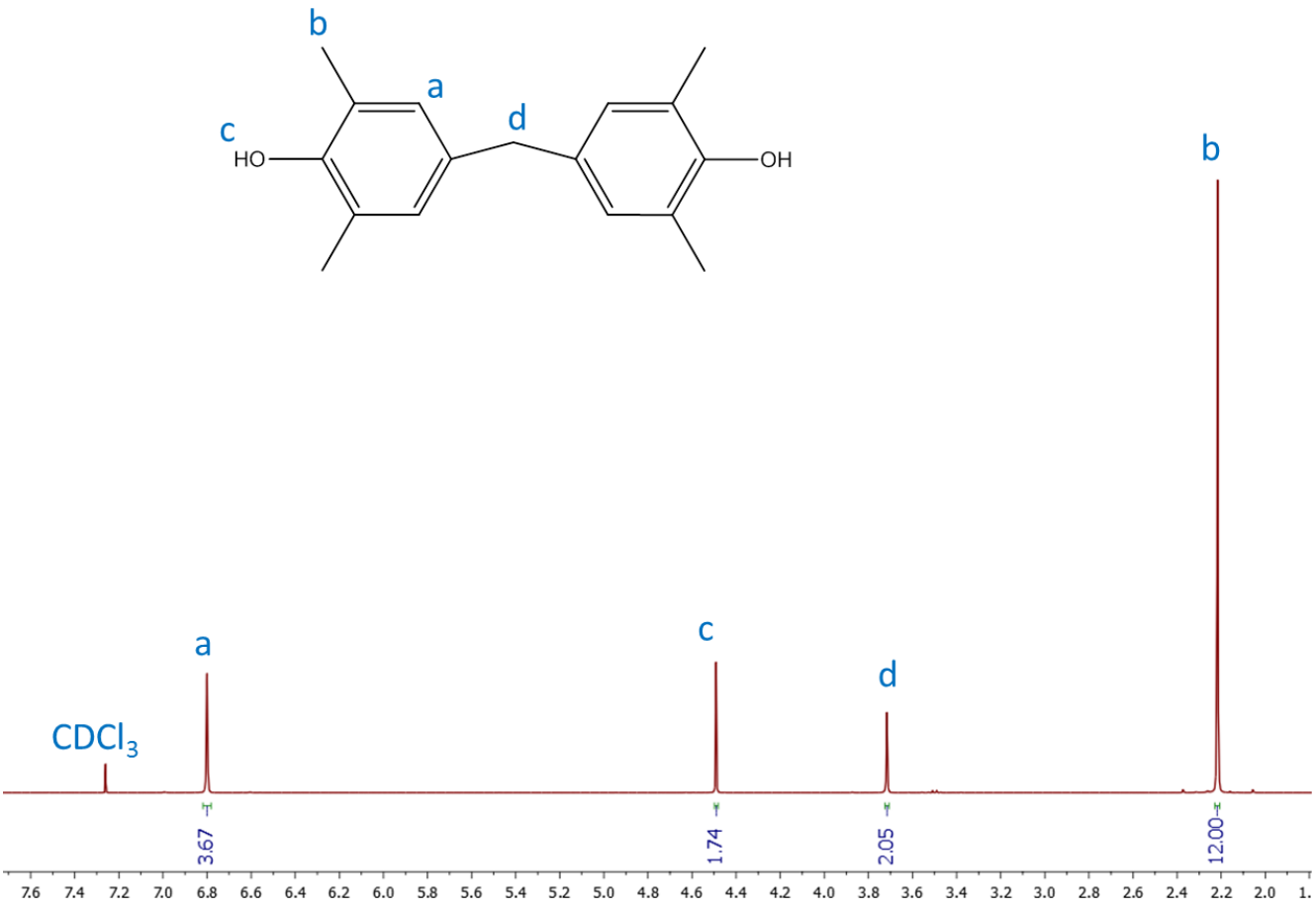

Figure 2.13 ^{1}H-NMR spectrum of tetramethyl bisphenol F

2.3.6. *4,4'-(2,2,2-Trifluoro-1-phenylethane-1,1-diyl)bis(2,6-dimethylphenol) (Tetramethyl bisphenol 3F-phenyl, 3F monomer)*

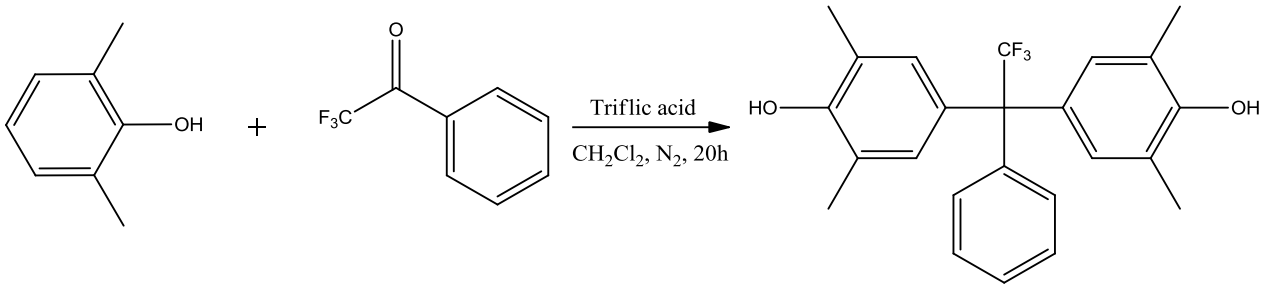

Figure 2.14 Synthesis of tetramethyl bisphenol 3F-phenyl

Molecular Weight: 400.43 g mol^{-1}

Experimental: Synthesis of the 3F monomer was adapted from a synthesis of 4,4'-(2,2,2-trifluoro-1-phenylethane-1,1-diyl)bisphenol.[5] To a 250-mL 4 necked flask, 2,6-xylenol (21.0476 g, 0.1723 mol) and 2,2,2-trifluoroacetophenone (5.0000 g, 0.0287 mol) were added to methylene chloride (34 mL). The flask was equipped with a condenser, mechanical stirrer, nitrogen inlet and addition funnel. The reaction was stirred at room temperature for the duration of the reaction. Trifluoromethanesulfonic acid (2.5352 g, 0.0169 mol) was added to the addition funnel and slowly dripped into the solution over 30 minutes. The solution quickly turned dark pink upon addition, and was a deep maroon color by the time all of the trifluoromethanesulfonic acid was added. The reaction was stirred overnight. The following day, methylene chloride was added to bring the final volume up to 50 mL. The product solution was transferred to a separatory funnel and 200 mL of DI water was added. The organic layer was extracted with the water, then with 100 mL of a 5 wt% $NaCO_3$ solution, and finally with 100 mL of DI water. The organic product layer was dried over sodium sulfate, filtered with an aspirator and evaporated to

obtain an off-white powder in high yield. Excess 2,6-xylenol may easily be disposed of by stirring the product in refluxing water, followed by hot filtration. The product was recrystallized from a 60:40, ethanol:water mixture. The melting point of the recrystallized solid was 163-165^{o}C, and this monomer was unreported in the literature. Figure 2.15 shows the ^{1}H-NMR spectrum of tetramethyl bisphenol 3F-phenyl.

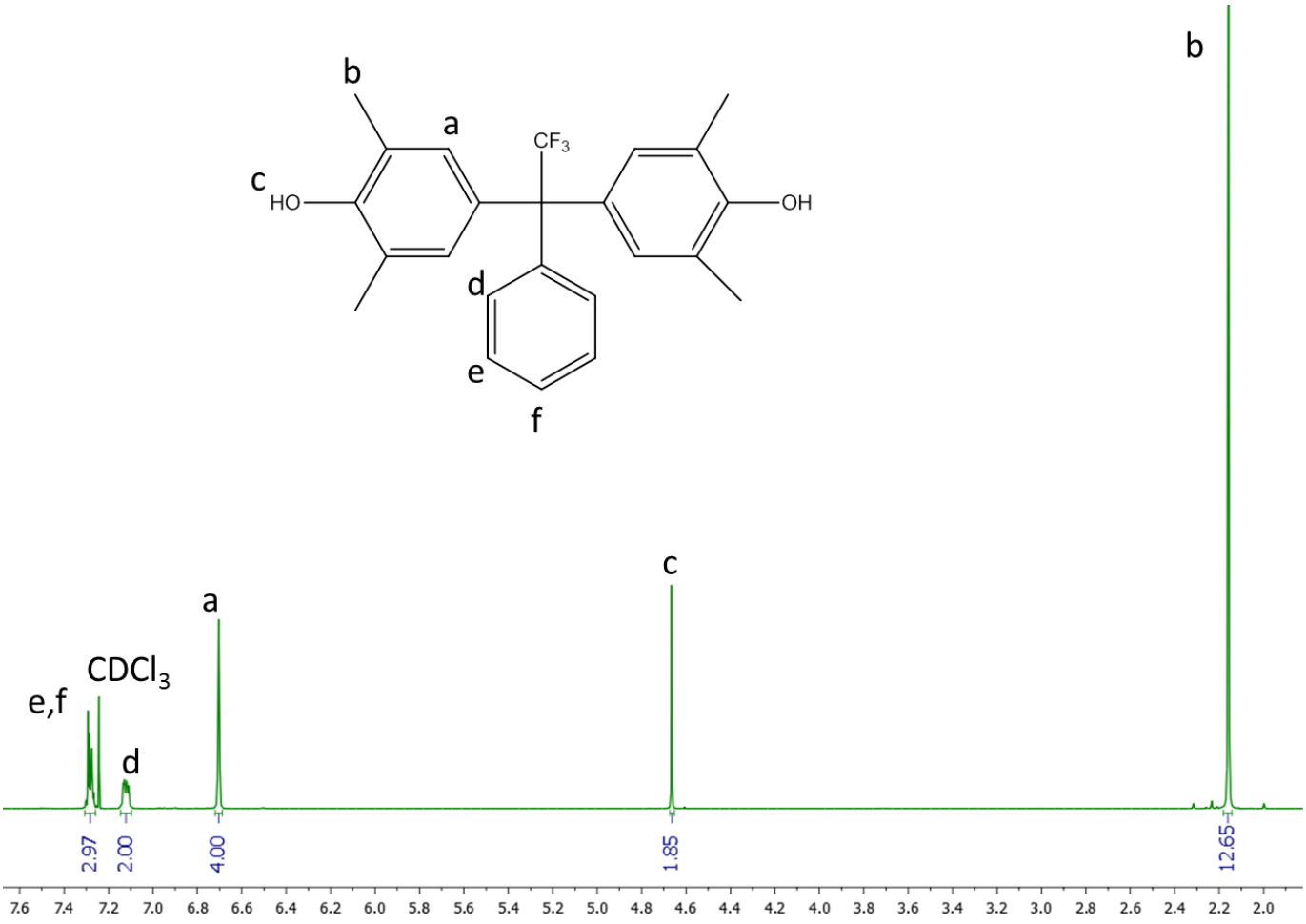

Figure 2.15 ^{1}H-NMR spectrum of tetramethyl bisphenol 3F-phen

2.3.7. *4,4'-Methylenebis(2,6-dimethylaniline) (Tetramethyl bisaniline F, MBDMA)*

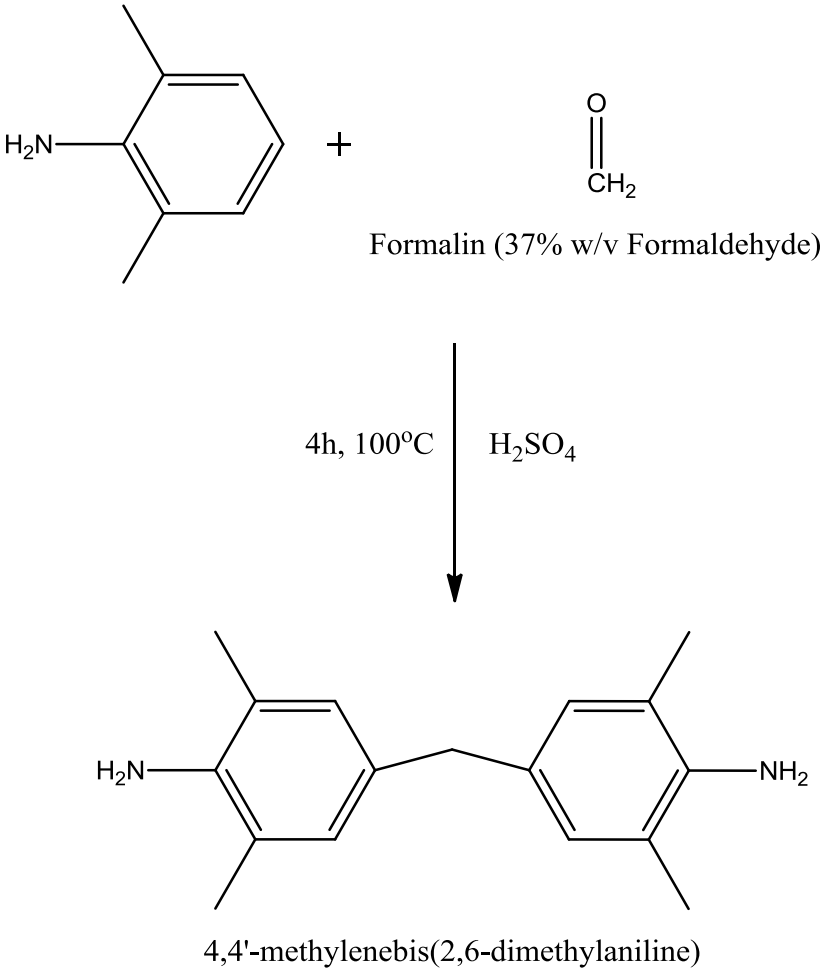

Figure 2.16 Synthesis of MBDMA

Molecular Weight: 254.37 g mol^{-1}

Experimental: The synthesis of 4,4'-methylenebis(2,6-dimethylaniline) (tetramethyl bisaniline F), hereafter referred to as MBDMA, was adapted from a traditional synthesis of a phenol-formaldehyde resin.[4] Excess 2,6-dimethylaniline (419.21 mmol, 50.80 g) was added to a 250-mL three-necked flask equipped with a condenser, mechanical stirrer, and addition funnel. The 2,6-

dimethylaniline was heated in a thermally regulated oil bath to 90^{o}C and stirred. Sulfuric acid (0.5 g) was added very slowly via the addition funnel, which made the reaction solution opaque. Formalin (37% by mass formaldehyde in H_2O, 15 mL) was added slowly via the addition funnel over the course of several hours; during this time, the reaction solution turned orange. As more product continued to form, the color changed from orange to a dark maroon and the reaction mixture transformed from a liquid to a viscous liquid/ partial solid. The addition funnel was removed and replaced with a 24/40 joint stopper. The reaction was allowed to stir for an additional 2.5 hours. The oil bath was heated to 110^{o}C and the mixture was stirred for 4 hours. After this last stage of reaction, the mixture was cooled to room temperature to yield a crude murky brown solid. The solid was extracted with DI water (700 mL) and diethyl ether (700 mL), which were transferred to a separatory funnel. Most of the product was contained in the organic layer, which was collected and set aside. The aqueous layer was washed with methylene chloride (200 mL), which was also collected and contained crude product. After sitting overnight, much of the organic phase had evaporated leaving crude product in the form of large yellow-brown crystals, shown in Figure 2.17.

Figure 2.17 Crude MBDMA crystals

Methylene chloride was also evaporated in the second organic layer which yielded darker, less pure product. The crude product was recrystallized from MeOH to obtain white crystals. Figure 2.18 shows the ^{1}H-NMR spectrum of MBDMA.

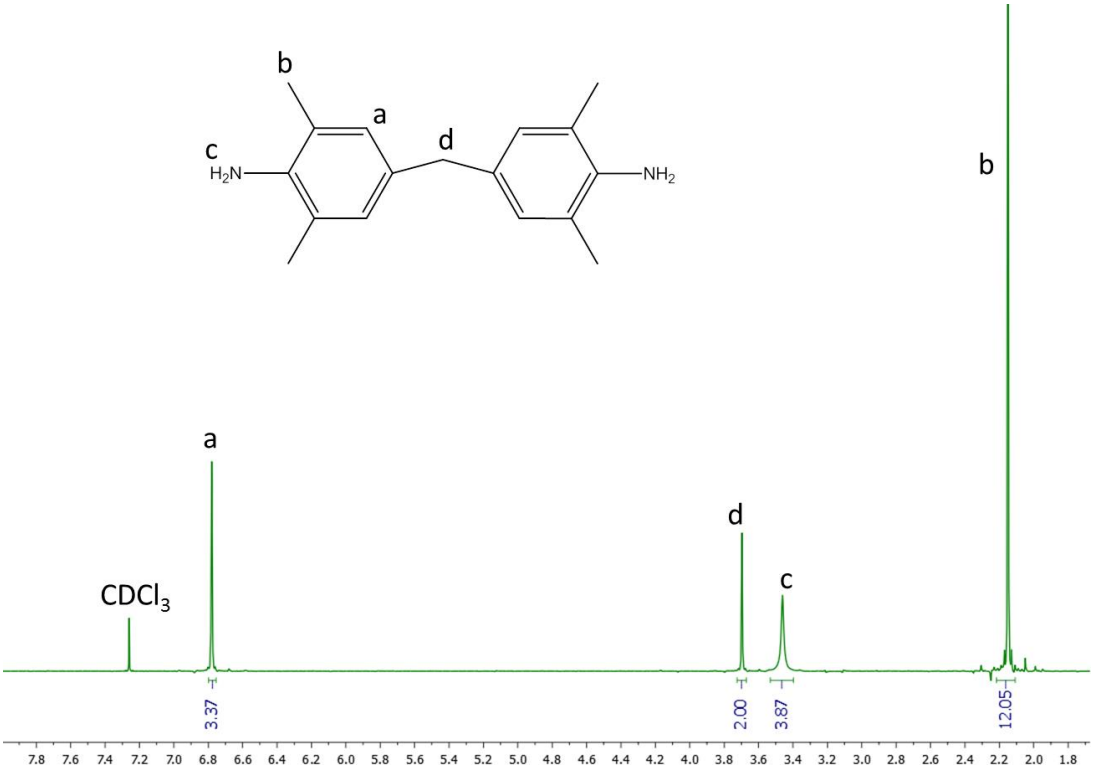

Figure 2.18 ^{1}H-NMR spectrum of MBDMA

2.3.8. *Disulfonated bis(4-(3-aminophenoxy)phenyl)sulfone (S-BAPS)*

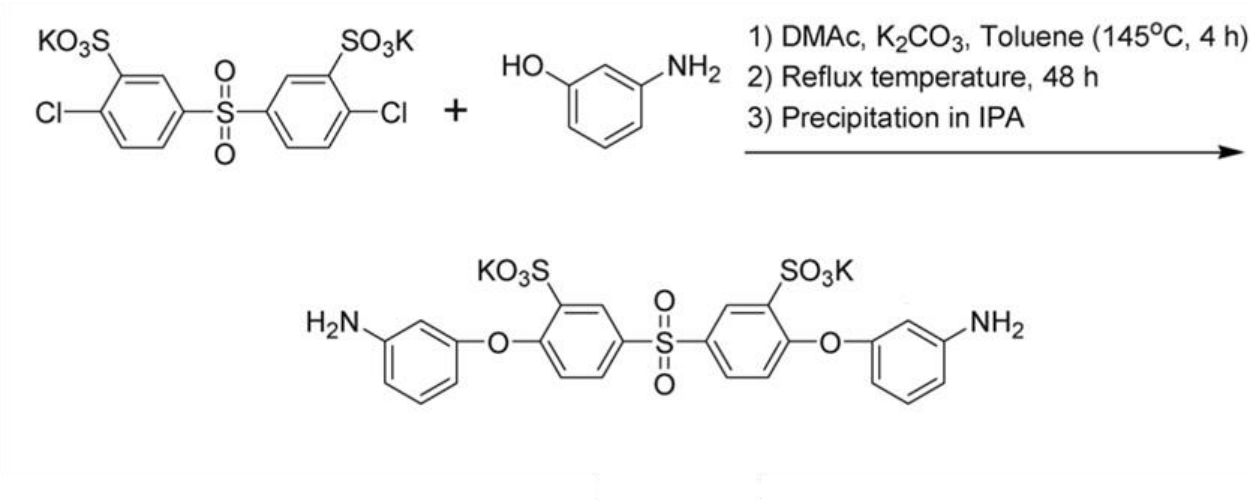

Figure 2.19 Synthesis of S-BAPS[6]

Molecular Weight: 668.80 g mol^{-1}

Experimental: SDCDPS and K_2CO_3 were dried at 160°C for several days under vacuum to ensure that all sorbed water was removed. SDCDPS (25.1923 g, 0.0500 mol) and *m*-AP (16.6134 g, 0.1507 mol) were added to a 250-mL 3 necked flask with distilled DMAc (120 mL). The reaction was equipped with a dean-stark trap filled with toluene, mechanical stirrer and nitrogen inlet. A thermally regulated oil bath was heated to 145°C while the reaction stirred. After reaching 145°C, K_2CO_3 (15.0426 g, 0.1088 mol) and toluene (60 mL) were added to the reaction which turned the solution an opaque white. The reaction was refluxed for 4 hours so that toluene could azeotropically remove any water given off by K_2CO_3 reaction with phenol. The temperature was then raised to 175°C and toluene was drained. The reaction mixture was light brown. The reaction was stirred at this temperature for two more days, during which it became noticeably darker in color. After 48 hours, the reaction was cooled to room temperature and filtered using an aspirator to remove salt byproducts. The amber, transparent filtrate was

precipitated drop wise from a separatory funnel into stirring IPA (1500 mL) to obtain an off-white solid powder. This powder was collected via filtration using an aspirator, dried under vacuum at 110^{o}C overnight and finally crushed with a mortar and pestle to obtain a gray/tan product powder. Figure 2.20 shows the ^{1}H-NMR spectrum of S-BAPS.

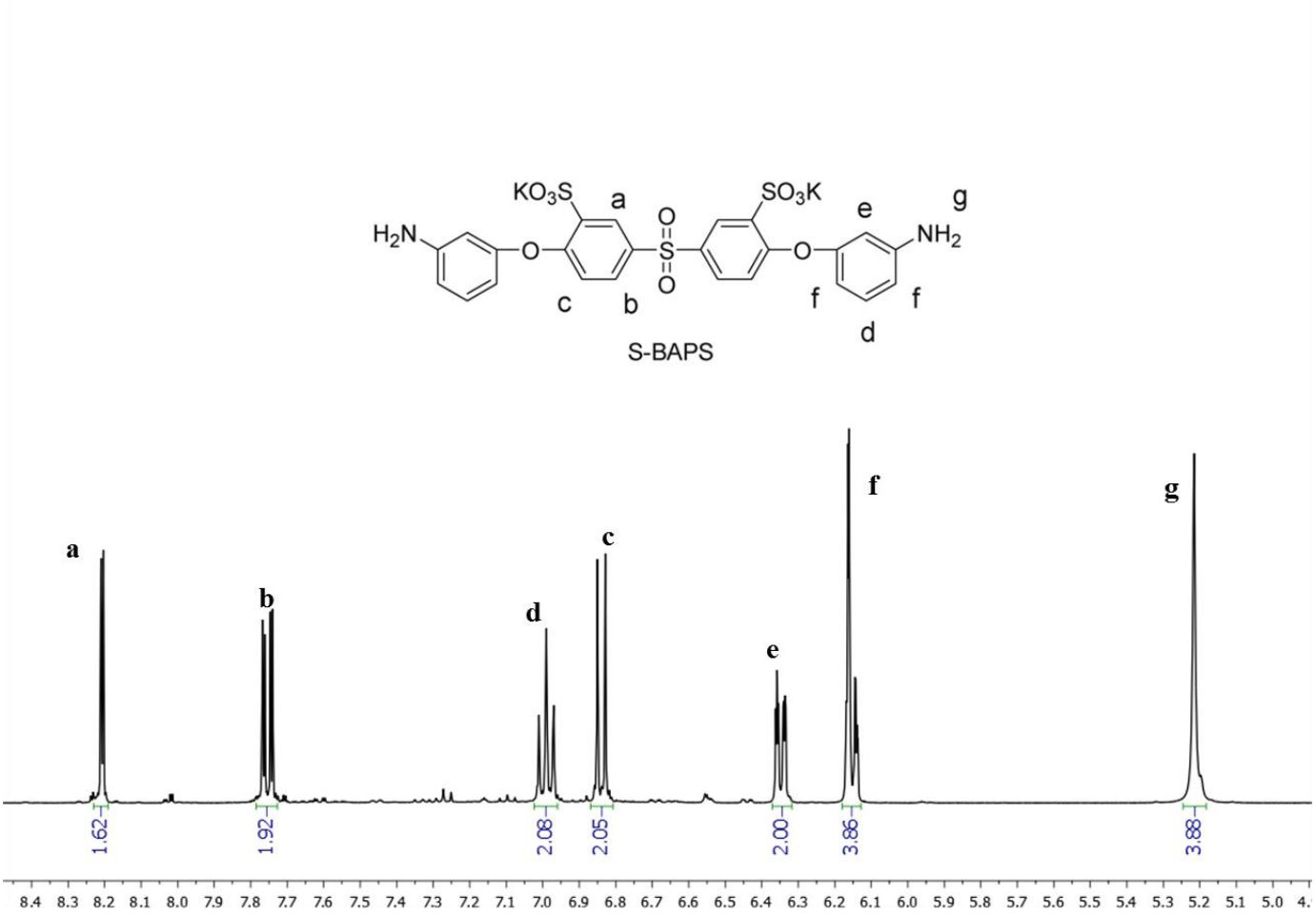

Figure 2.20 ^{1}H-NMR spectrum of S-BAPS

2.4. References

(1) Li, Y.; VanHouten, R. A.; Brink, A. E.; McGrath, J. E. Purity characterization of 3,3′-disulfonated-4,4′-dichlorodiphenyl sulfone (SDCDPS) monomer by UV–vis spectroscopy. *Polymer* **2008**, *49*, 3014.

(2) Paul, M.; Park, H. B.; Freeman, B. D.; Roy, A.; McGrath, J. E.; Riffle, J. S. Synthesis and crosslinking of partially disulfonated poly(arylene ether sulfone) random copolymers as candidates for chlorine resistant reverse osmosis membranes. *Polymer* **2008**, *49*, 2243.

(3) Farr, I. V.; Kratzner, D.; Glass, T. E.; Dunson, D.; Ji, Q.; McGrath, J. E. The Synthesis and Characterization of Polyimide Homopolymers Based on 5(6)-Amino-1-(4-aminophenyl)- 1,3,3-trimethylindane. *J. Polym. Sci., Part A: Polym. Chem.* **2000**, *38*, 2840.

(4) *Macromolecular Synthesis*; John Wiley & Sons: New York, **1977**; Vol. 1.

(5) Grubbs, H. J., Virginia Polytechnic Institute and State University, **1994**.

(6)Xie, W.; Geise, G. M.; Freeman, B. D.; Lee, H.-S.; Byun, G.; McGrath, J. E. Polyamide interfacial composite membranes prepared from m-phenylene diamine, trimesoyl chloride and a new disulfonated diamine. *J. Membr. Sci.* **2012**, *403-404*, 152.

CHAPTER 3: CROSSLINKING DISULFONATED POLY(ARYLENE ETHER SULFONE) TELECHELIC OLIGOMERS PART 1: SYNTHESIS, CHARACTERIZATION AND MEMBRANE PREPARATION

Benjamin J. Sundell [a], Kwan-soo Lee [a], Ali Nebipasagil [a], Andrew Shaver [a], Joseph R. Cook [b], Eui-Soung Jang [b], Benny D. Freeman [b], James E. McGrath [a]

[a] Macromolecules and Interfaces Institute, Virginia Polytechnic Institute and State University, Blacksburg, VA 24061, USA

[b] Department of Chemical Engineering, Center for Energy and Environmental Resources, The University of Texas at Austin, Austin, TX, 78758, USA

From Ind. Eng. Chem. Res.2014, 53, 2583. Used with permission of American Chemical Society, 2014.

3.1. Abstract

meta-Aminophenol was used during nucleophilic step copolymerization to endcap partially disulfonated bisphenol-A based random copolymers with controlled oligomeric molecular weights. The amine endgroups were thermally reacted with a tetrafunctional epoxy reagent to produce networks. Very high gel fractions, up to 99%, and ductile film formation were achieved. The oligomer was further functionalized with acryloyl chloride, phenylethynyl phthalic anhydride, and maleic anhydride to obtain several novel free radically crosslinkable oligomers. The structure and molecular weights (M_n) were established with ^{1}H NMR spectroscopy of the oligomers and endgroups. Thermogravimetric analysis demonstrated the

high thermal stability of these oligomers, DSC investigations showed that the oligomers had curing exotherms from 140°C to 330°C and that residual casting solvent during crosslinking was necessary to avoid vitrification during membrane formation. In addition to the thermally crosslinkable systems, photo-crosslinking was demonstrated with the telechelic acrylamide functionalized oligomers. Two compositions were identified as potential candidates for further development. Crosslinking disulfonated poly(arylene ether sulfone) copolymers limits the high water sorption and swelling of these hydrophilic materials, which enhances several properties for membrane applications. Initial transport results indicate that crosslinking greatly reduces salt permeability while modestly decreasing water permeability, resulting in improved water/NaCl selectivity.

3.2. Introduction

More than two billion people live with inadequate freshwater resources as a result of either physical or economic water scarcity.[1,2] This problem will be further exacerbated by rising population levels, which will necessitate the production of potable drinking water from alternative sources. Seawater accounts for 97% of the water on Earth and can be desalinated by methods such as multi-stage flash distillation and reverse osmosis (RO). The energy required for RO is now approaching theoretical minimums, resulting in its dominance for seawater desalination.[3,4]

The most critical component of the RO process is the polymeric membrane, often fabricated into thin asymmetric films.[2] These membranes have high salt rejection, high water flux, chemical resistance and satisfy many other requirements.[5-7] The state-of-the-art material for RO is a highly crosslinked aromatic polyamide, initially reported in 1980.[7-9] A major

shortcoming of this polymer is susceptibility to degradation by chlorinated disinfectants, which attack the amide bond and degrade the membrane by various mechanisms.[10-13] The seawater feed must be treated with disinfectant to reduce biofouling and the freshwater permeate should also contain chlorine to act as a biocide.[14,15] Somewhat more chlorine resistant cellulosic membranes have been demonstrated, but they exhibit significantly lower salt rejection than the state-of-the-art crosslinked aromatic polyamides.[16] Thus, it is an important goal to identify a desalination membrane with high chlorine tolerance while maintaining state-of-the-art transport properties.

Poly(arylene ether sulfone)s demonstrate both high chemical inertness and suitable mechanical properties for RO.[17,18] Sulfonation imparts hydrophilicity to these otherwise hydrophobic polymers.[19,20] The first sulfonation routes were post-polymerization reactions that resulted in side reactions and difficulties in controlling the extent of sulfonation .[21,22] McGrath et al. and Ueda et al. synthesized linear sulfonated polysulfones directly from a disulfonated monomer[23] and demonstrated high molecular weights.[24,25] The sulfonated copolymers showed high chlorine resistance in accelerated tests with modest levels of salt rejection and high water flux.[26] Recent fundamental studies of these linear copolymers have investigated the tradeoff between salt rejection and permeability,[27-29] effect of free volume on transport properties,[30] influence of processing history, and the ability to fabricate these materials into thin-film composite membranes.[31,32] Polymers with higher levels of sulfonation were more hydrophilic and had higher water flux. However, the ionic regions swelled significantly in water, leading to increased salt diffusion and lower salt rejection.

Crosslinked networks limits the swelling associated with increased levels of sulfonation.[33] Electrostatic physical crosslinking of polysulfones can be accomplished by

incorporating complementary acidic and basic units in the polymer backbone.[34-37] However, covalent crosslinks are less environmentally sensitive[38,39] and are more stable in an RO environment. Polysulfones have also been covalently crosslinked along the backbone of the polymer chain. Early work involved activation with diimidazole,[40] disproportionation of acid,[41] or S-alkylation of sulfinate groups,[42,43] all of which consumed sulfonate groups. More recently, main chain crosslinking was accomplished by reacting pendant hydroxyl groups with dihaloalkanes,[44] sulfonic acid groups with poly(vinyl alcohol),[45] and thermally curable allylic groups.[46] An alternative method to produce covalently crosslinked polysulfones synthesized oligomers with telechelic endgroups and then linked together chain ends into a network. One advantage of this approach is that oligomeric materials are more soluble and easily processed than their high molecular weight counterparts.[47] Several oligomers have been synthesized including thermally curable ethynyl,[47,48] allyl[49] and propargyl[49] endgroups, but with varying backbone structures and acidified forms for investigation as fuel cell materials. The first desalination studies with telechelic oligomers involved the crosslinking of phenoxide endgroups with a tetrafunctional epoxide.[33] Gel fractions up to 85% were obtained, and the reduced swelling drastically improved the desalination properties of these materials.

The present investigation has developed the synthesis of a novel sulfonated polysulfone oligomer with telechelic amine end groups. In addition, this amine terminated oligomer was used to synthesize acrylamide, 4-phenylethynyl phthalimide and maleimide termination with a constant polymer backbone structure. The properties of these materials as a function of crosslinking conditions and film fabrication were investigated and reported in this paper. The need for residual casting solvent during oligomeric crosslinking to reduce the T_g of these polymeric glasses was affirmed. Two oligomers capable of large-scale ductile film formation

were identified for further development. The acrylamide terminated oligomers were also photochemically initiated to afford crosslinking at room temperature, a first for sulfonated polysulfone oligomers. The amine terminated oligomers were crosslinked to over a 99% gel fraction. This value is the highest reported value for such sulfonated polysulfone oligomers. Initial transport results demonstrate that water/NaCl selectivity is drastically improved as a function of crosslinking, especially at high gel fractions. This paper, part I, focuses on the synthesis, characterization and fabrication of these crosslinkable materials; part II is investigating the influence of crosslinking, degree of sulfonation and oligomer backbone structure on water transport properties and will be reported later.

3.3. Experimental

Materials

4,4'-(propane-2,2-diyl)diphenol (BisA) and 4,4'-dichlorodiphenylsulphone (DCDPS, 99%) were kindly provided by Solvay and recrystallized from toluene before use. The 3-aminophenol (*m*-AP, 99%) monomer and *N*,*N*-dimethylacetamide (DMAc, 99%) were purchased from Acros Organics. The DMAc reaction solvent was dried with calcium hydride (CaH_2), distilled under reduced pressure and stored under molecular sieves before use. Calcium hydride (90-95%) was purchased from Alfa Aesar. Casting solvents for film preparation were used as received. *N*,*N*-dimethylformamide (DMF) was purchased from Spectrum. Akron Polymer Systems (Akron, OH) kindly provided 4-phenylethynylphthalic anhydride (4-PEPA) and 3,3-disulfonated-4,4'-dichlorodiphenylsulphone (SDCDPS, 98%) prepared using procedures developed earlier.[50,51] 1,2-dichlorobenzene (*o*-DCB, anhydrous), 2-propenoyl chloride (acryloyl chloride, 96%), triethylamine (TEA, 99.5%), potassium carbonate (K_2CO_3, 99%), maleic

anhydride (99%), 2,2'-azobis(2-methylpropionitrile) (AIBN, 98%), pentaerythritol tetraacrylate (PETA), 2,2-dimethoxy-2-phenylacetophenone (DMPA, 99%), triphenylphosphine (TPP, 99%) and tetraglycidyl bis(p-aminophenyl)methane (TGBAM, 92%[33]) were purchased from Aldrich. Toluene, cyclohexane, 2-propanol (IPA), 1-methyl-2-pyrrolidone (NMP) and bis(1-methyl-1-phenylethyl) peroxide (DCP, 99%) were purchased from Fisher Scientific.

Synthesis

Synthesis of a controlled 5,000 molecular weight (M_n) amine-endcapped bisphenol A based 50% disulfonated polysulfone copolymer (am-BisAS50)

The precursor oligomer (Fig. 1.) was produced by nucleophilic aromatic substitution step polymerization,[52,53] which directly incorporated the sulfonated monomer into the backbone.

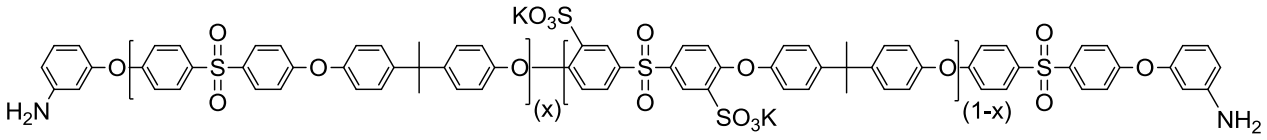

Figure 3.1 Structure of amine-endcapped bisphenol A based 50% disulfonated polysulfone copolymer

Prior to the reaction, it was necessary to dry the hydroscopic SDCDPS for 72 h at 160°C under vacuum to ensure removal of moisture. SDCDPS contains some NaCl impurities remaining from monomer synthesis, which were quantified using UV-visible light spectroscopy.[51] BisA (43.6 mmol, 9.9534 g), DCDPS (25 mmol, 7.1790 g), SDCDPS (25 mmol, 12.6611 g), *m*-AP (12.7 mmol, 1.3999 g), and DMAc (130 mL) were added to a 250-mL three-necked flask. The reaction flask was equipped with a mechanical stirrer, nitrogen inlet, and Dean-Stark trap filled with toluene. A stirring, thermocouple regulated, oil bath was used to heat the reaction mixture to 155°C. After the bath temperature reached 155°C, K_2CO_3 (78.48 mmol, 10.8467 g) was added with toluene (65 mL). The reaction was stirred at 155°C until all water was azeotropically

removed with toluene. The temperature was then increased to 175°C and water and toluene were drained. After 48 h, the amber opaque solution was cooled to room temperature and filtered. The resulting transparent solution was precipitated in isopropyl alcohol (IPA) as a white solid. The copolymer was filtered, washed with IPA, and dried in a vacuum oven at 120°C for one day.

Conversion of amine-endcapped oligomers to acrylamide-endcapped oligomers (AA-BisAS50)

Am-BisAS50 (0.517 mmol, 3.000 g) was dissolved in DMAc (45 mL) in a 100-mL round bottom flask. The flask was sealed with a septum and flushed with nitrogen and placed in an ice bath. Triethylamine (TEA, 10 mmol, 0.5856 g) was added via syringe as an acid scavenger. An excess of acryloyl chloride (3.47 mmol, 0.3143 g) dissolved in DMAc (5 mL) was added slowly via syringe, resulting in an opaque solution. The reaction was allowed to proceed for 4 h. Polymer isolation and drying was the same as described earlier.

Conversion of amine-endcapped oligomers to 4-phenylethynl phthalic anhydride-endcapped oligomers (PEPA-BisAS50)

4-PEPA terminated oligomers were synthesized via a two-step amic-acid route previously reported for the synthesis of polyetherimides.[54] The am-BisAS50 (2.08 mmol, 10.000 g) was dissolved in DMAc (67 mL) in a 250-mL three-necked flask. The reaction flask was equipped with a mechanical stirrer, nitrogen inlet and Dean-Stark trap. The solution was heated to 130°C, and cyclohexane (22 mL) was added and refluxed for 4 h. The trap was drained and the flask was cooled to room temperature. 4-PEPA (4.38 mmol, 1.086 g) was added and stirred for 3 h, resulting in a pale yellow solution. For cyclodehydration, the trap was filled with *o*-DCB, and additional *o*-DCB (15 mL) was added directly to the flask. The temperature was increased to

150°C for 30 min, then to 180°C for 24 h. Polymer isolation and drying was the same as described earlier.

Conversion of amine-endcapped oligomers to maleic anhydride-endcapped oligomers (MA-BisAS50)

Reactions to afford maleimide terminated oligomers involved a two-step amic-acid route, previously reported.[55] The reaction conditions and apparatus were similar to those used for the synthesis of PEPA-BisAS50. The am-BisAS50 (1 mmol, 5 g) was dissolved in DMAc (50 mL), then maleic anhydride (3 mmol, 0.2942 g) was added and stirred for 6 h. The reaction was heated to 130°C, the final reflux temperature and cyclodehydrated at 130°C with *o*-DCB (10 mL) overnight. Product isolation and drying was the same as described earlier.

Film casting and curing

Amine terminated oligomers

A mixture of am-BisAS50 (0.1633 mmol, 0.8 g), TGBAM (0.4083 mmol, 0.1917 g) and TPP (0.0187 mmol, 0.0049 g) were dissolved in DMAc (12 mL) and stirred until a homogenous solution was obtained. The solution was syringe filtered through a 0.45 μm PTFE filter. It was cast on a clean glass plate on a level surface inside a vacuum oven and dried under vacuum for 2 h at 100°C. Vacuum was released, and the oven was heated to the crosslinking temperature (150-160°C) for 90 min.

4-Phenylethynl phthalimide terminated oligomers

The PEPA-BisAS50 (0.36 mmol, 1.8 g) was dissolved in NMP (15 mL) and stirred until a homogenous solution was obtained. The solution was syringe filtered through a 0.45 μm PTFE and sonicated for two 60 min cycles to facilitate removal of dissolved gas. A glass plate was wrapped with aluminum foil to reduce adhesion of the cured membrane to the glass surface. The oligomeric solution was cast on this surface, placed on a level hot plate and covered with a glass dish that contained a nitrogen inlet and outlet. A nitrogen flow was applied, and the plate was heated to 180^{o}C. The hot plate was held at this temperature until the solution could no longer flow. The hot plate was then slowly heated to a temperature of 360^{o}C where it was cured for one hour.

Maleimide terminated oligomers

MA-BisAS50 (0.16 mmol, 0.8 g) was dissolved in DMAc (12 mL) and stirred until a homogenous solution was obtained. The solution was syringe filtered through a 0.45 μm PTFE and sonicated for two 60 min cycles to facilitate removal of dissolved gas, cast on a clean glass plate and dried under an infrared lamp until it could no longer flow. The membrane was then inserted into a forced air oven (Type 47900 Furnace, Thermolyne) at 300^{o}C under a nitrogen atmosphere. The film was cured for 1 h at this temperature.

Acrylamide terminated oligomers

The AA-BisAS50 (0.2 mmol, 1.000 g), PETA (0.1 mmol, 0.035 g) and DMF (2 mL) were stirred thoroughly to form a homogeneous mixture. DMPA UV initiator (2 wt. % of total mass, 15-20 mg) was added into the mixture and stirred thoroughly. The solution was cast on a 5

x 7.5 cm glass slide and placed in a Spectronics Corp. model XL-1000 UV crosslinker three times for 360 s to achieve photo-crosslinking. The typical intensity of the UV irradiation was between 3,500-4,500 $\mu W\ cm^{-2}$.

Polymer Characterization

Nuclear magnetic resonance spectroscopy (NMR)

^{1}H-NMR analysis of the oligomers was performed on a Varian Unity Plus spectrometer and a Varian Inova spectrometer, both operating at 400 MHz. The spectra of the oligomers were obtained from a 15% (w/v) 1 mL solution in DMSO-d_6.

Thermogravimetric analysis (TGA)

Thermal stability of the polymers in the range of their curing temperatures was probed using a TGA Q500 (TA Instruments). The samples were heated to at least 150°C and held isothermally for 10 min to remove any ambient water, then heated to 500°C at 10°C min^{-1} under nitrogen.

Differential scanning calorimetry (DSC)

The glass transition temperatures (T_g) and curing exotherms of the oligomers were obtained with a DSC Q200 (TA Instruments). The effect of solvent plasticization of the curing temperature was investigated with oligomers that were solution cast, dried until the material would not flow and collected into high volume pans capable of withstanding high pressures (TA Instruments). The solvent plasticized oligomers were heated at 10°C min^{-1} to 300°C. Baseline

corrections were applied to the heating curves obtained for the solvent plasticized oligomers, and thus the first derivative of the heating curve was used to quantify T_g's and cure temperatures.

Water uptake

Films were dried at 120°C under vacuum overnight, then removed and weighed to obtain the dry weight (W_{dry}). Next, they were immersed in DI water for at least 48 hours. The films were removed, quickly blotted dry to remove any water droplets and weighed to obtain the wet weight (W_{wet}). Water uptake values were calculated by equation 1.

$$Water\ Uptake\ (\%) = \frac{W_{wet} - W_{dry}}{W_{dry}} \times 100 \quad \text{Eq. 1}$$

Gel fractions

Gel fractions were performed to estimate the extent of crosslinking. Crosslinked films were dried at 120°C under vacuum overnight. Then 0.1-0.2 g of initial sample was placed in a 20 mL scintillation vial filled with DMAc and stirred at 100°C overnight. The remaining solid was filtered, transferred to a pre-weighed vial, and dried at 120°C under vacuum overnight. The final weight was taken the next day. Gel fraction values were calculated by equation 2.

$$Gel\ Fraction\ (\%) = \frac{W_{initial} - W_{final}}{W_{final}} \times 100 \quad \text{Eq. 2}$$

Initial Investigations of Water Transport Properties

The water permeability (L μm m^{-2} h^{-1} bar^{-1} or cm^2 s^{-1}), salt permeability (cm^2 s^{-1}), salt rejection (%) and water/NaCl selectivity were determined at 25°C in a previously described cross-flow filtration system using stainless steel crossflow cells machined at the University of

Texas at Austin.[56] The pressure difference across the membrane (15.1 cm^2) is listed in Table 1. The aqueous feed contained 2000 ppm NaCl, and the feed solution was circulated past the samples at a continuous flow rate of 3.8 (L min^{-1}). The feed pH was adjusted to a range between 6.5 and 7.5 using a 10 g/L sodium bicarbonate solution. NaCl concentrations in the feed water and permeate were measured with an Oakton 100 digital conductivity meter.

3.4. Results and Discussion

Oligomer Synthesis

The bisphenol monomer used was BisA instead of 4,4'-biphenol (Fig. 2.). BisA is more chemically reactive than 4,4'-biphenol, and contains the 2,2'-isopropylidene moiety in the middle of the molecule. This tetrahedral bond linkage leads to a lower density copolymer compared to a copolymer containing the less flexible 4,4'-biphenol. For example, the density of BisA polysulfone (Udel®) is lower than that of 4,4'-biphenol based polysulfone (Radel®). Initial unreported work in our group supports that this phenomenon remains true for the sulfonated copolymers. The lower density of BisA copolymers should lead to higher fractional free volume and thus more volume available for water transport.[30] The fractional free volume has been related mathematically to diffusion and permeability coefficients.[5]

Figure 3.2 Bisphenol A (left) and 4,4'-biphenol (right)

The synthesis of am-BisAS50 shown in Fig. 3 was performed using nucleophilic aromatic substitution with a weak base.[52] A monofunctional amine *m*-AP was added in amounts calculated by the modified Carothers equation[57] to target a number average molecular weight of 5,000 g mol^{-1} and to provide functional aromatic amine endgroups. Previous telechelic

oligomers were synthesized by adding an excess of the diphenol, which produces a relatively unstable *p*-phenoxide terminated species. Thus, the *m*-AP endgroup greatly extends the shelf life of these oligomers.

Toluene was used as the azeotropic solvent, removing any water sorbed by the monomers during weighing and also water formed by K_2CO_3 decomposition products. The water/toluene azeotrope appeared as a cloudy layer in the condenser of the Dean-Stark trap. Refluxing was continued until no more water was observed in the distillate. During the azeotropic period of the reaction, it was important to periodically use a heat gun to dry the joints connecting the three-necked flask to the Dean-Stark trap. The temperature was raised slowly to the final reaction temperature by heating the oil bath to 175^{o}C, and then toluene was slowly removed until the initial charged volume was collected. The reaction appeared unchanged in viscosity after 24 h and slightly more viscous after 48 h. Since the molecular weight of these copolymers was targeted at 5,000 g mol^{-1}, no drastic change in viscosity was anticipated or observed. The solution appeared off-white or wheat colored near the reactions end, compared to BisA phenoxide endgroups that impart a dark green color to the solution.

The nucleophilic substitution reaction that converted am-BisAS50 to AA-BisAS50 (Fig. 3) occurred very rapidly; thus, the reaction flask was cooled to 0^{o}C before addition of TEA and acryloyl chloride. The am-BisAS50 was dried overnight under vacuum to remove ambient water sorption, as water could also react with the acryloyl chloride.

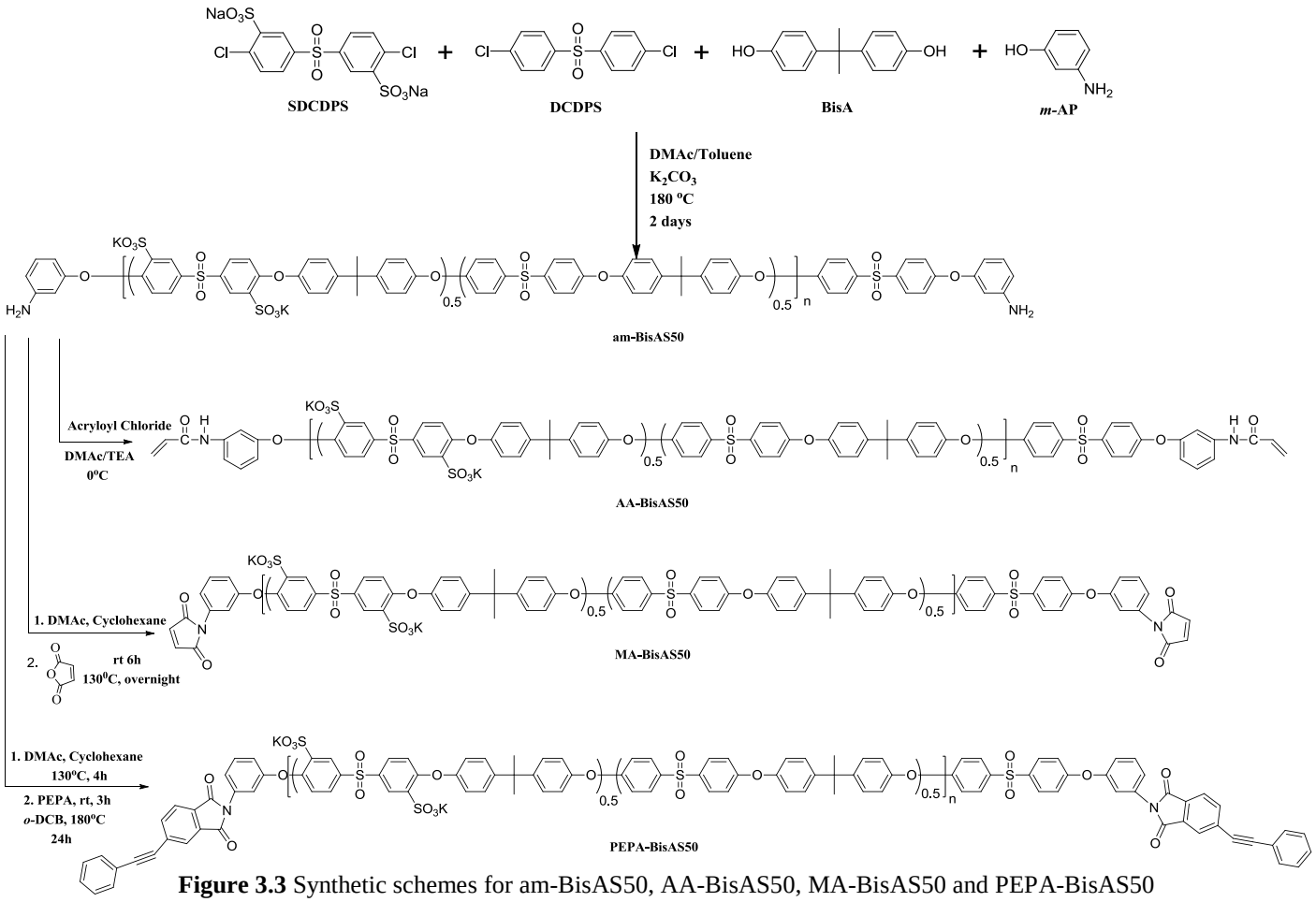

Figure 3.3 Synthetic schemes for am-BisAS50, AA-BisAS50, MA-BisAS50 and PEPA-BisAS50

The synthesis of the high temperature curing oligomers PEPA-BisAS50 and MA-BisAS50 are also shown in Fig. 3. The anhydride was added at lower temperatures because the ring opening reaction and formation of the amic-acid intermediate does not require elevated temperatures. ^{1}H-NMR was used to monitor the ring opening reactions by taking hourly aliquots of the reaction solution. The appearance of amic-acid peaks at 10.5 ppm indicated formation of the intermediate species, and the disappearance of the amine endgroups was used to judge sufficient reaction time for the first step. Similarly, sufficient time for cyclodehydration was found by monitoring the disappearance of the amic-acid intermediate.

Oligomer Characterization

The am-BisAS50 oligomer was characterized for degree of sulfonation (D.S.), M_n, and purity by ^{1}H-NMR. The ^{1}H-NMR spectrum of the am-BisAS50 oligomer is shown in Fig. 4. The solid sample completely dissolved in DMSO-d_6 and the spectrum showed no side products, residual monomer or solvent. The D.S. was calculated by equation 3. The measured D.S. was 49%, compared to the targeted D.S. of 50%.

Eq. 3
$$\text{D.S.} = \frac{[(H_a + H_B + H_c)/3]/2}{[(H_a + H_B + H_c)/3]/2 + [(H_f + H_g)/2]/4}$$

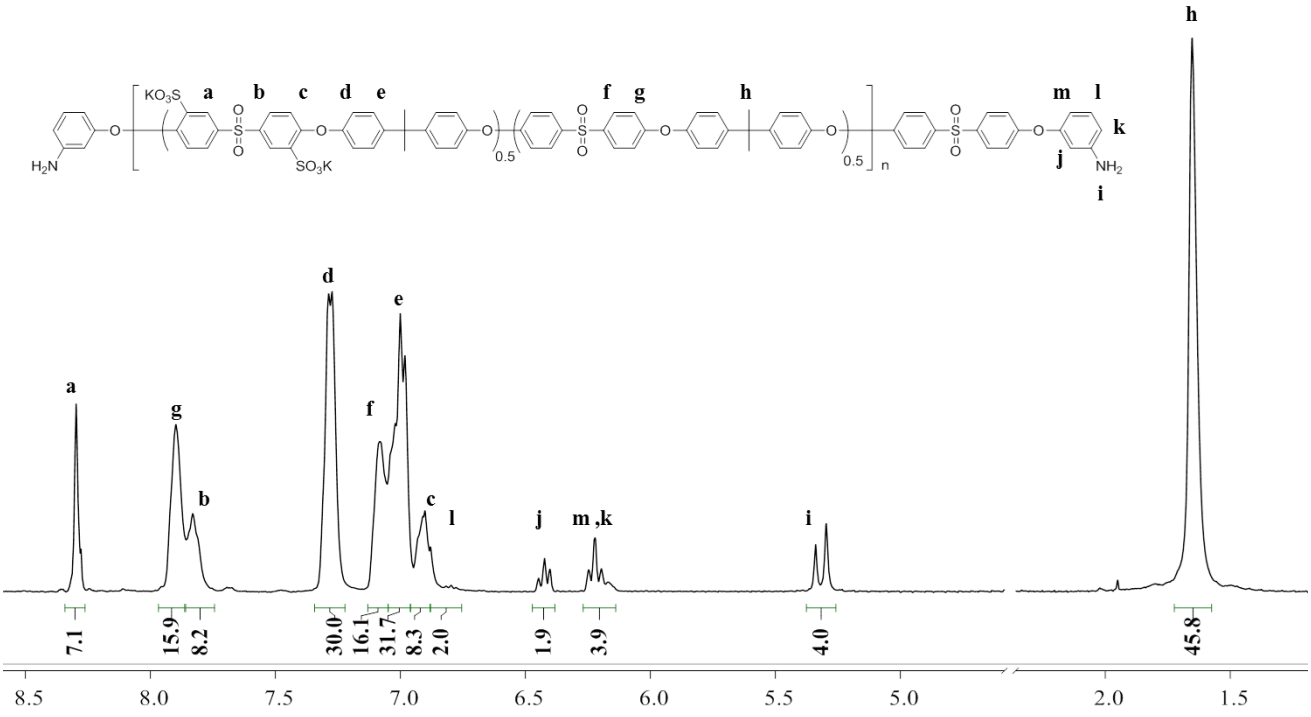

Figure 3.4 ^{1}H NMR of am-BisAS50

The chemical shifts of the *m*-AP endgroups differ depending on whether they are linked to DCDPS or SDCDPS. The *m*-AP endgroups adjacent to DCDPS occur at a slightly more downfield position compared to the SDCDPS linkage, and these closely related singlets (**i**) give the appearance of a doublet. The M_n calculated by ^{1}H-NMR was 4,800 g mol^{-1}, determined by

comparing the integration values of the amine endgroups (**i**) to the aromatic BisA peaks in the oligomer backbone (**d+e**). Calculation of M_n by this method assumes that there is no other endgroup species in the oligomer, the only other candidate being BisA endgroups. This assumption was considered reasonable, since the ^{1}H-NMR spectrum of a control reaction to produce 5,000 g mol^{-1} BisA terminated oligomer had strong endgroup peaks at 6.64 ppm, which are not observed in this spectrum.

The endgroup characterization for the further functionalized oligomers was also accomplished with ^{1}H-NMR. The aromatic regions in Fig. 5 are expanded to highlight the differences in endgroup structure. The complete disappearance of the amine peak was observed in AA-BisAS50, MA-BisAS50 and PEPA-BisAS50. This indicated complete endgroup conversion for AA-BisAS50. The absence of amic-acid intermediate peaks at 10.5 ppm indicated complete endgroup conversion and successful cyclodehydration for MA-BisAS50 and PEPA-BisAS50. Comparison of the final spectra to reagent ^{1}H-NMR showed no residual starting material left. The endgroup peak assignment of AA-BisAS50 and PEPA-BisAS50 was well defined and integrated out to appropriate values when compared to the starting oligomer. The endgroup peak assignment of MA-BisAS50 was more difficult, because the maleic anhydride endgroups overlap with backbone peaks in the aromatic region.[55]

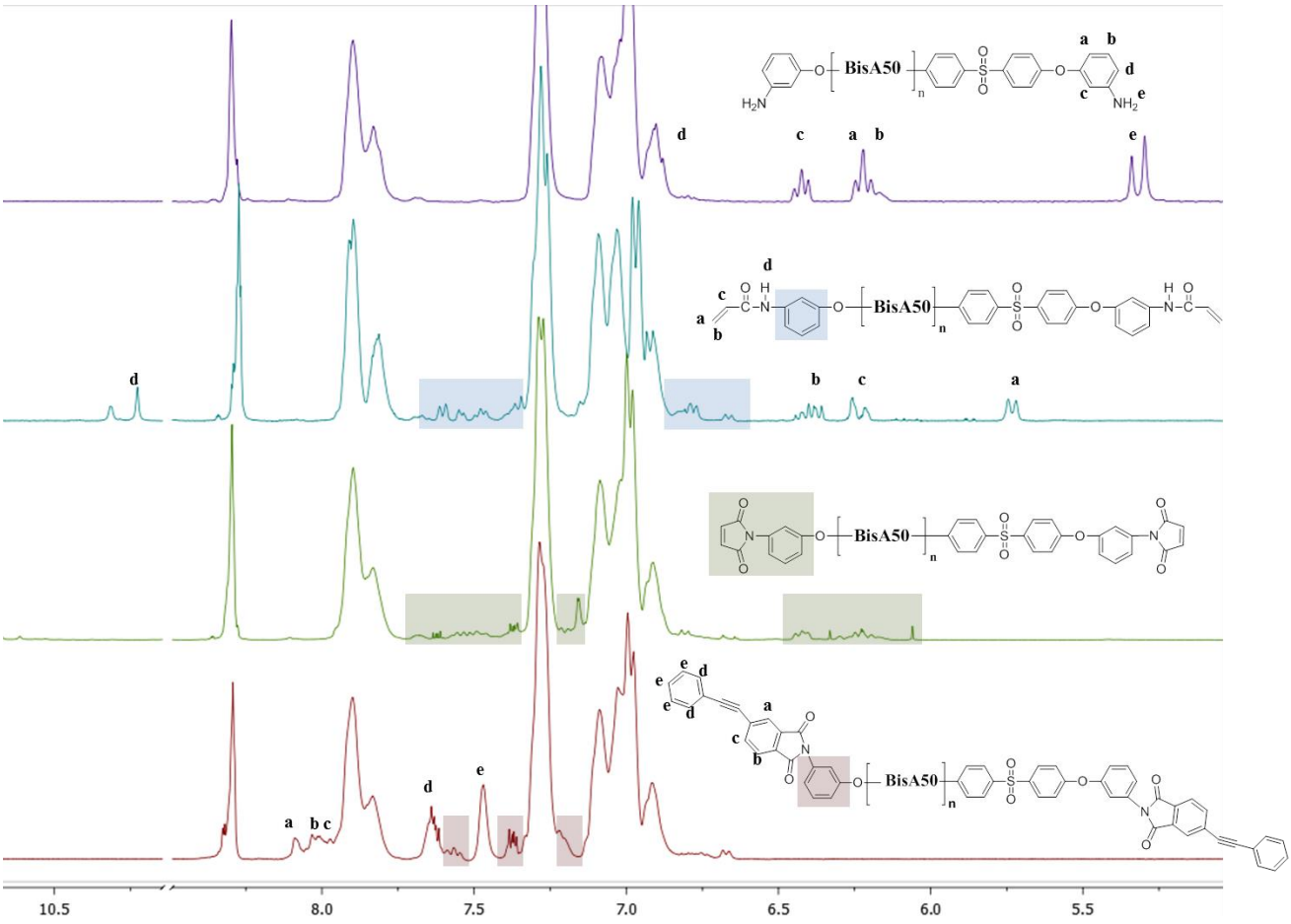

Figure 3.5 1H NMR comparison of am-BisAS50 starting oligomer shows complete conversion to further functionalized endgroups

Thermal Stability of the Oligomers

TGA studies were performed under N_2 at 10^{o}C/min to ensure that the oligomers were stable at high temperatures. This step is particularly important for ruling out oligomer degradation as a cause for exotherms observed in DSC heating curves. Fig. 6 shows that all of the oligomers had less than 1% weight loss in the range of 200 to 375^{o}C. The oligomers showed similar thermal behavior to high molecular weight BisAS50, denoted as BisAS50 Control in Fig. 6. The degradation temperature for this series was taken at values of 10% weight loss: 480^{o}C for the BisAS50 control, 470^{o}C for PEPA-BisAS50, 460^{o}C for am-BisAS50, and 440^{o}C for MA-BisAS50. These weight losses occur in the range expected for de-sulfonation, the primary

mechanism for initial sulfonated polysulfone degradation.[23] All of these degradations occurred well above the curing temperatures investigated.

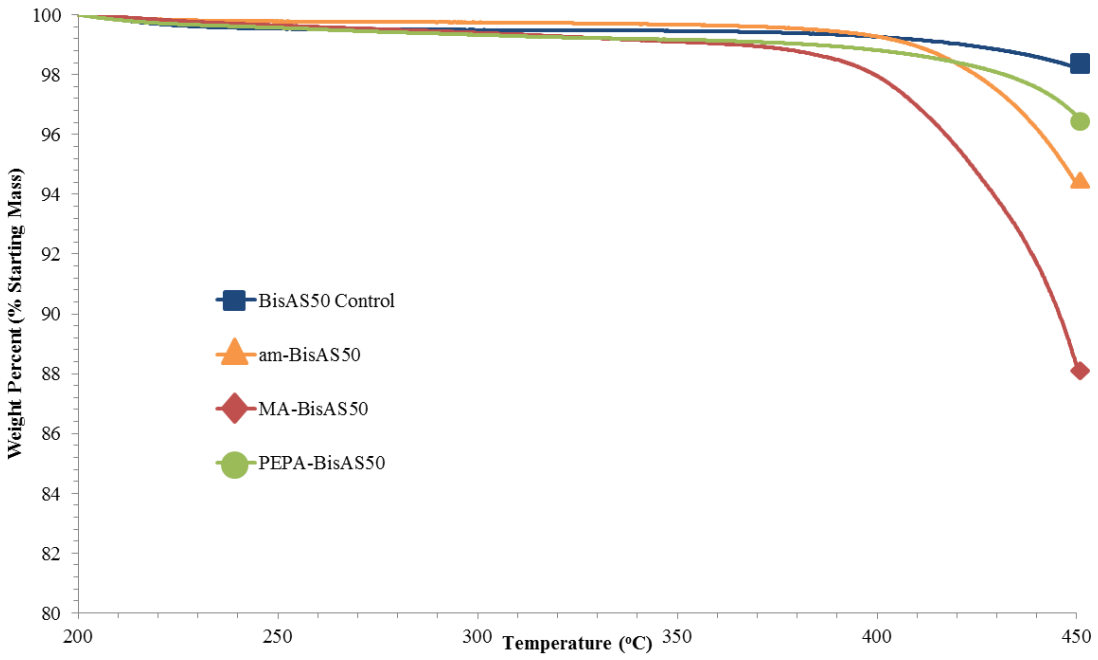

Figure 3.6 TGA shows that the oligomers are thermally stable in nitrogen at the curing conditions

Investigation of Oligomer Crosslinking Temperature

The determination of T_g for ionomers such as sulfonated polysulfones is not trivial. At high levels of sulfonation, the glass transition temperature becomes hard to distinguish from the baseline.[58] Because of the aforementioned phenomenon, the first derivative of the heating curve was used, and the T_g's were reported as the endothermic maxima. Previous work established the importance of crosslinking these high T_g copolymers in the presence of water and/or a high boiling point solvent. The T_g of a 5,000 g mol^{-1} 4,4'-biphenol based 50% sulfonated polysulfone (ph-BPS50) was lowered by over 100°C in the presence of NMP, enabling crosslinking at 150°C.[33] The oligomers in this study are well below the entanglement molecular weight and cannot produce free-standing films without crosslink formation. The formation of these

materials into a coherent ductile film is necessary for use as separation membranes. DSC studies were performed in pressurized pans on oligomers with a significant amount of DMAc left to plasticize their T_g's and afford crosslinking. The heating curves of the solvent plasticized oligomers are shown in Fig. 7.

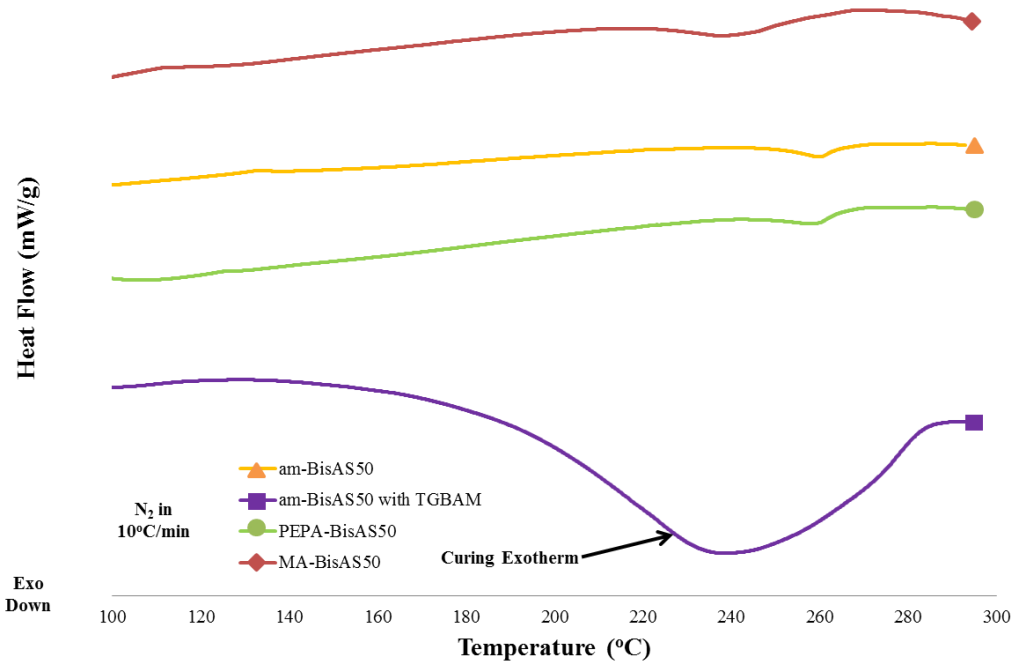

Figure 3.7 DSC thermogram comparison of solvent plasticized oligomers demonstrates that the epoxy cured system crosslinks at a much lower temperature than MA-BisAS50 and PEPA-BisAS50

The only oligomer to show strong evidence for crosslinking behavior was the am-BisAS50 with tetra-epoxide (TGBAM). Crosslinking in this system began at 140°C and had a maximum rate at 208°C. This curing behavior was not observed in the am-BisAS50 spectrum without TGBAM, as expected. The am-BisAS50 spectrum displayed a small endothermic maximum at 125°C, possibly a solvent plasticized T_g. The am-BisAS50 spectrum did have large endothermic maxima at 261 and 283°C, no exotherm was observed after these T_g's. PEPA-BisAS50 showed a solitary

T_g at 260°C and gave no indication of an exotherm afterwards. MA-BisAS50 showed a solitary T_g at 247°C with some indication of an exotherm occurring after 270°C.

The results from the solvent plasticized oligomer heating curves prove that curing am-BisAS50 with TGBAM occurs at much more facile conditions than MA-BisAS50 and PEPA-BisAS50. The T_g of the am-BisAS50 cured with TGBAM was raised 15°C, as crosslinks formed and restricted oligomer chain mobility. The cessation of the crosslinking reaction between 210 and 240°C may be a result of complete loss of the solvent DMAc, which has a boiling point of 165°C.

Crosslinking and Film Fabrication of am-BisAS50

The crosslinking reaction between am-BisAS50 and TGBAM (Fig. 8) was optimized to produce large ductile films with high extents of crosslinking. Small-scale films were prepared with varying molar ratios of TGBAM to determine which stoichiometry gave the highest gel fraction. These results are compared with the previous ph-BPS50 curing in Fig. 9.[33]

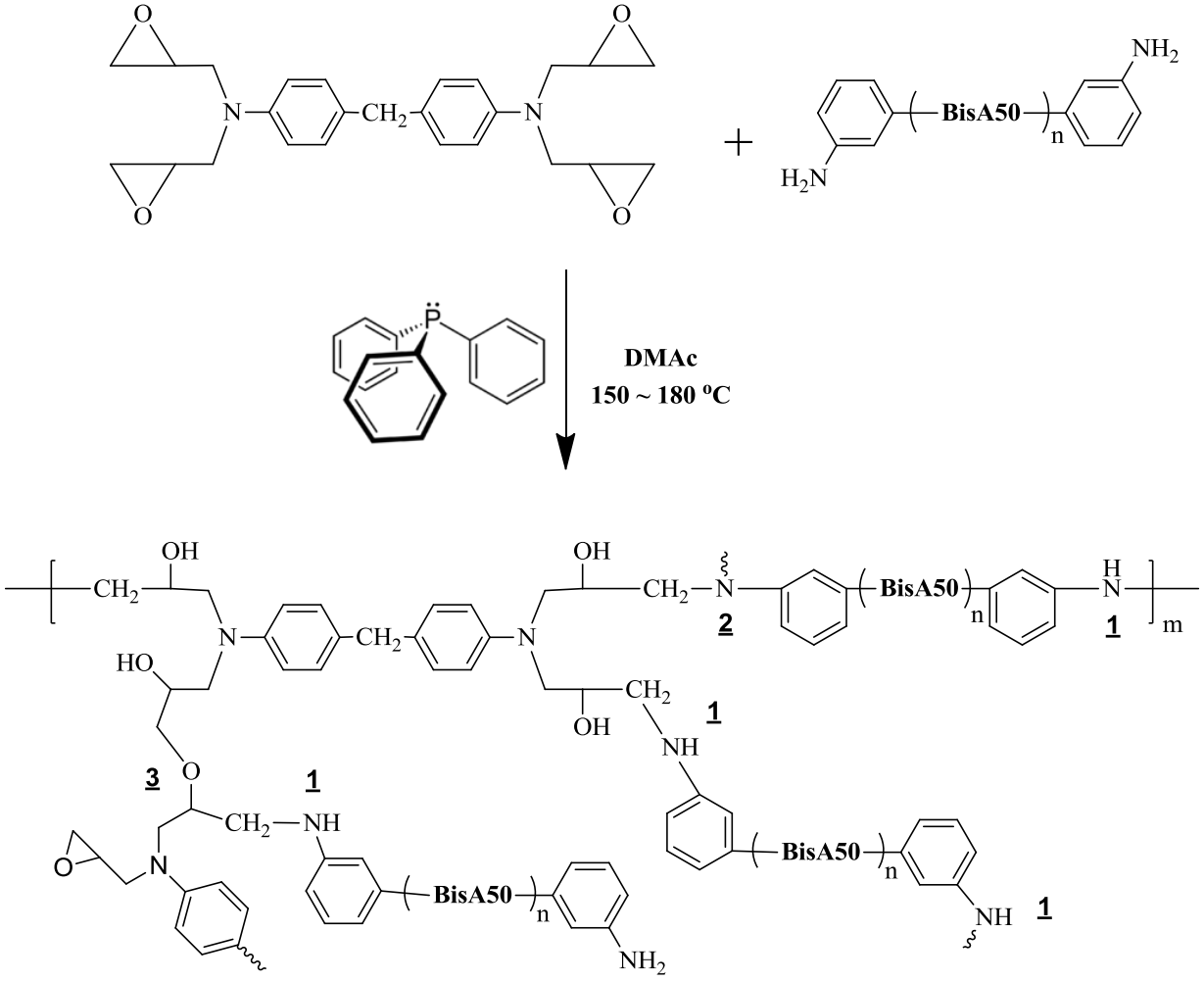

Figure 3.8 Schematic for crosslinking am-BisAS50 with TGBAM in the presence of TPP results in various linkages and some unreacted endgroups

The phenoxide terminated oligomers produced a maximum gel fraction at 2.1 molar equivalents of TGBAM. The amine terminated oligomers did not have a distinct maximum and continued to trend upwards with increasing epoxy concentration. This is possibly because the functionality of ph-BPS50 towards epoxy is 2 and for am-BisAS50 it is 4. The reactions of amines with glycidyl ethers are primary amine addition (**1**), secondary amine addition (**2**) and etherification (**3**),[59] all shown in Fig. 8. The kinetics of these competing reactions has been modeled in the literature.[59]

Primary amine addition occurs 2-10 times as quickly as secondary amine addition. Etherification has the lowest reaction rates and only occurs when the primary amines have all reacted. The soluble filtrates from gel fraction tests were also analyzed by ^{1}H NMR to determine remaining unreacted material. The sample prepared from a 3 molar equivalent of TGBAM contained excess epoxy, thus the optimal molar equivalency of TGBAM was taken to be 2.5. Figure 9 shows that the 2.5 molar equivalency sample had a gel fraction of 90%, and gel fractions up to 99% were obtained when the films were increased in size for transport testing. These are the highest reported gel fractions for sulfonated polysulfone oligomers to our knowledge.

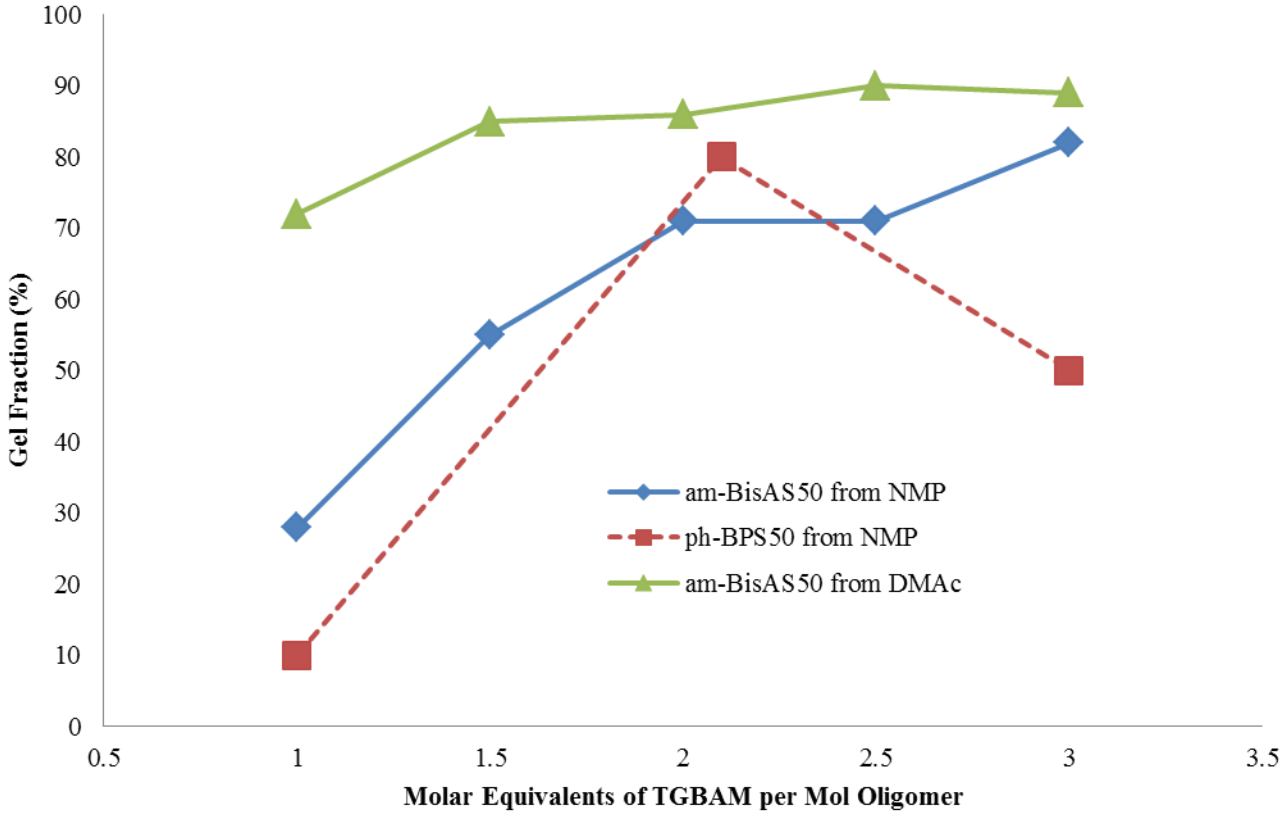

Figure 3.9 Optimal stoichiometry of TGBAM varies for phenoxide and amine terminated 5,000 Mn oligomers[33]

Several other variables were investigated to determine effect on final gel fractions. Both DMAc and NMP have been utilized as solvents for this curing reaction and produced similar results,

though films from DMAc had higher gel fractions. TPP was added in catalytic amounts to lower the onset of the curing exotherm. The kinetics of this reaction has been studied for epoxies and phenolic resins where it lowered cure temperatures by over 40^{o}C.[60] Varying the weight percent of TPP (relative to g TGBAM) from 0 to 2.5 to 5% had no impact on gel fraction. Increasing both the curing time and temperature improved gel fractions, and 90 min at 150-160^{o}C was sufficient to obtain a high extent of crosslinking.

Removal of the crosslinked film from the glass substrate was not trivial. It's hypothesized that epoxy reacts with both the glass surface and the oligomer. Silanation of the glass surface decreases the reaction of epoxy with glass, but caused the film to shrink as it dried. This problem was circumvented by soaking the crosslinked film and glass plate in a stirring solution of dilute K_2CO_3 dissolved in DI water. The weak base conditions had no effect on resulting gel fraction. After several days, the bonds between the film and glass plates was reduced and allowed for easy removal.

Crosslinking and Film Fabrication of PEPA-BisAS50

High gel fractions were consistently obtained with PEPA-BisAS50, though only at very high temperatures where large film fabrication was unsuccessful. The resulting deep brown membrane had several bubbles that disrupted the otherwise smooth surface. In addition to the procedure outlined in the experimental section, films were cast on glass substrates and cured in a Type 47900 Furnace or melt press. The final cure temperatures were in the range of 330-380^{o}C, producing blackened brittle materials that adhered to the casting surface and had gel fractions of over 90%. The best films obtained required a careful stepwise heating regimen using a hot plate. These films also had gel fractions over 90%, but bubble formation occurred between 200 and

300°C and disrupted the otherwise smooth surface area of the film. These results are consistent with the DSC heating curves, which indicated that the cure temperature was not sufficiently depressed and that solvent rapidly evaporated from the films while heating to the cure temperature. In other literature studies, the cure temperature of PEPA terminated polyetherimides was in the range of 345-360°C despite a T_g of 200°C, much lower than these sulfonated polysulfones.[54,61,62] Additionally, the curing of polyetherimides occurred above their melt temperature, whereas the PEPA terminated sulfonated poly(arylene ether sulfone) copolymers cure before any melt behavior is observed. Kinetic and mechanistic studies of the phenylethynyl curing reaction reported a minimum cure temperature of 318°C, and the reaction proceeded slowly under these conditions.[63]

Crosslinking and Film Fabrication of MA-BisAS50

The crosslinking results of MA-BisAS50 were similar to those of PEPA-BisAS50; high gel fractions were obtained at elevated temperatures and ductile film formations were not. The membrane produced from curing at 300°C in the forced air oven was free standing but very brittle. This material was wholly soluble in the casting solvent. The membrane was further crosslinked for 30 min by melt press at 330°C and 380°C. The 330°C cured membrane was partly soluble in gel fraction studies. The 380°C cured membrane was completely insoluble, but broke into many pieces when removed from the glass plate. Even if large crosslinked membranes of this oligomer could be fabricated, their inherent brittleness would prohibit use in high pressure water purification operations.

Crosslinking and Film Fabrication of AA-BisAS50

The thermal crosslinking of AA-BisAS50 without initiator was attempted, resulting in cracked membranes with 11.5 ± 1.5% gel fraction. The curing of the AA-BisAS50 oligomer was also attempted via thermally initiated free radical polymerization. AIBN was charged to polymer solutions in 0.5, 3, 5, 10 and 20 wt% relative to AA-BisAS50. The membranes were dried and cured at 100^{o}C for 12 h, resulting in extremely brittle membrane formation with no gel fraction. DCP was charged to polymer solutions in 1, 3 and 5 wt% relative to AA-BisAS50. This system was cured at 140^{o}C, 160^{o}C and 200^{o}C for several hours in a systematic series of experiments, all of which resulted in no membrane formation.

The successful crosslinking of AA-BisAS50 was photochemical, opposed to the thermal curing of the other oligomers. DMPA is a well-known initiator for photochemical reactions and its efficiency and mechanism have been elucidated.[64,65] Benzophenone initiators readily react with acrylates[66,67] and successfully crosslinked AA-BisAS50 with PETA. The resulting transparent films were free standing and ductile. The role of PETA equivalency was studied in a comparative test to am-BisAS50 and TGBAM. The molar equivalents of PETA to AA-BisAS50 ranged from 0.5 to 2.5 and gel fractions of up to 58% were obtained. However, no logical trend in crosslinker concentration to gel fraction was observed. We determined that the UV crosslinker used did not have sufficient intensity to penetrate the 30-40 μm thick films. Future research into this oligomers photochemical crosslinking is planned with a higher intensity UV crosslinker that can sufficiently penetrate the films thickness.

Effect of Gel Fraction on Water Uptake

The ultimate importance of crosslinking these oligomeric materials are to reduce the high degree of membrane swelling and sorption. The effect of crosslinking on water uptake was studied by curing am-BisAS50 oligomer with 2.5 molar equivalents of TGBAM. The oligomer was cured for 0, 10, 20, 45, 60 and 90 min at 150^{o}C. The samples cured for 0 and 10 min did not give free-standing films because of the low extent of crosslinking. The water uptake of the samples was measured before the gel fractions, with data plotted in Fig 10.

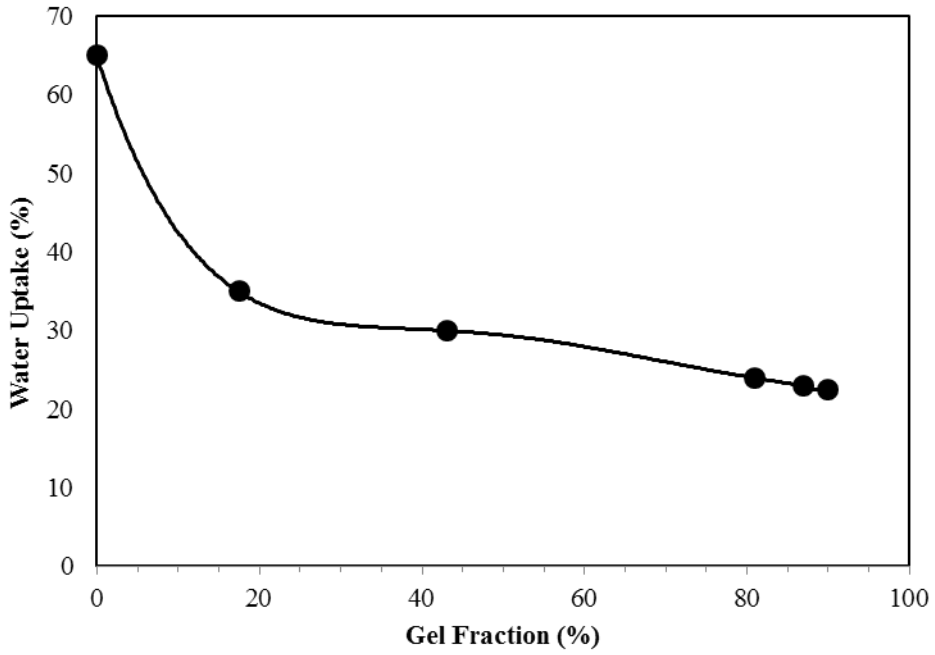

Figure 3.10 Water uptake of am-BisAS50 decreases rapidly and then plateaus as a function of increasing crosslinking with TGBAM

The water uptake of the films quickly dropped during the initial stages of crosslinking, which was similarly observed in the previous studies with ph-BPS50.[33] After the initial drop, water uptake plateaus, decreasing slowly to 90% gel fraction. The water uptake for the uncrosslinked am-BisAS50 was much higher than the BisAS50 control (35%), possibly because of the additional hydrophilic amine endgroups on the oligomer. The water uptake can be taken as

proportional to the free volume of the polymer and by extension related to water partition and permeability coefficients.[68] The loss in water permeability corresponds to an increase in water/NaCl selectivity, in accordance with fundamental tradeoff relationships.[29]

Initial Transport Results

The effect of crosslinking on the tradeoff relationship between water permeability and water/NaCl selectivity was investigated with preliminary cross-flow filtration experiments. The amine terminated oligomers were synthesized with a 60% degree of sulfonation to produce a material more hydrophilic than am-BisAS50. This oligomer (5k-am-BisAS60) was fabricated into large scale membranes at 45 and 93% extents of crosslinking. These crosslinked oligomers are listed with a high molecular weight linear control at the same level of sulfonation (BisAS60) and the state-of-the-art polyamide (SW30HR-380) material in Table 3.1. It is germane to note that water permeability standardizes these films for thickness when reported in (L μm / m^2 h bar); but that the state-of-the art material has a sub-micron film thickness while the dense crosslinked materials are in the range of 40-50 μm. The fabrication of sulfonated poly(arylene ether sulfone)s into films with a sub-micron thickness is currently being investigated.[31]

Table 3.1 Effect of crosslinking on water permeability, NaCl rejection and permeability, and water/NaCl selectivity for BisAS60 filmsa

Sample	Gel Fraction (%)	Water Uptake (%)	Pressure (psi)	Water Permeability (L μm / m^2 h bar)	NaCl Rejection (%)	Water Permeability ($x10^{-6}$, cm^2 / s)	NaCl Permeability ($x10^{-9}$, cm^2 / s)	Water/NaCl Selectivity
BisAS60	0	48	400	4.2 ± 0.6	88.1 ± 1.5	15.9 ± 2.3	43.5 ± 10.5	366
5k-am-BisAS60	45.1	26.8	200	1.2	91.8	4.4	7.7	580
5k-am-BisAS60	93.0	26.6	400	0.8 ± 0.1	97.1 ± 0.2	3.2 ± 0.2	1.9 ± 0.3	1700
SW30HR-380	-	-	800	0.05[b]	99.7[b]	-	-	-

[a] Three samples were used to obtain these average values, except for the mechanically weak 45% gel fraction material which yielded one measurement

[b] Commercial aromatic polyamide membrane,[69] test conditions: 32,000 mg L^{-1}, 25°C. Value is usually listed as 0.5 (L / m^2 h bar), and was converted to 0.05 (L μm / m^2 h bar) by assuming a thickness of 0.1 μm

The results clearly demonstrate that the water/NaCl selectivity greatly increases as the material becomes highly crosslinked and, in accordance with tradeoff relationships, that the water permeability decreases. The crosslinked membrane with a 45% gel fraction was much less ductile than the membrane with a 93% gel fraction. Thus, the 45% gel fraction membrane was run at a reduced trans-membrane pressure during cross-flow experiments compared to the linear control and highly crosslinked material. The NaCl rejection is not comparable for membranes tested at different pressures. Increasing the pressure will increase the water flux but will not substantially influence the salt flux, thus higher pressures will increase the NaCl rejection.[70]

However, the water permeability and salt permeability (cm^2 s^{-1}) and water/NaCl selectivity are intrinsic membrane properties and are comparable across varying pressures. The conversion of hydraulic water permeability (L μm m^{-2} h^{-1} bar^{-1}) to diffusive permeability (cm^2 s^{-1}) has been detailed in previous studies.[29]

The results across the intrinsic membrane properties vary greatly between the linear, modestly crosslinked (45% gel fraction) and highly crosslinked (93% gel fraction) samples. Notably, the modestly crosslinked sample has nearly twice as high selectivity compared to the linear control, but at the expense of a greatly reduced permeability. However, the highly crosslinked sample has a selectivity almost three times as high as the modestly crosslinked sample with only a minor decrease in water permeability. The water uptake was higher for the linear control (48%), but nearly identical for both the moderately and highly crosslinked materials (27%). It is surprising that the moderately and highly crosslinked membranes had nearly identical water uptake values despite very different transport properties. Part two of this paper will investigate this result in more depth. It appears that in this regime of high crosslinking that salt diffusion is increasingly limited despite only minor differences in water permeability. A very high extent of crosslinking is necessary for the high selectivity that the state-of-the-art aromatic polyamides demonstrate.13,71 It may follow that a high extent of crosslinking is necessary to achieve high selectivity and high water permeability for sulfonated polysulfones, and the amine terminated oligomers with epoxy can achieve this high extent of crosslinking while producing ductile films. Crosslinking certainly has a profound influence on the transport properties of these sulfonated poly(arylene ether sulfone) oligomers. Part two of this paper will compare the transport properties across a range of degree of sulfonation levels, crosslinking and

oligomer backbone structure to further develop the influence that crosslinking has on permeability and selectivity relationships for water purification.

3.5. Conclusions

In this paper, four novel crosslinkable oligomers were synthesized for use as water purification membranes and their structures were validated by ^{1}H-NMR. These oligomers have the same backbone structure with different telechelic functionalities, and the effects of endgroup structure on extent of crosslinking and film fabrication were investigated. The oligomers were all thermally stable to over 400^{o}C. The crosslinking reactions of the oligomers were very different mechanistically and occurred at varying temperatures and conditions. Oligomers endcapped with maleimide and phenylethynyl phthalimide produced networks with over 90% gel fraction at high temperatures, but crosslink formation occurred after a majority of the casting solvent evaporated. The necessity of residual casting solvent during crosslinking was demonstrated, and the aforementioned oligomers produced brittle discontinuous films. Acrylamide terminated BisAS50 oligomers were photochemically crosslinked to modest gel fractions with a multifunctional acrylate at low temperatures, resulting in ductile film formation. Amine terminated BisAS50 was reacted with a multifunctional epoxy to produce gel fractions of 99% and large-scale ductile films were fabricated. The water uptake of these polymers decreases drastically with initial network formation, then plateaus at higher extents of crosslinking. This upper regime with a high extent of crosslinking may be significant for developing these materials as water purification membranes.

Acknowledgements

The authors are grateful for the support of Dow Water & Process Solutions, Inc. This research was also supported by the U.S. National Science Foundation Partnerships for Innovation-Accelerating Innovative Research (PFI-AIR, Grant #1237858) and Partnerships for Innovation (PFI) -Partnerships for Water Purification (Grant #0650277).

3.6. References

(1) Oki, T.; Kanae, S. Global hydrological cycles and world water resources. *Science* **2006**, *313*, 1068.

(2) Lee, K. P.; Arnot, T. C.; Mattia, D. A review of reverse osmosis membrane materials for desalination. Development to date and future potential. *J. Membr. Sci.* **2011**, *370*, 1.

(3) Fritzmann, C.; Löwenberg, J.; Wintgens, T.; Melin, T. State-of-the-art of reverse osmosis desalination. *Desalination* **2007**, *216*, 1.

(4) Semiat, R. Energy Issues in Desalination Processes. *Enviromental Science & Technology* **2008**, *42*, 8193.

(5) Geise, G. M.; Lee, H.-S.; Miller, D. J.; Freeman, B. D.; McGrath, J. E.; Paul, D. R. Water purification by membranes: the role of polymer science. *J. Polym. Sci., Part B: Polym. Phys.* **2010**, *48*, 1685.

(6) Beasley, J. K. The evaluation and selection of polymeric materials for reverse osmosis membranes. *Desalination* **1977**, *22*, 181.

(7) Cadotte, J. E.; King, R. S.; Majerle, R. J.; Petersen, R. J. Interfacial synthesis in the preparation of reverse osmosis membranes. *J. Macromol. Sci., Chem.* **1981**, *A15*, 727.

(8) Cadotte, J. E. Interfacially synthesized reverse osmosis membrane and its use in removing solute from solute-containing water. EP15149A1,**1980**

(9) Cadotte, J. E.; Petersen, R. J.; Larson, R. E.; Erickson, E. E. A new thin-film composite seawater reverse osmosis membrane. *Desalination* **1980**, *32*, 25.

(10) Orton, K. J. P.; Soper, F. G.; Williams, G. Chlorination of anilides. III. N-Chlorination and C-chlorination as simultaneous side reactions. *J. Chem. Soc.* **1928**, 998.

(11) Avlonitis, S.; Hanbury, W. T.; Hodgkiess, T. Chlorine Degradation of Aromatic Polyamides. *Desalination* **1992**, *85*, 321.

(12) Glater, J.; Hong, S.-k.; Elimelech, M. The search for a chlorine resistant reverse osmosis membrane. *Desalination* **1994**, *95*, 325.

(13) Xie, W.; Geise, G. M.; Freeman, B. D.; Lee, H.-S.; Byun, G.; McGrath, J. E. Polyamide interfacial composite membranes prepared from m-phenylene diamine, trimesoyl chloride and a new disulfonated diamine. *J. of Membr. Sci.* **2012**, *403-404*, 152.

(14) Kissinger, J. C.; Willits, C. O. Preservation of Reverse Osmosis Membranes From Microbial Attack. *Food Technology* **1970**, *24*, 177.

(15) Mickols, W. E. In *Polymer Science: A Comprehensive Reference*; Matyjaszewski, K., Moller, M., Eds.; Elsevier: **2012**; Vol. 10, p 1060.

(16) Allegrezza, A. E., Jr.; Parekh, B. S.; Parise, P. L.; Swiniarski, E. J.; White, J. L. Chlorine resistant polysulfone reverse osmosis modules. *Desalination* **1987**, *64*, 285.

(17) Johnson, R. N.; Farnham, A. G.; Clendinning, R. A.; Hale, W. F.; Merriam, C. N. Poly(aryl ethers) by nucleophilic aromatic substitution. I. Synthesis and properties. *J. Polym. Sci., Part A: Polym. Chem.* **1967**, *5*, 2375.

(18) Rose, J. B. Preparation and properties of poly(arylene ether sulphones). *Polymer* **1974**, *15*, 456.

(19) Quentin, J. P. Polysulfones. DE2021383B2,**1970**

(20)Noshay, A.; Robeson, L. M. Sulfonated polysulfone. *J. Appl. Polym. Sci.* **1976**, *20*, 1885.

(21) Brousse, C.; Chapurlat, R.; Quentin, J. P. New Membranes for Reverse Osmosis 1. Characteristics of the Base Polymer: Sulphonated Polysulphones. *Desalination* **1976**, *18*, 137.

(22) Johnson, B. C.; Yilgor, I.; Tran, C.; Iqbal, M.; Wightman, J. P.; Lloyd, D. R.; Mcgrath, J. E. Synthesis and Characterization of Sulfonated Poly(Arylene Ether Sulfones). *J. Polym. Sci., Part A: Polym. Chem.* **1984**, *22*, 721.

(23) Ueda, M.; Toyota, H.; Ouchi, T.; Suciyama, J.-I.; Yonetake, K.; Masuko, T.; Teramoto, T. Synthesis and Characterization of Aromatic Poly (ether Sulfone)s Containing Pendant Sodium Sulfonate Groups. *J. Polym. Sci., Part A: Polym. Chem.* **1993**, *31*, 853.

(24) Wang, F.; Hickner, M.; Ji, Q.; Harrison, W.; Mecham, J.; Zawodzinski, T. A.; McGrath, J. E. Synthesis of Highly Sulfonated Poly(arylene ether sulfone) Random (Statistical) Copolymers Via Direct Polymerization. *Macromol. Symp* **2001**, *175*, 387.

(25) Wang, F.; Hickner, M.; Kim, Y. S.; Zawodzinski, T. A.; McGrath, J. E. Direct polymerization of sulfonated poly(arylene ether sulfone) random (statistical) copolymers: candidates for new proton exchange membranes. *J. of Membr. Sci.* **2002**, *197*, 231.

(26) Park, H. B.; Freeman, B. D.; Zhang, Z.-B.; Sankir, M.; McGrath, J. E. Highly chlorine-tolerant polymers for desalination. *Angew. Chem., Int. Ed.* **2008**, *47*, 6019.

(27) Xie, W.; Park, H.-B.; Cook, J.; Lee, C. H.; Byun, G.; Freeman, B. D.; McGrath, J. E. Advances in membrane materials: desalination membranes based on directly copolymerized disulfonated poly(arylene ether sulfone) random copolymers. *Water Sci. Technol.* **2010**, *61*, 619.

(28) Geise, G. M.; Park, H. B.; Sagle, A. C.; Freeman, B. D.; McGrath, J. E. Water permeability and water/salt selectivity tradeoff in polymers for desalination. *J. of Membr. Sci.* **2011**, *369*, 130.

(29) Xie, W.; Cook, J.; Park, H. B.; Freeman, B. D.; Lee, C. H.; McGrath, J. E. Fundamental salt and water transport properties in directly copolymerized disulfonated poly(arylene ether sulfone) random copolymers. *Polymer* **2011**, *52*, 2032.

(30) Xie, W.; Ju, H.; Geise, G. M.; Freeman, B. D.; Mardel, J. I.; Hill, A. J.; McGrath, J. E. Effect of Free Volume on Water and Salt Transport Properties in Directly Copolymerized Disulfonated Poly(arylene ether sulfone) Random Copolymers. *Macromolecules* **2011**, *44*, 4428.

(31) Lee, C. H.; McCloskey, B. D.; Cook, J.; Lane, O.; Xie, W.; Freeman, B. D.; Lee, Y. M.; McGrath, J. E. Disulfonated poly(arylene ether sulfone) random copolymer thin film composite membrane fabricated using a benign solvent for reverse osmosis applications. *J. of Membr. Sci.* **2012**, *389*, 363.

(32) Xie, W.; Geise, G. M.; Freeman, B. D.; Lee, C. H.; McGrath, J. E. Influence of processing history on water and salt transport properties of disulfonated polysulfone random copolymers. *Polymer* **2012**, *53*, 1581.

(33) Paul, M.; Park, H. B.; Freeman, B. D.; Roy, A.; McGrath, J. E.; Riffle, J. S. Synthesis and crosslinking of partially disulfonated poly(arylene ether sulfone) random copolymers as candidates for chlorine resistant reverse osmosis membranes. *Polymer* **2008**, *49*, 2243.

(34) Kerres, J.; Ullrich, A.; Meier, F.; Haring, T. Synthesis and characterization of novel acid-base polymer blends for application in membrane fuel cells. *Solid State Ionics* **1999**, *125*, 243.

(35) Hasiotis, C.; Li, Q.; Deimede, V.; Kallitsis, J. K.; Kontoyannis, C. G.; Bjerrum, N. J. Development and characterization of acid-doped polybenzimidazole/sulfonated polysulfone blend polymer electrolytes for fuel cells. *J. Electrochem. Soc.* **2001**, *148*, A513.

(36) Kerres, J.; Zhang, W.; Tang, C.-M. Covalently- and ionically-crosslinked polymers for use in membranes. DE10024576A1,**2001**

(37) Jorissen, L.; Gogel, V.; Kerres, J.; Garche, J. New membranes for direct methanol fuel cells. *J. Power Sources* **2002**, *105*, 267.

(38) Kerres, J.; Zhang, W.; Ullrich, A.; Tang, C. M.; Hein, M.; Gogel, V.; Frey, T.; Jorissen, L. Synthesis and characterization of polyaryl blend membranes having different composition, different covalent and/or ionic cross-linking density, and their application to DMFC. *Desalination* **2002**, *147*, 173.

(39) Kerres, J.; Hein, M.; Zhang, W.; Graf, S.; Nicoloso, N. Development of new blend membranes for polymer electrolyte fuel cell applications. *J. New Mater. Electrochem. Syst.* **2003**, *6*, 223.

(40) Nolte, R.; Ledjeff, K.; Bauer, M.; Muelhaupt, R. Partially sulfonated poly(arylene ether sulfone) - a versatile proton conducting membrane material for modern energy conversion technologies. *J. of Membr. Sci.* **1993**, *83*, 211.

(41) Kerres, J.; Cui, W.; Disson, R.; Neubrand, W. Development and characterization of crosslinked ionomer membranes based upon sulfinated and sulfonated PSU - Crosslinked PSU blend membranes by disproportionation of sulfinic acid groups. *J. of Membr. Sci.* **1998**, *139*, 211.

(42) Kerres, J.; Cui, W.; Junginger, M. Development and characterization of crosslinked ionomer membranes based upon sulfinated and sulfonated PSU - Crosslinked PSU blend membranes by alkylation of sulfinate groups with dihalogenoalkanes. *J. of Membr. Sci.* **1998**, *139*, 227.

(43) Kerres, J.; Zhang, W.; Cui, W. New sulfonated engineering polymers via the metalation route. II. Sulfinated/sulfonated poly(ether sulfone) PSU Udel and its crosslinking. *J. Polym. Sci., Part A: Polym. Chem.* **1998**, *36*, 1441.

(44) Voege, A.; Deimede, V. A.; Kallitsis, J. K. Side chain crosslinking of aromatic polyethers for high temperature polymer electrolyte membrane fuel cell applications. *J. Polym. Sci., Part A: Polym. Chem.* **2012**, *50*, 207.

(45) Gu, S.; He, G.; Wu, X.; Guo, Y.; Liu, H.; Peng, L.; Xiao, G. Preparation and characteristics of crosslinked sulfonated poly(phthalazinone ether sulfone ketone) with poly(vinyl alcohol) for proton exchange membrane. *J. Membr. Sci.* **2008**, *312*, 48.

(46) Feng, S.; Shang, Y.; Xie, X.; Wang, Y.; Xu, J. Synthesis and characterization of crosslinked sulfonated poly(arylene ether sulfone) membranes for DMFC applications. *J. Membr. Sci.* **2009**, *335*, 13.

(47) Delfort, B.; Lucotte, G.; Cormier, L. Ethynyl-terminated polyethers from new end-capping agents: synthesis and characterization. *J. Polym. Sci., Part A: Polym. Chem.* **1990**, *28*, 2451.

(48) Lucotte, G.; Cormier, L.; Delfort, B. Ethynyl-terminated polyethers from new end-capping agents. II. End-chain functionalization through nitro displacement. *J. Polym. Sci., Part A: Polym. Chem.* **1991**, *29*, 897.

(49) Chul, G. S.; Chul, K. J.; Ahn, D.; Jang, J.-S.; Kim, H.; Chul, J. J.; Lim, S.; Jung, D.-H.; Lee, W. Thermally crosslinked sulfonated polyethersulfone proton exchange membranes for direct methanol fuel cells. *J. Membr. Sci.* **2012**, *417-418*, 2.

(50) Sankir, M.; Bhanu, V. A.; Harrison, W. L.; Ghassemi, H.; Wiles, K. B.; Glass, T. E.; Brink, A. E.; Brink, M. H.; McGrath, J. E. Synthesis and characterization of 3,3 '-disulfonated-4,4 '-dichlorodiphenyl sulfone (SDCDPS) monomer for proton exchange membranes (PEM) in fuel cell applications. *J. of Appl. Polym. Sci.* **2006**, *100*, 4595.

(51) Li, Y.; VanHouten, R. A.; Brink, A. E.; McGrath, J. E. Purity characterization of 3,3′-disulfonated-4,4′-dichlorodiphenyl sulfone (SDCDPS) monomer by UV–vis spectroscopy. *Polymer* **2008**, *49*, 3014.

(52) Hedrick, J. L.; Mohanty, D. K.; Johnson, B. C.; Viswanathan, R.; Hinkley, J. A.; McGrath, J. E. Radiation resistant amorphous-all aromatic polyarylene ether sulfones: synthesis, characterization, and mechanical properties. *J. Polym. Sci., Part A: Polym. Chem.* **1986**, *24*, 287.

(53) Guo, R.; McGrath, J. E. In *Polymer Science: A Comprehensive Review*; Matyjaszewski, K., Moller, M., Eds.; Elsevier: **2012**; Vol. 5, p 769.

(54) Zhuang, H.; Sankarapandian, M. S.; Ji, Q.; McGrath, J. E. Thermosetting polyetherimides. The influence of reactive endgroup type and oligomer molecular weight on synthesis, network formation, adhesion strength, and thermal properties. *J. Adhes.* **1999**, *71*, 231.

(55) Lyle, G. D.; Senger, J. S.; Chen, D. H.; Kilic, S.; Wu, S. D.; Mohanty, D. K.; McGrath, J. E. Synthesis, curing and physical behavior of maleimide-terminated poly(ether ketones). *Polymer* **1989**, *30*, 978.

(56) Sagle, A. C.; Van, W. E. M.; Ju, H.; McCloskey, B. D.; Freeman, B. D.; Sharma, M. M. PEG-coated reverse osmosis membranes: Desalination properties and fouling resistance. *J. Membr. Sci.* **2009**, *340*, 92.

(57) Jurek, M. J.; McGrath, J. E. Synthesis and characterization of amine terminated poly(arylene ether sulphone) oligomers. *Polymer* **1989**, *30*, 1552.

(58) Johnson, B. C.; Yilgor, I.; Tran, C.; Iqbal, M.; Wightman, J. P.; Lloyd, D. R.; McGrath, J. E. Synthesis and characterization of sulfonated poly(arylene ether sulfones). *J. Polym. Sci., Polym. Chem. Ed.* **1984**, *22*, 721.

(59) Vyazovkin, S.; Sbirrazzuoli, N. Mechanism and Kinetics of Epoxy-Amine Cure Studied by Differential Scanning Calorimetry. *Macromolecules* **1996**, *29*, 1867.

(60) Han, S.; Kim, W. G.; Yoon, H. G.; Moon, T. J. Kinetic study of the effect of catalysts on the curing of biphenyl epoxy resin. *J. Appl. Polym. Sci.* **1998**, *68*, 1125.

(61) Tan, B.; Vasudevan, V.; Lee, Y. J.; Gardner, S.; Davis, R. M.; Bullions, T.; Loos, A. C.; Parvatareddy, H.; Dillard, D. A.; McGrath, E.; Cella, J. Design and characterization of thermosetting polyimide structural adhesive and composite matrix systems. *J. Polym. Sci., Part A: Polym. Chem.* **1997**, *35*, 2943.

(62) McGrath, J. E.; Meyer, G. W. Aryl ethynyl phthalic anhydrides and their use as modifying agents for amine-containing polymers. US5493002A,**1996**

(63) Fang, X.; Rogers, D. F.; Scola, D. A.; Stevens, M. P. A study of the thermal cure of a phenylethynyl-terminated imide model compound and a phenylethynyl-terminated imide oligomer (PETI-5). *J. Polym. Sci., Part A: Polym. Chem.* **1998**, *36*, 461.

(64) Kurdikar, D. L.; Peppas, N. A. Method of Determination of Initiator Efficiency: Application to UV Polymerizations Using 2-2-Dimethoxy-2-phenylacetophenone. *Macromolecules* **1994**, *27*, 733.

(65) Groenenboom, C. J.; Hageman, H. J.; Overeem, T.; Weber, A. J. M. Comparison of the Photodecompositions of α-Methoxy- and α α-Dimethoxydeoxybenzoin in 1-1-Diphenylethylene as Model Substrate. *Makromol. Chem.* **1982**, *183*, 281.

(66) Bradley, G.; Davidson, R. S.; Howgate, G. J.; Mouillat, C. G. J.; Turner, P. J. Photoinitiated polymerization reactions Application of a new real-time FTIR system for the rate of polymerization. *Journal of Photochemistry and Photobiology A: Chemistry* **1996**, *100*, 109.

(67) Phan, X. T.; Grubb, M. B. Effects of Additives on the Laser-Initiated Polymerization of 1,6-Hexanediol Diacrylate. *Journal of Macromolecular Science: Part A - Chemistry* **1988**, *25*, 143.

(68) Yasuda, H.; Lamaze, C. E.; Ikenberry, L. D. Permeability of solutes through hydrated polymer membranes. I. Diffusion of sodium chloride. *Makromol. Chem.* **1968**, *118*, 19.

(69) DowWebsite. http://www.dowwaterandprocess.com/products/f/filmtec_sw30hr_380 (70) Baker, R. W. *Membrane Technology and Applications*; McGraw-Hill, **2000**.

(71) Song, Y.; Sun, P.; Henry, L. L.; Sun, B. Mechanisms of structure and performance controlled thin film composite membrane formation via interfacial polymerization process. *J. Membr. Sci.* **2005**, *251*, 67.

CHAPTER 4: CROSSLINKING DISULFONATED POLY(ARYLENE ETHER SULFONE) TELECHELIC OLIGOMERS PART 2: EFFECT OF BACKBONE STRUCTURE, DEGREE OF SULFONATION AND CROSSLINKING ON TRANSPORT PROPERTIES

Benjamin J. Sundell, [a] *Eui-Soung Jang,* [b] *Chang Hyun Lee,* [a] *Joseph R. Cook,* [b] *Ozma Lane,* [a] *Benny D. Freeman,* [b] *Judy S. Riffle,* [a] *James E. McGrath* [a]

[a]Macromolecular Science and Engineering, Macromolecules and Interfaces Institute, Department of Chemistry, Virginia Polytechnic Institute and State University, Blacksburg, VA 24061, USA

[b]Department of Chemical Engineering, Center for Energy and Environmental Resources, University of Texas at Austin, Austin, TX 78758, USA

Article in preparation for submission

4.1. Abstract

Disulfonated poly(arylene ether sulfone) copolymer membranes are attractive candidates for water purification by reverse osmosis. The negatively charged disulfonated copolymers show low fouling and greatly improved resistance to oxidants such as chlorinated disinfectants compared to the state of the art highly crosslinked polyamide skin, porous polysulfone supported thin film composite (TFC) systems. A systematic series of controlled molecular weight 4,4'-biphenol and bisphenol-A based partially disulfonated poly(arylene ether sulfone)s were synthesized with terminal amine functionalities via end-capping with *m*-aminophenol. Number

average molecular weight and the degree of sulfonation were controlled by stoichiometric control of the bisphenols and two activated dihalide concentrations. The M_n's of the oligomers were verified by ^{1}H-NMR and molecular weight distributions were analyzed by size exclusion chromatography (SEC). The oligomers with controlled molecular weights and ionic content were thermally crosslinked with a multi-functional epoxy resin (TGBAM) derived from methylene dianiline. High gel fractions were confirmed by extracting the crosslinked copolymers in boiling solvents. The networks had improved salt rejection compared to linear controls due to reduced swelling, and this proved to be a valuable parameter for enhancing transport properties. Altering the variables of crosslinking, backbone structure and degree of sulfonation had large impacts on transport properties and the trends observed varied widely from the control systematic series. The crosslinked highly sulfonated copolymers produced the best water purification properties to date for sulfonated polysulfone membranes. For example, a crosslinked 4,4'-biphenol-based 50% disulfonated polysulfone had a salt rejection of 97.8% and a hydraulic water permeability of 0.43 (L μm m^{-2} h^{-1} bar^{-1}), compared to an analogous linear 4,4'-biphenol-based 50% disulfonated polysulfone that had a salt rejection of 73.4% and a hydraulic water permeability of 3.5 (L μm m^{-2} h^{-1} bar^{-1}).

4.2. Introduction

Crosslinked aromatic polyamides are the state-of-the-art membranes for water desalination by reverse osmosis, a commercially important method of purifying water in the 21st century.[1] These membranes can achieve over 99% solute rejection from seawater at relatively high water permeabilities.[2] However, despite excellent transport properties, the aromatic polyamides are extremely susceptible to biofouling and degradation by chlorinated disinfectants,

and this has prompted investigations of new desalination membranes such as sulfonated polysulfones.[3]

One of the greatest advantages of the state-of-the-art thin film composites is that they allow for separate optimization of the polysulfone support layer and the aromatic polyamide selective layer. For example, the aromatic polyamides are very highly crosslinked, brittle and weak, but can survive the high pressure reverse osmosis process because they are produced directly on a polysulfone support layer.[4] The high extent of crosslinking in the state-of-the-art membranes was identified early on as being important for the transport properties.[5] Permeate flux and salt rejection rely on membrane density and are therefore sensitive to crosslink density.[6] In some cases, the use of diamines bulkier than *m*-phenylene diamine have produced membranes with lower salt rejections, possibly because of decreased membrane density.[7] Despite the clear importance of crosslinking on transport properties, fundamental studies remain elusive because of the difficulty in studying the *in situ* produced aromatic polyamides as separate entities without the support layers. The aromatic polyamides are difficult to separate from the polysulfone support and they fail mechanically once removed. Recently, crosslink density of a state-of-the-art aromatic polyamide was studied by X-Ray reflectivity and X-Ray Photoelectron Spectroscopy. X-Ray reflectivity was used to measure an increase in film thickness and decrease in density upon membrane swelling. The membrane swelled up to 40% in water, yet the distance between crosslinks was quite small, equal to about five repeat units.[8] Because of the demonstrated importance of crosslinking in the state-of-the-art material, it is of interest to investigate effects of crosslinking in alternative water purification membranes such as sulfonated polysulfones.

Chapter 3 reviewed numerous examples of crosslinking sulfonated polysulfones and described several new reactions for crosslinking telechelic sulfonated polysulfone oligomers.[9] One crosslinking route was successful in producing ductile films with gel fractions up to 99%, among the highest reported to date for such sulfonated polysulfone copolymers. The reaction between amine terminated oligomers and a tetrafunctional epoxy resin was identified as a suitable candidate for further investigation into the effects of crosslinking on water purification properties.

In the present investigation, two systematic series of compositionally different disulfonated poly(arylene ether sulfone)s were synthesized. One series was based on the bisphenol-A (BisAS) monomer structure explored in Chapter 3, and the other series was based on 4,4'-biphenol (BPS). Each oligomeric series was produced with three levels of hydrophilicity corresponding to 40, 50 and 60% of disulfonated repeat units relative to non-sulfonated units. The compositions of the oligomers were verified by ^{1}H-NMR, and molecular weights were established by ^{1}H-NMR and SEC. Each of the oligomers was crosslinked with a tetrafunctional epoxy resin to achieve dense membranes with high gel fractions. These were studied to understand relationships among composition, crosslinking and transport properties. The crosslinked networks had significantly different transport properties than the linear controls. In particular, the salt rejection remained relatively constant across the crosslinked series, though water permeability drastically increased with increasing degrees of sulfonation. Therefore, the crosslinked oligomers were by far the most attractive sulfonated polysulfone candidates yet for reverse osmosis water purification. An initial investigation for producing thin film composites (TFC's) based on the crosslinked sulfonated polysulfones was also carried out.

4.3. Experimental

Materials

4,4'-(Propane-2,2-diyl)diphenol (BisA), 4,4'-biphenol (BP) and 4,4'-dichlorodiphenylsulfone (DCDPS, 99%) were purchased from Solvay and recrystallized from toluene before use. 3-Aminophenol (*m*-AP, 99%) was purchased from Acros Organics. Calcium hydride (90-95%) was purchased from Alfa Aesar. 3,3-Disulfonated-4,4'-dichlorodiphenylsulfone (SDCDPS, 98%) was purchased from Akron Polymer Systems, quantified for NaCl impurities and dried at 160°C for 72 h before use.[10] Toluene, *N*,*N*-dimethylacetamide (DMAc, 99%) and 2-propanol (isopropanol, IPA) were purchased from Fisher Scientific. The DMAc reaction solvent was dried with calcium hydride (CaH_2), distilled under reduced pressure and stored over molecular sieves. Triphenylphosphine (TPP, 99%), tetraglycidyl bis(*p*-aminophenyl)methane (TGBAM, 92%[11]), potassium carbonate (K_2CO_3, 99%), phosphorus pentoxide (P_2O_5) and lithium bromide (LiBr) were purchased from Aldrich. 1-Methyl-2-pyrrolidone (NMP) was purchased from Spectrum Chemicals. For the support material in the TFC development, Udel® polysulfone support (Dow Chemical, average pore size measured by porosimetry[12] = 25 nm) was utilized.

Synthesis of a 5,000 molecular weight (M_n) amine-endcapped 4,4'-biphenol based 50% disulfonated polysulfone oligomer (am-BPS50)

The BPS based oligomers were synthesized by nucleophilic aromatic substitution using the weak base approach as previously described in Chapter 3.[9,13] BP (43.9 mmol, 8.1711 g), DCDPS (25 mmol, 7.1790 g), SDCDPS (25 mmol, 12.6611 g), *m*-AP (12.2 mmol, 1.3481 g), and DMAc (96 mL) were added to a 250-mL three-necked flask. The reaction flask was

equipped with a mechanical stirrer, nitrogen inlet, and Dean-Stark trap filled with toluene. A stirring, thermally regulated, oil bath was used to heat the reaction mixture to 155^{o}C. After the bath temperature reached 155^{o}C, K_2CO_3 (70.0 mmol, 9.679 g) was added with toluene (48 mL). The reaction was stirred at 155^{o}C until all of the water was azeotropically removed with toluene. The temperature was increased to 175^{o}C and water and toluene were drained. After 48 h, the amber opaque solution was cooled to room temperature and filtered. The resulting transparent solution was precipitated in IPA (900 mL) to yield a white solid. The copolymer was filtered, washed with IPA (500 mL), and dried in a vacuum oven at 130^{o}C for one day. The 40 and 60% disulfonated oligomers were synthesized in a similar manner, with varying ratios of SDCDPS and DCDPS.

Nuclear Magnetic Resonance (^{1}H-NMR)

^{1}H-NMR analyses of the oligomeric copolymers were performed on a Varian Unity Plus spectrometer operating at 400 MHz. The spectra of the copolymers were obtained from 32 scans of a 15% (w/v) 1 mL solution in DMSO-d_6.

Size Exclusion Chromatography (SEC)

Intrinsic viscosities (IV) and molecular weights of the copolymers were obtained by size exclusion chromatography (SEC). The SEC system consisted of an isocratic pump (Agilent 1260 infinity, Agilent Technologies, Santa Clara, CA) with an online degasser (Agilent 1260, Agilent Technologies, Santa Clara, CA), autosampler and column oven used for mobile phase delivery and sample injection, and three Agilent PLgel 10 µm Mixed B-LS columns 300×7.5 mm connected in series with a guard column as the stationary phase. A system of multiple

detectors connected in series was used for the analysis. A multi-angle laser light scattering (MALS) detector (DAWN-HELEOS II, Wyatt Technology Corporation), operating at a wavelength of 658 nm, a viscometer detector (Viscostar, Wyatt Technology Corporation), and a refractive index detector operating at a wavelength of 658 nm (Optilab T-rEX, Wyatt Technology Corporation, Goleta, CA) provided online results. The system was corrected for interdetector delay and band broadening. The MALS signals were normalized using a 21,720 g/mol polystyrene standard obtained from Agilent Technologies or Varian. Data acquisitions and analysis were conducted using Astra 6 software (Wyatt Technology Corporation). The mobile phase of NMP was vacuum distilled over P_2O_5 before use. The salt, 0.05M dried LiBr, was added and dissolved in the NMP before the solvent was degassed and filtered. The sample solutions were prepared in a concentration range of 2~3 mg/mL and were filtered to remove any dust or insoluble particles using 0.22 μm PTFE filters. Molecular weights were measured using light scattering. Note that specific refractive index increments (dn/dc's) were calculated for each backbone type based on an assumption of 100% mass recovery using Astra 6 software.

Dense Film Preparation

The dense crosslinked films were prepared by adding the oligomers to TGBAM in a 1:2.5 molar ratio, respectively. TPP was added in a 2.5% by weight ratio relative to the weight of TGBAM. The following steps were completed to prepare a crosslinked film containing 5kamBPS-50. A mixture of amBPS-50 (0.3261 mmol, 1 eq. amine, 1.5000 g), TGBAM (0.8152 mmol, 2.5 eq. epoxy, 0.3764 g) and TPP (0.0358 mmol, 9.4 mg) were dissolved in DMAc (12 mL) and stirred until a homogeneous solution was obtained. The solution was syringe filtered through a 0.45 μm PTFE filter into a new vial. The solution was cast on a clean glass plate on a

level surface inside a vacuum oven and dried under vacuum for 2 h at 100°C. The vacuum was released and the oven was heated at the crosslinking temperature (180-200°C) for 90 min. The film was cooled to room temperature slowly overnight. The following day, the film was transferred to a stirring DI water bath containing dissolved potassium carbonate to aid in detaching the epoxy cured network from the glass substrate. Once separated, the film was transferred to a DI water bath.

Thin Film Composite (TFC) Preparation

Oligomeric amBisA-50 (3.0 g) was dissolved in monoglyme (57 g) at 30°C for 1 day with a 5 wt% concentration and TGBAM (0.045 and 0.06 g, respectively) at different total concentrations (1.5 and 2 wt% per the oligomer weight) were added into the oligomer solution. After filtering through a 0.45 μm PTFE filter, the solution was brush-coated onto a pretreated[12] support layer. For the pretreatment, the support layers are immersed in IPA-Glycerin mixture with a 75-25 weight ratio for at least one day. This was initially dried on a hot plate at 60°C for 0.5 h, and then heated to 90°C for 1 h. After vacuum drying at 90°C for 1 day, partially crosslinked am-BisA50 TFCs were obtained. The temperature of 90°C was selected as a stage one curing temperature to minimize pore shrinkage in the Udel® support during solvent evaporation.

Scanning Electron Microscopy

Samples of the TFC's were freeze-fractured in liquid nitrogen and sputter-coated with a gold/palladium alloy prior to imaging. Images were obtained using a LEO (Zeiss) Field-Emission Scanning Electron Microscope with a 5.0 kV accelerating voltage.

Gel Fraction measurements

Gel fractions were measured to estimate the extent of crosslinking. Crosslinked films were dried at 120°C under vacuum overnight. After drying, 0.1-0.2 g of the sample was placed in a 20-mL scintillation vial filled with DMAc and stirred at 100°C overnight. The remaining solid was filtered, transferred to a pre-weighed vial, and dried at 120°C under vacuum overnight. The final weight was taken the next day. One measurement was taken for each film and gel fractions were calculated by Equation 1.

Equation 1: $$\text{Gel Fraction (\%)} = \frac{Final\ mass\ of\ extracted\ film}{Initial\ mass\ of\ dried\ film} \text{ x } 100$$

Water uptake measurements

Films (0.1-0.2 g) were dried at 120°C under vacuum overnight, then weighed to obtain the dry weight (W_{dry}). Next, they were immersed in DI water for at least 48 hours. The films were removed, quickly blotted to remove any surface water droplets and weighed to obtain the wet weight (W_{wet}). Three measurements were taken for each film and water uptake values were calculated by Equation 2.

Equation 2: $$Water\ Uptake\ (\%) = \frac{W_{wet} - W_{dry}}{W_{dry}} \times 100$$

Water permeability and salt rejection

The water purification properties of the dense crosslinked oligomers and partially cured TFC's were determined at 25°C in a previously described cross-flow filtration system using stainless steel crossflow cells.[14] Permeate samples were collected and analyzed for their mass and conductivity, which were measured to calculate water permeability (L μm m^{-2} h^{-1} bar^{-1} or

$cm^2\ s^{-1}$), salt permeability ($cm^2\ s^{-1}$), salt rejection (%) and water/NaCl selectivity. The TFC membranes were evaluated for pure water flux ($L\ m^{-2}\ hr^{-1}$) and salt rejection (%). The pressure difference across the membrane was 400 psi (27.6 bar). The aqueous feed contained 2000 ppm NaCl and the feed solution was circulated past the samples at a continuous flow rate of 3.8 ($L\ min^{-1}$). The feed pH was adjusted to a range between 6.5 and 7.5 using a 10 ($g\ L^{-1}$) sodium bicarbonate solution. Sodium chloride concentrations in the feed water and permeate were measured as conductivities with an Oakton 100 digital conductivity meter.

4.4. Results and Discussion

Synthesis and structural characterization of the sulfonated oligomers

Recent results in the McGrath group have indicated that the transport properties of linear BPS and linear BisAS sulfonated polysulfones are significantly different. Linear BisAS copolymers have enhanced water permeabilities and slightly lower salt rejections at similar values of disulfonation. Polymeric composition greatly affects the chain packing and free volume available for transport. With regard to disulfonated polysulfones, BisAS based polymers have lower densities than BPS based polymers, and this has been hypothesized to lead to higher fractional free volumes and enhanced water permeabilities.[15] In this study, we sought to determine the effect of composition on the transport properties of crosslinked disulfonated polysulfones. The synthesis of telechelic amine end-capped disulfonated polysulfones based on a bisphenol-A backbone structure (amBisAS-50) were described in Chapter 3.[9] A similar approach was used to synthesize telechelic amine end-capped disulfonated polysulfones based on 4,4'-biphenol (amBPS-50) as shown in Figure 4.1. Oligomers with a number average molecular weight (M_n) equal to 5,000 $g\ mol^{-1}$ were targeted for consistency with prior studies.[9,11]

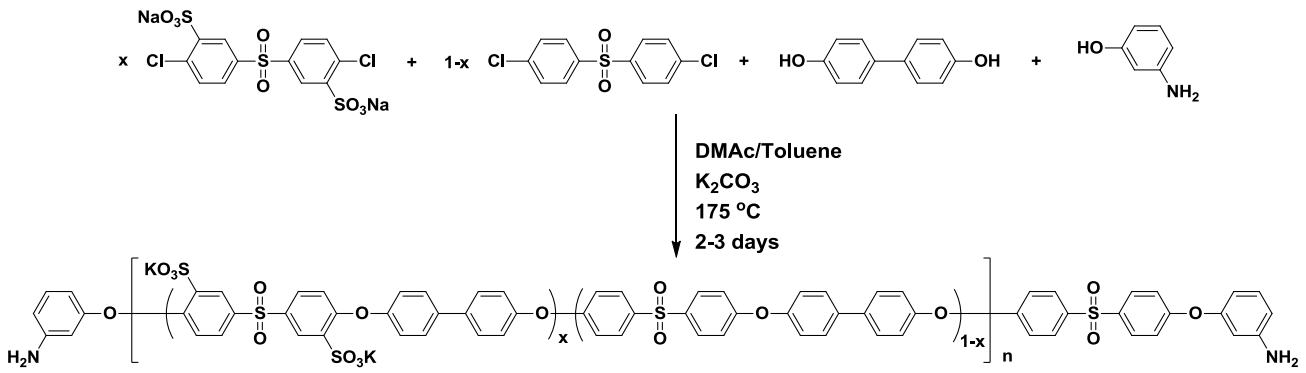

Figure 4.1 Synthesis of amBPS-X oligomers

The compositions of the new oligomers were confirmed with ^{1}H-NMR. The ^{1}H-NMR spectrum of amBPS-50 is shown in Figure 4.2. All of the peaks were represented in the aromatic region, unlike the amBisAS oligomers that had an isopropylidene peak in the aliphatic up-field region. The backbone peaks integrals were compared to the amine endgroup peaks (*i*) and used to calculate M_n.

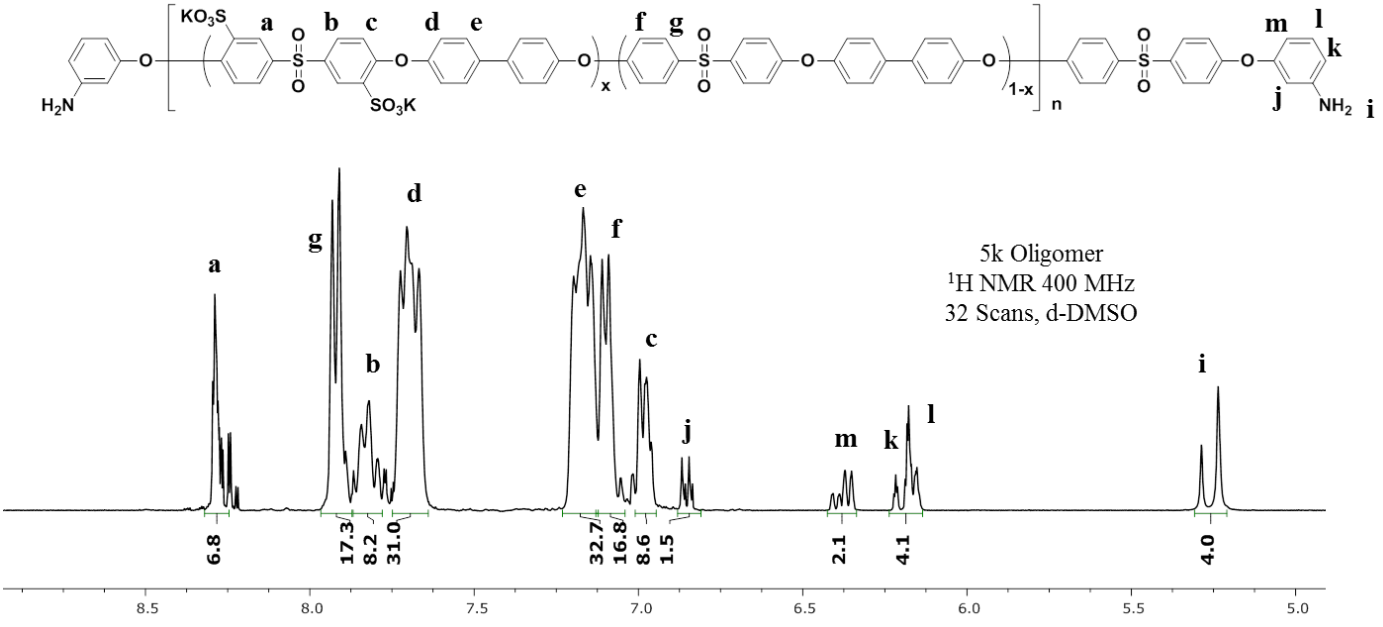

Figure 4.2 ^{1}H-NMR spectrum of an amBPS-50 oligomer

Integration of the sulfonated and non-sulfonated repeat units was also used to establish the degree of sulfonation (D.S.), a measure of hydrophilicity calculated by equation 3.

Equation 3: $$\text{D.S.} = \frac{[(H_a + H_B + H_c)/3]/2}{[(H_a + H_B + H_c)/3]/2 + [(H_f + H_g)/2]/4}$$

The increasing levels of hydrophilicity in both the amBisAS and amBPS series were numerically quantified by equation 3, and were also visually apparent in stacked ^{1}H-NMR spectra. Figure 4.3 shows the amBisAS series at 40, 50 and 60% D.S. The peaks corresponding to the hydrophilic repeat units (*a*, *b*, *c*) were larger compared to other peaks that remained constant, such as the bisphenol-A aromatic protons. Increasing hydrophilicity was also displayed in the telechelic amine endgroups (*i*), which appeared as two singlets since the endgroups were adjacent to both DCDPS and SDCDPS. The relative ratio of these two singlet peaks also validated increasing hydrophilicity as the D.S. was increased from 40 to 60%.

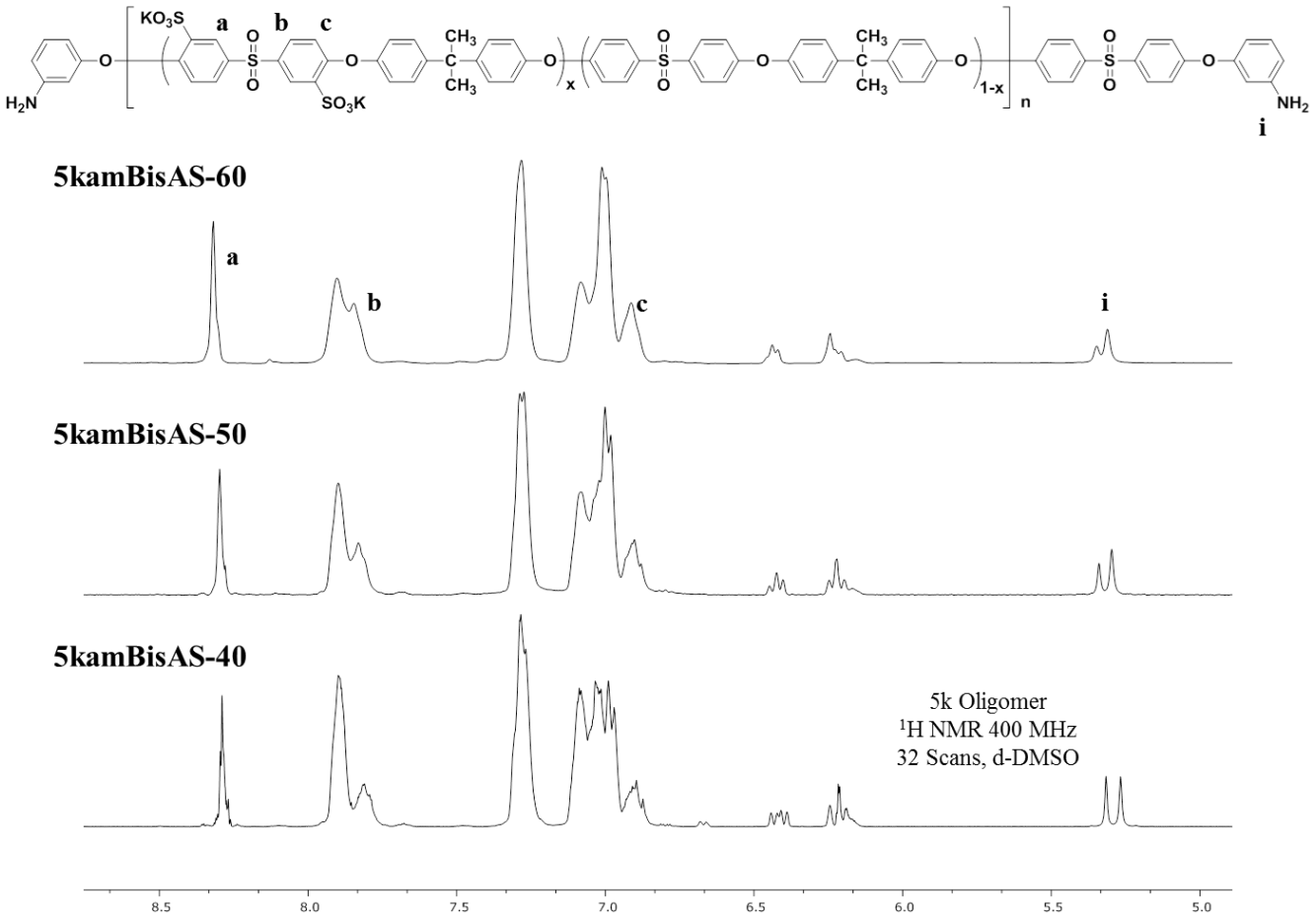

Figure 4.3 ^{1}H-NMR spectra of amBisAS-40, amBisAS-50 and amBisAS-60 oligomers

The targeted and measured degrees of sulfonation and molecular weights of the disulfonated oligomers are summarized in Table 4.1. Excellent success was obtained regarding control over hydrophilicity, as the measured degrees of sulfonation were all within 5% of the targeted composition. The M_n values calculated from the ^{1}H-NMR data were also very close to the targeted M_n of 5,000 g mol^{-1}, which indicated that the molecular weight could be controlled by addition of a monofunctional amine end-capping reagent. The results from SEC differed from both the targeted molecular weights and the ^{1}H-NMR calculated molecular weights. This could be a consequence of interaction between the sulfonated oligomers and the SEC column, which skewed the molecular weight analysis. ^{1}H-NMR is an accurate method for determining

molecular weights as low as 5,000 g mol^{-1}, and was therefore used for stoichiometric calculations to prepare dense crosslinked films.

Table 4.1 Hydrophilicity and molecular weight properties of amBisAS and amBPS oligomers

Sample	Targeted D.S.	Measured D.S. [a]	M_n (g/mol) [a]	M_w (g/mol) [b]	dn/dc (mL/g) [b]
5kamBisAS-40	40	38	4,800	6,200	0.1471
5kamBisAS-50	50	49	4,800	6,500	0.1495
5kamBisAS-60	60	57	5,400	8,100	0.1386
5kamBPS-40	40	40	5,200	8,700	0.1519
5kamBPS-50	50	50	4,600	8,400	0.1610
5kamBPS-60	60	60	4,600	9,100	0.1346

[a] Obtained from 1H-NMR spectra

[b] Obtained from SEC

Fabrication of sulfonated oligomers into crosslinked dense membranes

The amBPS and amBisAS oligomers were prepared as relatively large (10 x 15 cm^2) crosslinked membranes according to a previously established procedure.[9] All six of the crosslinked copolymers had gel fractions greater than 90%. With regard to water purification properties such as water and salt permeability, the crosslink density and molecular weight between crosslinks (M_c) are of interest. The crosslink density affects the free volume available for permeate transport. It was hypothesized that M_c should be approximately equal to the M_n's of

the oligomers. The telechelic amine end-groups were bifunctional towards the tetra functional epoxy resin, and therefore, it was expected that a crosslink site would occur at each endgroup. The gel fractions of the crosslinked dense membranes are listed in Table 4.2.

Table 4.2 Extent of crosslinking in amBisAS and amBPS oligomers crosslinked with TGBAM

Sample	Gel Fraction (%)
5kamBisAS-40	92
5kamBisAS-50	99
5kamBisAS-60	93
5kamBPS-40	90
5kamBPS-50	93
5kamBPS-60	93

Salt rejection, water permeability, salt permeability, and selectivity of crosslinked oligomeric disulfonated polysulfone dense membranes

Water and salt transport properties of the terminally crosslinked disulfonated oligomers were evaluated at by cross-flow filtration. Results from the cross-flow experiments are tabulated below (Table 4.3). The salt rejection was quite high (96-98%) for all of the networks, which indicated that the high amount of swelling that is observed with linear analogues of these disulfonated copolymers was controlled by crosslinking. Interestingly, the salt rejection did not change much despite considerably different water permeabilities and degrees of sulfonation.

Table 4.3 Water purification properties of amBisAS and amBPS oligomers crosslinked with TGBAM

Sample	Salt Rejection (%)	Water Permeability (L μm/(m² h bar))	Water Permeability (cm^2/s)	Salt permeability (cm^2/s)	Permeability Selectivity (P_w/P_s)
5kamBisAS-40	96.0 ± 0.99	0.11 ± 0.002	$4.10 \pm 0.07 \times 10^{-7}$	$3.30 \pm 0.80 \times 10^{-10}$	$1.32 \pm 0.34 \times 10^{3}$
5kamBisAS-50	96.6 ± 0.51	0.36 ± 0.01	$1.38 \pm 0.03 \times 10^{-6}$	$9.57 \pm 1.69 \times 10^{-10}$	$1.49 \pm 0.23 \times 10^{3}$
5kamBisAS-60	97.1 ± 0.18	0.83 ± 0.06	$3.17 \pm 0.24 \times 10^{-6}$	$1.88 \pm 0.26 \times 10^{-9}$	$1.70 \pm 0.10 \times 10^{3}$
5kamBPS-40	Results in Progress	Results in Progress	Results in Progress	Results in Progress	Results in Progress
5kamBPS-50	97.8 ± 0.82	0.43 ± 0.05	$1.63 \pm 0.20 \times 10^{-6}$	$6.81 \pm 1.33 \times 10^{-10}$	$2.54 \pm 0.70 \times 10^{3}$
5kamBPS-60	96.7 ± 0.17	1.18 ± 0.11	$4.52 \pm 0.43 \times 10^{-6}$	$2.96 \pm 0.13 \times 10^{-9}$	$1.52 \text{ x} \pm 0.08 \times 10^{3}$

The crosslinked amBPS networks are compared with previously data on linear disulfonated BPS based polysulfone copolymers in Figure 4.4.[16] The numbers adjacent to the data points are the targeted degrees of sulfonation values, for example the crosslinked amBPS-50 network has a salt rejection of 97.8% and a hydraulic water permeability of 0.43 (L μm m^{-2} h^{-1} bar^{-1}).

The transport properties of linear disulfonated polysulfone copolymers have been actively studied in recent years.[1,12,15-20] The hydrophilic disulfonated copolymers swell in aqueous environments, increasing the amount of free volume in the polymer and allowing higher fractional volumes of water to become incorporated into the copolymer. In a previous systematic series, as the degree of sulfonation increased the amount of swelling in the copolymers also increased, and this corresponded to enhanced permeation of both water and solutes.[16] The water permeability also increased with enhanced degrees of disulfonation because of higher water solubility coefficients. The disulfonated copolymers achieved high levels of salt rejection because of the fixed anionic sulfonate groups on the polymer backbone. These anionic groups actively repelled dissolved anions such as Cl^- by Donnan exclusion. However, this repulsive effect was sensitive to water purification operating conditions, including external salt

concentration (feed water concentration). Despite the role of the fixed anionic groups in salt rejection, the high swelling at large degrees of disulfonation greatly increased hole-type diffusion of salts throughout the polymer matrix and led to lower values of salt rejection. The expected trend for salt rejection versus water permeability in linear BPS copolymers is shown in Figure 4.4. The water permeability continually increased with growing degrees of disulfonation, but at the cost of decreased salt rejection.

Networks comprised of the terminally crosslinked amBPS oligomers showed improved transport properties compared to the linear BPS series. For example, the crosslinked amBPS-50 oligomer produced the same salt rejection as a linear BPS-30 copolymer, but twice as high water permeability. The difference between the crosslinked amBPS-50 oligomer and linear BPS-50 was even more drastic. BPS-50 had been reported elsewhere as having a salt rejection of 73.4% and a hydraulic water permeability of 3.5 (L μm m^{-2} h^{-1} bar^{-1}).[11] Therefore, by introducing crosslinks at the terminal ends of these oligomers, salt rejection was significantly improved. A numerical comparison could not be made between the crosslinked amBPS-60 network and linear BPS-60, because BPS-60 swelled so greatly that it lost all mechanical integrity and failed at high pressures in aqueous environments. However, the crosslinked amBPS-60 membrane also had the best combination of high salt rejection and high water permeability out of all the networks that were tested. The water permeability drastically improved as a function of increasing degree of disulfonation in the crosslinked amBPS series. The crosslinked amBPS-60 had water permeability nearly three times higher than the amBPS-50 network, but only 1% lower salt rejection. The results suggest relatively uniform swelling between the crosslinked materials and also similar levels of hole-type diffusion by salt particles. However, an advantage in water

permeability might be gained by exploiting the higher water solubility coefficients in more highly disulfonated copolymers.

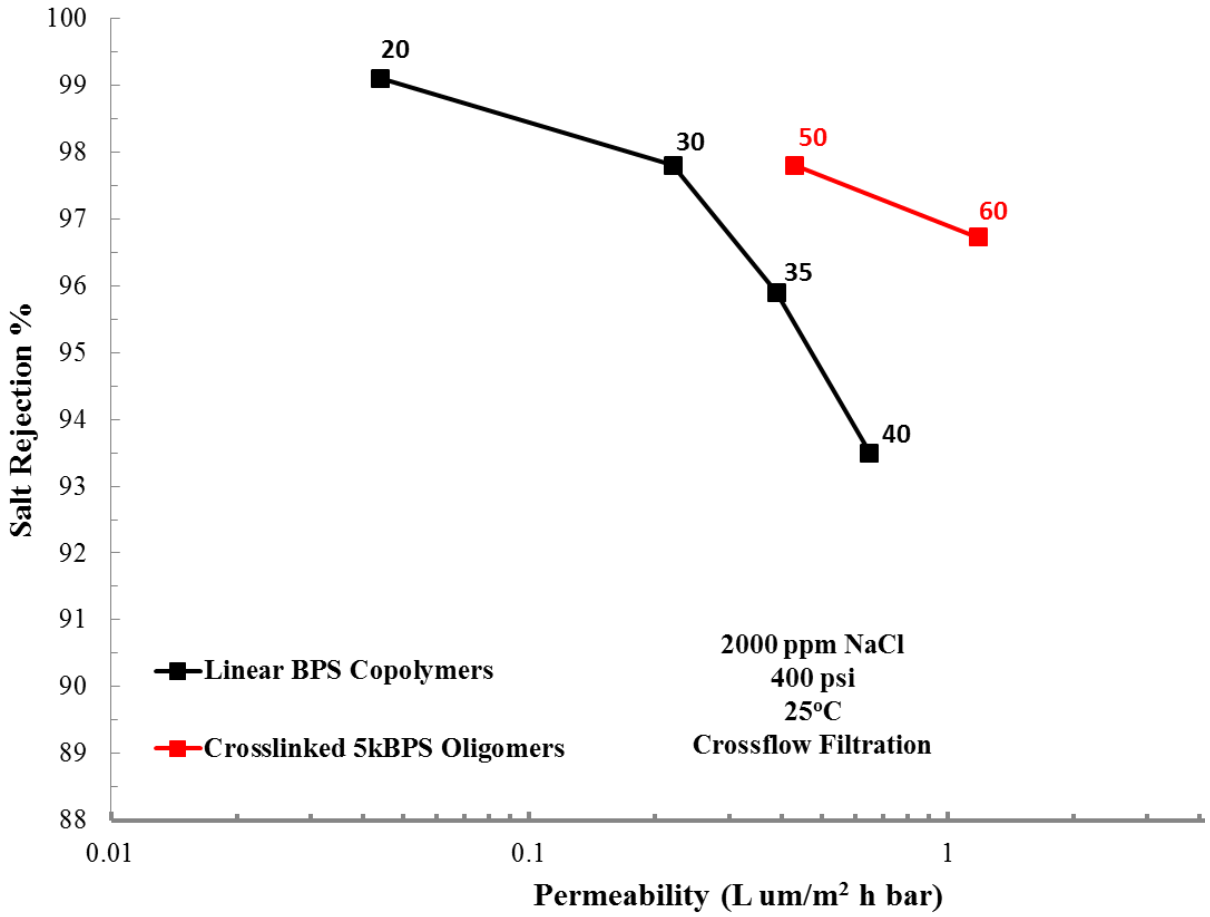

Figure 4.4 Salt rejection versus hydraulic water permeability in linear and crosslinked BPS copolymers

The crosslinked amBisAS oligomers were also compared with linear BisAS copolymers data in Figure 4.5. The linear BisAS series showed a similar trend to the linear BPS series, a higher degree of disulfonation led to decreased salt rejection and increased water permeability. However, the transport results for the crosslinked amBisAS oligomers varied widely from the linear control series. One of the networks, crosslinked amBisAS-60, had superior water purification properties compared to the linear BisAS copolymers. However, amBisAS-40 and amBisAS-50 networks both had inferior transport results compared to the linear series.

In all cases, the crosslinked oligomers resulted in higher salt rejection and lower water permeability than the analogous linear copolymer. For example, crosslinking the amBisAS-40 oligomer raised the salt rejection by approximately 3.5% compared to the linear BisAS-40 copolymer, but the huge decrease in water permeability made crosslinking an unattractive tradeoff. Alternatively, the crosslinking of amBisAS-60 increased the salt rejection by about 8.5% compared to a linear BisAS-60 copolymer, with a less drastic decrease in water permeability. The results emphasized that crosslinking was an effective way to control membrane swelling and raise rejection efficiency, though the overall effects on membrane performance were not always beneficial.

A remarkable trend was observed within the crosslinked amBisAS series. Both the salt rejection and water permeability increased as a function of increasing degree of disulfonation. The increase in water permeability was expected, but the increase in salt rejection was unanticipated. One reason for this phenomenon could be that swelling between the crosslinked amBisAS networks was relatively constant, but the increased ionic content of the crosslinked amBisAS-60 membrane could have contributed to heightened Donnan exclusion effects resulting in enhanced salt rejection compared to the amBisAS-40 and amBisAS-50 membranes.

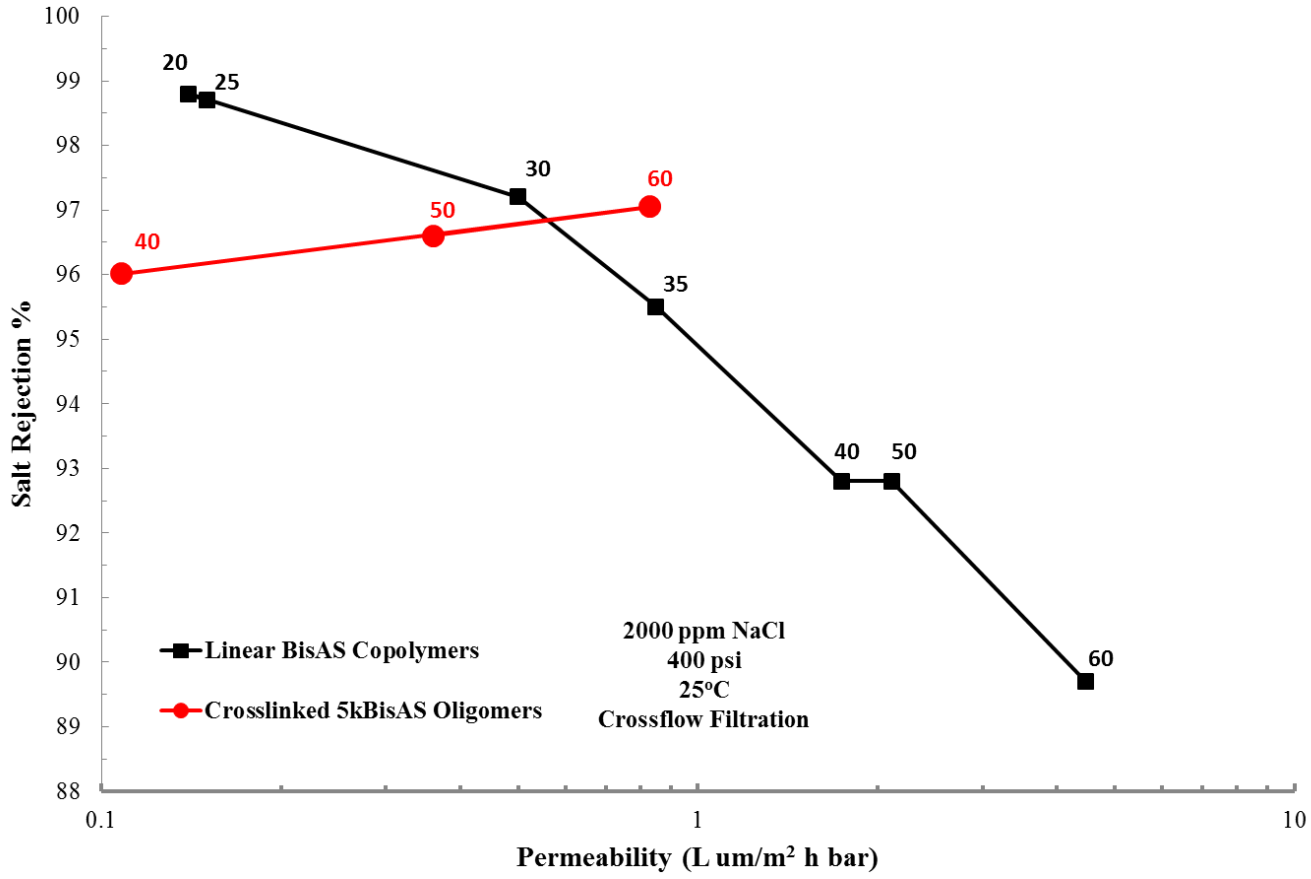

Figure 4.5 Salt rejection versus hydraulic water permeability in linear and crosslinked BisAS copolymers

Figures 4.4 and 4.5 provide useful comparisons between the linear copolymers and crosslinked oligomers. However, both salt rejection and hydraulic water permeability are dependent on the operating conditions. Increased applied pressures will increase the water flux while the salt flux remains relatively constant, artificially increasing the salt rejection of the membranes. For a true comparison to other water purification membranes, selectivity and diffusive water permeability must be used. Selectivity, another measure of rejection efficiency, is equal to the ratio of the diffusive water and salt permeabilities (P_w/P_s). Selectivity is an intrinsic membrane property similar to diffusive water permeability and diffusive salt permeability, because it does not depend on operating conditions such as applied pressure.

An "upper-bound" has been identified for water purification membranes by plotting the log of selectivity versus the log of diffusive water permeability.[17] The upper-bound is an empirically formulated line that represents the best transport results obtainable for a given combination of selectivity and water permeability. The best water purification membranes are the ones on or closest to the upper-bound. One main focus of material research is to transverse the upper-bound in the upper right direction. The crosslinked oligomers are graphed on an upper-bound plot in Figure 4.6, along with the linear disulfonated polysulfone copolymers, the state-of-the-art aromatic polyamides, and several other water purification membranes.

The results in Figure 4.6 show that crosslinking not only increases the salt rejection and selectivity of sulfonated polysulfones, but that it could also greatly improve their water purification properties. Both crosslinked networks with a 60% degree of disulfonation were much closer to the upper-bound than any of the linear disulfonated polysulfone copolymers. The linear disulfonated BPS copolymers in the graph span a wide range of selectivity and water permeability values; however, the selectivities of the crosslinked sulfonated oligomers remained relatively constant. Similar phenomena have previously been observed in crosslinked materials for use as fuel cell membranes, in which crosslinking simultaneously increased proton conductivity and membrane selectivity (conductivity/methanol permeability).[21] Crosslinking greatly reduced the swelling of sulfonated polysulfones and allowed for the development of sulfonated polysulfones with higher levels of hydrophilicity than previously used. In the future, crosslinked sulfonated polysulfone copolymers with a 70, 80, 90 and even 100% D.S. will be targeted to examine if even higher values of water permeability can be obtained while still maintaining relatively constant selectivity.

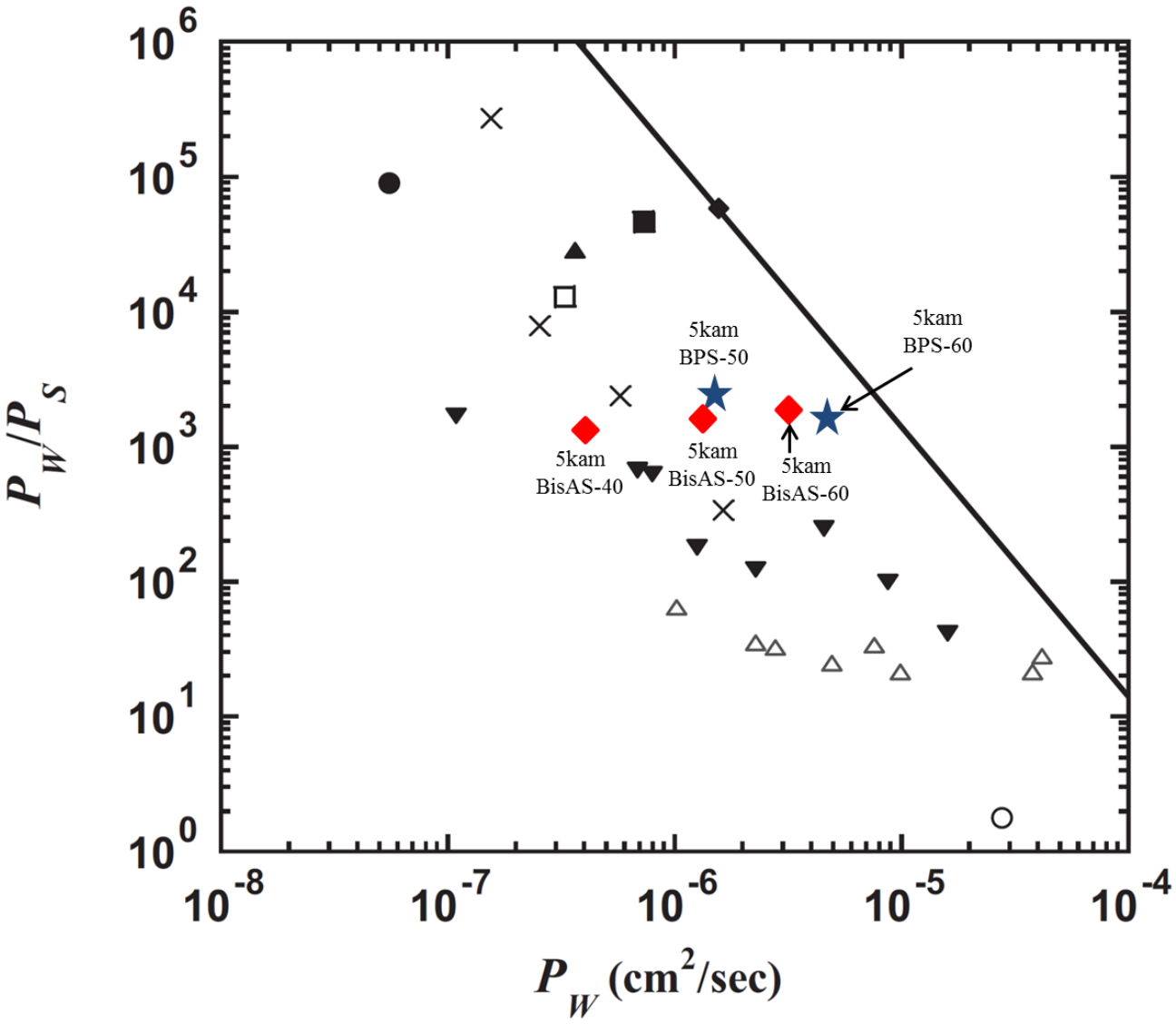

Figure 4.6 Fundamental transport properties water/NaCl permeability selectivity, P_w/P_s, and permeability coefficient, P_w, comparison between crosslinked amBPS oligomers (★), crosslinked amBisAS oligomers (◆), linear BPS copolymers (▼), state-of-the-art aromatic polyamide (■), PBP (polybenzimidazolepyrrolone,♦) and other water purification membranes[17]

Preparation, transport properties and morphology of amBisAS-50 TFC's

Although the dense crosslinked oligomers discussed above achieved promising transport results, commercial development would require substantially thinner materials. Water permeability is directly proportional to membrane thickness, and the dense oligomers were 50-60 μm thick, compared to the near 100 nm thickness of the state-of-the-art aromatic polyamide. The state-of-the-art material can be produced at this thickness because it is supported on a polysulfone support as a TFC. As a result, TFC development was attempted with the crosslinked disulfonated polysulfone oligomers.

Several challenges were encountered during preparation of an amBisAS-50 TFC. The DMAc casting solvent used for dense film preparation could not be used because it was also a co-solvent for the polysulfone support layer. Additionally, the dense oligomeric network layer could only be crosslinked at 90^{o}C as opposed to 180-200^{o}C. Temperatures higher than 90^{o}C resulted in pore shrinkage of the polysulfone support and very low water fluxes. Nevertheless, defect-free TFC's were obtained with similar values of salt rejection as the dense, more highly crosslinked amBisAS-50 membrane. Figure 4.7 shows a thin, defect-free crosslinked amBisA-50 layer formed on a Udel® support material. However, a high number of pores underneath the layer were filled with the crosslinked amBisA-50, and this could have hindered water molecules from quickly transporting through the crosslinked amBisA-50 skin.

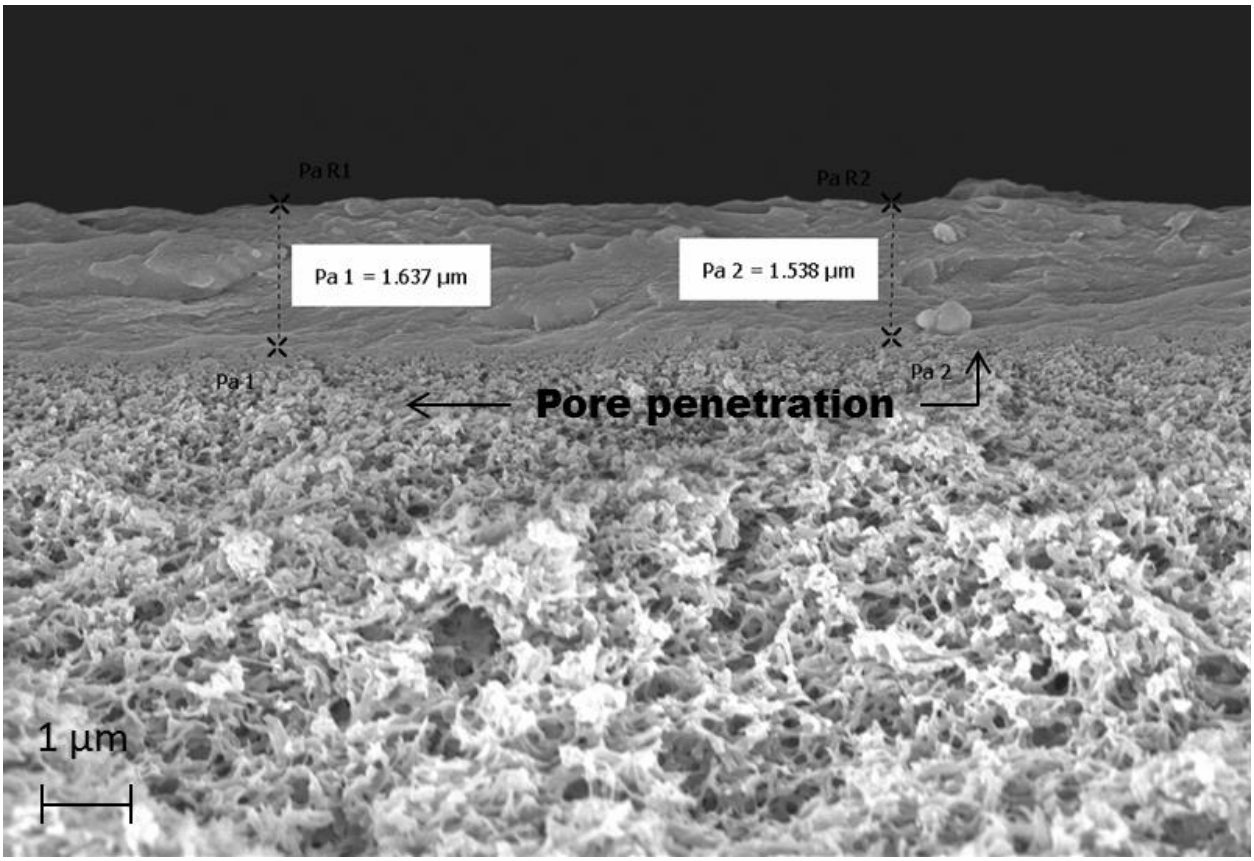

Figure 4.7 SEM cross-sectional images of a partially crosslinked amBisAS-50 TFC membrane, which was single-coated onto the pretreated Udel® support

As shown in Figure 4.8, the water flux values are still significantly lower than the state-of-the-art TFC, which measures near 50 (L m^{-2} h^{-1}).[7] Preparation of a TFC by a UV curing process would avoid undesirable high temperature treatments and perhaps greatly increase the flux of the membrane. Therefore, the current thrust of material research in the McGrath group is preparing UV curable telechelic oligomers and demonstrating their TFC fabrication.

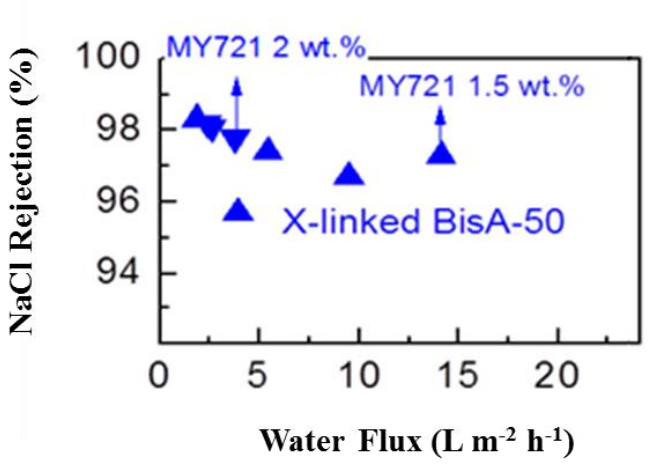

Figure 4.8 Salt rejection versus water flux in amBisAS-50 partially crosslinked TFCs with a Udel® polysulfone support layer

4.5. Conclusions

In this paper, the water and salt transport properties of membranes comprised of disulfonated polysulfone oligomers were systematically studied with regards to polymer composition, crosslinking, and degree of disulfonation/hydrophilicity. The disulfonated oligomers were well defined structurally by ^{1}H-NMR, ensuring that consistent molecular weights and end-group functionalities were obtained. All of the oligomers were fabricated into large films with gel fractions exceeding 90%, and transport properties were characterized. Crosslinking effectively reduced the swelling of the polymer membranes and controlled the salt rejection, though permeability was still influenced by degree of sulfonation. In particular, the crosslinked oligomers at the highest degree of sulfonation studied (60%) achieved superior transport results to previously studied linear sulfonated copolymers. Future work will study crosslinked oligomers at higher degrees of sulfonation and varying crosslink density. The fabrication of these crosslinked oligomers into thin film composites was also initially studied and showed promise for future development.

4.6. References

(1) Geise, G. M.; Paul, D. R.; Freeman, B. D. *Prog. Polym. Sci.* **2014**, *39*, 1.

(2) Elimelech, M.; Phillip, W. A. *Science* **2011**, *333*, 712.

(3) Park, H. B.; Freeman, B. D.; Zhang, Z.-B.; Sankir, M.; McGrath, J. E. *Angew. Chem., Int. Ed.* **2008**, *47*, 6019.

(4) Cadotte, J. E.; Petersen, R. J.; Larson, R. E.; Erickson, E. E. *Desalination* **1980**, *32*, 25.

(5) Petersen, R. J. *J. Membr. Sci.* **1993**, *83*, 81.

(6) Song, Y.; Sun, P.; Henry, L. L.; Sun, B. *J. Membr. Sci.* **2005**, *251*, 67.

(7) Xie, W.; Geise, G. M.; Freeman, B. D.; Lee, H.-S.; Byun, G.; McGrath, J. E. *J. Membr. Sci.* **2012**, *403-404*, 152.

(8) Chan, E. P.; Young, A. P.; Lee, J.-H.; Chung, J. Y.; Stafford, C. M. *J. Polym. Sci., Part B: Polym. Phys.* **2013**, *51*, 385.

(9) Sundell, B. J.; Lee, K.-s.; Nebipasagil, A.; Shaver, A.; Cook, J. R.; Jang, E.-S.; Freeman, B. D.; McGrath, J. E. *Ind. Eng. Chem. Res.* **2014**, *53*, 2583.

(10) Li, Y.; VanHouten, R. A.; Brink, A. E.; McGrath, J. E. *Polymer* **2008**, *49*, 3014.

(11) Paul, M.; Park, H. B.; Freeman, B. D.; Roy, A.; McGrath, J. E.; Riffle, J. S. *Polymer* **2008**, *49*, 2243.

(12) Lee, C. H.; McCloskey, B. D.; Cook, J.; Lane, O.; Xie, W.; Freeman, B. D.; Lee, Y. M.; McGrath, J. E. *J. Membr. Sci.* **2012**, *389*, 363.

(13) Hedrick, J. L.; Mohanty, D. K.; Johnson, B. C.; Viswanathan, R.; Hinkley, J. A.; McGrath, J. E. *J. Polym. Sci., Part A: Polym. Chem.* **1986**, *24*, 287.

(14) Sagle, A. C.; Van, W. E. M.; Ju, H.; McCloskey, B. D.; Freeman, B. D.; Sharma, M. M. *J. Membr. Sci.* **2009**, *340*, 92.

(15) Xie, W.; Ju, H.; Geise, G. M.; Freeman, B. D.; Mardel, J. I.; Hill, A. J.; McGrath, J. E. *Macromolecules* **2011**, *44*, 4428.

(16) Xie, W.; Cook, J.; Park, H. B.; Freeman, B. D.; Lee, C. H.; McGrath, J. E. *Polymer* **2011**, *52*, 2032.

(17) Geise, G. M.; Park, H. B.; Sagle, A. C.; Freeman, B. D.; McGrath, J. E. *J. Membr. Sci.* **2011**, *369*, 130.

(18) Geise, G. M.; Freeman, B. D.; Paul, D. R. *J. Membr. Sci.* **2013**, *427*, 186.

(19) Xie, W.; Geise, G. M.; Freeman, B. D.; Lee, C. H.; McGrath, J. E. *Polymer* **2012**, *53*, 1581.

(20) Xie, W.; Park, H.-B.; Cook, J.; Lee, C. H.; Byun, G.; Freeman, B. D.; McGrath, J. E. *Water Sci. Technol.* **2010**, *61*, 619.

(21) Chul, G. S.; Chul, K. J.; Ahn, D.; Jang, J.-S.; Kim, H.; Chul, J. J.; Lim, S.; Jung, D.-H.; Lee, W. *J. Membr. Sci.* **2012**, *417-418*, 2.

CHAPTER 5: SYNTHESIS AND CHARACTERIZATION OF SULFONATED HYDROQUINONE BASED POLY(ARYLENE ETHER SULFONE) RANDOM COPOLYMERS FOR USE AS WATER PURIFICATION MEMBRANES

Benjamin J. Sundell, [a] *Eui-Soung Jang,* [b] *Andrew T. Shaver,* [a] *Hailun Borjigin,* [a] *Priya Pisipati,* [a] *Judy S. Riffle,* [a] *Benny D. Freeman,* [b] *James E. McGrath* [a]

[a] Macromolecules and Interfaces Institute, Virginia Polytechnic Institute and State University, Blacksburg, VA 24061, USA

[b] Department of Chemical Engineering, Center for Energy and Environmental Resources, The University of Texas at Austin, Austin, TX, 78758, USA

Article in preparation for submission

5.1. Abstract

A systematic series of hydroquinone-based disulfonated poly(arylene ether sulfone) random copolymers were synthesized for use as water purification membranes. The copolymers were produced with varying levels of hydrophilicity, ranging from a 15 to 40% degree of disulfonation. The copolymer compositions were confirmed with ^{1}H-NMR and IR spectroscopy and SEC confirmed that high molecular weights were achieved. The copolymers were cast into tough, ductile, dense membranes and transport properties were elucidated by cross-flow filtration. The transport results showed an unexpected trend of both increasing salt rejection and water permeability as the degree of disulfonation was increased. In particular, the hydroquinone-based disulfonated copolymer with a 25% degree of disulfonation had significantly better water

permeability and salt rejection transport properties compared to previously studied 4,4'-biphenol- and bisphenol-A-based linear disulfonated polysulfone copolymers.

5.2. Introduction

Polymeric membranes for water purification enable an important technology platform to address several global challenges in the 21st century. Currently over one-third of the world's population lives in areas of high water stress, a number that is projected to increase.[1,2] Rising population levels, increased industrialization, and agricultural production all contribute to the need for increased amounts of potable water.[1,3] Desalination is an especially enticing route to produce potable water, as the oceans contain a virtually endless supply of salt water for the process. Membrane separations by reverse osmosis (RO) dominate the desalination market because of the low energy requirements compared to traditional distillation technologies.[1,4,5] Over 16 billion gallons of potable water are produced by desalination every day and this number is expected to double within the next decade.[1,4] The industries involved in water purification and energy production are intertwined; i.e., fresh water is needed to produce energy and vice-versa.[4] Thus, water purification membranes can also be used in the production of energy by forward osmosis, reverse electrodialysis, and pressure-retarded osmosis.[3,4]

Traditional materials for desalination membranes most notably include cellulose acetate and crosslinked aromatic polyamides.[6,7] Crosslinked aromatic polyamides, the current state-of-the-art materials, exhibit excellent salt rejection properties, reasonable water permeabilities, and very thin separation layers can be fabricated on a porous support as a thin film composite (TFC).[8,9] However, aromatic polyamides have poor oxidative chemical stability.[10,11] They polyamides degrade in the presence of chlorinated disinfectants by various chain scissioning

mechanisms, and chlorine is an essential additive to reduce biofouling and protect drinking water.[12,13] Additionally, the aromatic polyamide membranes cannot easily be prepared into dense free-standing films, and this hinders studies of fundamental structure-property relationships that guide membrane research.[4]

Poly(arylene ether sulfones) are an industrially important class of polymers that are used in gas separations and ultrafiltration water purification.[14,15] Polysulfones for ultrafiltration membranes have a porous morphology and discriminate by size-sieving mechanisms, in which water permeates through these materials by convective diffusion.[16] However, RO membranes must be nonporous (dense) to separate water from salt ions. Water permeates through the membrane by becoming solubilized at the membrane-feed interface and then diffuses through to the permeate side.[16,17] Thus, RO membranes must be partially hydrophilic, which is obtainable in polysulfones by several different routes.

One method of introducing hydrophilicity is by post-sulfonation, in which a hydrophobic polysulfone is treated with various sulfonic acids resulting in electrophilic aromatic substitution along the polymer backbone.[18] These post-sulfonated polysulfones have been identified as RO candidates,[19] but suffer from heterogeneous backbone microstructures and degradation during the harsh acidification process.[20] An alternative route towards hydrophilicity is direct-sulfonation.[21] In this process, a hydrophilic monomer is directly incorporated into the polymer during the polymerization, and this approach enables more controlled microstructures and allows for highly ionic compositions.[22,23]

In recent years, the McGrath and Freeman groups have collaborated to actively investigate syntheses and properties of disulfonated polysulfone copolymers. These membranes have reasonable RO properties, excellent resistance against chlorine,[24,25] they can be fabricated

into TFC's,[26,27] and recently they have been fabricated as asymmetric membranes.[28] Disulfonated polysulfones have also served as excellent model systems for investigating structure-property relationships for applications as RO membranes. McGrath and Freeman have investigated water and salt permeability, selectivity at different levels of disulfonation/hydrophilicity,[29] the effect of free volume,[30] effects of processing and thermal history on water transport properties,[31] the role of NaCl feed concentration on salt rejection,[32] and the effect of covalent crosslinking on transport properties.[33,34] One area that still needs development with regard to structure-property relationships of sulfonated polysulfones is the role of different chemical compositions.

The initial report on disulfonated polysulfones for RO membranes compared two series of sulfone and phosphine oxide-containing copolymers, each based on 4,4'-biphenol as the phenolic comonomer.[35] More recently, random copolymers based on 4,4'-(propane-2,2-diyl)diphenol (bisphenol A) were synthesized and diverse transport properties were obtained. The results showed that the compositions of the sulfonated polysulfones influence water permeability and salt rejection. It will be important to further investigate the effect of structure on transport properties. Benzene-1,4-diol (hydroquinone) based polysulfones are known in the literature[36] and have shown promise for application as fuel cells.[37,38] However, these materials have yet to be explored as water purification membranes.

This paper describes a series of random disulfonated polysulfone copolymers focused on hydroquinone as the bisphenol for potential use as reverse osmosis membranes. The compositions were systematically varied in disulfonation content and hydrophilicity. They were characterized structurally and thermally in addition to determination of their water purification properties. In comparison to 4,4'-biphenol and bisphenol A-based copolymers, the

hydroquinone-based copolymer with 25% of the repeat units disulfonated was identified as having the best combination of salt rejection and water permeability.

5.3. Experimental

Materials

4,4'-Dichlorodiphenylsulphone (DCDPS, 99%) was kindly provided by Solvay and recrystallized from toluene before use. Akron Polymer Systems (Akron, OH) prepared 3,3'-disulfonated-4,4'-dichlorodiphenylsulfone (SDCDPS, 98%) using procedures developed earlier.[39,40] Hydroquinone (HQ) was purchased from Eastman and used as received. Potassium carbonate (K_2CO_3), *N*,*N*-dimethylacetamide (DMAc, 99%), 2-propanol (IPA) and toluene were purchased from Fisher. The DMAc reaction solvent was dried over calcium hydride (CaH_2), distilled under reduced pressure and stored over molecular sieves before use. Calcium hydride (90-95%) was purchased from Alfa Aesar. Phosphorus pentoxide (P_2O_5) and lithium bromide (LiBr) were purchased from Aldrich. 1-Methyl-2-pyrrolidone (NMP) was purchased from Spectrum Chemicals.

Synthesis of a hydroquinone-based polysulfone copolymer with 25% of the repeat units disulfonated (HQS-25)

The hydroquinone-based random copolymers (Fig. 5.1) were synthesized using nucleophilic aromatic substitution step polymerization with a weak base.[23,41] This method allows for the disulfonated moieties to be directly incorporated into the backbone rather than utilizing post-sulfonation reactions. For a 25% disulfonated copolymer, x = 0.25 and 1-x = 0.75 in Figure 5.1.

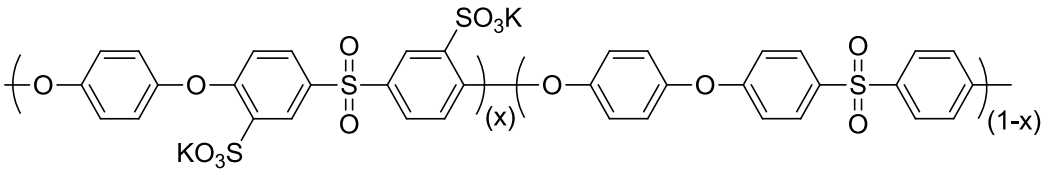

Figure 5.1 Structure of hydroquinone-based disulfonated polysulfone copolymer

The hygroscopic reagents SDCDPS and K_2CO_3 were dried for 72 h at 160°C under vacuum to ensure complete removal of water. The SDCDPS contained residual amounts of NaCl impurity (3% by weight) from the monomer synthesis. The impurity was quantified by UV-visible spectroscopy and additional SDCDPS was used to correct the reaction stoichiometry.[39] HQ (30 mmol, 3.3033 g), DCDPS (22.5 mmol, 6.4611 g), SDCDPS (7.5 mmol, 3.7788 g), and DMAc (54 mL) were added to a 100-mL three-necked flask. The reaction flask was equipped with a mechanical stirrer, nitrogen inlet, and Dean-Stark trap containing toluene. A stirring, thermally regulated oil bath was used to heat the reaction. After the oil bath reached 150°C, K_2CO_3 (42 mmol, 5.8048 g) and toluene (27 mL) were added via a funnel. The reaction was continued at 150°C for several hours until all of the water was azeotropically removed. The temperature was raised to 175°C and water and toluene were drained from the Dean-Stark trap. The reaction was continued for 48 h at 175°C until a viscous solution was obtained. The opaque, brown solution was diluted with additional DMAc (70 mL), cooled to room temperature, and filtered. The resulting solution was precipitated into stirring IPA (800 mL) to produce a white fibrous solid. The polymeric product was stirred in DI water for several hours at 60-70°C, filtered and then dried overnight at 110°C under vacuum. All of the other disulfonated copolymers were synthesized by this route, and the varying degrees of disulfonation were obtained by adjusting the ratios of DCDPS to SDCDPS.

Nuclear Magnetic Resonance (^{1}H-NMR)

^{1}H-NMR analysis of the copolymers was performed on a Varian Unity Plus spectrometer operating at 400 MHz. The spectra of the copolymers were obtained from a 15% (w/v) 1 mL solution in DMSO-d_6. For the HQS-15 copolymer, heat was required to fully dissolve the polymer sample.

Infrared Spectroscopy (IR)

FTIR-ATR spectra were recorded on an FTIR spectrometer (Varian 670 FTIR) equipped with an ATR attachment with a diamond crystal. The resolutions of the spectra were 4 cm^{-1} and 32 background scans were performed. A small amount of copolymer film was placed on the diamond crystal and the FTIR spectrum was measured with 32 scans. All measurements were performed at ambient temperature.

Size Exclusion Chromatography (SEC)

Intrinsic viscosities (IV) and molecular weights of the copolymers were obtained by size exclusion chromatography (SEC). The SEC system consisted of an isocratic pump (Agilent 1260 infinity, Agilent Technologies) with an online degasser (Agilent 1260, Agilent Technologies, Santa Clara, CA), autosampler and column oven used for mobile phase delivery and sample injection, and three Agilent PLgel 10 µm Mixed B-LS columns 300×7.5 mm connected in series with a guard column as the stationary phase. A system of multiple detectors connected in series was used for the analysis. A multi-angle laser light scattering (MALS) detector (DAWN-HELEOS II, Wyatt Technology Corporation, Goleta, CA) operating at a wavelength of 658 nm, a viscometer detector (Viscostar, Wyatt Technology Corporation), and a

refractive index detector operating at a wavelength of 658 nm (Optilab T-rEX, Wyatt Technology Corporation) provided online results. The system was corrected for interdetector delay, band broadening, and the MALS signals were normalized using a 21,720 g/mol polystyrene standard obtained from Agilent Technologies or Varian. Data acquisition and analysis was conducted using Astra 6 software (Wyatt Technology Corporation). The mobile phase was NMP, which was vacuum distilled over P_2O_5 before use. The salt, 0.05 M dried LiBr was dissolved in the NMP before the solvent was degassed and filtered. The sample solutions were prepared in a concentration range of 2~3 mg/mL and were filtered to remove any dust or insoluble particles using 0.22 μm PTFE filters. Molecular weights were measured using light scattering and the intrinsic viscosities were measured online. Note that specific refractive index increment (dn/dc) values were calculated for each backbone type based on the assumption of 100 % mass recovery using Astra 6 software.

Thermal Gravimetric Analysis (TGA)

The thermal stability of the copolymers was investigated using a TA Instruments TGA Q5000. The copolymers were first heated in nitrogen at a rate of $10^oC\ min^{-1}$ to 300^oC to ensure that any sorbed water was removed, cooled to 50^oC, and heated at $10^oC\ min^{-1}$ to 700^oC.

Film Preparation

The films were prepared by first dissolving 1.0 g of copolymer in 19 g of DMAc to obtain a 5 wt% mixture. The mixtures were stirred until a homogeneous solution was obtained and then syringe filtered through a 1.0 μm filter into a new vial. The solutions were cast on an (18 x 21.5) cm^2 clean, dry glass plate on a level surface in a vacuum oven. The films were dried

at 80°C for 24 h without vacuum, and then at 110°C for 48 h with vacuum. Films were removed from their glass substrates by soaking in water. A section was cut from the films for measuring water uptake, and the rest of the film was used to evaluate water permeability and salt rejection.

Water uptake measurements

Film coupons were dried overnight at 110°C under vacuum, removed, and weighed to obtain the dry weight (W_{dry}). The films were soaked in DI water for 48 hours, blotted to remove surface droplets and weighed to obtain the wet weight (W_{wet}). This protocol was repeated an additional time, and water uptake values were calculated by equation 5.1.

Equation 5.1: $$Water\ Uptake\ (\%) = \frac{W_{wet} - W_{dry}}{W_{dry}} \times 100$$

Transport Properties of water permeability and salt

The water permeability (L μm m^{-2} h^{-1} bar^{-1} or cm^2 s^{-1}), salt permeability (cm^2 s^{-1}), salt rejection (%) and water/NaCl selectivity were determined at 25°C using stainless steel crossflow cells machined at the University of Texas at Austin.[42] The pressure difference across the membrane (15.1 cm^2) was 400 psi. The aqueous feed contained 2000 ppm NaCl, and the feed solution was circulated past the samples at a continuous flow rate of 3.8 (L min^{-1}). The feed pH was adjusted to a range between 6.5 and 7.5 using a 10 g/L sodium bicarbonate solution. NaCl concentrations in the feed water and permeate were measured with an Oakton 100 digital conductivity meter.

5.4. Results and Discussion

Synthesis of hydroquinone-based disulfonated polysulfone copolymers (HQS)

Syntheses of HQS copolymers with varying levels of hydrophilicity were performed following established procedures for nucleophilic aromatic substitution, as shown in Figure 5.2.[22] Hydroquinone was used rather than bisphenol-A or 4,4'-biphenol in order to provide a compositional contrast to previous random copolymers. For equal molar loadings of the disulfonated monomer (equivalent degree of sulfonation), hydroquinone based copolymers were expected to have higher levels of hydrophilicity and water permeability because of the lower molecular weight of hydroquinone compared to previously studied bisphenol monomers.

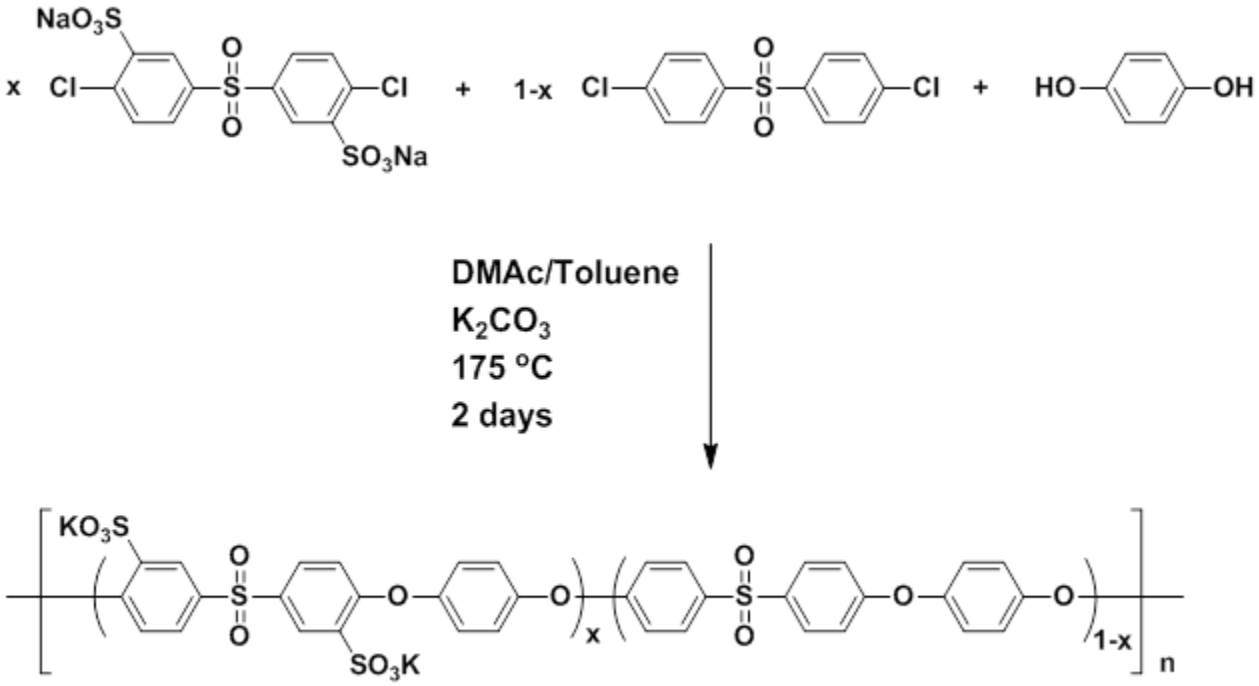

Figure 5.2 Synthesis of HQS copolymers

During the initial stages of the reaction, water was evolved from potassium carbonate decomposition which could potentially react with the activated dihalides and negatively

influence the reaction stoichiometry.[41] Toluene was added with the potassium carbonate and the reaction mixture was refluxed for several hours to azeotropically remove any water from the reaction. During this time, the reaction turned an opaque blue color. During the azeotropic removal and subsequent heat increase, it was important to occasionally heat the joints of the three-necked flask with a heat gun, as water/toluene azeotrope became trapped in these locations and could adversely affect the reaction during later stages.[43] As the reaction proceeded to higher molecular weight, the bluish color subsided and viscous, amber brown solutions were obtained.

After isolating the polymers, ^{1}H-NMR was used to characterize the copolymer compositions. Exemplary spectra are shown in Figure 5.3 where the expected compositions were confirmed. As shown below, the size and integrations of the hydrophilic protons continuously increased throughout the systematic series. The polymeric endgroups near 6.9 ppm were also identified, and their low integrations served as an indication of high molecular weight. Progress of the polymerization was tracked by taking aliquots of the reaction solution, precipitating the polymer, and integrating the endgroup moieties.

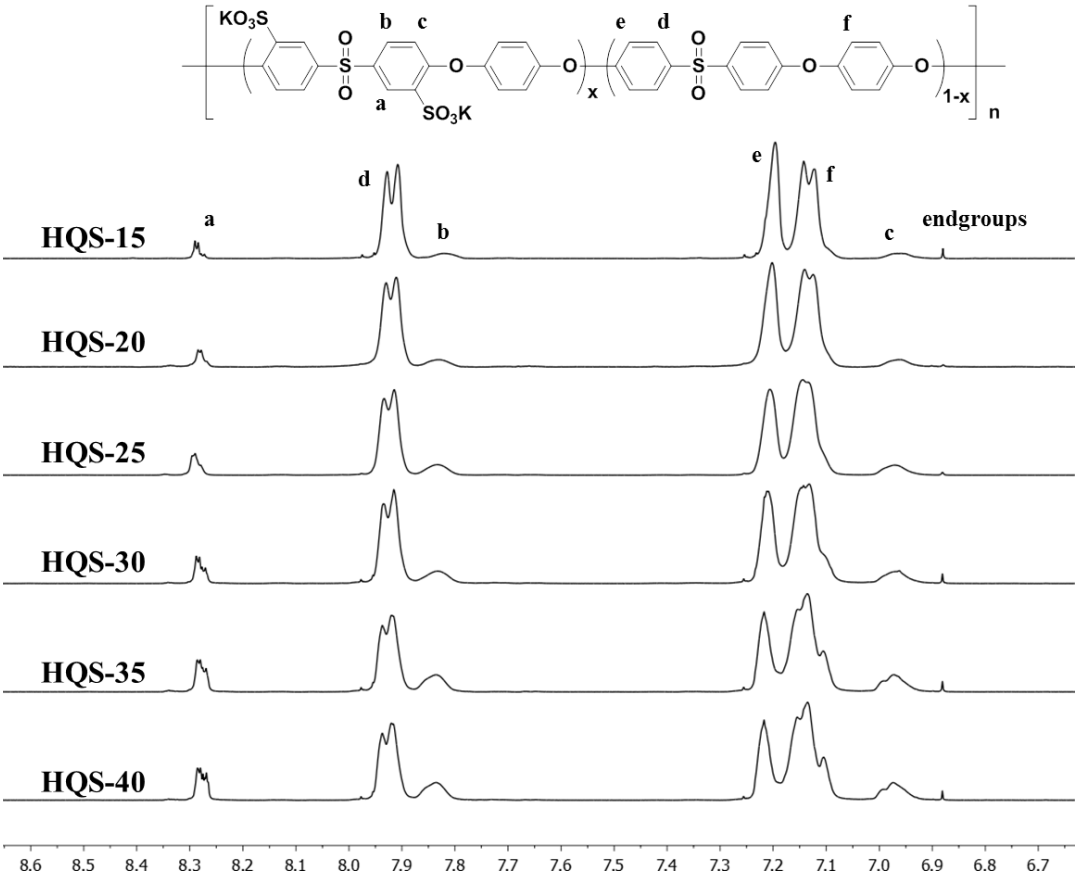

Figure 5.3 [1]H-NMR spectra of HQS copolymers

In addition, [1]H-NMR was used to characterize composition with regard to the degree of disulfonation (D.S.). The D.S. is the mole fraction of disulfonated units in the copolymer and this provides a measure of hydrophilicity. Similar to the ion exchange capacity (IEC) which characterizes the equivalents of ions per gram, increased values of D.S. corresponded to increased water uptake, and therefore higher values of water permeability in water purification processes. The D.S. was calculated by Equation 5.2, which compared the integrations of the protons on the hydrophilic moieties (*a, b, c*) to the hydrophobic moieties (*f, g*).

Equation 5.2: $$\text{D.S.} = \frac{[(H_a + H_B + H_c)/3]/2}{[(H_a + H_B + H_c)/3]/2 + [(H_f + H_g)/2]/4}$$

The D.S. was targeted between 15-40% at 5% increments to achieve a systematic series of hydroquinone-based copolymers with varying levels of hydrophilicity. The measured D.S. is listed in Table 5.1 with the corresponding IEC values. In all cases, the measured D.S. was within 10% of the targeted value.

Table 5.1 Hydrophilicity of HQS copolymers

Sample	**Targeted D.S.**	**Measured D.S.** [a]	**IEC** [b]	**Water Uptake**
HQS 15	15%	13%	0.73	7.8 ± 2.2%
HQS 20	20%	17%	0.93	11.9 ± 1.1%
HQS 25	25%	23%	1.21	13.3 ± 3.8%
HQS 30	30%	27%	1.39	12.3 ± 0.9%
HQS 35	35%	37%	1.80	20.9 ± 2.0%
HQS 40	40%	38%	1.83	25.6 ± 2.3%

[a] Measured from ^{1}H-NMR, potassium counterion

[b] Potassium counterion

IR of copolymers

Fourier transform infrared spectroscopy was also used to confirm the structures of the copolymers. The peak assignments for sulfonated polysulfones had been identified for both post-sulfonated and directly sulfonated copolymers.[22,44] In Figure 5.4, the ring vibrations of *p*-

substituted aryl ethers (1008 cm^{-1}) and symmetric O=S=O stretching of the sulfonate group (1026 cm^{-1}) are labeled. As the D.S. and hydrophilicity of the copolymers increase, the relative ratio of the sulfonate peak to the ether peak should increase. This trend was observed for the systematic series, which indicated that a set of increasingly hydrophilic copolymers were obtained.

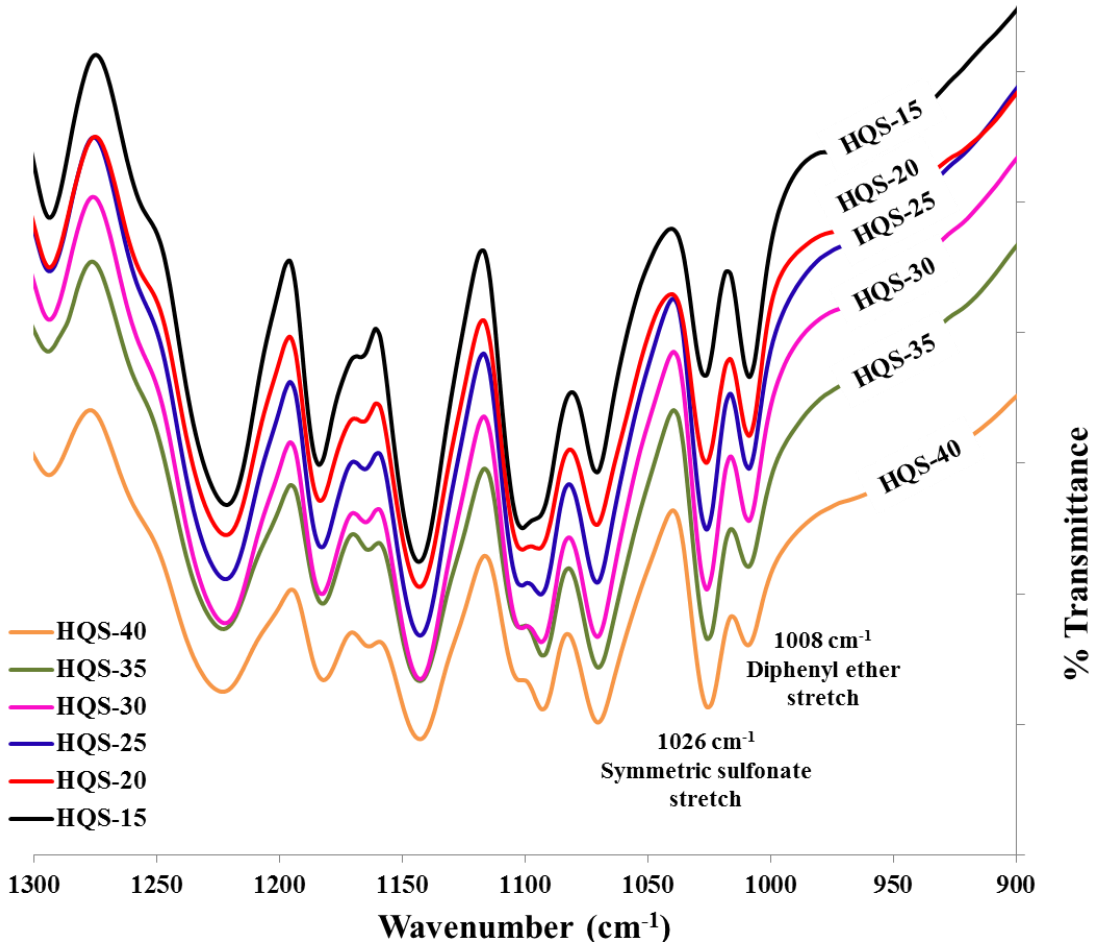

Figure 5.4 Infrared spectra of HQS copolymers

SEC of copolymers

All of the polymers were cast into tough, ductile films, which qualitatively indicated that high molecular weight was achieved in addition to the ^{1}H-NMR results. Molecular weights of the copolymers were quantitatively investigated by SEC (Figure 5.5). The chromatograms were

obtained from light scattering and have the Gaussian monomodal molecular weight distribution indicative of successful step growth polymerizations.

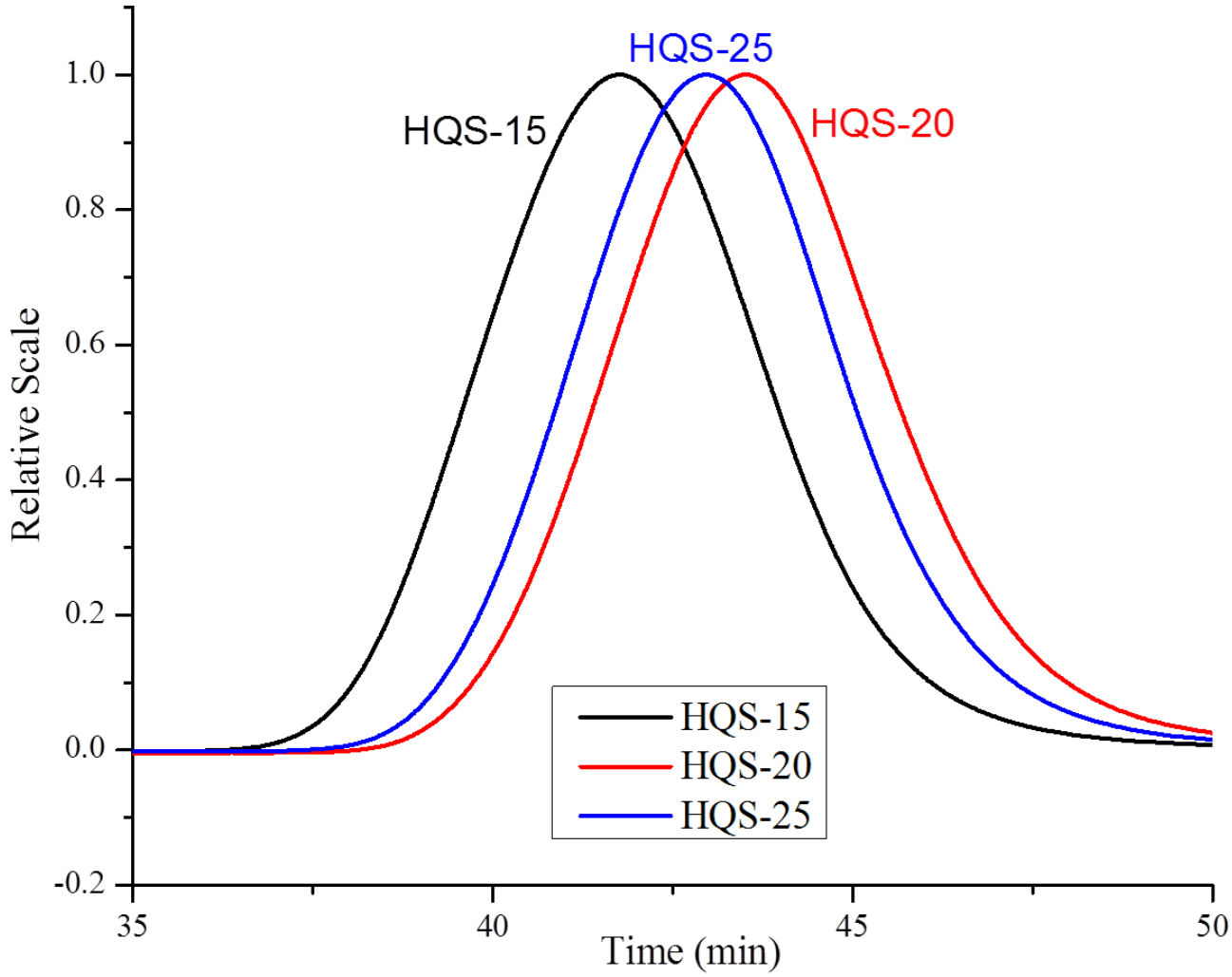

Figure 5.5 SEC chromatograms of HQS copolymers

The SEC molecular weight distributions were analyzed in dilute solutions of NMP containing 0.05 M LiBr, a good solvent for the disulfonated copolymers. The lithium bromide was added to disrupt any aggregation and to counteract any polyelectrolyte effect. In dilute solutions, polymeric chains with fixed ionic groups on the backbone undergo chain expansion.[45] The chain expansion results in an increased radius of gyration, intrinsic viscosity, and error in molecular weight measurements. Relatively constant ionic concentrations are achieved and chain

expansion is reduced by adding a mobile salt such as lithium bromide. Through this method, accurate intrinsic viscosities and molecular weights were obtained by SEC.

The molecular weights averages (M_n and M_w), molecular weight distributions (PDI), intrinsic viscosities ([η]), and change in refractive index with changing concentration (dn/dc) are listed in Table 5.2. Very high molecular weights were obtained in all of the copolymer systems, regardless of D.S. that was targeted. A PDI of 2 is expected for step-growth polymerizations, and the molecular weight distributions of the copolymers were somewhat narrower than this amount. The copolymers were boiled in water during the polymer workup to assist in salt and solvent removal. Some lower molecular weight materials were likely lost during this step, resulting in lower than expected PDI's. The M_w values are likely more accurate, since light scattering experiments directly measure M_w.

Table 5.2 Molecular weights and molecular weight distributions of HQS copolymers

Sample	M_w (kDa)	[η] (dL/g)	dn/dc (mL/g)
HQS 15	172.2	1.01	0.135
HQS 20	75.4	0.55	0.148
HQS 25	90.1	0.78	0.145
HQS 30	123.7	0.65	0.150
HQS 35	103.7	0.57	0.131
HQS 40	114.9	0.53	0.121

TGA of copolymers under N_2

Disulfonated polysulfones are recognized as high performance polymers with very high degradation temperatures and disulfonated dichlorodiphenylsulfone was even investigated for use as a flame retardant. The copolymers synthesized in this work also had very high thermal stabilities, as shown in Figure 5.6. All of the copolymers had 10% weight loss values above 500°C, which corresponded to degradation of the polymeric backbone.[23] The TGA thermograms confirmed that the copolymers had adequate thermal stability for RO processes.

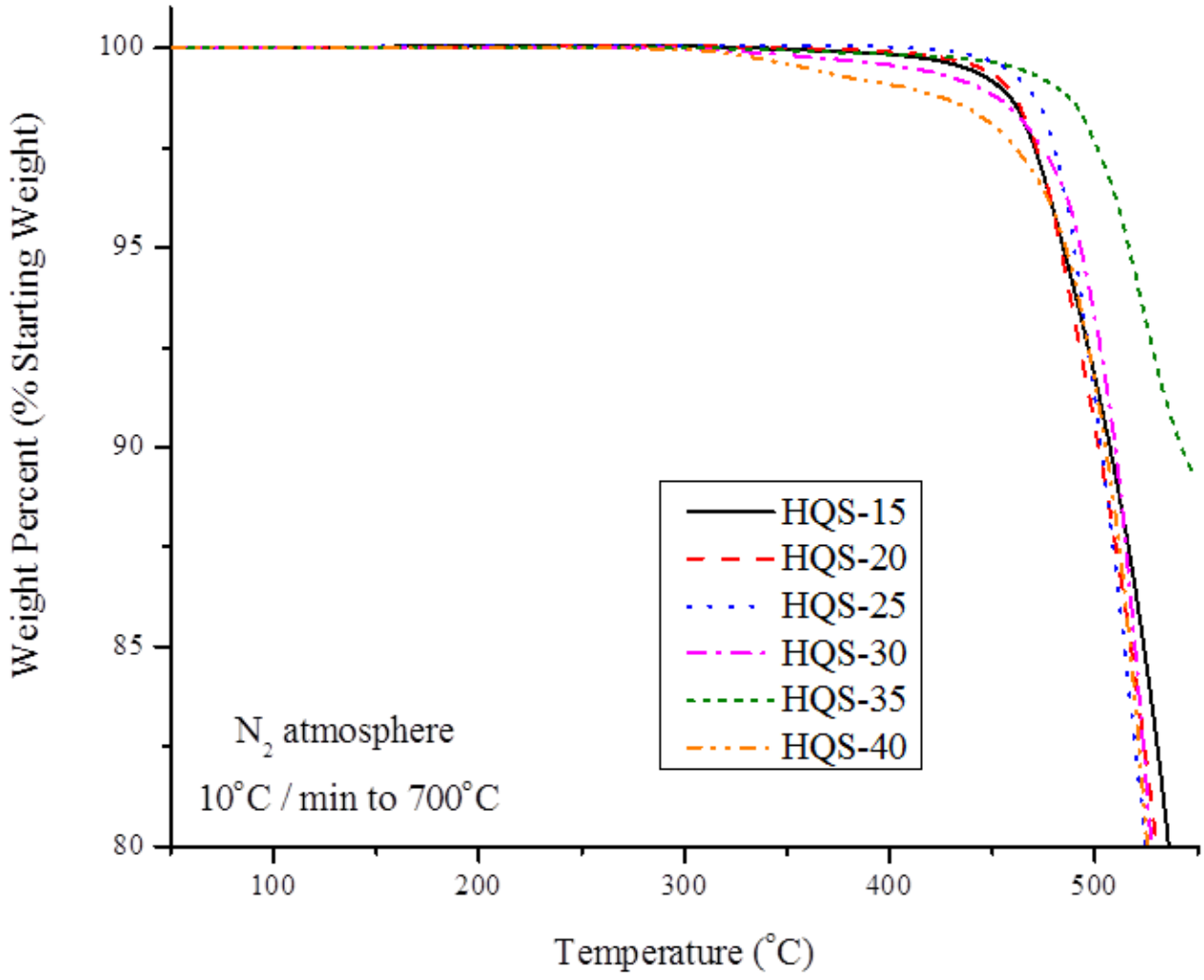

Figure 5.6 Thermal stability of HQS copolymers

Water uptake of HQS copolymer

The water uptakes of the disulfonated copolymers were measured as an early predictor of water permeability. The films were dried at 80^{o}C for 24 hours at ambient pressure and then at 110^{o}C for 48 hours under vacuum. The heating regimen was used to ensure that all of the DMAc casting solvent as well as moisture was removed.[29] The transport properties of disulfonated polysulfones are very sensitive to processing conditions, drying temperatures, and thermal annealing.[31] The water uptake values are shown below in Figure 5.7.

The water uptake was plotted as a function of degree of disulfonation (measured from ^{1}H-NMR). Eight measurements were made for every level of hydrophilicity and minor standard deviations were obtained in all cases, except for the 23% disulfonated copolymer. A nonlinear increase in water uptake was observed, which differed from the disulfonated 4,4'-biphenol based system.[29] At higher levels of sulfonation, the water uptake drastically increased because of a morphological change. The data points at 37 and 38% disulfonation possibly showed this trend, though smaller error bars would be needed for confirmation.

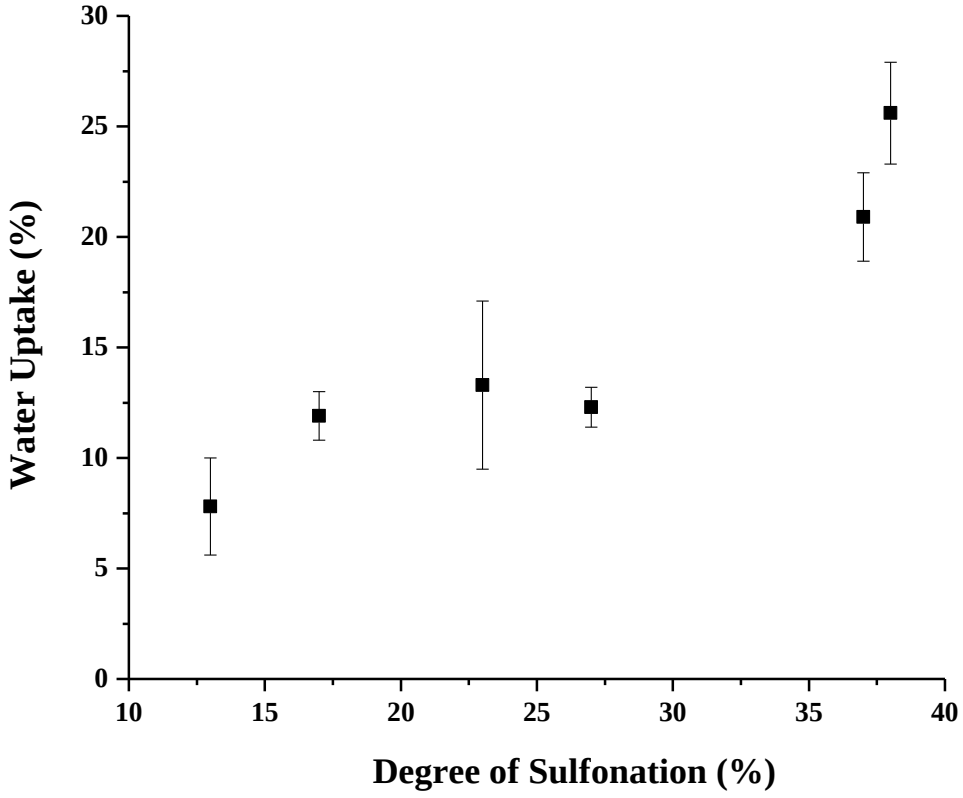

Figure 5.7 Water uptake as a function of the measured degree of disulfonation

Salt rejection and water permeability of HQS copolymers

The transport properties of the copolymers were tested at the University of Texas at Austin by crossflow filtration. A variety of membrane properties were tested and are summarized in Table 5.3. The permeability of the eluting species was quantified by hydraulic water permeability (L μm/(m^2 h bar)), diffusive water permeability (cm^2/s), and diffusive salt permeability (cm^2/s). The separation efficiency was quantified by permeability selectivity (the ratio of diffusive water and salt permeability) and salt rejection (% NaCl rejected).

Table 5.3 Water transport properties of HQS copolymers

Sample	Salt Rejection (%)	Water Permeability (L μm/(m² h bar))	Water Permeability (cm²/s)	Salt permeability (cm²/s)	Permeability Selectivity (P_w/P_s)
HQS 15	94.1	0.064	2.43×10^{-7}	2.95×10^{-10}	8.24×10^{2}
HQS 20	97.2 ± 0.05	0.33 ± 0.01	$1.27 \pm 0.03 \times 10^{-6}$	$7.01 \pm 0.05 \times 10^{-10}$	$1.81 \pm 0.03 \times 10^{3}$
HQS 25	97.9 ± 0.07	1.06 ± 0.06	$4.05 \pm 0.25 \times 10^{-6}$	$1.66 \pm 0.16 \times 10^{-9}$	$2.45 \pm 0.09 \times 10^{3}$

The transport of water and salt through disulfonated polysulfones has been extensively studied in the Freeman laboratories.[4,16,29,32] The ionic domains in the polymer backbone aggregated to form discrete domains that had been discerned through atomic force microscopy for both random and block disulfonated polysulfone copolymers. For random copolymers at low levels of sulfonation, the ionic domains take the form of isolated ionic regions in a matrix of non-ionic regions. At a high enough level of sulfonation, the ionic domains become continuous and formed large ionic channels throughout the polymer microstructure. A drastic increase in water uptake and permeability often accompanies the transition from ionic clusters to continuous domains. In general, increasing the amount of hydrophilic charged groups on the polymer backbone increased water uptake and water and salt permeability. At the most fundamental level, Yasuda showed that permeability and diffusion of water and salt through hydrated polymers increased with higher volume fractions of water and free volume inside the polymer.[46] Higher loadings of ionic domains resulted in enhanced swelling in aqueous environments, higher water volume fractions and free volume, and thus higher permeabilities, which were observed in Table 5.3.

Compared to water transport, salt transport through sulfonated polysulfones was much more nuanced due to the fixed anionic groups on the polymeric backbone that actively attracted cations and repelled anions. Additionally, salt sorption coefficients were very sensitive to

external salt concentration in charged polymers. As the external salt concentration increased, the ability of the sulfonate groups to repel anionic mobile salts by Donnan exclusion was effectively screened.[32] Thus, both salt diffusivity and sorption increased with heightened external salt concentration, whereas salt diffusivity and sorption remained relatively constant in uncharged polymers at varying levels of external salt concentration.[4]

The transport results for the disulfonated hydroquinone-based copolymers are shown in Figure 5.8 along with a series of disulfonated biphenol-based copolymers and a series of disulfonated bisphenol A-based copolymers.[29] The separation efficiency was quantified by a rejection coefficient (% NaCl rejected). Equation 5.3 for salt rejection is shown below, where c_{sl} is the salt concentration on the permeate side of the membrane, and c_{s0} is the salt concentration on the feed side of the membrane.

Equation 5.3: $R = \left(1 - \frac{c_{sl}}{c_{s0}} \right) * 100\%$

Due to the sensitivity of salt rejection, all of the results shown in Figure 5.8 were tested at 400 psi. Water permeability was proportional to applied pressure, whereas salt permeability was not. Therefore, higher applied pressures artificially inflate the salt rejection term. Water permeability was quantified by hydraulic water permeability, which standardized the membranes to a 1.0 μm thickness, and further standardized the membranes surface area, experimental time and pressure in the denominator.

Transport results that were obtained previously for the disulfonated biphenol copolymer series and disulfonated bisphenol A copolymer series followed a logical trend of increased water permeability and decreased salt rejection at higher levels of disulfonation. The higher levels of disulfonation swelled the polymers, and this led to higher water volume fractions and more free volume in the polymer. Accordingly, water and salt permeability increased through the

membrane at higher levels of disulfonation, which corresponded to decreased salt rejection. Notably, the bisphenol A copolymer series had superior transport properties compared to the biphenol copolymers, including higher values of water permeability at a similar % salt rejection. Also, the bisphenol A copolymer with a 30% D.S. had a higher water permeability than the biphenol copolymer with a 30% D.S., even though the biphenol copolymers had higher I.E.C. values at the same D.S. It was hypothesized that the tetrahedral isopropylidene group in the backbone of the bisphenol A component created a kink in the structure, lowered the polymer density, and increased free volume.

The 15, 20 and 25% disulfonated hydroquinone-based copolymers also demonstrated the trend of increased water permeability at higher levels of disulfonation. Surprisingly, however, the salt rejection also increased at higher levels. The 20% disulfonated hydroquinone copolymer (HQS-20) had transport properties in line with the disulfonated biphenol and disulfonated bisphenol A results. Comparatively, HQS-15 had very poor transport properties and the HQS-25 had excellent transport results. Further research is warranted to understand whether those very different results are due to differing morphologies. The other three films in the series, HQS-30, HQS-35 and HQS-40 are currently being tested in Texas and will aid in the understanding of these results. These films are expected to follow the trend of decreasing salt rejection and increasing water permeability.

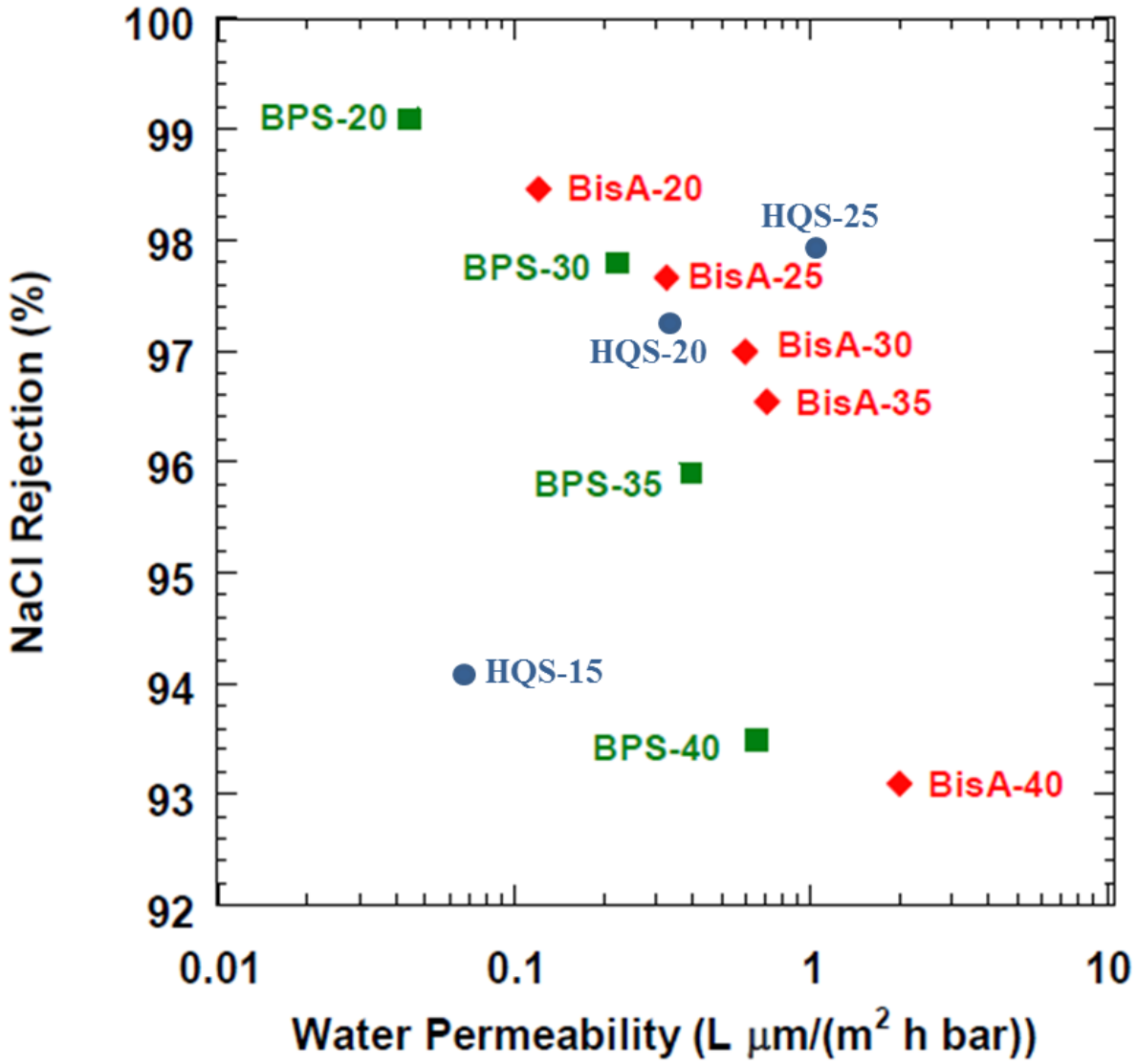

Figure 5.8 Salt rejection and water permeability comparison between HQS, BPS and BisA copolymers

Selectivity and pure water permeability of HQS copolymers

Salt rejection and hydraulic water permeability are often quoted in the literature, but these are not solely material properties because they depend on applied pressure and other testing conditions. Therefore, it was also useful to examine the transport properties of the disulfonated hydroquinone-based copolymers by fundamental measurements such as diffusive water and salt permeability, P_w and P_s (cm^2/s). These measurements did not vary with crossflow operating conditions and were also used to calculate the selectivity of the membrane (Equation 5.4). This

measured separation efficiency and also did not depend on operating conditions. Similar to salt rejection, high values of selectivity are most desirable in a separation process.

Equation 5.4: $\alpha_{w/s} = \frac{P_W}{P_S} = \frac{K_W}{K_S} * \frac{D_W}{D_S}$

Together, selectivity and diffusive water permeability were used to plot the intrinsic membrane properties of a material and were used to construct upper-bound tradeoff plots for reverse osmosis membranes.[47] These properties are plotted in Figure 5.9, along with other linear disulfonated bisphenol-based copolymers, the state-of-the-art aromatic polyamide, and several other reverse osmosis membranes.

The fundamental transport results were similar to the salt rejection vs. water permeability comparison. The HQS-15 and HQS-20 materials were similar to other disulfonated polysulfone random copolymers, but HQS-25 had improved transport properties relative to any of the disulfonated polysulfones. The HQS-25 copolymer approached the upper bound, the black line on the figure, which has been considered the limit of transport properties obtainable for solution-diffusion membranes in reverse osmosis. The HQS-25 proved to be the best linear disulfonated polysulfone copolymer that we have prepared to date for water purification by achieving selectivity values a magnitude greater than any of the other copolymers at similar levels of water permeability. The trend of increasing selectivity and permeability with higher levels of sulfonation will be better understood with further research in this area. The HQS-30, HQS-35 and HQS-40 are currently being tested in Texas and will soon become incorporated into this figure, hopefully leading to increased understanding of the transport properties of these materials. The disulfonated hydroquinone-based copolymers are also excellent candidates for crosslinking reactions as described in Chapters 3 and 4.

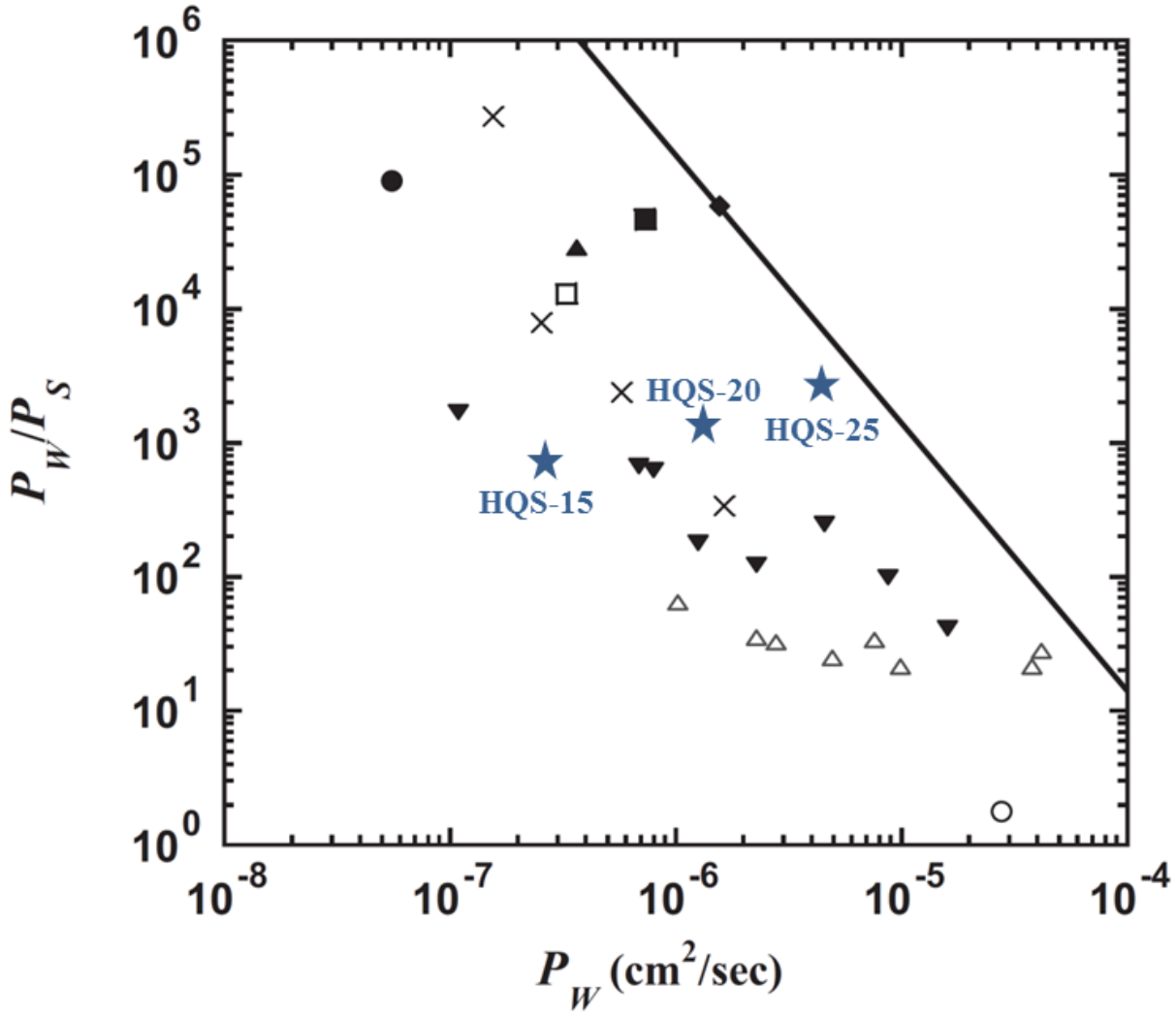

Figure 5.9 Fundamental transport properties water/NaCl permeability selectivity, P_w/P_s, and permeability coefficient, P_w, comparison between HQS (★), BPS (▼), state-of-the-art aromatic polyamide (■) and other water purification membranes[47]

5.5. Conclusions

In this paper, a series of high molecular weight, thermally stable, ductile disulfonated hydroquinone-based polysulfone copolymers were designed and synthesized for use as water purification membranes. The copolymers varied widely in hydrophilicity, which was controlled by targeting incrementally higher degrees of disulfonation. The water purification properties of the copolymers were analyzed by crossflow filtration, which surprisingly showed that both salt

rejection and water permeability increased at higher levels of disulfonation. One membrane based on a 25% disulfonated hydroquinone-based copolymer was found to have water purification properties superior to any previously reported disulfonated polysulfone.

5.6. References

(1) Elimelech, M.; Phillip, W. A. The future of seawater desalination: energy, technology, and the environment. *Science* 2011, *333*, 712.

(2) Oki, T.; Kanae, S. Global hydrological cycles and world water resources. *Science* 2006, *313*, 1068.

(3) Bennett, A. Desalination trends: What's the future for desalination? *Filtration+Separation* 2012.

(4) Geise, G. M.; Paul, D. R.; Freeman, B. D. Fundamental water and salt transport properties of polymeric materials. *Prog. Polym. Sci.* 2014, *39*, 1.

(5) Semiat, R. Energy Issues in Desalination Processes. *Enviromental Science & Technology* 2008, *42*, 8193.

(6) Frommer, M. A.; Murday, J. S.; Messalem, R. M. Solubility and diffusivity of water and of salts in an aromatic polyamide film. *Eur. Polym. J.* 1973, *9*, 367.

(7) Cadotte, J. E.; Rozelle, L. T.; Petersen, R. J.; Francis, P. S. Water transport across ultrathin membranes of mixed cellulose ester and ether derivatives. *Appl. Polym. Symp.* 1970, *No. 13*, 73.

(8) Cadotte, J. E.; Petersen, R. J.; Larson, R. E.; Erickson, E. E. A new thin-film composite seawater reverse osmosis membrane. *Desalination* 1980, *32*, 25.

(9) Cadotte, J. E.; King, R. S.; Majerle, R. J.; Petersen, R. J. Interfacial synthesis in the preparation of reverse osmosis membranes. *J. Macromol. Sci., Chem.* 1981, *A15*, 727.

(10) Orton, K. J. P.; Soper, F. G.; Williams, G. Chlorination of anilides. III. N-Chlorination and C-chlorination as simultaneous side reactions. *J. Chem. Soc.* 1928, 998.

(11) Shintani, T.; Matsuyama, H.; Kurata, N. Effect of heat treatment on performance of chlorine-resistant polyamide reverse osmosis membranes. *Desalination* 2009, *247*, 370.

(12) Avlonitis, S.; Hanbury, W. T.; Hodgkiess, T. Chlorine Degradation of Aromatic Polyamides. *Desalination* 1992, *85*, 321.

(13) Jayarani, M. M.; Rajmohanan, P. R.; Kulkarni, S. S.; Kharul, U. K. Synthesis of model diamide, diester and esteramide adducts and studies on their chlorine tolerance. *Desalination* 2000, *130*, 1.

(14) Ulbricht, M. Advanced functional polymer membranes. *Polymer* 2006, *47*, 2217.

(15) McHattie, J. S.; Koros, W. J.; Paul, D. R. Gas transport properties of polysulfones. 2. Effect of bisphenol connector groups. *Polymer* 1991, *32*, 2618.

(16) Geise, G. M.; Lee, H.-S.; Miller, D. J.; Freeman, B. D.; McGrath, J. E.; Paul, D. R. Water purification by membranes: the role of polymer science. *J. Polym. Sci., Part B: Polym. Phys.* 2010, *48*, 1685.

(17) Wijmans, J. G.; Baker, R. W. The solution-diffusion model: a review. *Journal of Membrane Science* 1995, *107*, 1.

(18) Noshay, A.; Robeson, L. M. Sulfonated polysulfone. *J. Appl. Polym. Sci.* 1976, *20*, 1885.

(19) Brousse, C.; Chapurlat, R.; Quentin, J. P. New Membranes for Reverse Osmosis 1. Characteristics of the Base Polymer: Sulphonated Polysulphones. *Desalination* 1976, *18*, 137.

(20) O'Gara, J. F.; Williams, D. J.; MacKnight, W. J.; Karasz, F. E. Random homogeneous sodium sulfonate polysulfone ionomers: preparation, characterization, and blend studies. *Journal of Polymer Science, Part B: Polymer Physics* 1987, *25*, 1519.

(21) Ueda, M.; Toyota, H.; Ouchi, T.; Suciyama, J.-I.; Yonetake, K.; Masuko, T.; Teramoto, T. Synthesis and Characterization of Aromatic Poly (ether Sulfone)s Containing Pendant Sodium Sulfonate Groups. *Journal of Polymer Science: Part A Polymer Chemistry* 1993, *31*, 853.

(22) Wang, F.; Hickner, M.; Ji, Q.; Harrison, W.; Mecham, J.; Zawodzinski, T. A.; McGrath, J. E. Synthesis of Highly Sulfonated Poly(arylene ether sulfone) Random (Statistical) Copolymers Via Direct Polymerization. *Macromol. Symp* 2001, *175*, 387.

(23) Wang, F.; Hickner, M.; Kim, Y. S.; Zawodzinski, T. A.; McGrath, J. E. Direct polymerization of sulfonated poly(arylene ether sulfone) random (statistical) copolymers: candidates for new proton exchange membranes. *Journal of Membrane Science* 2002, *197*, 231.

(24) Fan, Y.; Cornelius, C. J.; Lee, H.-S.; McGrath, J. E.; Zhang, M.; Moore, R.; Staiger, C. L. The effect of block length upon structure, physical properties, and transport within a series of sulfonated poly(arylene ether sulfone)s. *J. Membr. Sci.* 2013, *430*, 106.

(25) Xie, W.; Park, H.-B.; Cook, J.; Lee, C. H.; Byun, G.; Freeman, B. D.; McGrath, J. E. Advances in membrane materials: desalination membranes based on directly copolymerized disulfonated poly(arylene ether sulfone) random copolymers. *Water Sci. Technol.* 2010, *61*, 619.

(26) Lee, C. H.; McCloskey, B. D.; Cook, J.; Lane, O.; Xie, W.; Freeman, B. D.; Lee, Y. M.; McGrath, J. E. Disulfonated poly(arylene ether sulfone) random copolymer thin film composite membrane fabricated using a benign solvent for reverse osmosis applications. *Journal of Membrane Science* 2012, *389*, 363.

(27) Widjojo, N.; Chung, T.-S.; Weber, M.; Maletzko, C.; Warzelhan, V. A sulfonated polyphenylenesulfone (sPPSU) as the supporting substrate in thin film composite (TFC) membranes with enhanced performance for forward osmosis (FO). *Chemical Engineering Journal* 2013, *220*, 15.

(28) Stevens, D. M.; Mickols, B.; Funk, C. V. Asymmetric reverse osmosis sulfonated poly(arylene ether sulfone) copolymer membranes. *J. Membr. Sci.* 2014, *452*, 193.

(29) Xie, W.; Cook, J.; Park, H. B.; Freeman, B. D.; Lee, C. H.; McGrath, J. E. Fundamental salt and water transport properties in directly copolymerized disulfonated poly(arylene ether sulfone) random copolymers. *Polymer* 2011, *52*, 2032.

(30) Xie, W.; Ju, H.; Geise, G. M.; Freeman, B. D.; Mardel, J. I.; Hill, A. J.; McGrath, J. E. Effect of Free Volume on Water and Salt Transport Properties in Directly Copolymerized Disulfonated Poly(arylene ether sulfone) Random Copolymers. *Macromolecules* 2011, *44*, 4428.

(31) Xie, W.; Geise, G. M.; Freeman, B. D.; Lee, C. H.; McGrath, J. E. Influence of processing history on water and salt transport properties of disulfonated polysulfone random copolymers. *Polymer* 2012, *53*, 1581.

(32) Geise, G. M.; Freeman, B. D.; Paul, D. R. Sodium chloride diffusion in sulfonated polymers for membrane applications. *J. Membr. Sci.* 2013, *427*, 186.

(33) Paul, M.; Park, H. B.; Freeman, B. D.; Roy, A.; McGrath, J. E.; Riffle, J. S. Synthesis and crosslinking of partially disulfonated poly(arylene ether sulfone) random copolymers as candidates for chlorine resistant reverse osmosis membranes. *Polymer* 2008, *49*, 2243.

(34) Sundell, B. J.; Lee, K.-s.; Nebipasagil, A.; Shaver, A.; Cook, J. R.; Jang, E.-S.; Freeman, B. D.; McGrath, J. E. Cross-Linking Disulfonated Poly(arylene ether sulfone) Telechelic

Oligomers. 1. Synthesis, Characterization, and Membrane Preparation. *Ind. Eng. Chem. Res.* 2014, *53*, 2583.

(35) Park, H. B.; Freeman, B. D.; Zhang, Z.-B.; Sankir, M.; McGrath, J. E. Highly chlorine-tolerant polymers for desalination. *Angew. Chem., Int. Ed.* 2008, *47*, 6019.

(36) Bunn, A.; Rose, J. B. Sulfonation of poly(phenylene ether sulfones) containing hydroquinone residues. *Polymer* 1993, *34*, 1114.

(37) Wang, Z.; Ni, H.; Zhao, C.; Li, X.; Zhang, G.; Shao, K.; Na, H. Influence of the hydroquinone with different pendant groups on physical and electrochemical behaviors of directly polymerized sulfonated poly(ether ether sulfone) copolymers for proton exchange membranes. *J. Membr. Sci.* 2006, *285*, 239.

(38) Geormezi, M.; Deimede, V.; Gourdoupi, N.; Triantafyllopoulos, N.; Neophytides, S.; Kallitsis, J. K. Novel Pyridine-Based Poly(ether sulfones) and their Study in High Temperature PEM Fuel Cells. *Macromolecules (Washington, DC, U. S.)* 2008, *41*, 9051.

(39) Li, Y.; VanHouten, R. A.; Brink, A. E.; McGrath, J. E. Purity characterization of 3,3′-disulfonated-4,4′-dichlorodiphenyl sulfone (SDCDPS) monomer by UV–vis spectroscopy. *Polymer* 2008, *49*, 3014.

(40) Sankir, M.; Bhanu, V. A.; Harrison, W. L.; Ghassemi, H.; Wiles, K. B.; Glass, T. E.; Brink, A. E.; Brink, M. H.; McGrath, J. E. Synthesis and characterization of 3,3 '-disulfonated-4,4 '-dichlorodiphenyl sulfone (SDCDPS) monomer for proton exchange membranes (PEM) in fuel cell applications. *Journal of Applied Polymer Science* 2006, *100*, 4595.

(41) Viswanathan, R.; Johnson, B. C.; McGrath*, J. E. In *Polymer* 1984; Vol. 25, p 1827.

(42) Sagle, A. C.; Van, W. E. M.; Ju, H.; McCloskey, B. D.; Freeman, B. D.; Sharma, M. M. PEG-coated reverse osmosis membranes: Desalination properties and fouling resistance. *J. Membr. Sci.* 2009, *340*, 92.

(43) Hedrick, J. L.; Mohanty, D. K.; Johnson, B. C.; Viswanathan, R.; Hinkley, J. A.; McGrath, J. E. Radiation resistant amorphous-all aromatic polyarylene ether sulfones: synthesis, characterization, and mechanical properties. *J. Polym. Sci., Part A: Polym. Chem.* 1986, *24*, 287.

(44) Johnson, B. C.; Yilgor, I.; Tran, C.; Iqbal, M.; Wightman, J. P.; Lloyd, D. R.; McGrath, J. E. Synthesis and characterization of sulfonated poly(arylene ether sulfones). *J. Polym. Sci., Polym. Chem. Ed.* 1984, *22*, 721.

(45) Eisenberg, H. Polyelectrolyte excluded volume and expansion compared to non-ionic polymers. *Acta Polym.* 1998, *49*, 534.

(46) Yasuda, H.; Lamaze, C. E.; Ikenberry, L. D. Permeability of solutes through hydrated polymer membranes. I. Diffusion of sodium chloride. *Makromol. Chem.* 1968, *118*, 19.

(47) Geise, G. M.; Park, H. B.; Sagle, A. C.; Freeman, B. D.; McGrath, J. E. Water permeability and water/salt selectivity tradeoff in polymers for desalination. *Journal of Membrane Science* 2011, *369*, 130.

CHAPTER 6: SYNTHESIS, OXIDATION AND CROSSLINKING OF TETRAMETHYL BISPHENOL F (TMBPF)-BASED POLYMERS FOR OXYGEN/NITROGEN GAS SEPARATIONS

Benjamin J. Sundell, [a] *Andrew T. Shaver,* [a] *Qiang Liu,* [b] *Ali Nebipasagil,* [a] *Priya Pisipati,* [a] *Sue J. Mecham,* [a] *Judy S. Riffle,* [a] *Benny D. Freeman,* [b] *James E. McGrath* [a]

[a] Macromolecules and Interfaces Institute, Virginia Polytechnic Institute and State University, Blacksburg, VA 24061, USA

[b] Department of Chemical Engineering, Center for Energy and Environmental Resources, The University of Texas at Austin, Austin, TX, 78758, USA

Article in press, Polymer

6.1. Abstract

Amorphous, high glass transition, crosslinkable poly(arylene ether)s for gas purification membranes have been synthesized. The polymers include a moiety capable of several oxidation reactions and UV crosslinking. Structural identification was confirmed by ^{1}H-NMR and IR spectroscopy and molecular weights were determined by size exclusion chromatography. The polymers were subjected to oxidation under two different conditions, one by chemical treatment using Oxone and KBr and one by elevated thermal treatment in air. Differential scanning calorimetrey and thermogravimetric analysis were used for thermal characterization, and thermogravimetric analysis, ^{1}H-NMR and attenuated total reflectance fourier transform infrared spectroscopy revealed the progress of the thermal oxidation reactions. Both polymers produced tough, ductile films and gas transport properties of the non-crosslinked linear polymers and

crosslinked polymer are compared. The O_2 permeability of one exemplary non-crosslinked poly(arylene ether) was 2.8 Barrer, with an O_2/N_2 selectivity of 5.4. Following UV crosslinking, the O_2 permeability decreased to 1.8 Barrer, and the O_2/N_2 selectivity increased to 6.2.

6.2. Introduction

Polymeric membranes are important for the separation of gases in a variety of industrial applications.[1] Several excellent reviews have detailed industrial gas separations including the removal of carbon dioxide from natural gas,[2] nitrogen enrichment from air,[3] hydrogen recovery and a variety of smaller membrane markets.[1,4] These reviews also discuss some of the challenges associated with gas separation membranes such as achieving higher selectivity to provide higher purity products at high yield and making membranes more robust to harsh operating conditions and resistant to plasticization.

Transport of gases in dense polymeric membranes is based on the solution-diffusion model; the permeability of a gas across the membrane is the product of diffusion and solubility coefficients.[3,5] One measure of the ability of a membrane to separate a pair of gases is the ratio of the permeability coefficient of the more permeable gas to that of the less permeable gas, known as selectivity. The selectivity may be further separated into the product of solubility selectivity and diffusivity selectivity, the latter generally being the dominant factor controlling overall selectivity of glassy polymers.[6] Gas diffusion is very sensitive to the size of the diffusing gases and the availability of free volume within the polymer membrane.[7,8] A desirable gas separation membrane exhibits both high permeability and selectivity; however, an inherent trade-off relationship between these two properties has been identified. Membranes with high gas permeability typically have lower selectivity, and vice-versa. This observation led to the

development of the concept of the upper-bound by Robeson, which is typically represented as a log-log plot of selectivity versus permeability.[5] The upper-bound plots were revised upwards once[9] based on the development of new classes of polymer membrane materials and have a mathematical and theoretical basis derived by Freeman.[6] Freeman, among others, noted that the most widely used approach to prepare materials with properties above the upper bound was to simultaneously increase polymer backbone stiffness and interrupt interchain packing to increase diffusivity.

Several families of glassy polymers have been investigated to explore the influence of polymer structure on gas transport properties. For example, one early effort studied the effect of tacticity on poly(methyl methacrylate).[10] Polyimides typically have good gas separation properties and are of significant interest in the field because of their chemical robustness and low chain mobility.[11,12] Another candidate for gas separation polymers are polysulfones due to their chemical stability and excellent mechanical properties, along with inherent rigidity due to in chain aromatic rings. The effect of variations in backbone chemical structure on permeability and selectivity of polysulfones has been studied.[13,14] For example, changes to the isopropylidene group, which influences bond rotation and intersegmental packing,[15] the effect of symmetry of phenylene linkages, and methyl group placement[16] all have significant influence on gas separation properties of polysulfones. Several specialty polyimides have exceeded the upper bound by undergoing a chemical transformation to form carbon membranes at very high temperatures, such as that induced via pyrolysis between 550-800^{o}C.[17] Additionally, thermal rearrangement of *ortho*-positioned polyhydroxyimide precursors produce crosslinked polybenzoxazoles with much narrower pore size distributions than the precursor polyimides and, in some cases, gas separation properties beyond the upper bound.[18]

One intriguing approach for improving the properties of gas separation membranes is to crosslink them, which is a well-known method to decrease chain mobility. In the late 1980s, Hayes demonstrated that UV crosslinked aromatic polyimides had a significantly higher selectivity than their linear analogs.[19] The effect of UV crosslinking on gas separation properties of the polyimides has been studied,[20-23] and the effects of crosslinking have also been decoupled from thermal annealing.[24,25] These crosslinked membranes are especially effective in CO_2/CH_4 separations, because crosslinking greatly improves resistance to plasticization by CO_2[26] or in some cases interrupts polymer crystallization.[27]

In this paper, a poly(arylene ether sulfone) and poly(arylene ether ketone) have been synthesized from inexpensive reagents that contain moieties for UV crosslinking and an additional site for chemical oxidation. The materials considered in this study contain, in each repeat unit, a moiety derived from 4,4'-methylenebis(2,6-dimethylphenol), which has been used previously in polymers for forward osmosis[28] and as a self-cross-linked material for fuel cells.[29] This benzylic methylene group may be oxidized to a carbonyl by several routes and then UV crosslinked by benzylic hydrogen abstraction. This structure also provides the ability to UV crosslink a poly(arylene ether ketone) to increase backbone stiffness and interrupt chain packing by oxidizing the crosslinked polymeric backbone in the solid state. The synthesis and characterization of these polymers are described, and investigations of several oxidation routes are discussed. Initial film casting, UV crosslinking, and gas transport properties are also discussed.

6.3. Experimental

Materials

2,6-Dimethylphenol (2,6-xylenol, 99+%), 37% formaldehyde in H_2O (formalin), phosphorous pentoxide (P_2O_5), lithium bromide (LiBr) and potassium bromide (KBr) were purchased from Sigma-Aldrich. *N*-Methyl-2-pyrrolidone (NMP), methanol (MeOH) and sulfuric acid were purchased from Spectrum Chemical. Chloroform ($CHCl_3$), *N*,*N*-dimethylacetamide (DMAc) and acetonitrile (CH_3CN) were purchased from Fisher. DMAc used as a reaction solvent was dried with calcium hydride (CaH_2), distilled under reduced pressure and stored over 3Å molecular sieves before use. Calcium hydride (90-95%) and potassium peroxymonosulfate (Oxone) were purchased from Alfa Aesar. 4,4'-Difluorobenzophenone (DFB) was purchased from TCI. 4,4'-Dichlorodiphenylsulfone (DCDPS) was kindly provided by Solvay and recrystallized from toluene before use.

Synthesis of 4,4'-methylenebis(2,6-dimethylphenol)

The synthesis of 4,4'-methylenebis(2,6-dimethylphenol), tetramethyl bisphenol F, hereafter referred to as TMBPF, was adapted from a traditional synthesis of a phenol-formaldehyde resin.[30] Excess 2,6-xylenol (415.83 mmol, 50.80 g) was added to a 250-mL three-necked flask equipped with a condenser, mechanical stirrer, and addition funnel. The 2,6-xylenol was heated in a thermocouple regulated oil bath to 90^{o}C and stirred as it began to melt. Sulfuric acid (0.5 g) was added very slowly via the addition funnel, which changed the reaction solution to a dark pink color. The addition funnel was rinsed with DI water to ensure that all of the acid catalyst was transferred into the reaction flask. Formalin (37% by mass formaldehyde in H_2O, 15 mL) was added slowly via the addition funnel over the course of several hours; during this time,

the reaction solution turned lighter in color and significantly more opaque. As more product continued to form, the reaction mixture transformed from a liquid to a solid. The crude product was removed from the flask and filtered using an aspirator and washed copiously with hot DI water. The crude product was dried at 70^{o}C in a convection oven and was recrystallized from MeOH to obtain a 90% yield. The melting point of the recrystallized solid was 177^{o}C.

Synthesis of bis-(2,6-xylenol)-F-DFB poly(arylene ether) ketone (TMBPF-DFB)

The TMBPF-DFB polymer was synthesized using a nucleophilic aromatic substitution procedure previously reported.[31] TMBPF (39.01 mmol, 10.0000 g), DFB (39.01 mmol, 8.5121 g) and DMAc (62 mL) were added to a 250-mL three necked flask. The reaction flask was equipped with a mechanical stirrer, nitrogen inlet, and Dean-Stark trap filled with toluene. A stirring, thermocouple regulated oil bath was heated to 155^{o}C. After a homogeneous solution was obtained and the oil bath was at 155^{o}C, K_2CO_3 (54.61 mmol, 7.5482 g) and toluene (31 mL) were added, which immediately turned the light yellow solution a deep violet color. The reaction was stirred at 155^{o}C for 3 h to azeotropically remove any water, and then the bath was heated to 175^{o}C. Toluene and water were drained from the Dean Stark trap, and the reaction was maintained at this final temperature overnight. After 16 h, the viscous solution was diluted with additional DMAc (62 mL) and filtered through celite using an aspirator. The polymer solution was precipitated into rapidly stirring DI water to produce a fibrous white solid, filtered using an aspirator, and then boiled several times in DI water to remove any residual salt by-product. The solid polymer was finally dried at 150^{o}C in *vacuo*.

Synthesis of bis-(2,6-xylenol)-F-DCDPS poly(arylene ether) sulfone (TMBPF-DCDPS)

The TMBPF-DCDPS polymer was synthesized in the same manner as the TMBPF-DBF polymer, except DCDPS (39.01 mmol, 11.2023 g) was used instead of DFB, and more DMAc (71 mL) was used to obtain the same monomer concentration due to higher total monomer mass.

Oxidation of TMBPF-DCDPS polymer with Oxone/KBr

Oxidation of the TMBPF-DCDPS polymer was adapted from a literature procedure for the oxidation of small molecules with benzylic methylene linkages.[32] TMBPF-DCDPS polymer (1.0 g) was added to CH_3CN (26 mL) and DI water (2 mL) in a 100-mL round bottom flask. Oxone (4.675 mmol, 0.712 g) and KBr (1.063 mmol, 0.126 g) were added to the flask. The flask, under air, was sealed with septa and stirred in a thermocouple regulated water bath at 45^{o}C. After several hours, the temperature was raised to 60^{o}C, and the reaction was stirred overnight. The heterogeneous reaction was poured directly into stirring DI water (250 mL), stirred for several hours, filtered on an aspirator, and dried overnight at 70^{o}C in a convection oven.

Thermal oxidation of TMBPF polymers

The TMBPF polymers were thermally treated in air in a Lindberg/Blue M 1200^{o}C box furnace. Once the oven reached the specified temperature, the polymer inside of an open scintillation vial was placed into the oven. After a designated time, the vial was removed and sealed for analysis.

Structural Characterization

Proton nuclear magnetic resonance (^{1}H NMR) spectroscopy was performed on a Varian Inova spectrometer operating at 400 MHz. All spectra were obtained from 15% (w/v) 1 mL solutions in deuterated chloroform ($CDCl_3$). Fourier Transform Infrared Spectroscopy with attenuated total reflectance (FTIR-ATR) was applied to the polymers to observe the conversion of the methylene bridge to the carbonyl group as a result of oxidation. The FTIR-ATR spectra were recorded on an FTIR spectrometer (Varian 670 FTIR) equipped with an ATR attachment with a diamond crystal. The spectral resolution was 4 cm^{-1}, and 32 background scans were performed. A small amount of polymer was placed on the diamond crystal, and the FTIR spectrum was measured with 32 scans. The spectra were baseline corrected and normalized based on the initial C=O group stretch at ca. 1525 cm^{-1}. All measurements were performed at ambient temperature. Intrinsic viscosities (IV) and molecular weights of the polymers were obtained by size exclusion chromatography (SEC). The SEC system consisted of an isocratic pump (Agilent 1260 infinity, Agilent Technologies, Santa Clara, CA) with an online degasser (Agilent 1260, Agilent Technologies, Santa Clara, CA), autosampler and column oven used for mobile phase delivery and sample injection, and three Agilent PLgel 10µm Mixed B-LS columns 300×7.5mm connected in series with a guard column as the stationary phase. A system of multiple detectors connected in series was used for the analysis. A multi-angle laser light scattering (MALS) detector (DAWN-HELEOS II, Wyatt Technology Corporation, Goleta, CA), operating at a wavelength of 658 nm, a viscometer detector (Viscostar, Wyatt Technology Corporation, Goleta, CA), and a refractive index detector operating at a wavelength of 658 nm (Optilab T-rEX, Wyatt Technology Corporation, Goleta, CA) provided online results. The system was corrected for interdetector delay, band broadening, and the MALS signals were

normalized using a 21,720 g/mol polystyrene standard obtained from Agilent Technologies or Varian. Data acquisition and analysis was conducted using Astra 6 software (Wyatt Technology Corporation, Goleta, CA). The mobile phase was NMP, which was vacuum distilled over P_2O_5 before use. The salt, 0.05M dried LiBr, was added and dissolved in the NMP before the solvent was degassed and filtered. The sample solutions were prepared in a concentration range of 2~3 mg/mL and were filtered to remove any dust or insoluble particles using 0.22 μm PTFE filters. Molecular weight values were measured using light scattering, and the intrinsic viscosity values were measured online. Specific refractive index increment (dn/dc) values were calculated for each backbone type based on 100 % mass recovery using the Astra 6 software.

Thermogravimetric analysis (TGA)

The thermal stability and oxidation of the polymers were investigated using a TA Instruments TGA Q5000. The polymers were first heated under a nitrogen atmosphere at a rate of $10^oC\ min^{-1}$ to 600^oC to test the thermal stability in an inert atmosphere. The thermal oxidation reaction and consequent weight gain were performed in air by heating at $10^oC\ min^{-1}$ to 220^oC, then $1^oC\ min^{-1}$ to 450^oC, and finally $10^oC\ min^{-1}$ to 700^oC.

Differential scanning calorimetry (DSC)

The glass transition temperatures (T_g) of the polymers were investigated with a TA Instruments DSC Q200. The polymers were heated under nitrogen at a rate of $10^oC\ min^{-1}$ to 350^oC, cooled to 50^oC, and heated again at a rate of $10^oC\ min^{-1}$ to 350^oC. The DSC thermograms shown are the second scan.

Film preparation

To prepare films, 0.8 g of polymer was added to 20 mL of chloroform ($CHCl_3$) in a scintillation vial, and the mixture was stirred until a homogeneous, transparent solution was obtained. The solution was syringe filtered through a 1.0 μm filter into a new vial. The vial was sonicated 3 times for 60 minutes each to remove dissolved gases. The solution was cast on a 10 x 15 cm clean, dry glass plate on a level casting surface and then dried in air at ambient conditions overnight. The following day the air dried film was removed, the edges were trimmed, and the film was dried at 120^{o}C under vacuum before gas transport experiments. TGA thermograms showed that these drying conditions were suitable for the complete removal of solvent.

UV Crosslinking

Crosslinking was performed by irradiating polymer films in air under a 100W high intensity, long-wave UV lamp equipped with a 365-nm light filter (Blak-Ray B-100, UVP). The film was placed about 3.5 cm from the UV lamp and irradiated for one hour on each side. At this distance, the UV intensity was measured to be 19.7 mW cm^{-2}.

Gel Fractions

Crosslinked films were dried at 120°C under vacuum overnight. Then 0.1-0.2 g of the crosslinked film was placed in a 20 mL scintillation vial filled with $CHCl_3$ and stirred overnight. The remaining solid was filtered, transferred to a pre-weighed vial, and dried at 120°C under vacuum overnight to the final weight. Gel Fractions were calculated by equation 1.

Equation 6.1
$$Gel\ Fraction\ (\%) = \frac{W_{final}}{W_{initial}} \text{ x } 100$$

Density Measurements

Density was measured using a Mettler Toledo balance equipped with a density measurement kit. Ethanol was chosen as the reference liquid because the samples tested showed low ethanol uptake over the time scale of the density measurement.

Gas Permeation Measurements

Gas permeation properties were measured using a constant-volume/variable-pressure method.[33] The upstream portion of the system was constructed from commercially available Swagelok parts using Swagelok tube fittings. Welded joints and VCR connections were used in the downstream portion to minimize leaks. The membrane was housed in a stainless steel Millipore filter holder (Millipore, Billerica, MA, USA) with an included support. A Honeywell Super TJE 1500 psi (10.3 MPa) transducer (Honeywell Sensotec, Columbus, Ohio, USA) was used to track upstream pressure, and a MKS Baratron 626 transducer (MKS, Andover, MA, USA) was used to measure downstream pressure. The permeabilities of N_2 and O_2 were measured at 35^{o}C at 10 atm feed pressure.

6.4. Results and Discussion

Synthesis of Tetramethyl Bisphenol F monomer (TMBPF)

An appealing feature of these polymers is the low cost of starting materials. The TMBPF monomer is commercially available, or may be easily synthesized from inexpensive 2,6-xylenol and formalin via electrophilic aromatic substitution as shown in Figure 6.1.

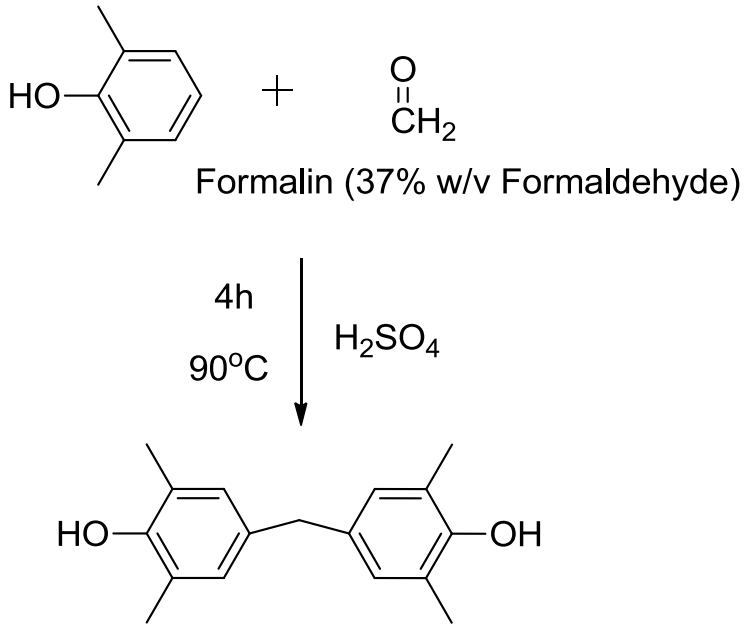

Figure 6.1 Synthesis of TMBPF via electrophilic aromatic substitution

TMBPF is the key monomer in these polymers, because the benzylic methyl groups are necessary for UV crosslinking and the benzylic methylene group may undergo an oxidative chemical transformation.[32] A slight excess of 2,6-xylenol was used to drive the reaction to completion.[34] The reaction occurs very rapidly at the conditions used; however a temperature of 90°C was necessary to ensure that the 2,6-xylenol was melted and that homogeneous stirring could occur. Upon formalin addition, the reaction shifted from a liquid to solid phase in addition to exhibiting a color change, which indicates the formation of product as TMBPF has a significantly higher melting point than 90°C and is insoluble in water. Isolation of the monomer product was also very efficient. Washing with near boiling water is effective at removing residual acid and residual starting material. Upon drying, any residual 2,6-xylenol impurity in the crude product was assessed qualitatively by the presence of an orange/pink color, which is completely removed when recrystallized from methanol to yield white crystals.

Characterization of TMBPF monomer

The ^{1}H-NMR spectrum of TMBPF is shown in Figure 6.2. All of the peaks integrate quantitatively with regard to the molecular structure. The ^{1}H-NMR also showed no organic side products or contaminants, including starting material. The melting point of the recrystallized product was measured at 177^{o}C via melting point apparatus and found to be in good agreement with reported values (177^{o}C).[35]

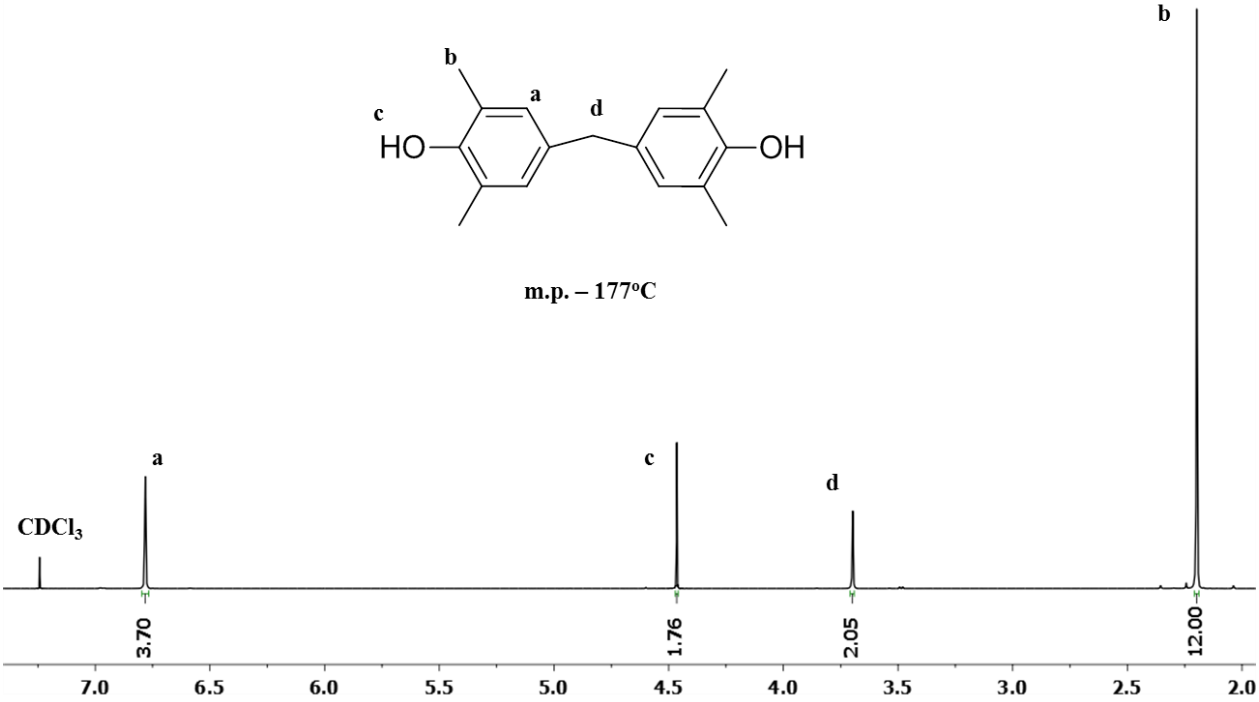

Figure 6.2 ^{1}H-NMR spectrum of TMBPF monomer

Synthesis and NMR of TMBPF polymers

Poly(arylene ether)s are potentially important candidates for gas separation materials, and poly(arylene ether sulfone)s in particular have already found wide application in the field.[1,36] The success of poly(arylene ether)s as gas separation membranes is in part due to their mechanical robustness and high chemical stability.[37,38]

The TMBPF containing poly(arylene ether ketone) (TMBPF-DFB) and poly(arylene ether sulfone) (TMBPF-DCDPS) in this study were synthesized by nucleophilic aromatic

substitution with a weak base.[31,39] The syntheses of the poly(arylene ether sulfone) and poly(arylene ether ketone) are shown in Figures 6.3 and 6.4 respectively. Upon addition of toluene and K_2CO_3, both reaction solutions turned a deep violet color immediately, which persisted throughout the course of the reaction. In both reactions, toluene was used as an azeotropic solvent to remove water formed by K_2CO_3 reaction and subsequent decomposition. Water could potentially react with the activated dihalide monomer at higher temperatures and upset the reaction stoichiometry, leading to low molecular weight polymers. It was important to use a heat gun to dry the joints on the three-necked flask during the azeotropic reflux, where water may become trapped. After the water was removed from the reaction, toluene was drained, and the flask was brought to the final reaction temperature. Difluorobenzophenone is a more reactive than dichlorodiphenyl sulfone, because the carbon fluorine bond is more polarized than the carbon chlorine bond, and therefore, more efficiently stabilizes the Meisenheimer complex intermediate.[40] Thus, the final temperature of the poly(arylene ether ketone) reaction was 20^{o}C lower than that of the poly(arylene ether sulfone) reaction. Both reactions exhibited high viscosity after 16 hours and were stopped at this time.

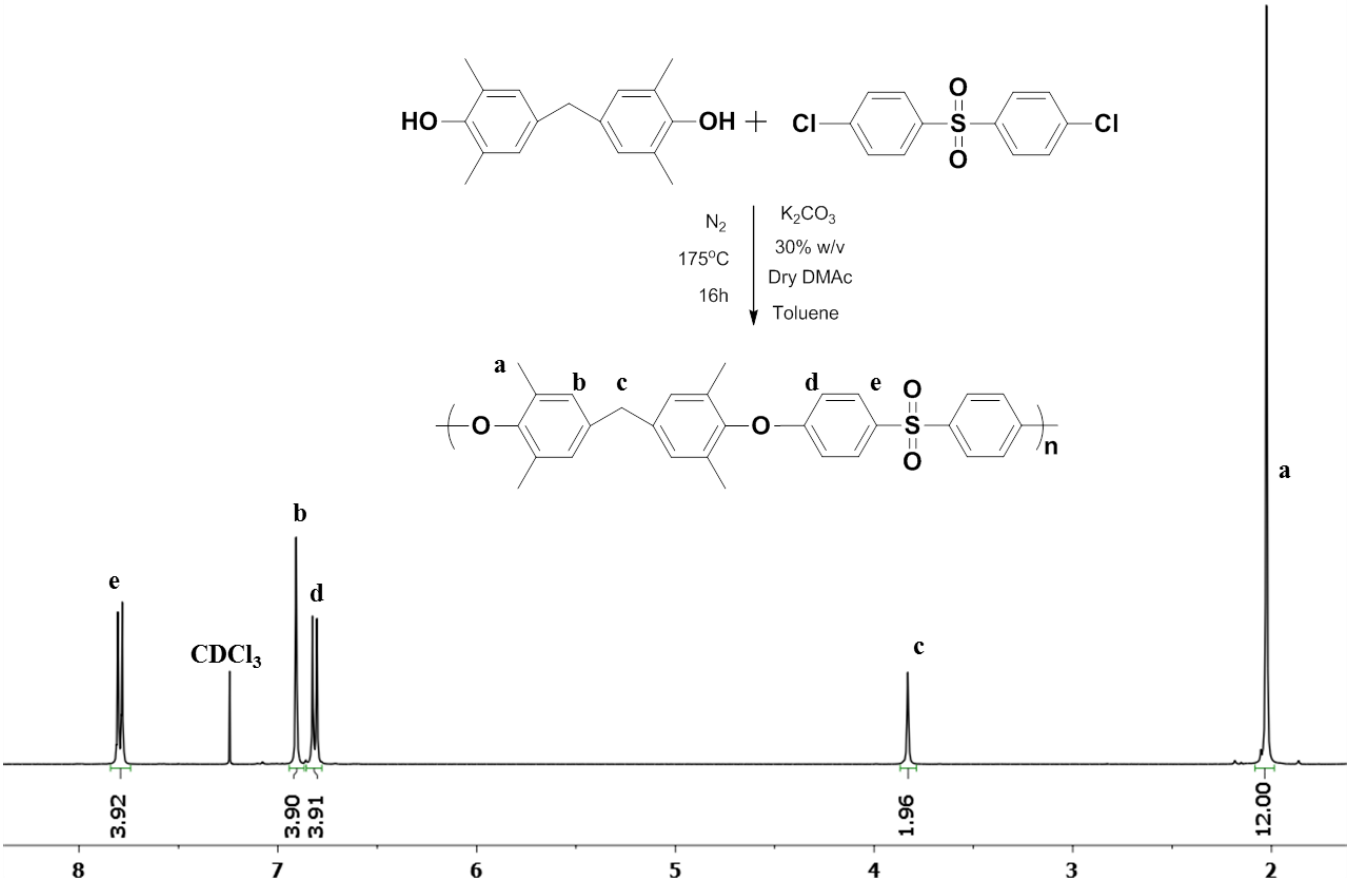

Figure 6.3 Synthesis and ^{1}H-NMR spectrum of TMBPF-DCDPS polymer

After polymer isolation and drying, the TMBPF polymers were characterized by a variety of spectral and thermal methods. ^{1}H-NMR was performed to ensure polymer purity, structural identification and removal of solvent. Figures 6.3 and 6.4 demonstrate that all of these objectives were achieved, as the integrations corresponded to the expected structures and no impurities or endgroups were observed in the spectra, an indication of high molecular weight.

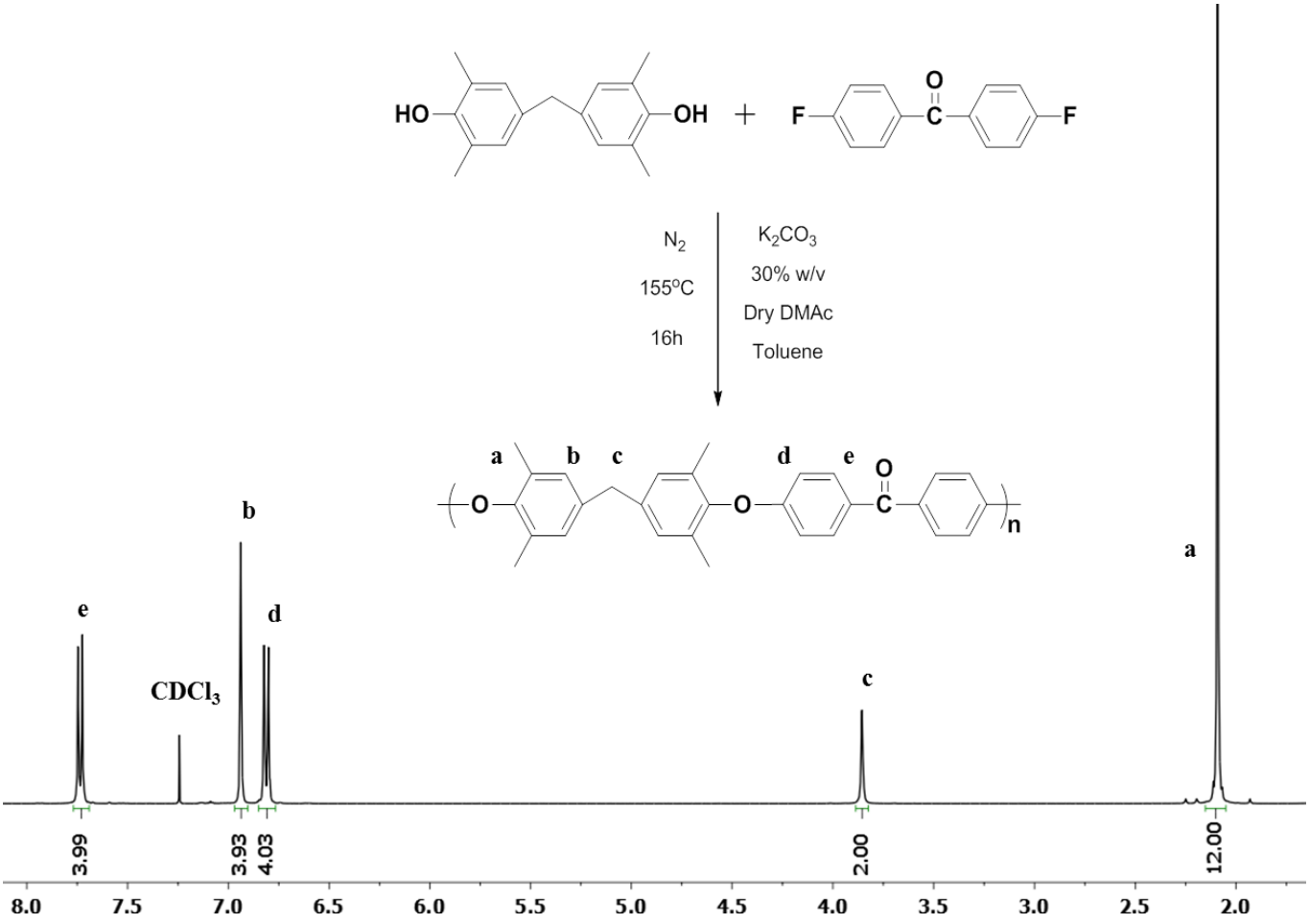

Figure 6.4 Synthesis and ^{1}H-NMR spectrum of TMBPF-DFB polymer

SEC of TMBPF polymers

The polymers were sufficiently high in molecular weight to form transparent, ductile films. SEC of the polymers quantitatively substantiated high molecular weight, and these results are shown in Figure 6.5 and Table 6.1. The polymers have a monomodal Gaussian distribution and polydispersity index (PDI) that one would expect from a step growth polymerization. The PDI should theoretically be 2. However, some lower molecular weight material is likely lost during polymer isolation, thereby decreasing the observed PDI.

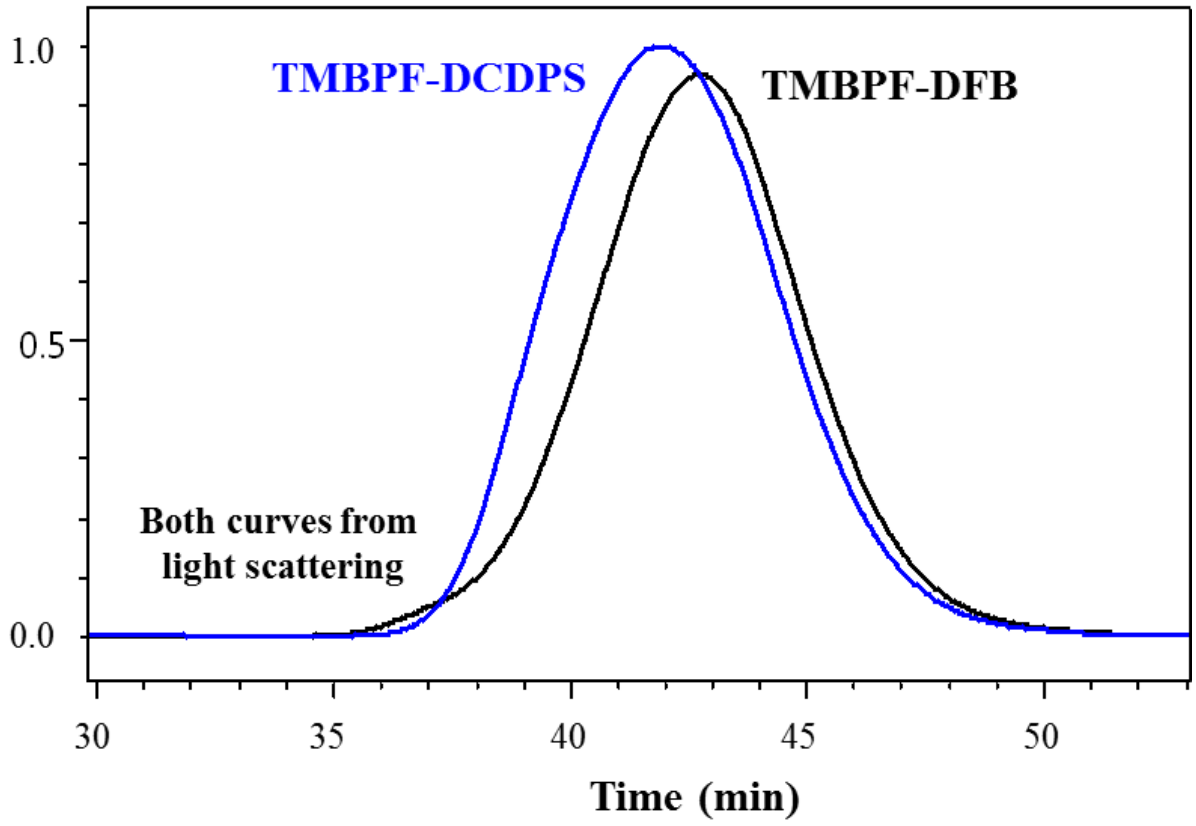

Figure 6.5 SEC of TMBPF containing polymers

Table 6.1 SEC of TMBPF containing polymers

Sample	Mn (kDa)	Mw (kDa)	PDI	[η] (dL/g)	dn/dc (mL/g)
TMBPF-DCDPS	66.2	127.5	1.9	0.61	0.14
TMBPF-DFB	51.7	92.7	1.8	0.54	0.15

Oxidation of TMBPF-DCDPS polymer with Oxone/KBr

To UV crosslink these polymers requires the presence of aromatic carbonyl groups in the backbone and benzylic methyl groups.[41] The methylene bridge of the TMBPF group in the backbone of the polymer can be converted to a carbonyl via oxidation.[42] The oxidation of the TMBPF containing poly(arylene ether sulfone) was initially attempted using potassium

peroxymonosulfate (Oxone®) and KBr in a procedure adapted from the oxidation of small molecules containing benzylic methylene linkages.[32] The poly(arylene ether sulfone) was initially tested for this oxidation route because the un-oxidized form does not contain carbonyl linkages, so the success of this reaction may be followed by tracking the growth of this peak by FTIR spectroscopy.

The small molecule procedure called for the addition of Oxone and KBr by molar equivalencies of 2.2 and 0.5 respectively. Because each repeat unit contains one benzylic methylene group capable of oxidation, the molecular weight of the repeat unit was used as the molar mass to determine 1 equivalent for stoichiometric considerations.

Addition of TMBPF-DCDPS polymer to aqueous acetonitrile turned the liquid a light amber color, and addition of Oxone and KBr produced a slight red tint that quickly disappeared upon stirring. It was apparent that the polymer was mostly insoluble in the solvent mixture, and gradually heating to 45°C or 60°C did not noticeably improve the solubility. The solvent system of aqueous acetonitrile was important for the success of oxidation in the small molecule reactions.[32] Water is the source of oxygen in the oxidized product, and changing the solvent to DMSO or DMF produced very low yields. One reaction for oxidizing TMBPF-DCDPS was performed in chloroform, a good solvent for this polymer, but this led to similar levels of conversion with side reactions including crosslinking.

Spectral verification of the oxidation reaction was done using ^{1}H-NMR and FTIR-ATR spectroscopy. The ^{1}H-NMR spectra of TMBPF-DCDPS and its partially oxidized analog are shown in Figure 6.6. Most notably, the benzylic methylene peak *c* decreased to about 80% of its initial value, indicating near 20% conversion to the oxidized product. The peaks nearest to the benzylic methylene moiety, *a* and *b*, also decreased and new peaks, *a'* and *b'* appeared downfield

relative to the initial control peaks. This downfield shift is consistent with the electron withdrawing nature of the new carbonyl linkage compared to the original methylene group. Peaks *d* and *e* are less affected by this chemical transformation because of their distance from the methylene or carbonyl group, but a broadening of these peaks was still observed. FTIR-ATR spectra of the TMBPF-DCDPS polymer and its partially oxidized analog are presented in Figure 6.7. Several signature peaks of the control polymer structure are highlighted, including the sulfone linkage and the benzylic methylene linkage. Most importantly, the partially oxidized polymer had a signature peak at 1656 cm^{-1}, indicating the appearance of a carbonyl group not observed in the control polymer.

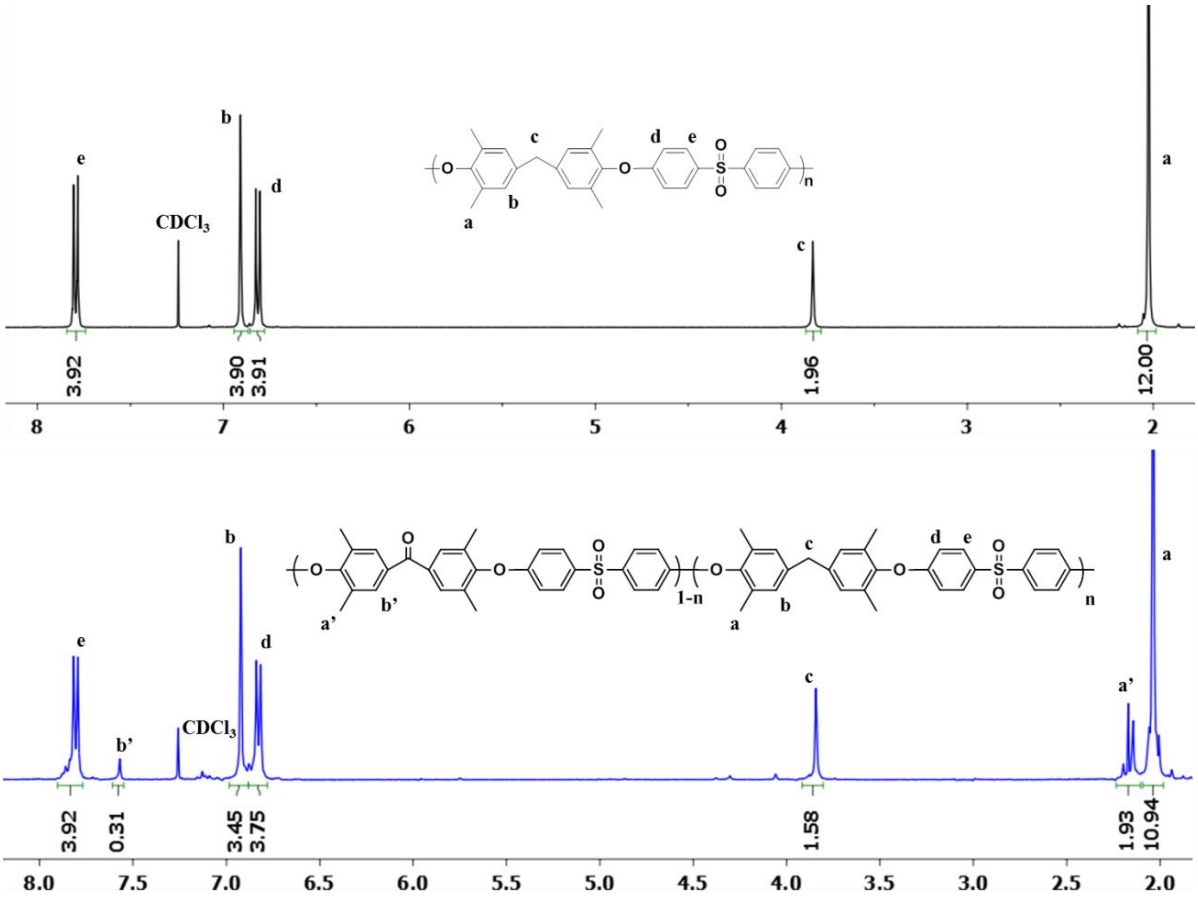

Figure 6.6 ^{1}H-NMR of TMBPF-DCDPS before and after oxidation with Oxone/KBr

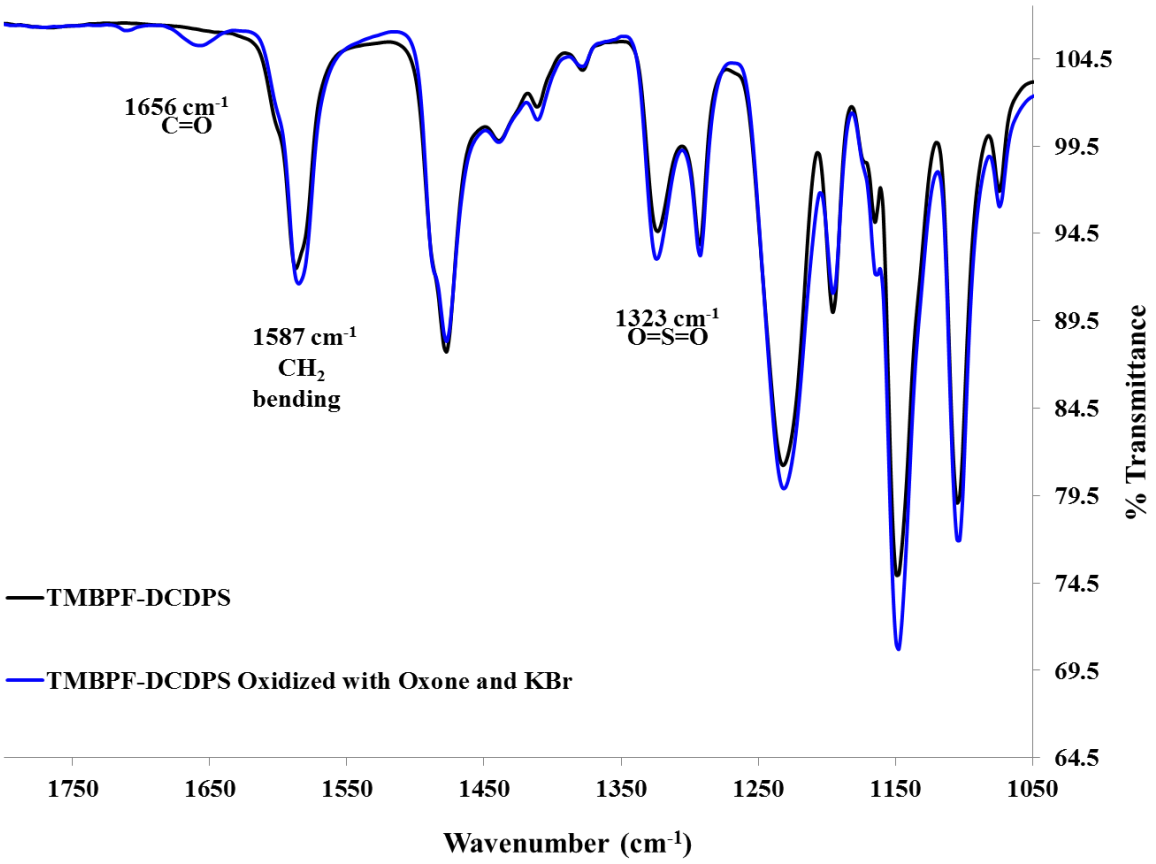

Figure 6.7 IR of TMBPF-DCDPS before and after oxidation with Oxone/KBr

UV crosslinking of oxidized TMBPF-DCDPS polymer

One important test on the partially oxidized TMBPF-DCDPS polymer was the ability of the polymer to UV self-crosslink. The UV crosslinking mechanism of interest was benzylic hydrogen abstraction by a benzophenone moiety, which generated two radicals that led to a crosslinked site upon recombination.[43] The TMBPF-DCDPS control polymer lacked the benzophenone moiety and was incapable of UV crosslinking. Two films were prepared to test the self-crosslinking reaction, one of the TMBPF-DCDPS control and one of the partially oxidized system. Both films were cast from chloroform, dried, and then exposed to UV light. After irradiation, both films were weighed and extracted with chloroform. The TMBPF-DCDPS film quickly dissolved, indicating 0% gel fraction and no crosslinking. However, the partially

oxidized TMBPF-DCDPS film was largely undissolved after one day and had a gel fraction of 80%, demonstrating a high level of network formation.

TGA of TMBPF polymers under N_2

In addition to chemical and mechanical stability, high thermal stability is also desired for gas separation membranes. Some hydrogen separations are performed near 100°C today, and there is discussion of performing separations at even higher temperatures, such as those involved in production of synthesis gas, which potentially require membrane stability above 300°C,[1] and pre-combustion carbon capture, which might need membranes that are stable at up to 150°C or higher.[44] The thermal stability of the TMBPF polymers was initially tested under pure nitrogen, as shown in Figure 6.8. Both polymers had very high thermal stabilities, showing no weight loss until 400°C and a 10% weight loss above 450°C.

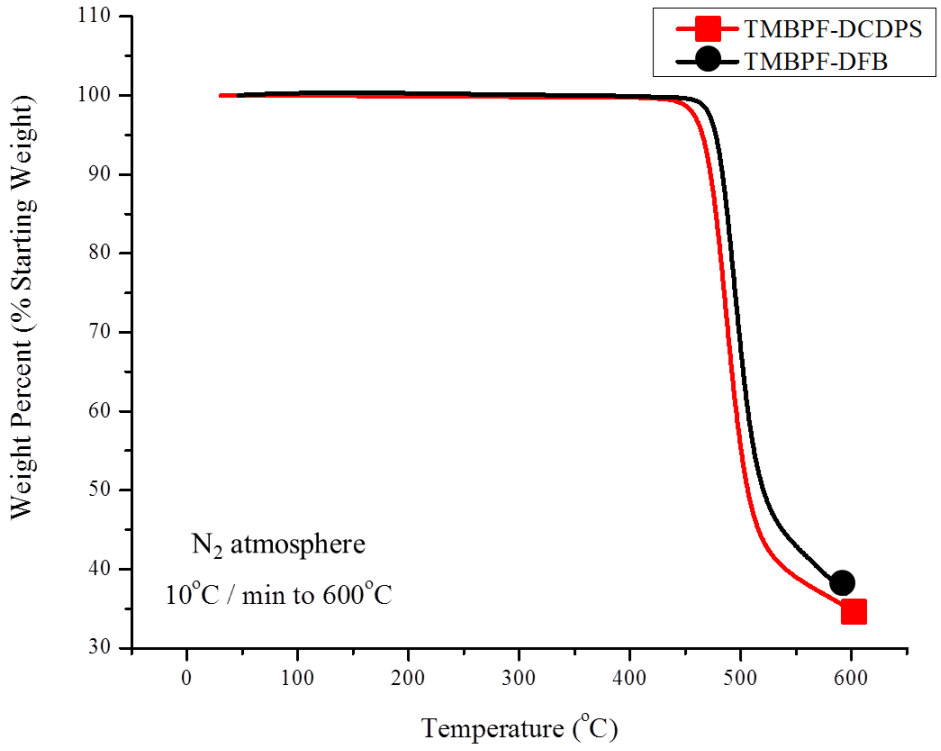

Figure 6.8 TGA of TMBPF containing polymers in N_2

TGA of TMBPF polymers in Air

Thermogravimetric analysis of the TMBPF polymers was also performed in air, and the results are presented in Figure 6.9. The polymers both showed a very interesting phenomenon, weight gain in the region of 250 to 325^{o}C. Initially, these polymers were only investigated for their ability to chemically oxidize, but it became apparent that the benzylic methylene linkage could also thermally oxidize at elevated temperatures in the presence of oxygen. The molecular mass difference between non-oxidized and oxidized polymer was calculated for both TMBPF containing poly(arylene ether ketone) and poly(arylene ether sulfone). The theoretical weight gain required to oxidize each methylene group to a carbonyl in the TMBPF-DFB polymer was 3.2%, and it was 3.0% for the TMBPF-DCDPS polymer. The theoretical weight percent increase was higher for the ketone system because of its lower molecular weight repeat unit. The actual weight gains shown in Figure 6.9 were approximately 90% of the theoretically possible weight gains, suggesting a high level of oxidation. The temperature ramp above 220^{o}C was done at 1^{o}C/min, because incomplete oxidation was observed at higher heating rates (i.e., 10 ^{o}C/min). The rates of thermal oxidation at various fixed temperatures will be detailed in a subsequent publication.

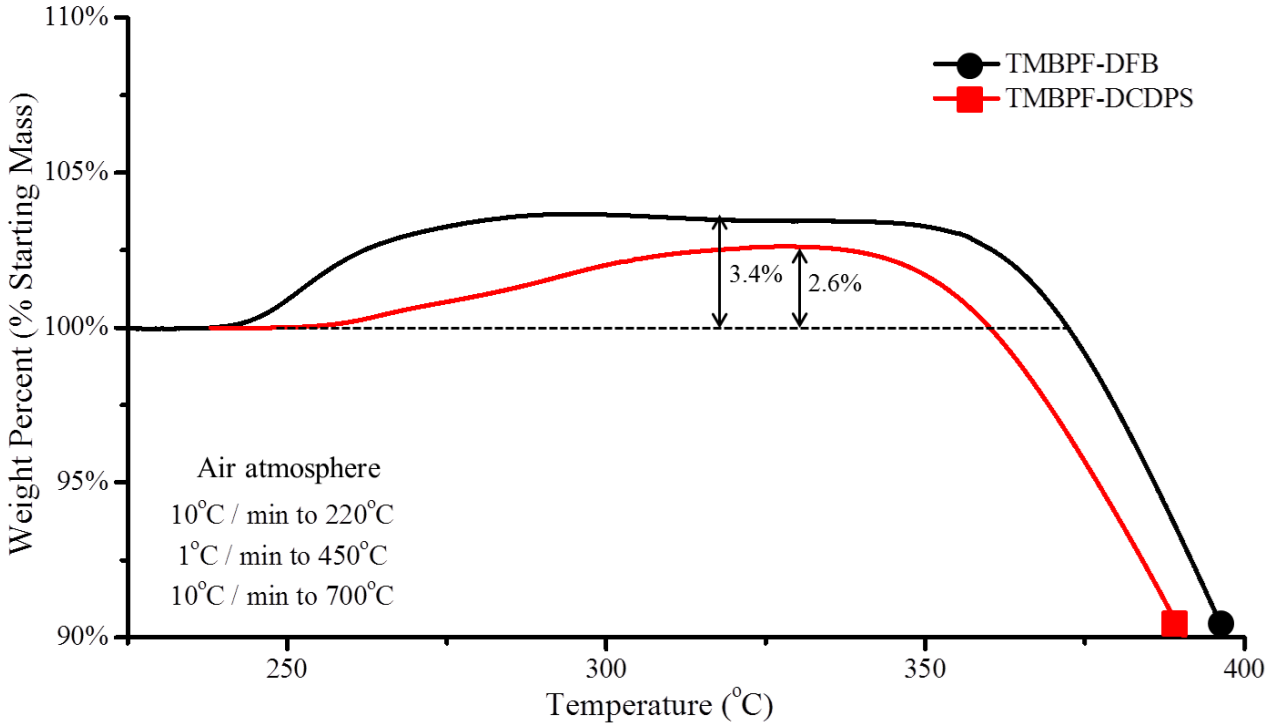

Figure 6.9 TGA of TMBPF containing polymers in air

Thermal properties of TMBPF polymers under N_2

DSC was performed to identify the glass transition temperatures (T_g's) of the TMBPF polymers. The samples were heated to 350°C to erase their thermal history, cooled, and then heated again to 350°C to produce the thermograms in Figure 6.10. DSC was performed under an inert atmosphere to eliminate the possibility of thermal oxidation. Distinct endothermic transitions indicative of the T_g were found at 213°C for TMBPF-DFB and 235°C TMBPF-DCDPS. The T_g's were in the range expected for poly(arylene ethers); notably, the T_g of TMBPF-DCDPS was in excellent agreement with a prior literature study investigating the effect of polysulfone backbone structure on T_g.[45] The poly(arylene ether sulfone) has a T_g more than 20°C higher than that of the poly(arylene ether ketone), likely due to the increased restrictions to rotation about the sulfone linkage relative to the carbonyl linkage. Results indicated that thermal

oxidation in air began nearly 20°C above the T_g of the polymers, as shown in Figure 6.9 by weight gain. These results seem to suggest that extensive chain motion is needed for the oxidation process.

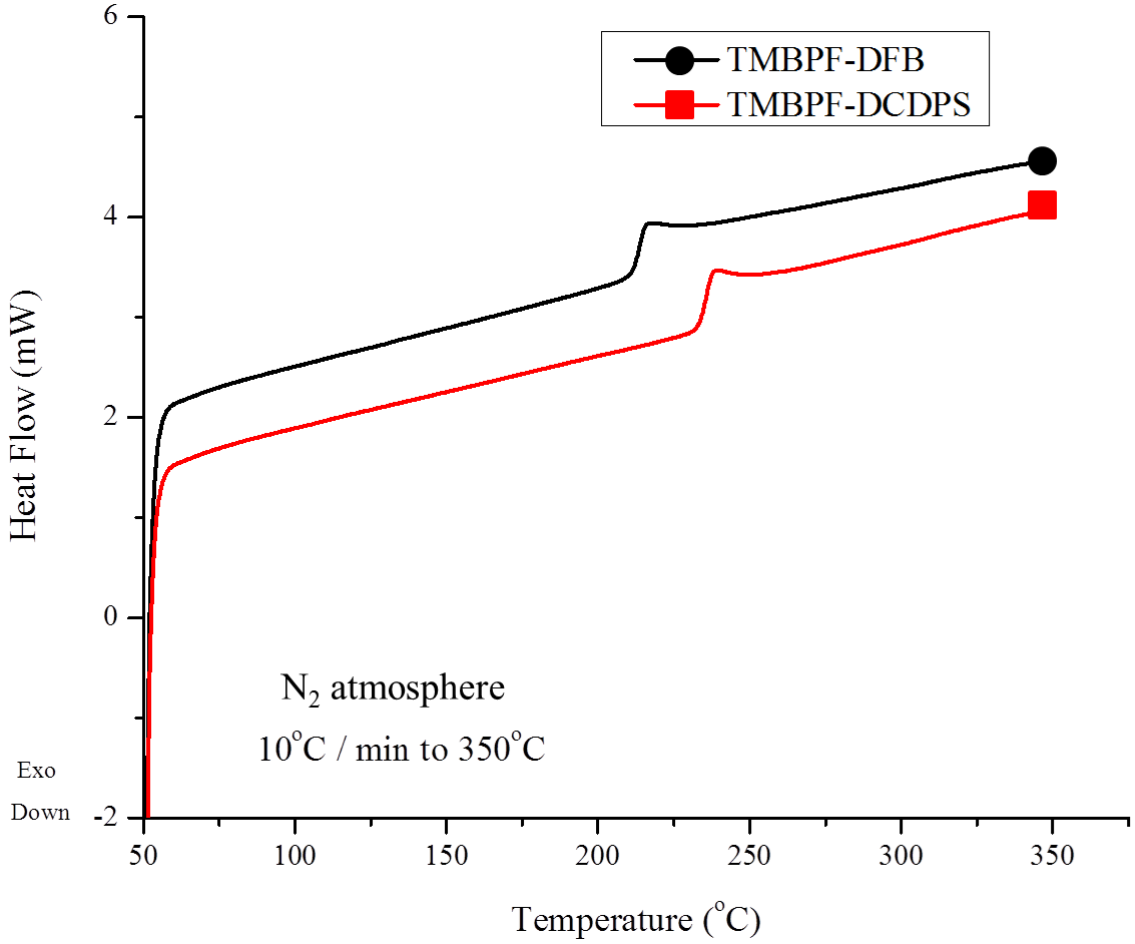

Figure 6.10 DSC of TMBPF containing polymers in N_2

NMR of thermally oxidized TMBPF-DFB polymer

To further test the thermal oxidation reactions, the TMBPF-DFB polymer was heated in air to 260°C, well above T_g, and held for 10 min. The TMBPF-DCDPS polymer was heated to 280°C in air, well above T_g, and held for 120 min. The TMBPF-DCDPS polymer was heated at a higher temperature and for a longer period of time to account for the slower oxidation rates observed via TGA. During these times, the polymers changed from white to a light yellow color.

The ^{1}H-NMR spectrum of the soluble fraction of the thermally oxidized TMBPF-DFB is shown in Figure 6.11, and the spectrum for oxidized TMBPF-DCDPS is shown in Figure 6.12.

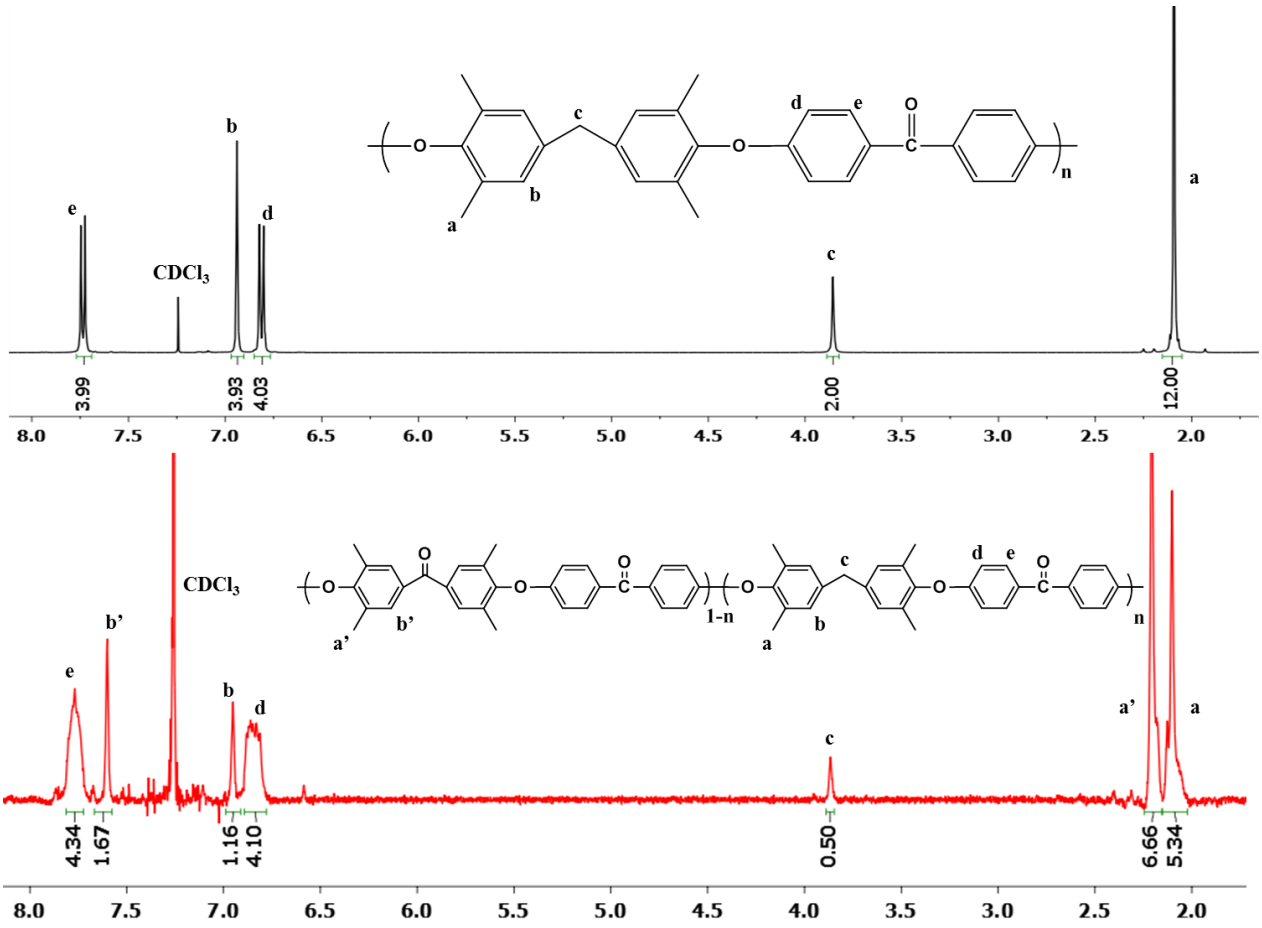

Figure 6.11 ^{1}H-NMR of thermally oxidized TMBPF-DFB

Similar to the results obtained via partial Oxone/KBr oxidation, the thermal oxidation reactions were analyzed by ^{1}H-NMR spectroscopy. The spectra show that the TMBPF-DFB polymer was oxidized to 75% conversion, and the TMBPF-DCDPS polymer was oxidized to 45% conversion, based on integration of the benzylic methylene peak (i.e., peak c in Figures 6.11 and 6.12) before and after thermal oxidation. The signal-to-noise ratio was lower in the thermal oxidation spectra compared to the Oxone/KBr oxidation because of poor solubility in the deuterated solvent, presumably as a result of thermal crosslinking concurrent with the oxidation reaction. The growth of several small peaks (Figures 6.11 and 6.12) may also indicate increased structural

complexity as the polymers began to crosslink. The rate and exact temperature of these thermal oxidation reactions and how they can be decoupled from crosslinking will be further explored in a subsequent publication.

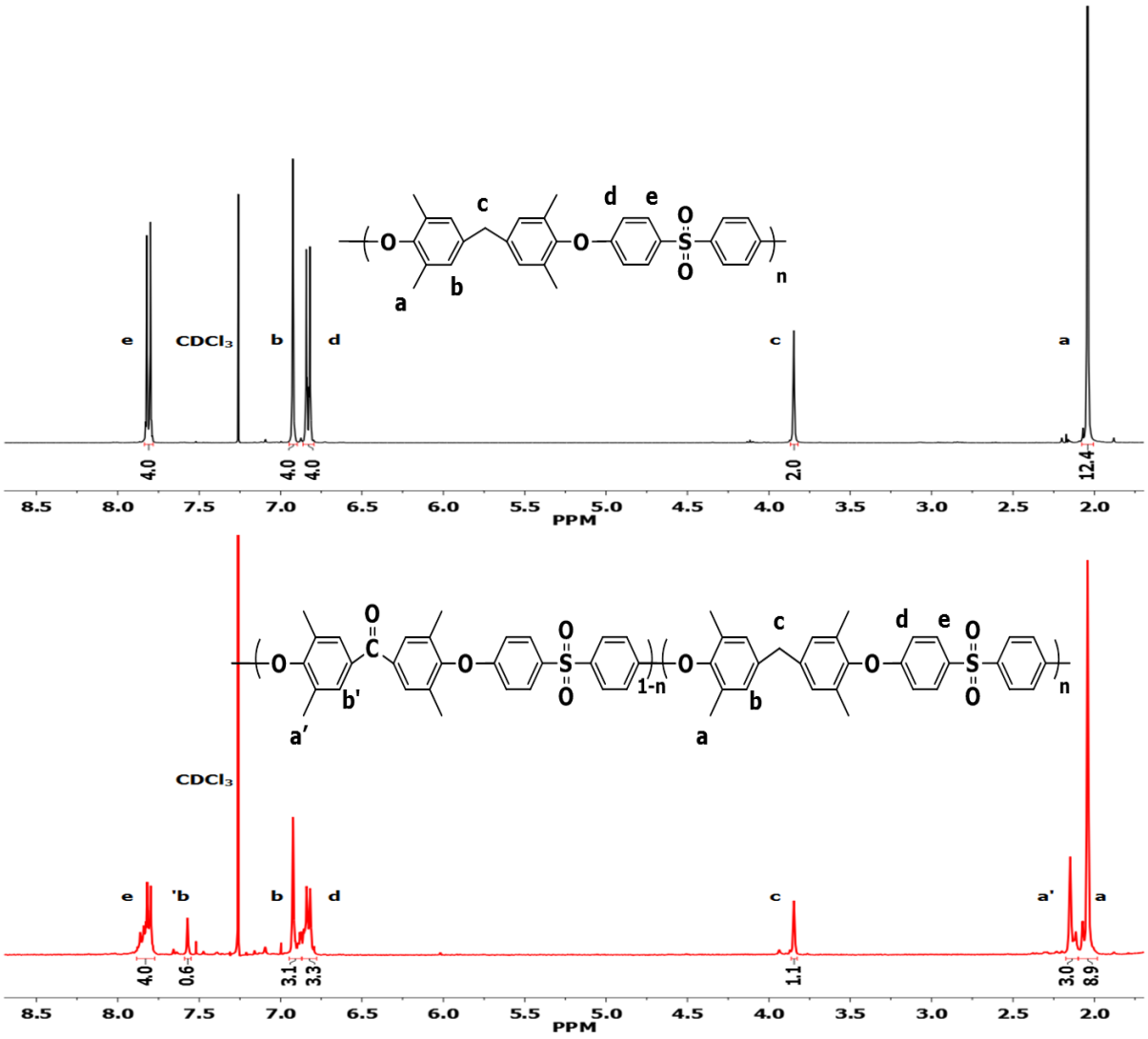

Figure 6.12 ^{1}H-NMR of thermally oxidized TMBPF-DCDPS

FTIR of the thermally oxidized TMBPF-DCDPS polymer

Figure 6.13 shows the FTIR spectrum of the thermally oxidized TMBPF-DCDPS compared to the untreated sample. The thermally oxidized sample had significantly larger carbonyl peaks than the Oxone/KBr oxidized product in Figure 6.7. This comparison of the FTIR

spectra supports the ^{1}H-NMR result that thermal oxidation proceeds to higher conversion than Oxone/KBr conversion.

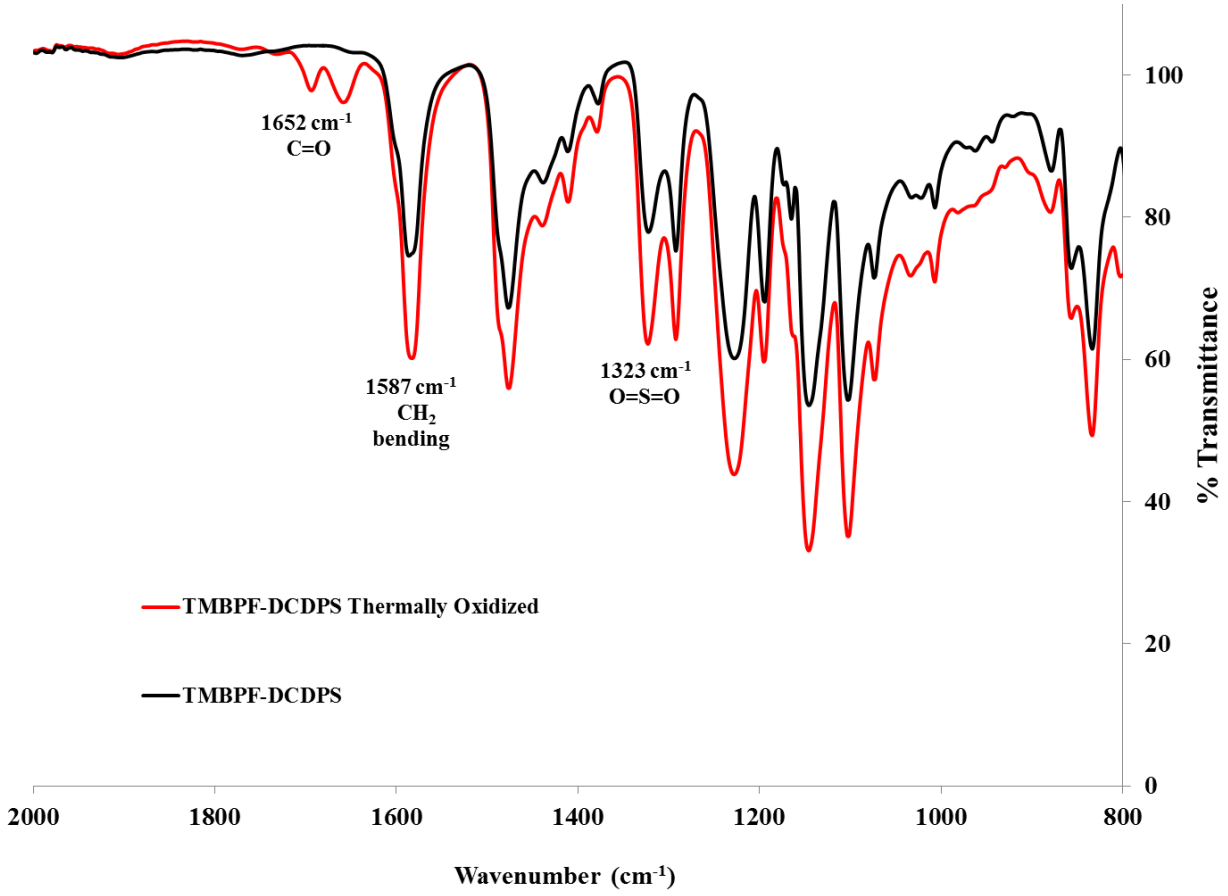

Figure 6.13 IR of thermally oxidized TMBPF-DCDPS

Initial gas transport results

As the effect of UV crosslinking on gas permeation properties was of interest for this research, gas transport results were obtained to compare the linear TMBPF containing poly(arylene ether ketone) and its UV crosslinked analog. A control film was cast from the TMBPF-DFB polymer and then cut in half. Permeabilities and selectivities of five different gases were directly tested on one half. The other half was exposed to UV irradiation to induce photochemical crosslinking. The mechanism for this photochemical reaction is benzylic hydrogen abstraction by an excited state benzophenone moiety,[43,46] which has been shown to

produce polyimides with high selectivity.[19] The gel fraction of this UV irradiated half was measured to be 100%, indicating that a highly crosslinked network was obtained. The density of the linear TMBPF-DFB polymer was 1.116 ± 0.003 g mL^{-1} and the density of the crosslinked TMBPF-DFB polymer was 1.146 ± 0.004 g mL^{-1}. The densification of the polymer membrane upon UV crosslinking was expected based on prior literature, and reflects a decrease in interchain spacing.[47] The pure gas permeabilities and selectivities of these two films are shown in Tables 6.2 and 6.3, where they are compared with UDEL polysulfone.

Table 6.2 Initial pure gas permeability of linear and crosslinked TMBPF-DFB

	Gas Permeability (Barrer) at 10 atm & 35 °C				
	O_2	N_2	CO_2	CH_4	H_2
TMBPF-DFB Linear	2.8	0.52	10	0.54	29
TMBPF-DFB Crosslinked	1.8	0.29	7.1	0.25	23
Polysulfone [a]	1.4	0.25	5.6	0.25	14

[a] Polysulfone[16]: CO_2, CH_4 at 10 bar and 35°C; O_2, N_2, H_2 at 1 bar and 35°C

Table 6.3 Initial pure gas selectivity of linear and crosslinked TMBPF-DFB

	Gas Selectivity at 10 atm & 35 °C				
	O_2/N_2	CO_2/CH_4	H_2/N_2	H_2/CH_4	CO_2/N_2
TMBPF-DFB Linear	5.4	19	75	72	19
TMBPF-DFB Crosslinked	6.2	28	79	92	24
Polysulfone [a]	5.6	22.4	56	56	22.4

[a] Polysulfone[16]: CO_2, CH_4 at 10 bar and 35°C; O_2, N_2, H_2 at 1 bar and 35°C

The films demonstrate the expected relationship of crosslinking decreasing gas permeability and improving selectivity. An additional benefit of crosslinking for thin films is a reduction in physical aging.[46] The reduction of permeability after UV crosslinking has also been attributed to membrane densification.[48] Notably, the crosslinked TMBPF-DFB films had both

higher permeability and selectivity compared to UDEL polysulfone. One reason for the greatly enhanced gas permeability of the TMBPF systems is the presence of the numerous bulky methyl groups along the polymeric backbone. These two samples represent a minor set that was obtainable from these TMBPF polymer series. In a subsequent publication, the effect of oxidation before and after UV crosslinking will be explored for both the TMBPF-DFB and the TMBPF-DCDPS polymers. The pure gas permeability was measured at five different pressures, which is graphed in Figures 6.14 and 6.15.

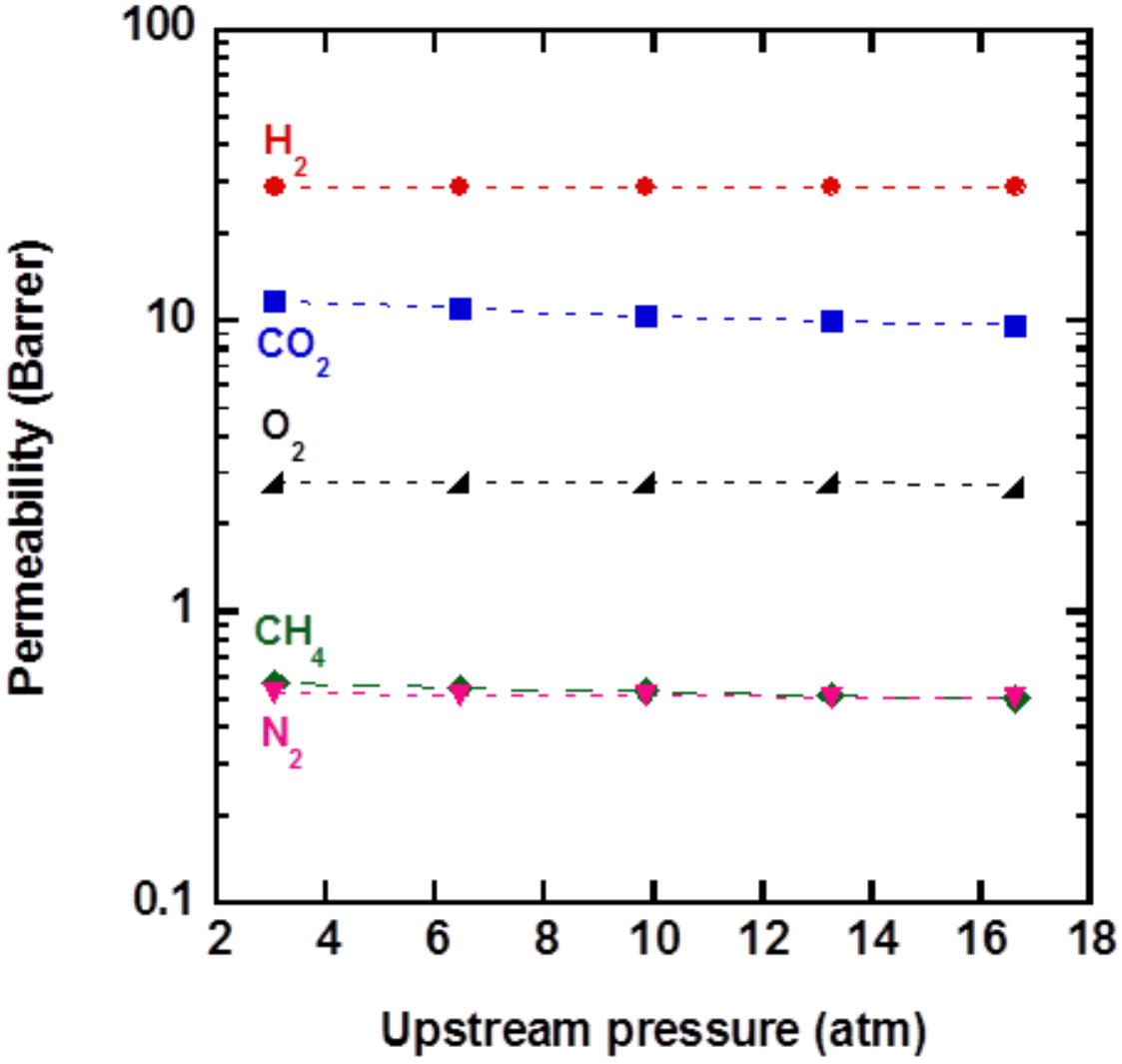

Figure 6.14 Permeability as a function of feed pressure for linear TMBPF-DFB

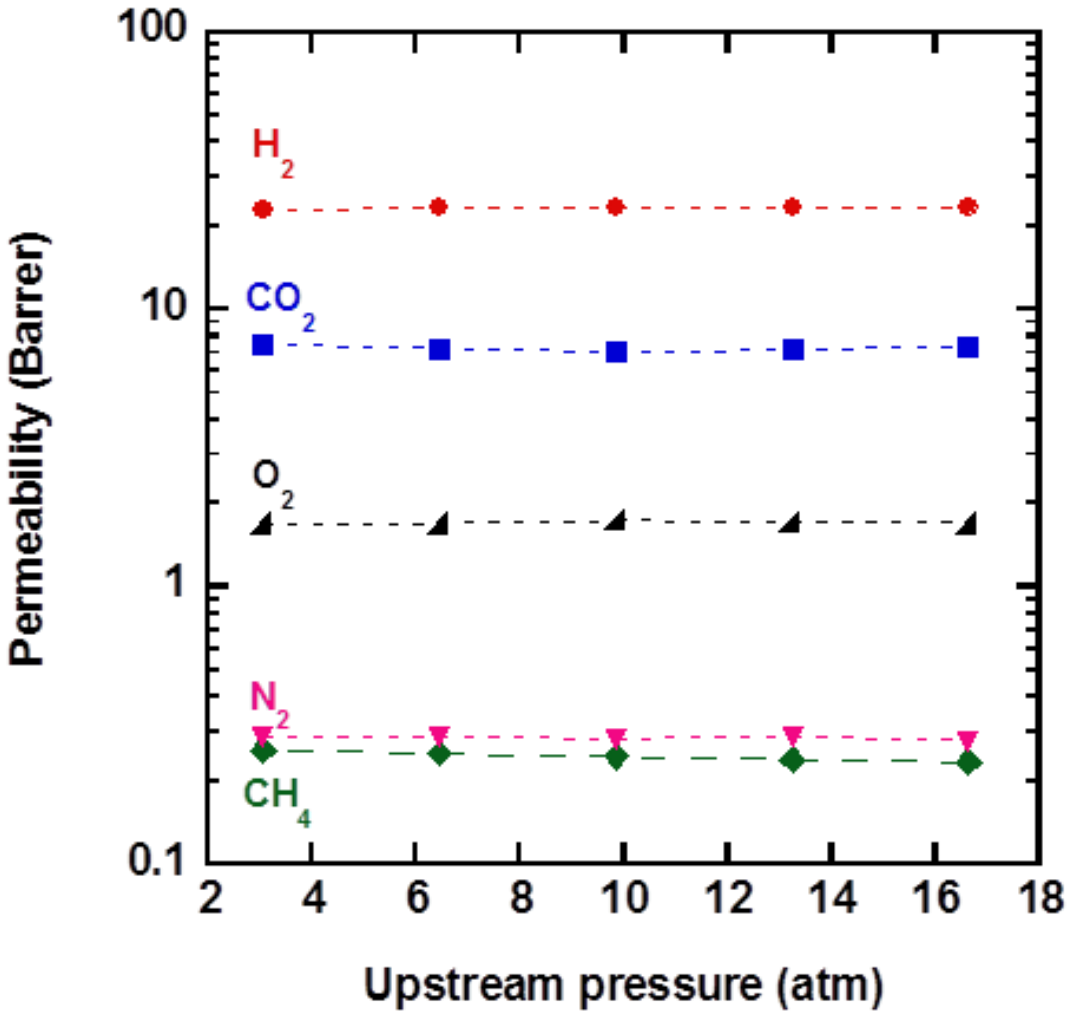

Figure 6.15 Permeability as a function of feed pressure for crosslinked TMBPF-DFB

In Figure 6.14, the permeability of CH_4 and CO_2 decreased slightly as upstream pressure was increased, because of their condensability.[49] The effect of decreasing permeability in glassy polymers as a function of upstream pressure has been attributed to the dual-sorption model.[50] An increase in upstream pressure effectively reduces the Langmuir term and thus reduces permeability. Interestingly this phenomenon was less pronounced in Figure 6.15 for the highly crosslinked TMBPF-DFB.

6.5. Conclusions

In this paper, an economical route was presented to synthesize the TMBPF monomer and two TMBPF containing poly(arylene ether) materials. High molecular weights were demonstrated quantitatively by SEC, and ductile films were obtained. The polymers are capable of backbone modifications that include oxidation and photochemical crosslinking. Solid state thermal oxidation of the benzylic methylene groups was more successful than solution oxidation, in terms of conversion. Both polymers were capable of producing crosslinked films with high gel fractions. ^{1}H-NMR and FTIR spectroscopy were used for structural verification of the TMBPF monomer, TMBPF containing polymers, and conversion of the polymers to their oxidized form. The thermal oxidation reaction was also studied by TGA, and quantitative proof of the oxidation was presented by demonstrating theoretical weight gains. Initial gas transport properties demonstrated that crosslinking these polymers produced more highly selective membranes at the cost of reduced gas permeability.

Acknowledgements

The authors gratefully acknowledge the financial support of Air Products, Inc. (212-153-P), and the National Science Foundation under contracts (NSF-AIR: IIP-1237857) and (NSF-MRI: DMR-1126534).

6.6. References

(1) Bernardo, P.; Drioli, E.; Golemme, G. Membrane Gas Separation: A Review/State of the Art. *Ind. Eng. Chem. Res.* **2009**, *48*, 4638.

(2) Baker, R. W.; Lokhandwala, K. Natural Gas Processing with Membranes: An Overview. *Ind. Eng. Chem. Res.* **2008**, *47*, 2109.

(3) Koros, W. J.; Fleming, G. K. Membrane-based gas separation. *J. Membr. Sci.* **1993**, *83*, 1.

(4) Baker, R. W. Future Directions of Membrane Gas Separation Technology. *Ind. Eng. Chem. Res.* **2002**, *41*, 1393.

(5) Robeson, L. M. Correlation of separation factor versus permeability for polymeric membranes. *J. Membr. Sci.* **1991**, *62*, 165.

(6) Freeman, B. D. Basis of Permeability/Selectivity Tradeoff Relations in Polymeric Gas Separation Membranes. *Macromolecules* **1999**, *32*, 375.

(7) Doolittle, A. K. Newtonian flow. II. The dependence of the viscosity of liquids on free space. *J. Appl. Phys.* **1951**, *22*, 1471.

(8) Cohen, M. H.; Turnbull, D. Molecular transport in liquids and glasses. *J. Chem. Phys.* **1959**, *31*, 1164.

(9) Robeson, L. M. The upper bound revisited. *J. of Membr. Sci.* **2008**, *320*, 390.

(10) Min, K. E.; Paul, D. R. Effect of tacticity on permeation properties of poly(methyl methacrylate). *J. Polym. Sci., Part B: Polym. Phys.* **1988**, *26*, 1021.

(11) Miyata, S.; Sato, S.; Nagai, K.; Nakagawa, T.; Kudo, K. Relationship between gas transport properties and fractional free volume determined from dielectric constant in polyimide films containing the hexafluoroisopropylidene group. *J. Appl. Polym. Sci.* **2008**, *107*, 3933.

(12) Stern, S. A. Polymers for gas separations: the next decade. *J. Membr. Sci.* **1994**, *94*, 1.

(13) McHattie, J. S.; Koros, W. J.; Paul, D. R. Gas transport properties of polysulfones. 1. Role of symmetry of methyl group placement on bisphenol. *Polymer* **1991**, *32*, 840.

(14) Kim, I.-W.; Lee, K. J.; Jho, J. Y.; Park, H. C.; Won, J.; Kang, Y. S.; Guiver, M. D.; Robertson, G. P.; Dai, Y. Correlation between Structure and Gas Transport Properties of Silyl-Modified Polysulfones and Poly(phenyl sulfone)s. *Macromolecules* **2001**, *34*, 2908.

(15) McHattie, J. S.; Koros, W. J.; Paul, D. R. Gas transport properties of polysulfones. 2. Effect of bisphenol connector groups. *Polymer* **1991**, *32*, 2618.

(16) Aitken, C. L.; Koros, W. J.; Paul, D. R. Effect of structural symmetry on gas transport properties of polysulfones. *Macromolecules* **1992**, *25*, 3424.

(17) Xiao, Y.; Chung, T.-S.; Chng, M. L.; Tamai, S.; Yamaguchi, A. Structure and Properties Relationships for Aromatic Polyimides and Their Derived Carbon Membranes: Experimental and Simulation Approaches. *J. Phys. Chem. B* **2005**, *109*, 18741.

(18) Park, H. B.; Jung, C. H.; Lee, Y. M.; Hill, A. J.; Pas, S. J.; Mudie, S. T.; Van Wagner, E.; Freeman, B. D.; Cookson, D. J. Polymers with Cavities Tuned for Fast Selective Transport of Small Molecules and Ions. *Science* **2007**, *318*, 254.

(19) Hayes, R. A. Polyimide gas-separation membranes. US4717393A,**1988**

(20) Bennett, C. L.; Richards, R. E. Copolyimides for use as gas separation membranes. GB2244997A,**1991**

(21) Kita, H.; Inada, T.; Tanaka, K.; Okamoto, K. Effect of photocrosslinking on permeability and permselectivity of gases through benzophenone-containing polyimide. *J. Membr. Sci.* **1994**, *87*, 139.

(22) Ouyang, M.; Muisener, R. J.; Boulares, A.; Koberstein, J. T. UV-ozone induced growth of a SiOx surface layer on a cross-linked polysiloxane film: characterization and gas separation properties. *J. Membr. Sci.* **2000**, *177*, 177.

(23) Kwisnek, L.; Heinz, S.; Wiggins, J. S.; Nazarenko, S. Multifunctional thiols as additives in UV-cured PEG-diacrylate membranes for CO2 separation. *J. Membr. Sci.* **2011**, *369*, 429.

(24) Wind, J. D.; Paul, D. R.; Koros, W. J. Natural gas permeation in polyimide membranes. *J. Membr. Sci.* **2004**, *228*, 227.

(25) Shao, L.; Samseth, J.; Hagg, M.-B. Crosslinking and stabilization of high fractional free volume polymers for gas separation. *Int. J. Greenhouse Gas Control* **2008**, *2*, 492.

(26) Staudt-Bickel, C.; Koros, W. J. Improvement of CO2/CH4 separation characteristics of polyimides by chemical crosslinking. *J. Membr. Sci.* **1999**, *155*, 145.

(27) Lin, H.; Van Wagner, E.; Freeman, B. D.; Toy, L. G.; Gupta, R. P. Plasticization-enhanced hydrogen purification using polymeric membranes. *Science* **2006**, *311*, 639.

(28) Han, G.; Chung, T.-S.; Toriida, M.; Tamai, S. Thin-film composite forward osmosis membranes with novel hydrophilic supports for desalination. *J. Membr. Sci.* **2012**, *423-424*, 543.

(29) Sun, H.; Zhang, G.; Liu, Z.; Zhang, N.; Zhang, L.; Ma, W.; Zhao, C.; Qi, D.; Li, G.; Na, H. Self-crosslinked alkaline electrolyte membranes based on quaternary ammonium poly (ether sulfone) for high-performance alkaline fuel cells. *Int. J. Hydrogen Energy* **2012**, *37*, 9873.

(30) *Macromolecular Synthesis*; John Wiley & Sons: New York, **1977**; Vol. 1.

(31) Hedrick, J. L.; Mohanty, D. K.; Johnson, B. C.; Viswanathan, R.; Hinkley, J. A.; McGrath, J. E. Radiation resistant amorphous-all aromatic polyarylene ether sulfones: synthesis, characterization, and mechanical properties. *J. Polym. Sci., Part A: Polym. Chem.* **1986**, *24*, 287.

(32) Yin, L.; Wu, J.; Xiao, J.; Cao, S. Oxidation of benzylic methylenes to ketones with Oxone–KBr in aqueous acetonitrile under transition metal free conditions. *Tetrahedron Letters* **2012**, *53*, 4418.

(33) Lin, H., Freeman, B.D. In *Spring Handbook of Metrology and Testing*; 2nd Edition ed.; H. Czichos, T. S., L. Smith, Ed.; Springer: Berlin, **2011**, p 426.

(34) Olah, G. A.; Kobayashi, S.; Nishimura, J. Aromatic Substitution. XXXI. Friedel-Crafts Sulfonylation of Benzene and Toluene with
Alkyl- and Arylsulfonyl Halides and Anhydrides. *J. Amer. Chem. Soc.* **1973**, *95*, 564.

(35) Bowman, P. J.; Brown, B. R.; Chapman, M. A.; Doyle, P. M. Synthesis and reactions of phenolic alkylbenzylnitrosamines. *J. Chem. Res., Synop.* **1984**, 72.

(36) Sanders, D. F.; Smith, Z. P.; Guo, R.; Robeson, L. M.; McGrath, J. E.; Paul, D. R.; Freeman, B. D. Energy-efficient polymeric gas separation membranes for a sustainable future: A review. *Polymer* **2013**, *54*, 4729.

(37) Robeson, L. M.; Farnham, A. G.; McGrath, J. E. Synthesis and dynamic mechanical characteristics of poly(aryl ethers). *Appl. Polym. Symp.* **1975**, *26*, 373.

(38) Rose, J. B. Preparation and properties of poly(arylene ether sulphones). *Polymer* **1974**, *15*, 456.

(39) Viswanathan, R.; Johnson, B. C.; McGrath*, J. E. In *Polymer* **1984**; Vol. 25, p 1827.

(40) Bunnett, J. F. Mechanism and reactivity in aromatic nucleophilic substitution reactions. *Quarterly Reviews, Chemical Society* **1958**, *12*, 1.

(41) Mohanty, D. K.; Sachdeva, Y.; Hedrick, J. L.; Wolfe, J. F.; McGrath, J. E. Synthesis and transformations of tetramethyl bis[phenol] A polyaryl ethers. *Polym. Prepr. (Am. Chem. Soc., Div. Polym. Chem.)* **1984**, *25*, 19.

(42) Chen, M. S.; White, M. C. Combined Effects on Selectivity in Fe-Catalyzed Methylene Oxidation. *Science* **2010**, *327*, 566.

(43) Wright, C. T.; Paul, D. R. Gas sorption and transport in UV-irradiated polyarylate copolymers based on tetramethylbisphenol-A and dihydroxybenzophenone. *J. Membr. Sci.* **1997**, *124*, 161.

(44) Merkel, T. C.; Zhou, M.; Baker, R. W. Carbon dioxide capture with membranes at an IGCC power plant. *J. Membr. Sci.* **2012**, *389*, 441.

(45) Aitken, C. L.; McHattie, J. S.; Paul, D. R. Dynamic mechanical behavior of polysulfones. *Macromolecules* **1992**, *25*, 2910.

(46) McCaig, M. S.; Paul, D. R. Effect of UV crosslinking and physical aging on the gas permeability of thin glassy polyarylate films. *Polymer* **1999**, *40*, 7209.

(47) Matsui, S.; Ishiguro, T.; Higuchi, A.; Nakagawa, T. Effect of ultraviolet light irradiation on gas permeability in polyimide membranes. 1. Irradiation with low pressure mercury lamp on photosensitive and non-photosensitive membranes. *J. Polym. Sci., Part B: Polym. Phys.* **1997**, *35*, 2259.

(48) Matsui, S.; Sato, H.; Nakagawa, T. Effects of low molecular weight photosensitizer and UV irradiation on gas permeability and selectivity of polyimide membrane. *J. Membr. Sci.* **1998**, *141*, 31.

(49) Sanders, D. F.; Smith, Z. P.; Ribeiro, C. P., Jr.; Guo, R.; McGrath, J. E.; Paul, D. R.; Freeman, B. D. Gas permeability, diffusivity, and free volume of thermally rearranged polymers based on 3,3'-dihydroxy-4,4'-diamino-biphenyl (HAB) and 2,2'-bis-(3,4-dicarboxyphenyl) hexafluoropropane dianhydride (6FDA). *J. Membr. Sci.* **2012**, *409-410*, 232.

(50) Koros, W. J.; Chan, A. H.; Paul, D. R. Sorption and transport of various gases in polycarbonate. *J. Membr. Sci.* **1977**, *2*, 165.

CHAPTER 7: FUTURE AND SUGGESTED RESEARCH

7.1. Suggested Direction for Water Purification Research

An article was recently published by Stevens et al. of Dow Water and Process Solutions that demonstrated the production of an asymmetric membrane from sulfonated polysulfones.[1] The paper was a breakthrough for these materials in that 99% salt rejection was demonstrated with very thin membranes that were produced by a phase inversion process. Unfortunately, this paper also demonstrated a vital flaw in the sulfonated polysulfone membranes. The authors revealed that divalent salts such as Ca^{2+} bind strongly to the anionic sulfonate groups in the polymer backbone. The binding of these ions screens the repulsive Donnan exclusion effect that is necessary to achieve high salt rejection. Figure 7.1 compares the salt passage of the state-of-the-art aromatic polyamide with a sulfonated polysulfone as a function of calcium concentration.

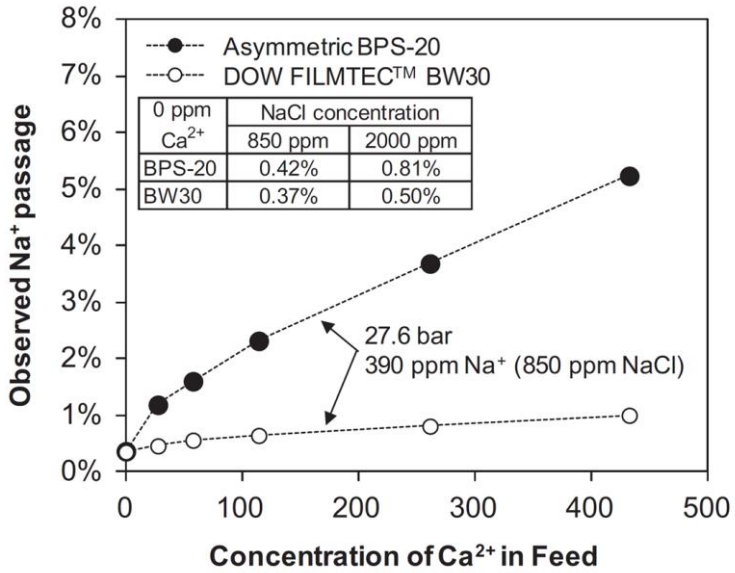

Figure 7.1 Salt passage of BPS copolymers and aromatic polyamides in the presence of calcium. From J. of Membr. Sci. 2014, 452, 193. Stevens, D. M.; Mickols, B.; Funk, C. V. Asymmetric reverse osmosis sulfonated poly(arylene ether sulfone) copolymer membranes. Used with permission of Elsevier, 2014[1]

The figure shows that the disulfonated polysulfones have a much greater susceptibility to divalent ions than the state-of-the-art polyamide. The concentration of calcium in seawater is approximately 400 ppm so the selectivity for divalent versus monovalent cations represents a challenge. Though this experiment was only performed on linear disulfonated polysulfones, it follows that this weakness would extend to the crosslinked disulfonated polysulfones studied in this dissertation. Therefore, it is of paramount importance to identify hydrophilic polysulfones that achieve high water permeability without the tendency to be selective for multivalent cations.

I propose that emphasis should be placed on incorporating the carboxylate group into polysulfones, and then crosslinking them by similar mechanisms discussed in this dissertation. There are several advantages to this approach. Most importantly, the carboxylate groups emulate the hydrophilicity of the state-of-the-art aromatic polyamides, but lacks the oxidatively unstable amide group and could therefore still achieve high chlorine resistance. This approach might also resolve the calcium sensitivity issue by eliminating the sulfonate groups on the polymer backbone. These carboxylate containing polysulfones could be achieved by a variety of methods, discussed below.

The ability to incorporate carboxylate groups into polysulfones has been known for nearly 25 years but to my knowledge has never been applied in the area of water purification, and has certainly not been combined with crosslinking in the field. Guiver et al. published the following scheme to incorporate carboxylate into polysulfones.[2]

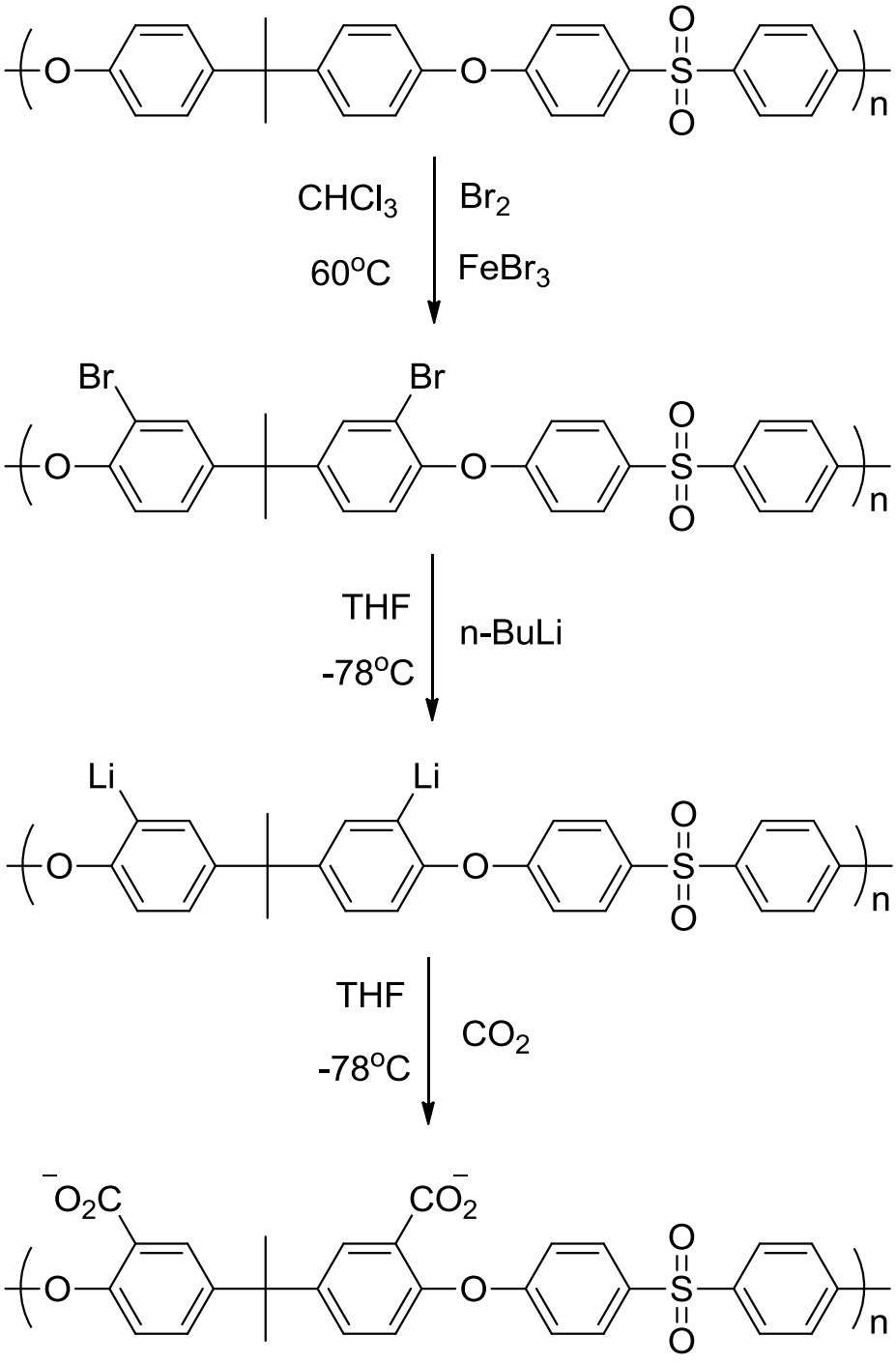

Figure 7.2 Synthetic scheme to produce carboxylate containing polysulfones[2]

The bromination reaction will occur ortho to the aryl ether linkage on the bisphenol moiety of the polymer chains, because the sulfone group deactivates adjacent rings toward electrophilic aromatic substitution. The hydrophilicity and water uptake may also be altered by

synthesizing copolymers containing bisphenol S instead of solely bisphenol A or 4,4'-biphenol. Copolymers containing bisphenol S would produce additional sites that are unreactive to electrophilic aromatic substitution and therefore less hydrophilic polymers.

An alternative way to directly introduce carboxylate groups into polysulfones has recently been studied by Kim et al.[3] The authors used phenolphthalin (PP), a bisphenol monomer that contains a carboxylic acid. This monomer could be used in a copolymerization with bisphenol A, dichlorodiphenyl sulfone and meta-aminophenol by the following scheme.

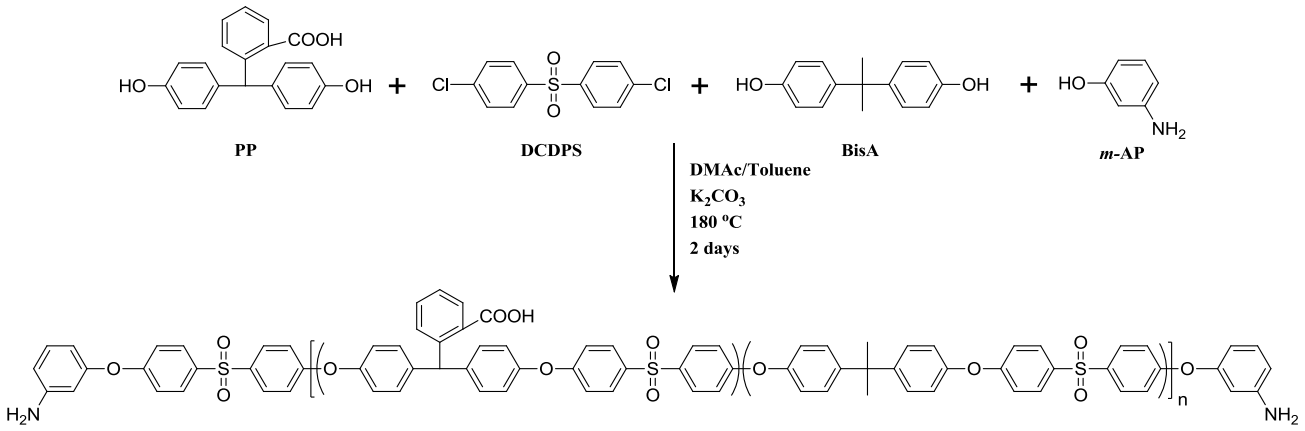

Figure 7.3 Alternative route to produce carboxylate containing crosslinkable polysulfones

The molecular weight would be controlled by the amount of *m*-AP charged to the reaction, which also functionalizes the endgroups for a variety of crosslinking reactions as discussed in Chapter 3. This oligomer could be directly crosslinked with epoxy, or first functionalized with acryloyl chloride to prepare a UV crosslinkable variant. The primary amine is much more nucleophilic than the benzoic acid moiety on the polymer backbone, and reaction with stoichiometric amounts of acryloyl chloride should result in solely acrylamide terminated oligomers. Systematic studies could then be performed with varying levels of hydrophilicity and varying molecular weights of the telechelic oligomers.

7.2. Suggested Project for Gas Separation Membranes

The crosslinked polymers and copolymers produced in this dissertation were primarily characterized by gel fraction amongst other spectroscopic methods. The precedent for this was that the literature is rich with gel fraction measurements and perhaps mechanical properties of the crosslinked polymers, but fails to take into account the importance of crosslink density. The difference between crosslink density and gel fraction is somewhat subtle, though it is of tremendous importance. The gel fraction is the percentage of chains included in the gel or crosslinked network, whereas the crosslink density is the average molecular weight between two crosslinks (M_c). For Chapters 3 and 4 of this dissertation the molecular weight of the oligomer should set the crosslink density, assuming no chain extension. The number average molecular weight of the oligomers was 5,000 g mol^{-1} and the M_c should also be 5,000 g mol^{-1}, even though the gel fractions were between 90-100%. The crosslink situation for the gas separation research in Chapter 6 is much less certain. Here the gel fraction of the materials was near 100%, meaning that all of the polymer chains were incorporated into the network. However, because each repeat unit could be crosslinked the crosslink density could be as low as the molecular weight of a repeat unit (~500 g mol^{-1}) and as high as the ten thousands (the length of the polymer chains).

Crosslinking increases the selectivity of polymers primarily through densification of the polymer matrix, which limits the diffusion of gases through the polymer membrane. However, crosslinking also reduces the interchain spacing between polymer chains and decreases the free volume gases can travel through, thereby decreasing gas diffusion and permeability and increasing selectivity. It follows that a highly crosslinked network with a small M_c will have less free volume available for transport and higher membrane selectivity than a similar crosslinked network with a relatively large M_c. However, the relationship between crosslink density and gas

transport properties is largely unknown. Preliminary results in our research group indicate that crosslinking a polymer under different UV wavelengths (254 and 365 nm) produces membranes with distinctly different transport results, even though both membranes had near 100% gel fraction. This membrane crosslinked at 254 nm had markedly higher selectivity than the membrane irradiated at 365 nm, likely a result of the 254 nm irradiation producing a membrane with a higher crosslink density. Based upon this initial result, elucidation of crosslink density and how it affects membrane performance would be of great fundamental and industrial importance.

A research plan for a systematic study that could separate crosslink density from gel fraction is described below. The study is based on the same monomers used in Chapter 6 and would be an excellent comparison to the already completed study. The direction of the research would be to synthesize oligomers and chain extend them with a crosslinkable functionality. In the scheme shown below the oligomers contain benzylic methyl groups, which will crosslink under UV irradiation with the benzophenone used to chain extend the oligomers.

After the membranes have been prepared and structurally characterized, gas transport properties could be tested at the University of Texas at Austin as discussed in Chapter 6. The crosslink density would be determined by performing dynamic mechanical analysis (DMA) or stress-strain measurements and utilizing the following equation. Where ρ is the polymer density, E is the elastic modulus, R is the gas constant and T is the temperature in kelvin.

Equation 7.1: $E = \frac{3\rho RT}{2M_c}$

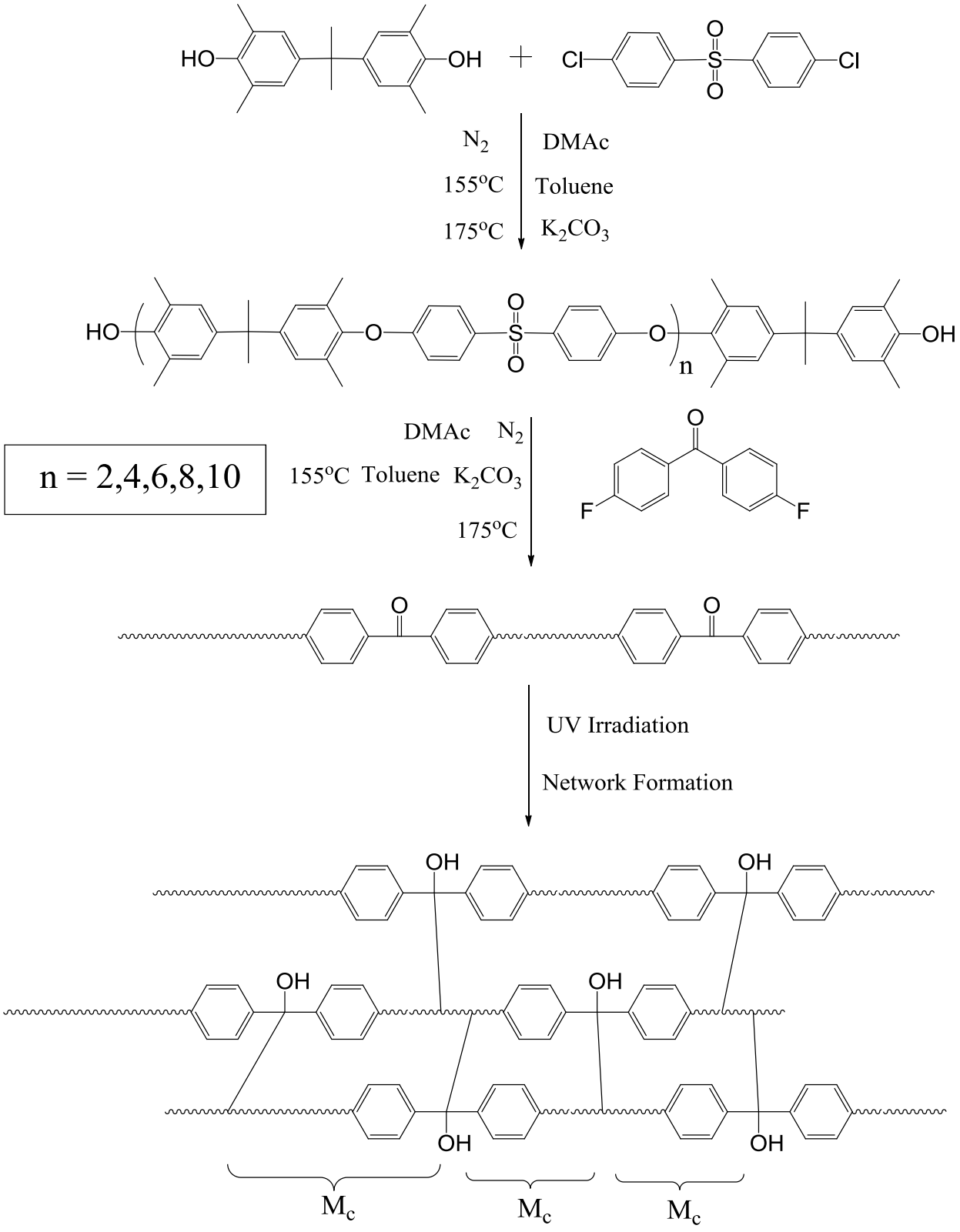

Figure 7.4 Research scheme to investigate effect of crosslink density on gas transport properties

The mechanism for this reaction is benzylic hydrogen abstraction by an excited ketone, radical formation and subsequent radical recombination. The mechanism for this reaction is shown below.

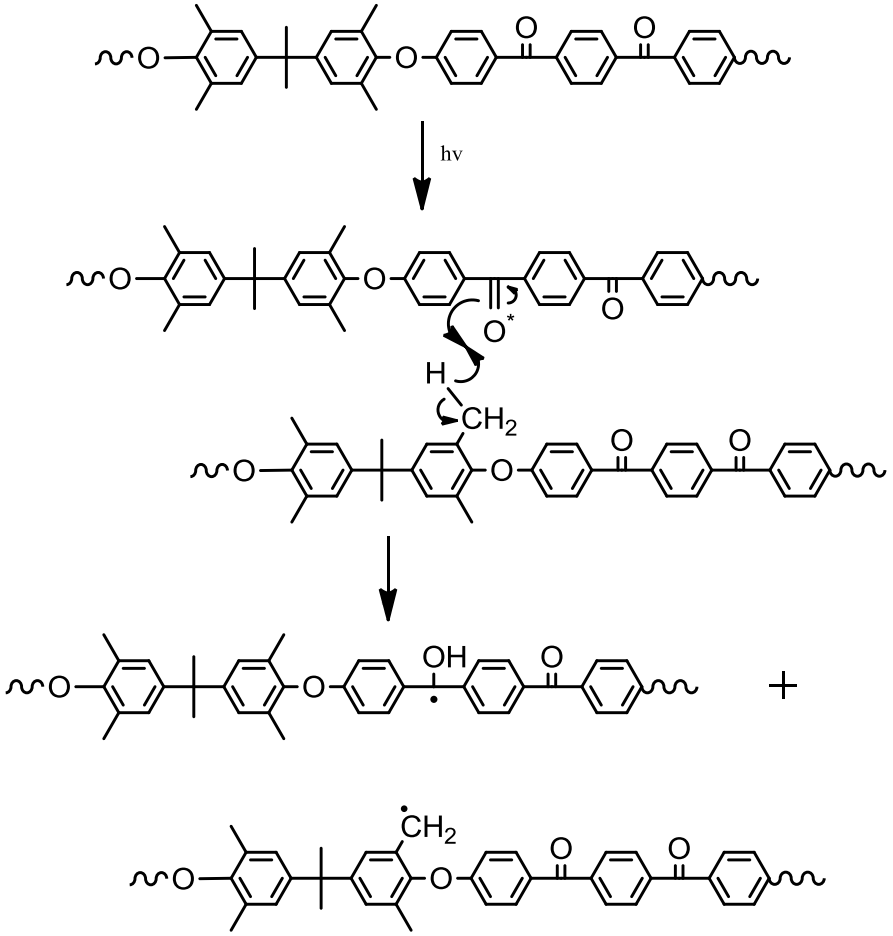

Figure 7.5 Benzylic hydrogen abstraction by ketone excited to triplet state

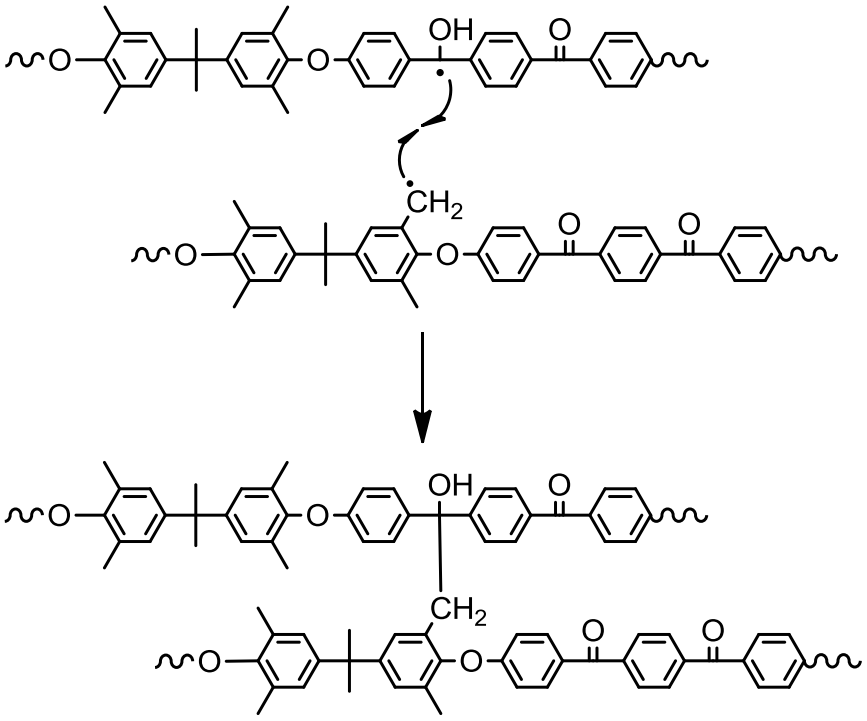

Figure 7.6 Intermolecular radical recombination leading to crosslink site

7.3. References

(1) Stevens, D. M.; Mickols, B.; Funk, C. V. Asymmetric reverse osmosis sulfonated poly(arylene ether sulfone) copolymer membranes. *J. Membr. Sci.* **2014**, *452*, 193.

(2) Guiver, M. D.; Kutowy, O.; ApSimon, J. W. Functional group polysulfones by bromination-metalation. *Polymer* **1989**, *30*, 1137.

(3) Kim, D. S.; Shin, K. H.; Park, H. B.; Chung, Y. S.; Nam, S. Y.; Lee, Y. M. Synthesis and characterization of sulfonated poly(arylene ether sulfone) copolymers containing carboxyl groups for direct methanol fuel cells. *J. Membr. Sci.* **2006**, *278*, 428.